

**A Thesis Submitted for the Degree of PhD at the University of Warwick**

**Permanent WRAP URL:**

<http://wrap.warwick.ac.uk/79688>

**Copyright and reuse:**

This thesis is made available online and is protected by original copyright.

Please scroll down to view the document itself.

Please refer to the repository record for this item for information to help you to cite it.

Our policy information is available from the repository home page.

For more information, please contact the WRAP Team at: [wrap@warwick.ac.uk](mailto:wrap@warwick.ac.uk)

# **Synthesis of Glycopolymers for the Study of Lectin-Carbohydrate Interactions**

**by**

**Yanzi Gou (苟燕子)**

**A thesis submitted in fulfilment of the requirements for the degree  
of  
Doctor of Philosophy in Chemistry.**

**Department of Chemistry  
University of Warwick**

**November 2011**



“A man should look for what is, and not for what he thinks should be”

— **Albert Einstein**

“Nothing in life is to be feared, it is only to be understood. Now is the time to understand more, so that we may fear less.”

— **Marie Curie**

“Just do it.”

— **David M. Haddleton**

# Table of Contents

Table of Contents ..... i

Table of Figures ..... vi

Table of Tables ..... xvii

Abbreviations ..... xviii

Acknowledgments ..... xxiv

Declaration ..... xxvi

Abstract ..... xxvii

**Chapter 1. From Glycobiology to Glycopolymers ..... 1**

    1.1 Chemical glycobiology ..... 2

    1.2 Direct synthesis of oligosaccharides ..... 2

        1.2.1 Chemical synthesis ..... 3

        1.2.2 Enzymatic synthesis ..... 6

    1.3 Synthesis of glycopolymers ..... 8

        1.3.1 Linear glycopolymers ..... 9

        1.3.2 Hyperbranched glycopolymers ..... 19

        1.3.3 Glycodendrimers ..... 22

        1.3.4 Star glycopolymers ..... 28

    1.4 Biological application of glycopolymers ..... 31

    1.5 References ..... 32

**Chapter 2. Lectin-Carbohydrate Interactions ..... 44**

    2.1 Background ..... 45

    2.2 Glycoside cluster effect ..... 48

    2.3 Investigation of lectin-carbohydrate interactions ..... 49

        2.3.1 Traditional methods ..... 51

        2.3.2 Quartz crystal microbalance biosensor with dissipation monitoring (QCM-D) ..... 58

## Table of Contents

---

2.3.3 Surface plasmon resonance (SPR) .....	66
2.4 References .....	71
<b>Chapter 3. Synthesis of Glycopolymers via the Combination of CCTP and Click Chemistry</b> .....	<b>83</b>
3.1 Introduction .....	84
3.1.1 Catalytic chain transfer polymerisation (CCTP) .....	85
3.1.2 Click chemistry .....	89
3.1.3 Conclusions .....	94
3.2 Results and discussion .....	96
3.2.1 CCTP of methyl methacrylate (MMA) .....	96
3.2.1.1 Determination of the chain transfer constant of CoBF .....	96
3.2.1.2 Bulk catalytic chain transfer polymerisation of MMA .....	98
3.2.2 Preparation of clickable polymer scaffolds .....	101
3.2.2.1 Polymerisation of propargyl methacrylate (PMA) via CCTP .....	101
3.2.2.2 Synthesis of TMS-protected propargyl methacrylate .....	104
3.2.2.3 CCTP of TMS-protected propargyl methacrylate .....	107
3.2.3 Post-modification of polymers via click reactions .....	115
3.2.3.1 CuAAC click reaction with poly(ethylene glycol) (PEG) azide ...	115
3.2.3.2 Thiol-ene click reaction with benzyl mercaptan .....	117
3.2.4 Synthesis of glycopolymers via CuAAC with sugar azides .....	119
3.2.4.1 Synthesis of sugar azides .....	119
3.2.4.2 CuAAC reaction of precursor polymers with sugar azides. ....	124
3.3 Conclusions .....	128
3.4 References .....	130
<b>Chapter 4. Well-defined Multivalent Glycopolymers for the Lectin-Carbohydrate Interaction</b> .....	<b>140</b>
4.1 Introduction .....	141
4.1.1 The interaction mechanisms of ligands with receptors .....	141

---

## Table of Contents

4.1.2 Investigation into lectin-glycopolymer interactions.....	144
4.1.3 Conclusions.....	146
4.2 Results and discussion.....	148
4.2.1 Synthesis of glycopolymers.....	148
4.2.2 The stoichiometry of the glycopolymer–Con A complexes.....	150
4.2.3 The rate of glycopolymer–Con A clustering.....	155
4.2.4 Inhibitory potency of the glycopolymers.....	160
4.2.5 Stability of the glycopolymer–Con A cluster.....	164
4.2.5 The influence of polymer chain length.....	168
4.3 Conclusions.....	172
4.4 References.....	173
<b>Chapter 5. Controlled Interactions of Lectins and Glycopolymers Using QCM-D and SPR...</b>	<b>177</b>
5.1 Layer-by-layer self-assembly by QCM-D.....	178
5.1.1 Introduction.....	178
5.1.2 Immobilisation of lectin on an Au chip.....	181
5.1.2.1 Con A on bare Au chip surface.....	181
5.1.2.2 Con A on a modified Au chip surface.....	182
5.1.2.3 The self-assembly of lectin and glycopolymer.....	184
5.1.3 Immobilisation of glycopolymers on a Au chip.....	186
5.1.3.1 Mannose glycopolymer on a bare gold chip surface.....	186
5.1.3.2 Disulfide mannose glycopolymer on a bare gold chip surface....	187
5.1.3.3 Multilayer self-assembly on Au chip surface.....	190
5.1.4 Conclusions.....	195
5.2 Lectin-glycopolymer interactions monitored by QCM-D.....	195
5.2.1 Interactions of Con A with glycopolymers.....	197
5.2.1.1 Glycopolymer P4 binding with Con A.....	197
5.2.1.2 Glycopolymer P5 binding with Con A.....	203

## Table of Contents

5.2.1.3 Glycopolymer <b>P6</b> binding with Con A.....	205
5.2.1.4 Glycopolymer <b>P1</b> binding with Con A.....	208
5.2.1.5 Comparison of all glycopolymers in the interactions with Con A.....	209
5.2.2 Interactions of DC-SIGN with glycopolymers .....	213
5.3 Investigation into the specific lectin-glycopolymer interactions by SPR.....	219
5.3.1 The routine of SPR experiments .....	219
5.3.2 Comparison of glycopolymers on the basis of sugar moieties.....	222
5.3.3 Kinetic properties of the interaction between DC-SIGN and synthetic glycopolymers .....	223
5.4 Conclusions .....	226
5.5 References .....	227
<b>Chapter 6. Conclusions and Outlook .....</b>	<b>232</b>
6.1 Conclusions .....	233
6.2 Outlook .....	235
<b>Chapter 7. Experimental.....</b>	<b>236</b>
7.1 Materials.....	237
7.2 Characterisation.....	237
7.2.1 Nuclear Magnetic Resonance.....	237
7.2.2 Gel Permeation Chromatography (GPC) .....	238
7.2.3 Electrospray Ionization Mass Spectrometry (ESI-MS).....	239
7.2.4 Matrix Assisted Laser Desorption Ionisation–Time of Flight (MALDI-TOF) Spectrometry.....	239
7.2.5 Fourier Transform Infra Red (FTIR) Spectroscopy.....	240
7.2.6 Ultraviolet (UV) Spectroscopy .....	240
7.2.7 Quartz Crystal Microbalance with Dissipation Monitoring (QCM-D).....	240
7.2.8 Surface Plasmon Resonance (SPR).....	241
7.3 Chapter 3 Experimental .....	241
7.3.1 CCTP of Methyl Methacrylate (MMA) .....	241

## Table of Contents

---

7.3.2 Synthesis of TMS-Protected Propargyl Methacrylate .....	242
7.3.3 CCTP of TMS-Protected Propargyl Methacrylate (General Procedure) ....	243
7.3.4 Deprotection of TMS-Protected Polymers (General Procedure) .....	243
7.3.5 CuAAC of Clickable Polymers and Poly(ethylene glycol) (PEG) Azide .....	244
7.3.6 Thiol-ene reaction of Clickable Polymers with Benzyl Mercaptan .....	245
7.3.7 One-Step Synthesis of Sugar Azides .....	245
7.3.8 CuAAC of Clickable Polymers with Sugar Azides (General Procedure) ....	249
7.4 Chapter 4 Experimental .....	249
7.4.1 Synthesis of TMS-Protected Polymers by ATRP (General Procedure) .....	250
7.4.2 Deprotection of the TMS-Protected Polymers (General Procedure) .....	250
7.4.3 Synthesis of Sugar Azides .....	251
7.4.4 Synthesis of Glycopolymers by CuAAC (General Procedure) .....	254
7.4.5 Quantitative Precipitation .....	254
7.4.6 Turbidimetry .....	255
7.4.7 Reversal Aggregation Assay .....	256
7.4.8 Inhibitory Potency Assay .....	256
7.5 Chapter 5 Experimental .....	256
7.5.1 Typical Conditions for QCM-D Experiment .....	256
7.5.2 Modification of Au Chip with MUA, EDC and NHS .....	257
7.5.3 Typical Conditions for SPR Experiment .....	258
7.6 References .....	259

---

## Table of Figures

Figure 1.1 Automated solid-phase synthesis of oligosaccharides. Ref. 34.....	4
Figure 1.2 Examples of oligosaccharides synthesised by a solid-phase synthesiser. Ref. 34.....	5
Figure 1.3 OptiMer's programmed one-pot synthesis. Ref. 43. ....	6
Figure 1.4 Enzymatic synthesis of oligosaccharides. Ref. 43. ....	7
Figure 1.5 Glycomonomers and the resulting glycopolymers as glycomimetics of natural polysaccharides, chondroitin sulfate (CS) glycosaminoglycans. Ref. 58. .....	10
Figure 1.6 Synthesis of (a) linear block glycopolymer PS-b-PAcGEMA, (b) linear random glycopolymer PS-r-PAcGEMA, and (c) comb-like glycopolymer PS-b- (PHEMA-g- PAcGEMA. From ref. 59.....	11
Figure 1.7 Preparation of dual-end-functionalised glycopolymers as mucin mimics. Ref. 60.....	12
Figure 1.8 Synthesis of glycopolymers by CCTP and double click reactions. Ref. 65. .....	13
Figure 1.9 Monomers used for the preparation of hyperbranched glycopolymers via combination of self-condensing vinyl copolymerisation and ATRP. Ref.106~109. ....	20
Figure 1.10 Synthesis of (a) highly branched and (b) hyperbranched glycopolymers by RAFT polymerisation and click chemistry. Ref. 110. ....	21
Figure 1.11 Mannose conjugates based on hyperbranched polyglycerols. Ref. 111.	22
Figure 1.12 Unsymmetrical fluorescent mannose glycodendrimers synthesised by click chemistry. Ref. 119. ....	23
Figure 1.13 Polysulfated poly(ethylene oxide) (PEO) dendrimer-like glycopolymers bearing sulfated lactose. Ref. 120. ....	24

## Table of Figures

Figure 1.14 Dendritic glycopolymer synthesised by RAFT and click chemistry. Ref. 121. ....	24
Figure 1.15 Glycodendrimers obtained by click chemistry. Ref. 122. ....	25
Figure 1.16 Supramolecular glycodendrimers based on the use of cyclodextrin. Ref. 125. ....	26
Figure 1.17 Glycodendrimer-cyclodextrin conjugates. Ref. 126. ....	27
Figure 1.18 Star-shaped multivalent ligands with low valency. Ref. 127. ....	28
Figure 1.19 Synthesis of star-shaped SPBLG-PGAMA biohybrids. Ref.129. ....	29
Figure 1.20 Synthesis of star glycopolymer by RAFT. Ref.133. ....	30
Figure 1.21 Structure of seven-arm $\beta$ -CD-(PHEA <sub>10</sub> -b-PAGAx). Ref. 134. ....	31
Figure 2.1 An example of hydrogen-bonding and calcium coordination bonding patters in the binding of a mannoside to the MBL binding sites. Ref. 26. ....	47
Figure 2.2 Representative glycodendrimer involved in the study against bacterial adhesion. Ref. 57. ....	54
Figure 2.3 QCM-D instrument images obtained from Q-Sense website. ....	59
Figure 2.4 Different thiols used for the construction of carbohydrate libraries. Ref. 126. ....	63
Figure 2.5 Synthetic functional glycopolymer to be immobilised on Au surface for screening different lectins. Ref. 127. ....	64
Figure 2.6 Frequency changes by binding glycoproteins onto immobilised lectin surface in the investigation of various lectins and different glycoproteins. Ref. 128. ....	65
Figure 2.7 Schematic presentation of bacterial detection mediated by Con A. Ref. 129. ....	66
Figure 2.8 A schematic representation of a typical SPR-sensing configuration. Ref. 134. ....	67
Figure 2.9 Representative heteroglycocluster based on $\beta$ CD. Ref. 155. ....	70
Figure 2.10 Synthesis of dodecavalent fullerene-based glycocluster. Ref. 156. ....	71



## Table of Figures

Figure 3.1 Catalysts commonly used in CCTP. Ref. 33 ~ 38.....	86
Figure 3.2 Proposed mechanism for CCTP of methacrylates catalysed by cobalt chelates. Ref. 41 and 42. ....	87
Figure 3.3 CoBF as the catalyst in CCTP. Ref. 51. ....	88
Figure 3.4 The preliminary 1,3-dipolar cycloaddition of azides and alkynes. Ref. 92 and 93.....	90
Figure 3.5 Copper(I)-catalysed azide–alkyne cycloadditions (CuAAC). Ref. 94 and 95. ....	91
Figure 3.6 The proposed mechanism of CuAAC. Ref. 80.....	92
Figure 3.7 The mechanism of thiol-ene radical reaction. Ref. 107. ....	93
Figure 3.8 The thiol-Michael addition to various enes bearing electron-withdrawing (EWG) moiety.....	94
Figure 3.9 The proposed mechanism of the thiol-ene Michael addition catalysed by phosphines. Ref. 106.....	94
Figure 3.10 Preparation of glycopolymers by CCTP and CuAAC.....	95
Figure 3.11 CCTP of methyl methacrylate.....	96
Figure 3.12 Mayo plot of the CCTP of MMA at 60 °C.....	98
Figure 3.13 SEC spectra of samples obtained from the CCTP of MMA at 60 °C. (a) High concentration of CoBF (0.1 mg/mL). (b) Low concentration of CoBF (0.05 mg/mL). ....	99
Figure 3.14 The changes of molecular weight $M_n$ and polydispersity PDI during the CCTP of MMA. (a) High concentration of CoBF (0.1 mg/mL). (b) Low concentration of CoBF (0.05 mg/mL). ....	101
Figure 3.15 The conversion vs. time during the CCTP of MMA calculated from $^1\text{H}$ NMR spectra. (a) High concentration of CoBF (0.1 mg/mL). (b) Low concentration of CoBF (0.05 mg/mL). ....	101
Figure 3.16 CCTP of propargyl methacrylate. ....	102

## Table of Figures

Figure 3.17 The conversion vs. time during the CCTP of PMA calculated from SEC results. ....	102
Figure 3.18 $^1\text{H}$ NMR spectrum of one sample during the CCTP of PMA. ....	103
Figure 3.19 SEC result of the sample taken at $t = 2$ h during the CCTP of PMA... ..	104
Figure 3.20 Synthesis of TMS-PMA. ....	104
Figure 3.21 $^1\text{H}$ NMR spectrum of the crude pale yellow oil in $\text{CDCl}_3$ . ....	105
Figure 3.22 $^1\text{H}$ NMR spectrum of impurities from the process in $\text{CDCl}_3$ . ....	106
Figure 3.23 $^1\text{H}$ NMR spectrum of pure TMS-PMA in $\text{CDCl}_3$ . ....	106
Figure 3.24 Preparation of clickable polymer scaffolds by CCTP of TMS-PMA and deprotection. ....	107
Figure 3.25 CCTP of the monomer TMS-PMA. ....	107
Figure 3.26 $^1\text{H}$ NMR spectrum of TMS-protected polymers in $\text{CDCl}_3$ . ....	108
Figure 3.27 SEC spectra of samples obtained from the CCTP of TMS-PMA. ....	109
Figure 3.28 The changes of molecular weight $M_n$ and polydispersity $\text{PDI}$ with time during the CCTP of TMS-PMA.....	109
Figure 3.29 SEC traces of polymers prepared by CCTP of TMS-PMA.....	111
Figure 3.30 The difference of conversions from $^1\text{H}$ NMR spectra and those from SEC analysis. ....	112
Figure 3.31 The changes of conversions with time in CCTP of TMS-PMA. ....	113
Figure 3.32 Deprotection of polymers prepared by CCTP of TMS-PMA. ....	114
Figure 3.33 $^1\text{H}$ NMR spectrum of polymers after deprotection. ....	114
Figure 3.34 MALDI-TOF spectra of polymers before (left) and after (right) deprotection. ....	115
Figure 3.35 CuAAC click reaction with PEG azide. ....	115
Figure 3.36 Conversion vs. time in CuAAC click reaction with PEG azide. ....	116
Figure 3.37 $^1\text{H}$ NMR spectrum of CuAAC click product with PEG azide. ....	117
Figure 3.38 Thiol-ene click reaction with benzyl mercaptan. ....	117

## Table of Figures

Figure 3.39 Conversion vs. time of the thiol-ene click reaction.....	118
Figure 3.40 $^1\text{H}$ NMR spectrum of the thiol-ene click product in $\text{CDCl}_3$ .....	119
Figure 3.41 MALDI-TOF spectrum of the thiol-ene click product.....	119
Figure 3.42 One-step synthesis of $\beta$ -D-glucopyranosyl azide.....	120
Figure 3.43 The proposed mechanism for the one-step synthesis of sugar azide....	121
Figure 3.44 $^1\text{H}$ NMR spectrum of $\alpha$ -D-mannopyranosyl azide in $\text{D}_2\text{O}$ .....	122
Figure 3.45 $^{13}\text{C}$ NMR spectrum of $\alpha$ -D-mannopyranosyl azide in $\text{D}_2\text{O}$ .....	122
Figure 3.46 FTIR spectrum of $\alpha$ -D-mannopyranosyl azide.....	123
Figure 3.47 Glycosyl azides prepared in the work. ....	123
Figure 3.48 Synthesis of fucose glycopolymers via CuAAC reaction. ....	124
Figure 3.49 $^1\text{H}$ NMR spectrum of fucose glycopolymer in $\text{D}_2\text{O}$ .....	125
Figure 3.50 MALDI-TOF spectrum of fucose glycopolymer. ....	126
Figure 3.51 SEC results of polymers before and after CuAAC reaction.....	126
Figure 3.52 FTIR spectra of polymers before and after CuAAC reaction. ....	127
Figure 4.1 Binding mechanisms of monovalent ligands with receptors.....	142
Figure 4.2 Proposed binding mechanisms of multivalent ligands with receptors. ..	143
Figure 4.3 The strategy used in this study. ....	147
Figure 4.4 The crystallographic structure of concanavalin A (Con A): The four subunits are coloured with cyan, magenta, red, green. The gold and grey spheres represent calcium and manganese cations respectively.....	147
Figure 4.5 Synthesis of glycopolymers by ATRP and CuAAC click reaction. Reagents and conditions: (a) N-(ethyl)-2-pyridylmethanimine/CuBr, toluene, 70 °C; (b) TBAF, acetic acid, THF; (c) $\text{RN}_3$ , CuBr, bipyridine, $\text{Et}_3\text{N}$ .....	148
Figure 4.6 The sigmoidal curves fitted to the data from quantitative precipitation assays using glycopolymers (3 ~ 7) containing pendant mannose or galactose. ....	151

## Table of Figures

Figure 4.7 The sigmoidal curves fitted to the data from quantitative precipitation assays using glycopolymers (8 ~ 10) containing pendant galactose and glucose. .....	152
Figure 4.8 The sigmoidal curves fitted to the data from quantitative precipitation assays using glycopolymers (11 ~ 13) containing pendant mannose and glucose. .....	152
Figure 4.9 The sigmoidal curves fitted to the data from quantitative precipitation assays using glycopolymers (14 ~ 17) containing pendant mannose, galactose and glucose of different ratios. ....	153
Figure 4.10 Quantitative precipitation results. (a) The concentration required for half-maximal precipitation. The error bars represent the standard deviation. (b) The number of Con A units bound per glycopolymer chain. ....	154
Figure 4.11 Plots of Abs <sub>420</sub> vs. time in turbidimetry experiments of glycopolymers (3 ~ 7) containing pendant mannose or galactose. ....	156
Figure 4.12 Plots of Abs <sub>420</sub> vs. time in turbidimetry experiments of glycopolymers (8 ~ 10) containing pendant galactose and glucose. ....	157
Figure 4.13 Plots of Abs <sub>420</sub> vs. time in turbidimetry experiments of glycopolymers (11 ~ 13) containing pendant mannose and glucose. ....	157
Figure 4.14 Plots of Abs <sub>420</sub> vs. time in turbidimetry experiments of glycopolymers (14 ~ 17) containing pendant mannose, galactose and glucose of different ratios. .....	158
Figure 4.15 Results of turbidimetry experiments. (a) The initial rate of the clustering. (b) The time for half-maximum precipitation of Con A. ....	159
Figure 4.16 The absorbance of turbidities at 420 nm in the inhibitory potency experiments of glycopolymers (3 ~ 7) containing pendant mannose or galactose. .....	160
Figure 4.17 The absorbance of turbidities at 420 nm in the inhibitory potency experiments of glycopolymers (8 ~ 10) containing pendant galactose and glucose. ....	161

## Table of Figures

Figure 4.18 The absorbance of turbidities at 420 nm in the inhibitory potency experiments of glycopolymers (11 ~ 13) containing pendant mannose and glucose. ....	161
Figure 4.19 The absorbance of turbidities at 420 nm in the inhibitory potency experiments of glycopolymers (14 ~ 17) containing pendant mannose, galactose and glucose of different ratios. ....	162
Figure 4.20 Results of inhibitory potency assays. (a) The MIC <sub>50</sub> values of $\alpha$ MeMan for all the glycopolymers. (b) The rate of clustering and inhibitory potency for all of the multivalent ligands tested. ....	163
Figure 4.21 Plots of Abs <sub>420</sub> vs. time in the reversal aggregation experiments of glycopolymers (3 ~ 7) containing pendant mannose or galactose. ....	164
Figure 4.22 Plots of Abs <sub>420</sub> vs. time in the reversal aggregation experiments of glycopolymers (8 ~ 10) containing pendant galactose and glucose. ....	165
Figure 4.23 Plots of Abs <sub>420</sub> vs. time in the reversal aggregation experiments of glycopolymers (11 ~ 13) containing pendant mannose and glucose. ....	165
Figure 4.24 Plots of Abs <sub>420</sub> vs. time in the reversal aggregation experiments of glycopolymers (14 ~ 17) containing pendant mannose, galactose and glucose of different ratios. ....	166
Figure 4.25 Results of reversal aggregation assays. (a) The rate of the reverse interaction between the Con A-glycopolymer aggregates and $\alpha$ MeMan. (b) The percent change of the turbidity after 10 min with the addition of $\alpha$ MeMan solution. ....	167
Figure 4.26 Mannose-containing glycopolymers with different chain lengths. ....	169
Figure 4.27 Sigmoidal curves fitted to quantitative precipitation data. ....	169
Figure 4.28 The results of turbidimetry experiments. ....	170
Figure 4.29 The data from inhibitory potency experiments. ....	170
Figure 5.1 Schematic diagram of the self-assembly in this study. ....	180
Figure 5.2 QCM-D plot of Con A on the Au chip surface. (A) HBS buffer; (B) Con A in HBS solution (1 mg/mL). ....	181

## Table of Figures

Figure 5.3 Modification of Au chip surface with MUA, EDC and NHS. ....	182
Figure 5.4 QCM-D plot of Con A on modified Au chip surface. (A) HBS buffer; (B) Con A solution (0.1 mg/mL). ....	183
Figure 5.5 Synthesis of mannose glycopolymer <b>P1</b> . (a) N-(ethyl)-2-pyridylmethanimine/CuBr, toluene, 70 °C. (b) TBAF, acetic acid, THF. (c) mannose azide, CuBr, bipyridine, Et <sub>3</sub> N. ....	184
Figure 5.6 QCM-D plot of the self-assembly of Con A and mannose glycopolymer <b>P1</b> : (A) HBS buffer; (B) Con A in HBS buffer (0.5 mg/mL); (C) ethanolamine HCl in HBS buffer (1M, pH 8.5); (D) <b>P1</b> in HBS buffer (0.5 mg/mL). ....	185
Figure 5.7 Estimated mass and thickness of materials deposited on the modified Au chip over time. ....	185
Figure 5.8 Glycopolymer on a bare gold chip surface. (A) HBS buffer; (B) glycopolymer <b>P1</b> solution. ....	186
Figure 5.9 Synthesis of disulfide mannose glycopolymer <b>P2</b> . (a) N-(ethyl)-2-pyridylmethanimine/CuBr, [M]:[I]:[Cu(I)]:[L] = 141:1:1:2 in toluene, 90 °C (b) TBAF, acetic acid, THF. (c) mannose azide, CuBr, N-(ethyl)-2-pyridylmethanimine, Et <sub>3</sub> N. ....	187
Figure 5.10 Absorption of glycopolymer <b>P2</b> onto the bare gold surface: (A) HBS buffer; (B) <b>P2</b> solution. ....	188
Figure 5.11 QCM-D plot of two self-assembled layers formed by interaction between <b>P2</b> and Con A: (A) HBS buffer; (B) <b>P2</b> in HBS buffer (0.5 mg/mL); (C) Con A in HBS buffer (left: 0.1 mg/mL; right: 0.5 mg/mL). ....	189
Figure 5.12 D-f plot of two layers formed by interaction between <b>P2</b> and Con A. ....	190
Figure 5.13 Schematic diagram of composition of the multilayer surface. ....	191
Figure 5.14 Synthesis of mannose-galactose glycopolymer <b>P3</b> : (a) N-(ethyl)-2-pyridylmethanimine/CuBr, toluene, 70 °C. (b) TBAF, acetic acid, THF. (c) mannose azide, galactose azide, CuBr, bipyridine, Et <sub>3</sub> N. ....	191

## Table of Figures

Figure 5.15 Multilayer assembly of <b>P2</b> , Con A, <b>P3</b> and PNA: (A) HBS buffer; (B) <b>P2</b> in HBS buffer (0.5 mg/mL); (C) Con A in HBS buffer (0.5 mg/mL); (D) <b>P3</b> in HBS buffer (0.5 mg/mL); (E) PNA in HBS buffer (0.5 mg/mL). ....	192
Figure 5.16 D-f plot of the multilayer films assembly.....	193
Figure 5.17 Synthetic glycopolymers employed in QCM-D measurements.....	196
Figure 5.18 The frequency changes with different concentrations of glycopolymer <b>P4</b> .....	198
Figure 5.19 The frequency shift over time for glycopolymer <b>P4</b> of different concentrations. ....	201
Figure 5.20 D-f plots of the interactions of Con A with glycopolymer <b>P4</b> of different concentration.....	202
Figure 5.21 The frequency changes with different concentrations of glycopolymer <b>P5</b> .....	203
Figure 5.22 The frequency shift over time for glycopolymer <b>P5</b> of different concentrations. ....	204
Figure 5.23 D-f plots of the interactions of Con A with glycopolymer <b>P5</b> of different concentration.....	205
Figure 5.24 The frequency changes with different concentrations of glycopolymer <b>P6</b> .....	206
Figure 5.25 The frequency shift over time for glycopolymer <b>P6</b> of different concentrations. ....	206
Figure 5.26 D-f plots of the interactions of Con A with glycopolymer <b>P6</b> of different concentration.....	207
Figure 5.27 The frequency changes with different concentrations of glycopolymer <b>P1</b> .....	208
Figure 5.28 The frequency shift over time for glycopolymer <b>P1</b> of different concentrations. ....	208
Figure 5.29 D-f plots of the interactions of Con A with glycopolymer <b>P1</b> of different concentrations. ....	209

## Table of Figures

Figure 5.30 The frequency changes for different concentrations of glycopolymers. .....	210
Figure 5.31 The changes of energy dissipation for different concentrations of glycopolymers.....	211
Figure 5.32 Schematic diagrams of the glycopolymer layer on gold chip surface..	212
Figure 5.33 The structure of lectin DC-SIGN from Wikipedia.....	213
Figure 5.34 Fucose-containing glycopolymers employed in the interactions with DC-SIGN. ....	214
Figure 5.35 The binding of DC-SIGN to the modified gold surface comparing with Con A.....	215
Figure 5.36 QCM-D plot of the interaction of DC-SIGN with mannose glycopolymer <b>P4</b> : (A) buffer; (B) DC-SIGN solution (0.1 mg/mL); (C) the solution of ethanolamine HCl (1M, pH 8.5); (D) the solution of glycopolymer <b>P4</b> (0.5 mg/mL). ....	216
Figure 5.37 Regeneration of the lectin surface: (A) buffer; (B) glycopolymer <b>P4</b> solution (0.5 mg/mL); (C) 10 mM glycine hydrochloride, pH 2.5.....	217
Figure 5.38 The changes of frequency and energy dissipation for all the glycopolymers (0.5 mg/mL) binding with DC-SIGN (* The concentration was 2.0 mg/mL). ....	218
Figure 5.39 The routine for a SPR measurement of the interaction between DC-SIGN and gp120: (A) the mixture of 0.4 M EDC and 0.1M NHS (1:1, v/v); (B) the solution of DC-SIGN (50 $\mu$ M) in acetate buffer (pH = 5.0); (C) the solution of ethanolamine HCl (1M, pH 8.5); (D) HBS buffer solutions of gp120 with different concentrations (0.31 nM ~ 10.0 nM); (E) 10 mM glycine hydrochloride, pH 2.5. ....	220
Figure 5.40 The linear dependency of the inverse of relaxation time on concentration of gp120. ....	221
Figure 5.41 The resonance responses for the binding of glycopolymer <b>P5</b> and <b>P1</b> to the lectin (a) Con A and (b) DC-SIGN, respectively.....	222
Figure 5.42 Glycopolymers used in SPR kinetic measurements. ....	223



## Table of Figures

---

Figure 5.43 SPR sensorgrams by binding of glycopolymers to immobilised DC-SIGN with different concentrations. ....	224
--	-----

## Table of Tables

Table 1.1 Direct polymerisation of glycomonomers. ....	13
Table 1.2 Post-functionalisation of precursor polymers. ....	18
Table 2.1 Examples of lectins and their binding carbohydrates. ....	46
Table 2.2 Studies of the lectin-carbohydrate interactions by traditional methods. ....	54
Table 2.3 QCM-D measurements of the lectin-carbohydrate interactions. ....	62
Table 2.4 Investigations of lectin-carbohydrate interactions based on SPR approach. .....	67
Table 3.1 C <sub>s</sub> Values of CCTP at 60 °C using CoBF as the chain transfer agent. ....	89
Table 3.2 Determination of the chain transfer constant in CCTP of MMA. ....	97
Table 3.3 Polymers of different M <sub>n</sub> and PDI obtained by CCTP of TMS-PMA. ....	110
Table 3.4 The glycopolymer prepared by CuAAC. ....	128
Table 4.1 Glycopolymers synthesised in this study. ....	150
Table 4.2 The results from four different assays. ....	171
Table 5.1 Estimated mass by two different immobilisation methods using the same concentration (T: 25 °C; pH: 7.4; flow rate: 50 µL/min; concentration: 0.5 mg/mL). ....	194
Table 5.2 The association constants of different mannose glycopolymers. ....	211
Table 5.3 Kinetic parameters of the interactions between different glycopolymers and DC-SIGN. ....	225

## Abbreviations

AIBN	Azobisisobutyronitrile
ATR	Attenuated total reflection
AHL	Alligator hepatic lectin
ATRP	Atom transfer radical polymerisation
BA	Butyl acrylate
BLG-NCA	$\gamma$ -Benzyl-L-glutamate <i>N</i> -carboxyanhydride
BPEA	2-(2-Bromopropionyloxy)ethyl acrylate
Bipy	2,2'-Bipyridine
BMA	<i>n</i> -Butyl methacrylate
BA	<i>n</i> -Butyl acrylate
BSA	Bovine serum albumin
CCTP	Catalytic chain transfer polymerisation
CDs	Cyclodextrins
$\beta$ CD	$\beta$ -cyclodextrin
CS	Chondroitin sulfate
Con A	Concanavalin A
CHL	Chicken hepatic lectin
CD-MPR	Cation-dependent mannose 6-phosphate receptor
CRD	Carbohydrate recognition domain
CRP	Controlled radical polymerisation
CLD	Chain length distribution
CTA	Chain transfer agent
CuAAC	Cu(I)-catalysed azide-alkyne cycloaddition

## Abbreviations

---

DP	Degree of polymerisation
DCM	Dichloromethane
CoBF	Bis(boron difluorodimethylglyoximate) cobalt(II)
DMPP	Dimethylphenylphosphine
DEGMA	Diethylene glycol methacrylate
DMC	2-Chloro-1,3-dimethylimidazolidinium chloride
DMI	1,3-Dimethyl-2-imidazolidinone
DIPEA	Diisopropylethylamine
DMF	Dimethyl formamide
DMSO	Dimethyl sulfoxide
DRI	Differential refractive index
DEGDVE	Di(ethylene glycol) divinylether
DC-SIGN	Dendritic cell specific ICAM-3 grabbing nonintegrin
ELLA	Enzyme-linked linked assay
ELISA	Enzyme-linked immunosorbent assay
EDC	1-[3-(Dimethylamino)propyl]-3-ethyl carbodiimide
FITC-ConA	Fluorescein isothiocyanate-conjugated concanavalin A
ECA	<i>Erythrina cristagalli</i>
ECL	<i>Erythrina cristagalli</i> lectin
EMA	Ethyl methacrylate
ESI-MS	Electrospray ionisation mass spectrometry
FRP	Free radical polymerisation
FT-IR	Fourier-transform infrared
FTA	Fluorescence titration assay
FRET	Fluorescence resonance energy transfer

## Abbreviations

---

GPC	Gel permeation chromatography
GAMA	D-gluconamidoethyl methacrylate
GalNAc	<i>N</i> -Acetylgalactosamine
GOx	Glucose oxidase
Gal	Galactose
Glc	Glucose
GlcNAc	<i>N</i> -Acetylglucosamine
HEMA	2-Hydroxyethyl methacrylate
HIA	Hemagglutination inhibition assay
HPA	<i>Helix pomatia</i> agglutinin
HPG	Hyperbranched polyglycerols
HRP	Horseradish peroxidase
IGF-II/CI-MPR	Insulin-like growth factor II/cation-independent mannose 6-phosphate receptor
ITC	Isothermal titration microcalorimetry
iCVD	Initiated chemical vapour deposition
LBL	Layer-by-layer
LCA	<i>Lens culinaris</i> agglutinin
LCST	Lower critical solution temperature
MUA	11-Mercaptoundecanoic acid
MA	Methyl acrylate
MAA	Methacrylic acid
Man	Mannose
MHL	Mammalian hepatic lectin
MBL	Mannose-binding lectin

## Abbreviations

---

MALDI-TOF	Matrix assisted laser desorption ionisation - time of flight
MS	mass spectrometry
$M_n$	Number average molecular weight
$M_w$	Weight average molecular weight
MMA	Methyl methacrylate
MA	Methyl acrylate
MEK	Methyl ethyl ketone
$\alpha$ MeMan	Methyl- $\alpha$ -D-mannopyranoside
MIC <sub>50</sub>	Minimum inhibitory concentration for half-maximum precipitation
NHS	<i>N</i> -Hydroxysuccinimide
NIPAAm	<i>N</i> -Isopropyl acrylamide
NPs	Nanoparticles
NMP	Nitroxide mediated polymerisation
NMR	Nuclear magnetic resonance
PA	<i>Pseudomonas aeruginosa</i>
PDVB	Poly(divinylbenzene)
PDI	Polydispersity index
PCL	Poly( $\epsilon$ -caprolactone)
PGAMA	Poly(D-gluconamidoethyl methacrylate)
PAMAM	Poly(amido amine)
PGA	Poly(L-glutamic acid)
PEG	Poly(ethylene glycol)
PEGMA <sub>1100</sub>	Poly(ethylene glycol) methyl ether methacrylate, average molecular weight 1100 g mol <sup>-1</sup>
PEO	Poly(ethylene oxide)

---

## Abbreviations

---

PDS	Pyridyl disulfide
PS	Polystyrene
PNA	Peanut agglutinin
PPO	Poly(propylene oxide)
PMA	Propargyl methacrylate
pNIPAAm	Poly(N-isopropylacrylamide)
ppm	Parts per million
QPA	Quantitative precipitation assay
QCM	Quartz crystal microbalance
QCM-D	Quartz crystal microbalance biosensor with dissipation monitoring
RAFT	Reversible addition fragmentation chain transfer
ROMP	Ring-opening metathesis polymerisation
ROP	Ring-opening polymerisation
siRNA	Short interfering RNA
SET-LRP	Single electron transfer living radical polymerisation
SAMs	Self-assembled monolayers
SPR	Surface plasmon resonance
SBA	Solid-phase binding assay
STY	Styrene
SEC	Size Exclusion Chromatography
TEA	Triethylamine
TBTA	Tris(benzyltriazolyl)methyl amine
TMS-PMA	TMS-protected propargyl methacrylate
THF	Tetrahydrofuran

## Abbreviations

---

TBAF	Tetrabutylammonium fluoride
TMS	Tetramethylsilane
UEA	Ulex europaeus agglutinin
UV-VIS	Ultra violet-visible
VBC	Vinyl benzyl chloride
WGA	Wheat germ agglutinin



## Acknowledgments

First of all, I would like to thank my academic supervisor Professor David Haddleton. He is one of the greatest supervisor and the nicest person I have ever met. I am really appreciated to his continuous support, encouragement and advice for my work. I feel really lucky to do my Ph.D. project under the supervision of him.

A huge thank you will be given to my former supervisor Professor Xiaodong Li for encouraging me to study abroad. I am so grateful for the hospitality of his family to invite me to spend the Spring Festival in 2009 with them.

I would like to thank the China Scholarship Council (CSC) and Warwick University for funding. Many thanks go to the National University of Defense Technology for the permission to let me study abroad.

I would like to thank all members of the group past and present to make my life in UK to be just like at home. Stacy Slavin, my best friend. She is an angel to me. With so much help and fun from her, I feel very happy to study here. Moreover, a lot of thanks will go to James Burns for his English teaching, Dr. Mathew Jones for being my 'second best friend' (He want it to be 'the best friend' which I've already given to Stacy☺), Dr. Jay Syrett for a lot of fun in our office, Dr. Remzi Becer and Dr. Mathew Gibson for very helpful discussion, Jasmine Menzel for sharing the room with me during the conferences, Dr. Anthony Grice for helping me with GPC stuff, Guangzhao Li for showing me around at the beginning of my study, Kayleigh McEwan and Georgina Rayner for having a successful conference in America and Rajan Randev for general help. Additional thanks go to Dr. Jin Geng, Dr. Lijiang Song, Dr. Zoe Lethbridge, Dr. Anne de Cuendias, Dr. Tomasz Kreft, Dr. Nicole

## Acknowledgements

---

Jagielski, Dr. Julien Rosselgong, Dr. Florence Gayet, Dr. Paul Wilson, Chris Summers, Zaidong Li, Qiang Zhang, Jamie Godfrey, Muxiu Li, Athina Anastasaki and Chris Waldron. Thank them all deeply for sharing the precious and happy three years with me. They will always be my friends of life no matter where they are.

Many thanks should go to my housemates past and present, Lingling Song, Xi Cheng, Zijin Li, Jia Zhou, Yao Zhao, Qiang Zhang, Fan Yang and also my friend Dr. Jing Liu, Jingjing Qian for the wonderful time and delicious food sharing with me.

I wish to thank very much my friends in China, Lin Liu, Dafang Zhao, Gongyi Li, Haizhe Wang, Qingling Fang, Tianjiao Hu, Molin Qing, Jun Ma, Wenjin Pu for supporting me. A lot of thanks will be given to my friend Jianxia Liu, Juan Liu, Ning Zhao, Yanyan Wei, Shengchun Huang, Lingfang Zhang and Fangjun Yin for always helping me when I need it. My life is worth to be more appreciated because of you guys being my friends.

Special thanks to Shuyong Zhu for loving me and encouraging me over these three years. I am grateful for everything he has done for me.

Finally, I would like to thank my parents and relatives for their encouragements and supports. Grandpa, Mum, Dad and younger brother Yanling Gou, I love you forever. Thank all my uncles, aunties, cousins for general help in daily life and for making a sweet big family.

## **Declaration**

Experimental work contained in this thesis is original research carried out by the author, unless otherwise stated, in the Department of Chemistry at the University of Warwick, between January 2009 and November 2011. No Material contained herein has been submitted for any other degree, or at any other institution.

Results from other authors are referenced in the usual manner throughout the text.

Date:

---

**Yanzi Gou**

## Abstract

Saccharides act important roles in many biological processes as recognition molecules, signalling molecules and adhesion molecules. However, due to the complexity and diversity of oligosaccharides the direct synthetic approaches cannot fully meet the demands for all of the pure and well-defined oligosaccharides being studied in glycobiology. The efficient synthesis of glycomimetics, glycopolymers, offers an attractive route to solve this problem. Thus, the synthesis and application of glycopolymers of various architectures has been extensively investigated. Meanwhile, In order to explore the mechanism of the lectin-carbohydrate interactions and to get a better understanding of the structure-function relationship of oligosaccharides, the assays employed in studies of lectin-carbohydrate interactions become much more sophisticated and accurate with fast development of various analytical approaches.

In this work, well-defined glycopolymers were prepared by the combination of CCTP and CuAAC click reactions. Alkyne-containing polymer scaffolds were synthesised by CCTP, followed by post-modification of the *clickable* polymer scaffolds with sugar azides. Moreover, a library of well-defined synthetic glycopolymers featuring the same macromolecular properties (architecture, polydispersity, valency, polarity, *etc.*) with difference only in the densities of different sugars (mannose, galactose and glucose) were employed to investigate the influence of different pendant epitopes on the interactions with a model lectin Con A by the traditional methods. Additionally, two powerful modern detection techniques

QCM-D and SPR were also exploited to investigate the interactions of the lectin Con A, PNA, or DC-SIGN with a series of different glycopolymers.

The diversities of binding properties contributed by different clustering parameters can make it possible to define the structures of the multivalent ligands and densities of binding epitopes for specific functions in the lectin-carbohydrate interactions. These conclusions can be employed as the springboard to develop new glycopolymeric drugs and therapeutic agents and to assess the mechanisms by which they work.

# **Chapter 1.**

## **From Glycobiology to Glycopolymers**

## 1.1 Chemical glycobiology

Glycobiology, a term coined in 1988 by biochemist Raymond Dwek,<sup>1</sup> is the branch of biology that deals with the role of saccharides in biological events.<sup>2</sup> Saccharides are one of the four major classes of organic molecules in living systems along with proteins, lipids, nucleic acids and exist on the surface of nearly every cell in the form of oligosaccharides, polysaccharides, glycolipids, glycoproteins or other glycoconjugates.<sup>3</sup> Although being a source of energy and an integral part of cellular structure for a long time, it has been widely acknowledged that they also act important roles in many biological processes, including inflammation,<sup>4</sup> immune response,<sup>5</sup> signal transmission,<sup>6</sup> disease development,<sup>7</sup> metastasis and intracellular localisation.<sup>8-10</sup>

The complex heterogeneity of oligosaccharides, such as different types and numbers of sugar residues, the multiple glycosidic linkages and various branching structures,<sup>11-12</sup> enable them to encode information to act as recognition molecules, signalling molecules and adhesion molecules.<sup>13-15</sup> However, it is this structural complexity and diversity of the saccharides that frustrates the efforts of scientists to explore the relationship between their structures and functions. For example, nine monosaccharides that commonly found in human can produce more than 15 million possible tetrasaccharides depending on how they are linked together.<sup>16</sup>

## 1.2 Direct synthesis of oligosaccharides

Although oligosaccharide functions are now being illustrated in molecular detail, advances in glycobiology are relatively very slow compared with the pace of other

parts of biochemistry.<sup>17</sup> In a general process, a mixture of carbohydrate groups are released from the relative glycans in a cell by chemical or enzymatic treatment. Then sequential separation of individual saccharides and structural analysis enables the duplication of the structures artificially to produce various carbohydrate-based materials.<sup>18</sup> Despite huge progress in analytical techniques, detailed information on the structure and function of each carbohydrate moiety and determination of their sequences in a specific glycan are still difficult to obtain, especially if the glycan is present in low concentration in cells.<sup>16</sup>

Interdisciplinary studies have been employed in glycobiology to synthesise and analyse carbohydrates which have involved methods from genetics, biochemistry, organic chemistry, analytical chemistry and cell biology.<sup>19</sup> They are very essential in providing oligosaccharides for establishment of the structural features for relative functions, elucidation of their interactions with lectins and production of carbohydrate-based therapeutic agents. With improvement in techniques to change the traditional laborious work, two general strategies are commonly used for the synthesis of oligosaccharides *in vitro*: chemical synthesis<sup>20-26</sup> and enzymatic synthesis<sup>27-32</sup>.

### 1.2.1 Chemical synthesis

Chemical synthesis includes solid-phase and one-pot synthesis. Since the successful construction of oligosaccharides on a polymer support in 1971 by Frechet and co-workers,<sup>33</sup> solid-phase synthesis of oligosaccharide has been developed dramatically. Seeberger and coworkers re-engineered an existing apparatus used in automated



peptide synthesis to a solid-phase synthesiser for the automation of oligosaccharide synthesis,<sup>34</sup> **Figure 1.1**.

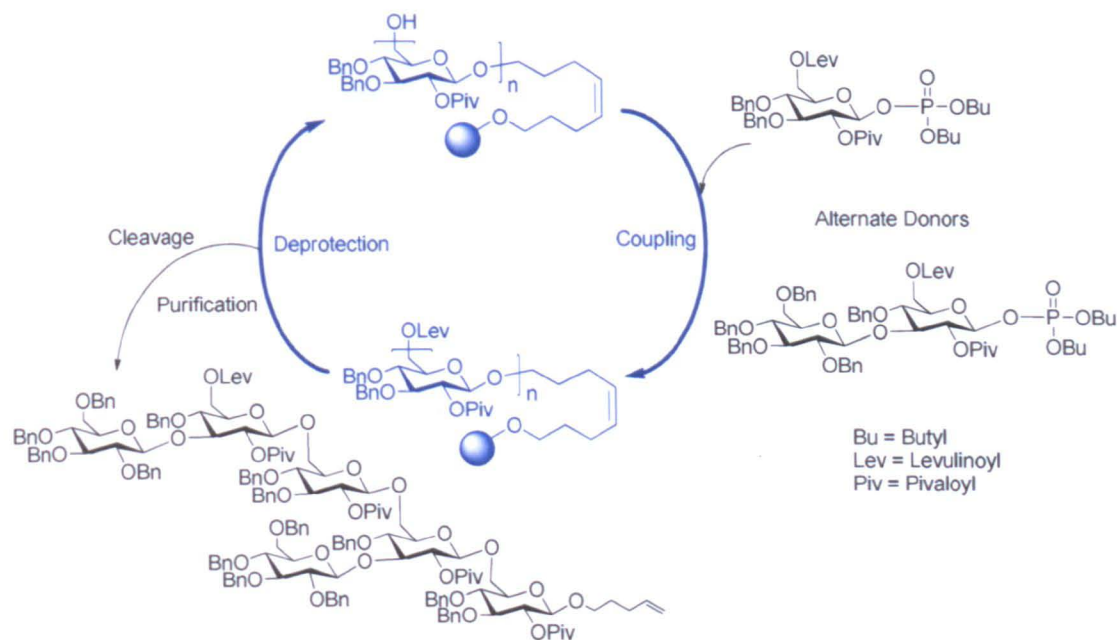


*Figure 1.1 Automated solid-phase synthesis of oligosaccharides. Ref. 34.*

Linear and branched oligosaccharides were synthesised with high yield within several cycles under controlled temperature, **Figure 1.2**. While cutting down the multiple purification and separation steps in carbohydrate synthesis, there are still several problems in this methods to be addressed, including the availability of excess building blocks, the incorporation of certain monosaccharides such as sialic acid and the cleavage of the linker to the resin.<sup>35</sup>

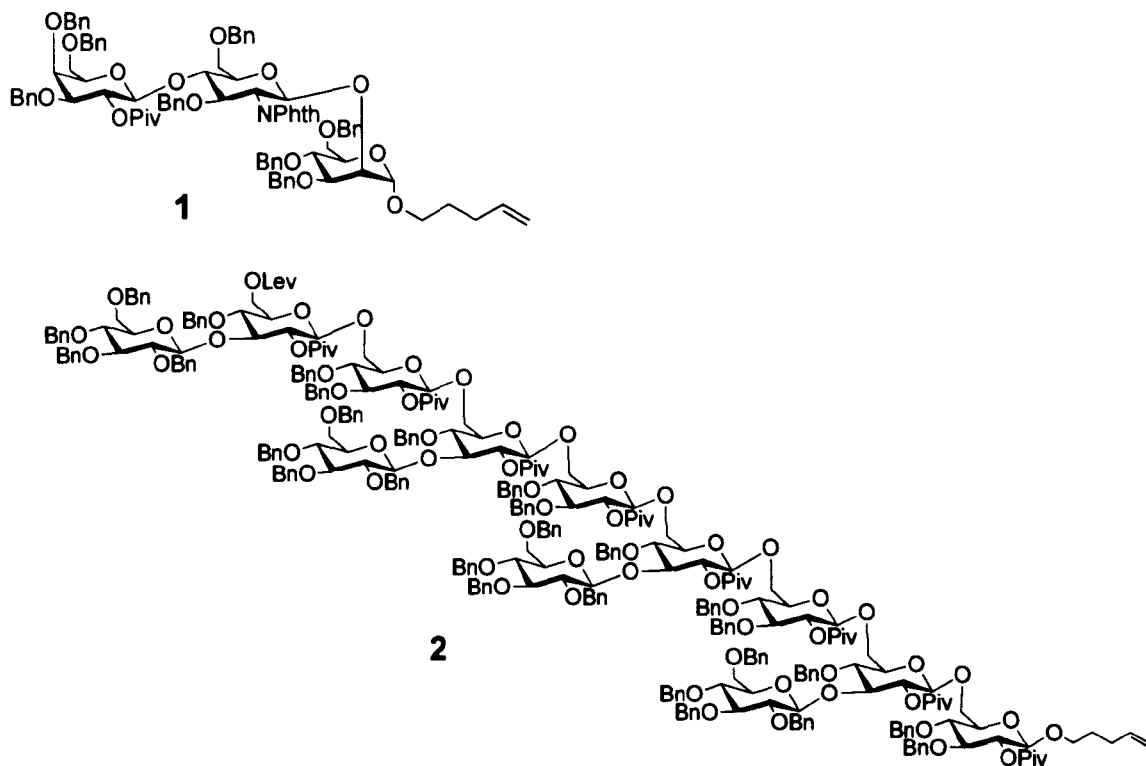


Figure 1.2 Examples of oligosaccharides synthesised by a solid-phase synthesiser. Ref. 34.

A further chemical approach to oligosaccharides is the one-pot synthesis. Since its proposal by Kahne *etc* in 1993<sup>36</sup>, numerous efforts have been dedicated into this area, which has resulted in the appearance of the programmable one-pot synthesis,<sup>37-38</sup> **Figure 1.3.** A desired oligosaccharide could be synthesised by adding sequentially from most reactive substrates to least reactive substrates into a single reaction vessel which was controlled by a computer program, OptiMer. Globo H hexasaccharide, a cancer antigen, was prepared under control of OptiMer.<sup>39</sup> The different reactivities of various protected sugars are dependent on the protecting groups and the anomeric activating groups. It is essential to expand the repertoire of building blocks of different reactivity which can be applied in the programmable one-pot synthesis.

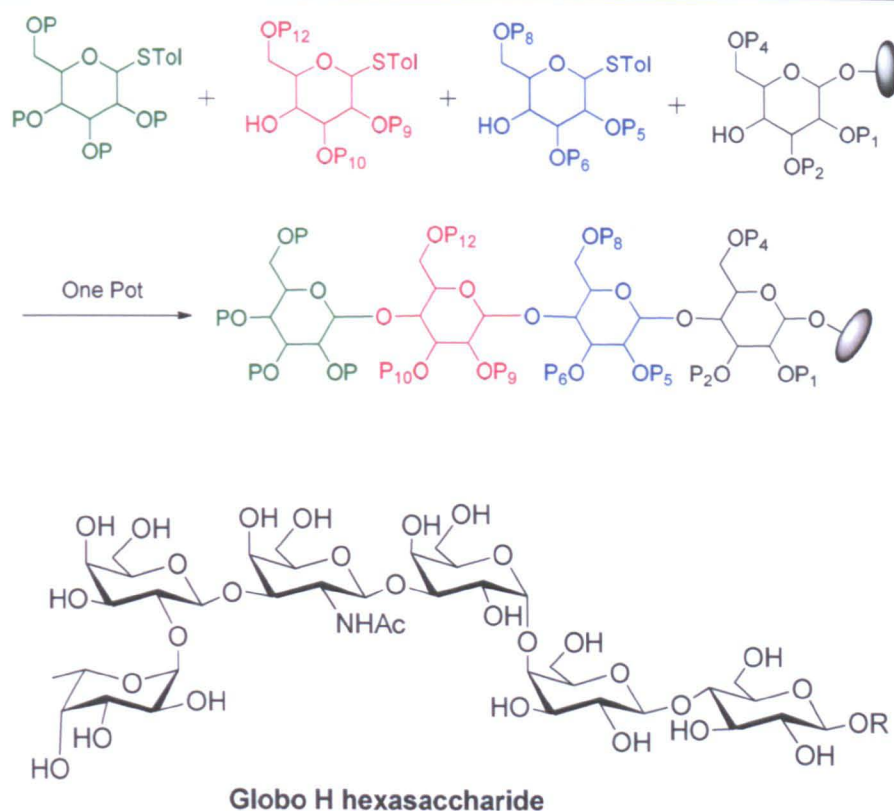


Figure 1.3 OptiMer's programmed one-pot synthesis. Ref. 43.

### 1.2.2 Enzymatic synthesis

In enzymatic synthesis, including chemoenzymatic synthesis, several enzymes are used to elaborate the saccharide intermediates to generate oligosaccharides. These enzymes are usually the glycosyltransferases, which are used naturally to synthesise saccharides, and glycosidases, which are normally used to hydrolyse glycosidic bonds. With good control of the stereoselectivity, anomeric configuration and regioselectivity under mild reaction conditions, protection and deprotection steps are not always necessary in enzymatic synthesis. A solution of enzymatic catalyst can be passed through the solid phase which the growing saccharides are attached to.<sup>40-41</sup> The enzymes can also be immobilised in columns with the growing saccharides dissolved in the water soluble solution phase,<sup>42</sup> **Figure 1.4.**

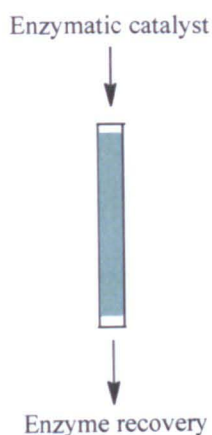
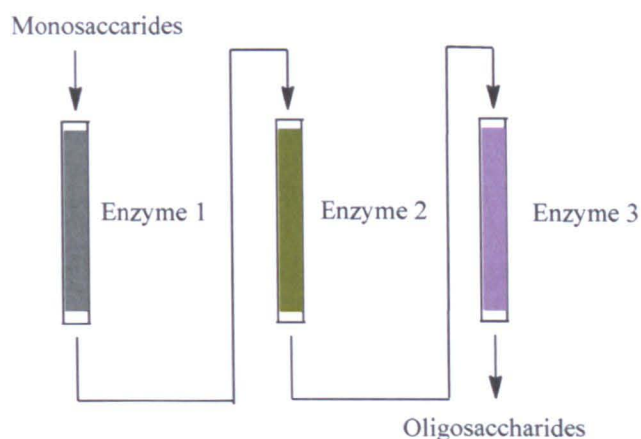
**(a) Immobilised substrate:****(b) Immobilised enzymes:**

Figure 1.4 Enzymatic synthesis of oligosaccharides. Ref. 43.

However, the enzymatic approach is limited by the availability and the cost of enzyme catalysts needed to synthesise all of the oligosaccharides researchers may be interested in. In addition, recovery of the enzymes is often required. A further drawback is that for synthesis of novel oligosaccharides with unnatural sugars most enzymes are not usually as efficient as in the catalysis of the synthesis of natural products.<sup>43</sup> Thus it is still necessary to explore other enzyme catalysts with high activity.

Chemical synthesis and enzymatic approaches are very complementary. Enzymes can be used for the synthesis of oligosaccharides very efficiently with absolute regio- and stereo-control. In contrast, chemical synthesis can be very flexible. Natural and non-natural saccharide building blocks can be assembled with natural or non-natural linkages to generate a large range of oligosaccharides and glycoconjugates.<sup>17</sup> However, due to the complexity and diversity of oligosaccharides these direct

synthetic approaches cannot fully meet the demands for all of the pure and well-defined oligosaccharides being studied in glycobiology.<sup>44</sup>

### 1.3 Synthesis of glycopolymers

The development of glycobiology can be hindered by the limited access to oligosaccharides using direct synthetic approaches. The efficient synthesis of glycomimetics offers an attractive route to solve this problem. Glycopolymers, as synthetic carbohydrate polymers, can often interact with lectins in a similar way to natural oligosaccharides. In order to get a better understanding of the structure-function relationship of oligosaccharides and to mimic, or even exceed, the properties of oligosaccharides in some specific applications, glycopolymers of various architectures have been synthesised and investigated in recent years since the precipitation of lectins using copolymers of acrylamide and allyl glycosides by Hořejší *et al.*<sup>45</sup> The synthesis of glycopolymers has been reviewed many times in recent years based on the developed synthetic techniques.<sup>46-53</sup> However, the reviews on the basis of various glycopolymer architectures are very few.<sup>54-55</sup> The architecture of glycopolymers is vital to their application as the factors such as orientation of recognition element, scaffold shape, flexibility, size and valency can influence biological activity of the glycopolymers and mechanism of their interactions with lectins.<sup>56</sup> Herein, we report recent developments in the synthesis of glycopolymers with a variety of architectures.

### 1.3.1 Linear glycopolymers

Linear architecture is the most commonly used structure of glycopolymers of different properties in many applications. Controlled polymerisation techniques such as nitroxide-mediated polymerisation (NMP), atom transfer radical polymerisation (ATRP), reversible addition-fragmentation chain transfer (RAFT) polymerisation and ring-opening metathesis polymerisation (ROMP) together with click chemistry have been widely employed in the synthesis of glycopolymers. The synthesis of polysaccharide-containing block copolymers has been summarised by Lecommandoux and Schatz,<sup>57</sup> so here we mainly focus on the preparation of oligosaccharide-containing glycopolymers.

Linear glycopolymers of targeted molecular weights and polydispersities can be prepared directly from the controlled polymerisation of glycomonomers. Glycomimetics of natural polysaccharides, chondroitin sulfate (CS) glycosaminoglycans, were generated by Hsieh-Wilson and co-workers using ROMP of fully protected, sulphated glycomonomers,<sup>58</sup> **Figure 1.5**. A series of protected glycopolymers with controllable molecular weights ( $DP = 25 \sim 80$ ) were obtained from synthetic disaccharide and tetrasaccharide monomers (**1**, **2** and **3**) with relatively narrow polydispersities (1.24  $\sim$  1.63). The desired glycopolymers (**4**, **5** and **6**) were prepared by the following desilylation and sequential LiOOH-NaOH treatment. The potencies of the sulphated glycopolymers to inhibit neuronal growth were comparable to those of natural CS polysaccharides, which showed dependency on the valency of the corresponding polymers.

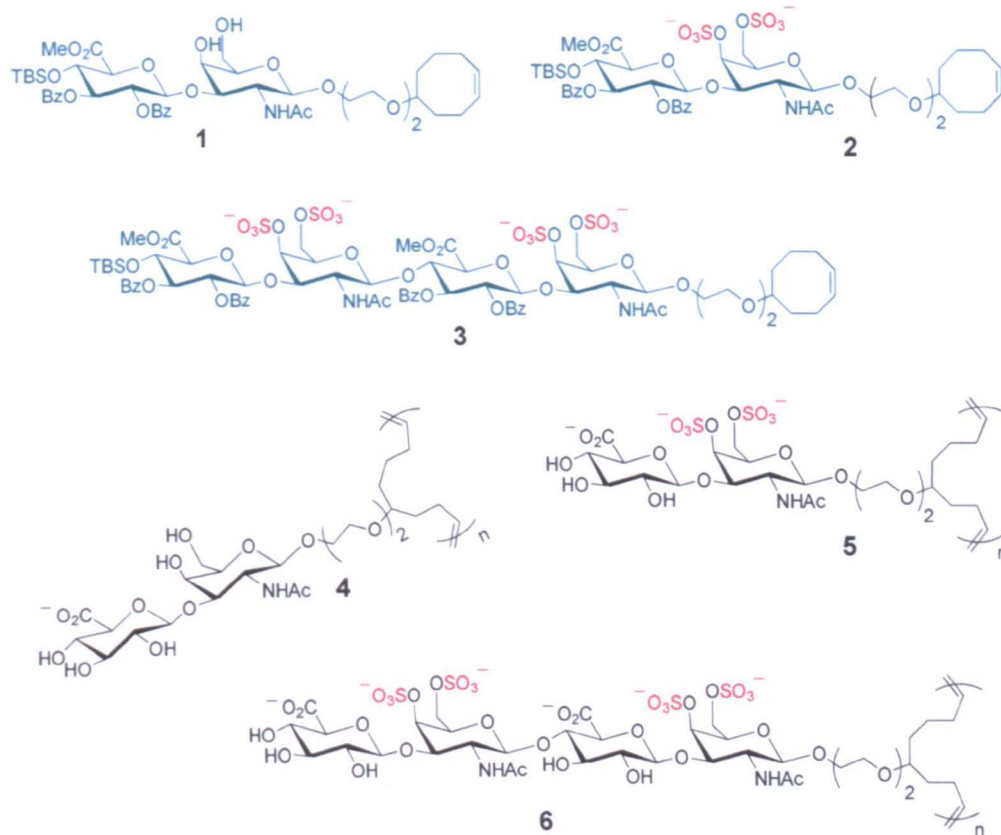


Figure 1.5 Glycomonomers and the resulting glycopolymers as glycomimetics of natural polysaccharides, chondroitin sulfate (CS) glycosaminoglycans. Ref. 58.

Xu *et al.* exploited ATRP to synthesise the linear block glycopolymer PS-*b*-PAcGEMA, linear random glycopolymer PS-*r*-PAcGEMA, and comb-like glycopolymer PS-*b*-(PHEMA-*g*-PAcGEMA),<sup>59</sup> **Figure 1.6.**



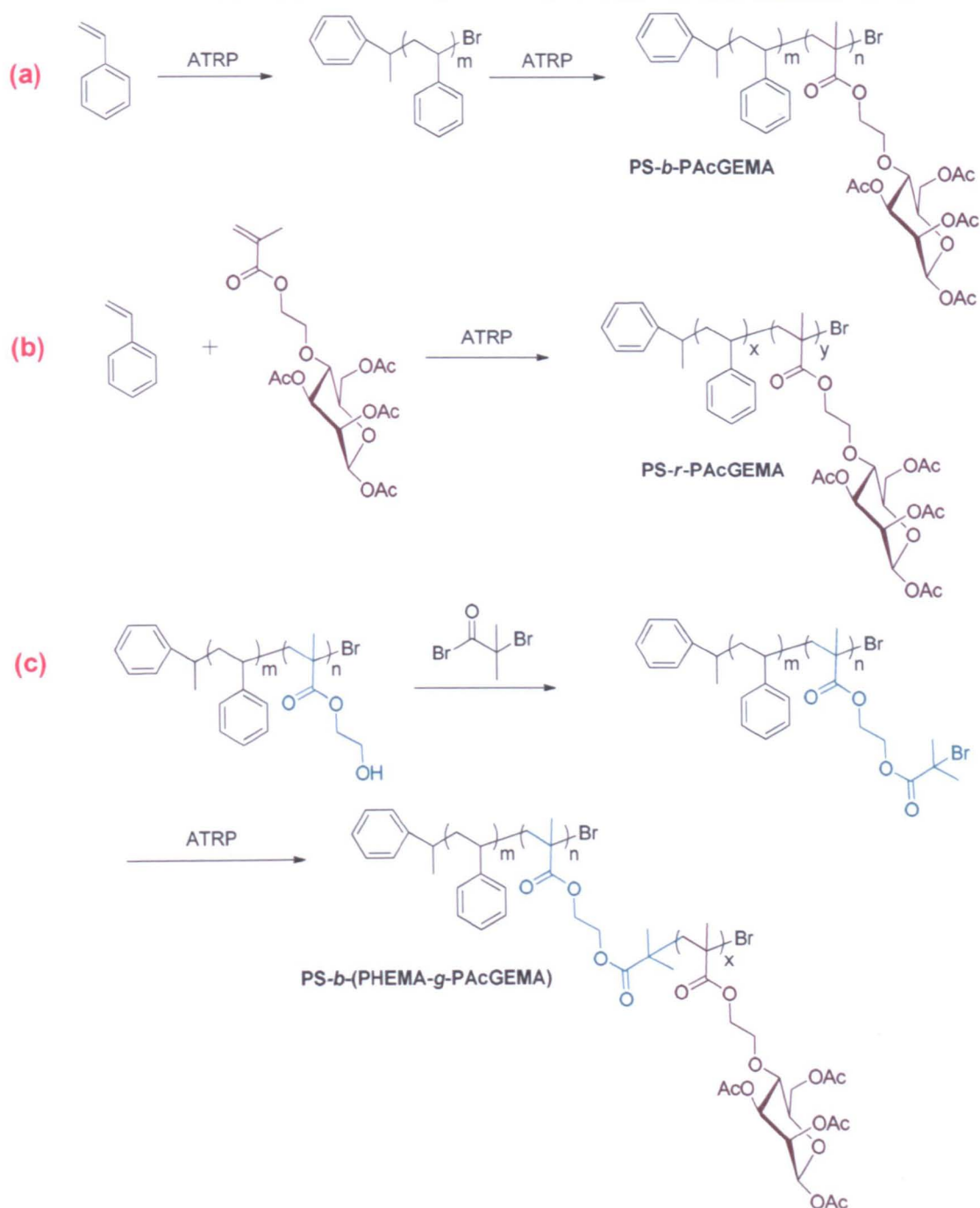


Figure 1.6 Synthesis of (a) linear block glycopolymer PS-b-PAcGEMA, (b) linear random glycopolymer PS-r-PAcGEMA, and (c) comb-like glycopolymer PS-b-(PHEMA-g-PAcGEMA). From ref. 59.

Glycopolymers have also been synthesised by the post-functionalisation of precursor polymers. Bertozzi and co-workers<sup>60</sup> synthesised dual-end-functionalised glycopolymers as mucin mimics for microarray applications. The attachment of



maleimide-conjugated Texas Red fluorophore and alkyne groups to the glycopolymers containing *N*-acetylgalactosamine (GalNAc) moieties made them suitable for application of the microcontact printing, **Figure 1.7**. The specific binding of the printed glycopolymers with *Helix pomatia* agglutinin (HPA), a lectin that recognises  $\alpha$ -GalNAc, was tested using fluorescence microscopy.

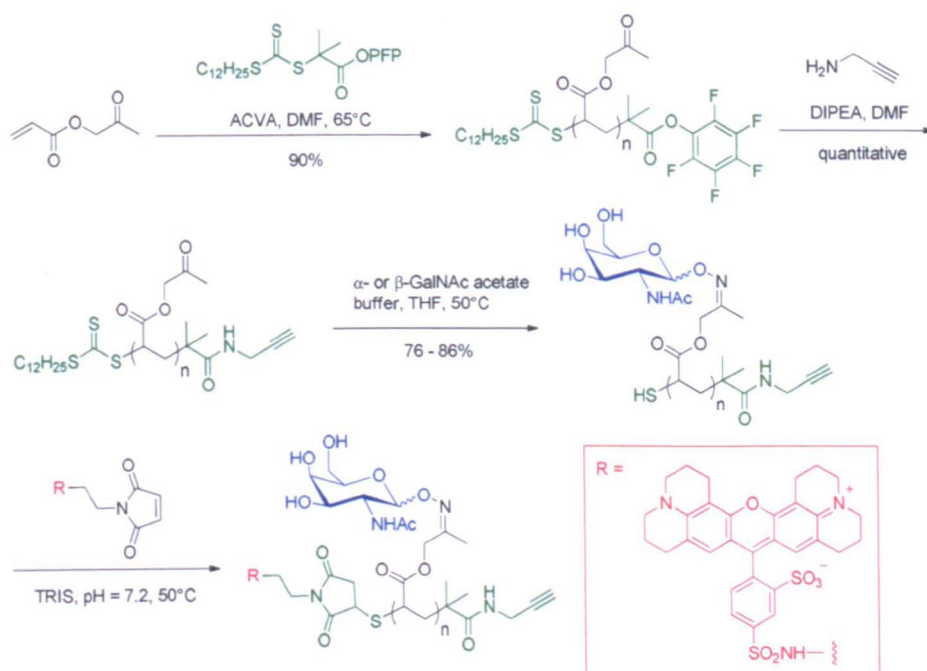


Figure 1.7 Preparation of dual-end-functionalised glycopolymers as mucin mimics. Ref. 60.

Both ATRP and catalytic chain transfer polymerisation (CCTP) have been employed by Haddleton *et al.* to prepare glycopolymers with different pendant sugars,<sup>61–64</sup> and to synthesise glycopolymers in a double click route,<sup>65–66</sup> **Figure 1.8**. The interactions of the resulting glycopolymers of different chain lengths with lectin Con A and human DC-SIGN were investigated by quantitative precipitation and turbidity assays,<sup>67</sup> QCM-D<sup>68</sup> and SPR<sup>69</sup> respectively.

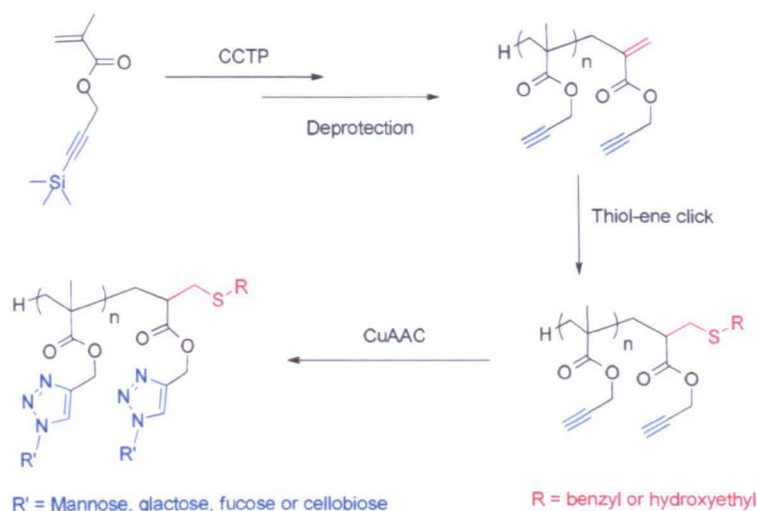
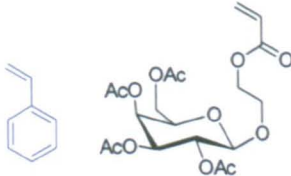
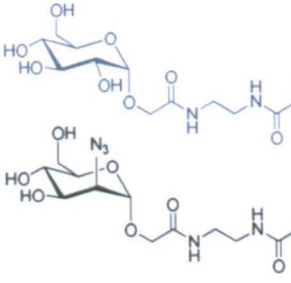
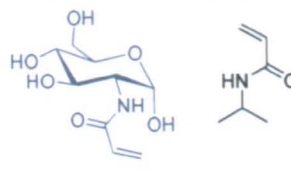
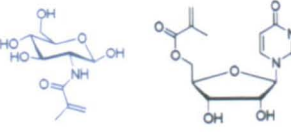
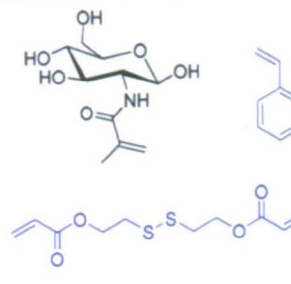
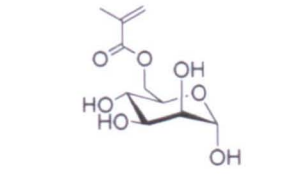
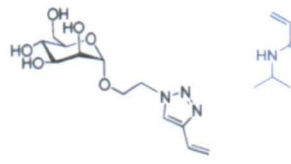


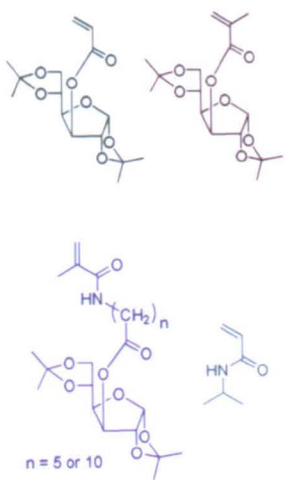
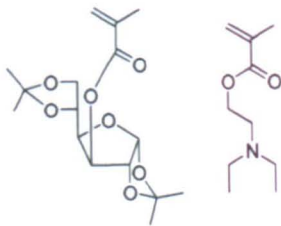
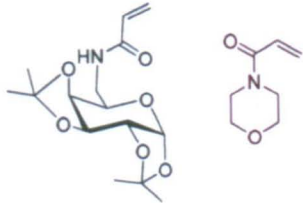
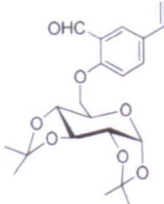
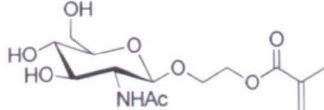
Figure 1.8 Synthesis of glycopolymers by CCTP and double click reactions. Ref. 65.

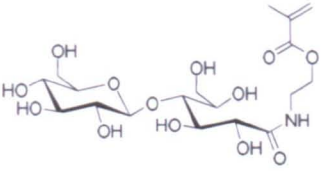
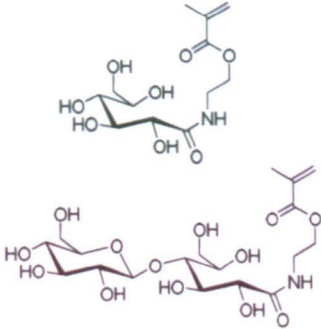
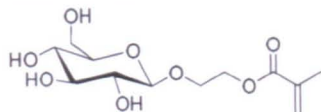
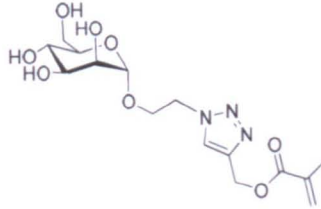
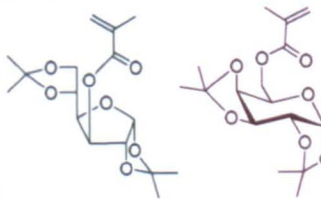
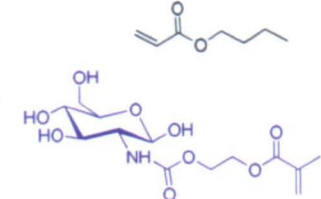
According to the different synthetic approaches, a range of linear glycopolymers have been summarised in **Table 1.1** and **Table 1.2**.

Table 1.1 Direct polymerisation of glycomonomers.

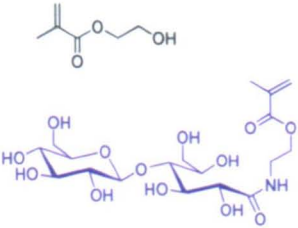
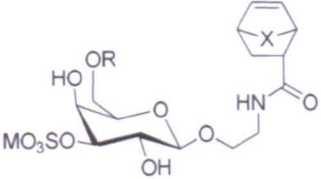
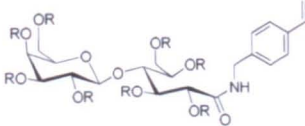
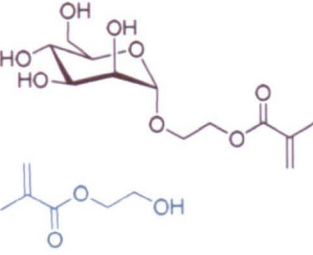
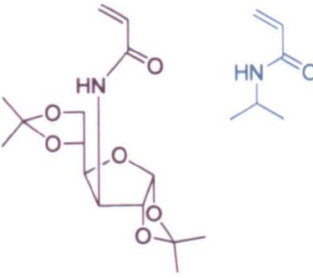
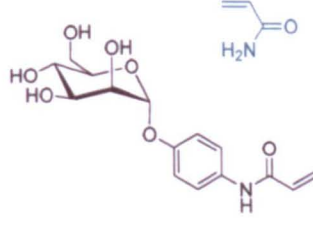
Monomer	Technique	Properties	Ref.
	RAFT	Diblock glycopolymer with different sugars	70
	RAFT	Well-defined glycopolymers, amphiphilic copolymers and biologically active glyconanoparticles	71-72
	RAFT	Diblock glycopolymers for effective pDNA and siRNA delivery	73

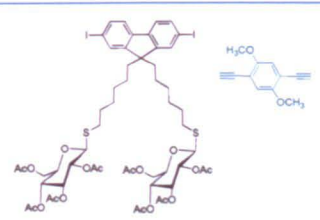
	RAFT	Gradient copolymers used to prepare glycopolymer-based porous films	74
	RAFT	Clickable glycopolymers	75
	RAFT	Thermosensitive diblock glycopolymers	76
	RAFT	Homoglycopolymers and amphiphilic block copolymers	77
	RAFT	Cross-linked glyco-particles with capability to bind Con A and bacteria lectin <i>fimH</i>	78
	RAFT	Mannose glycopolymers from chemo-enzymatic synthesised glycomonomer	79
	RAFT	Thermo-responsive block copolymers	80

 <p><math>n = 5 \text{ or } 10</math></p>	RAFT	Thermoresponsive random and block glycol-copolymers with different comonomer content, spacer chain length of the glycomonomer	81
	RAFT	pH-sensitive block glycopolymers	82
	RAFT	Biotinylated gradient glycopolymers based on the use of a biotin-CTA	83
	RAFT	Aldehyde-functionalised glycopolymer	84
	ATRP	Pyridyl disulfide end-functionalised glycopolymer for conjugation to biomolecules and patterning on gold surfaces	85

	ATRP	Glycopolymer with cyclic sugar ring	86
	ATRP	Stimuli-responsive diblock and triblock glycol-copolymers by copolymerisation with other monomers.	87
	ATRP	Virus-glycopolymer conjugates	88
	ATRP	Glycopolymer conjugations with protein to form glycoprotein mimics	63
	ATRP	$\alpha$ -Functional glycopolymers for (poly)peptide conjugation	89
	ATRP	Homoglycopolymer and diblock, triblock amphiphilic glycopolymers	90

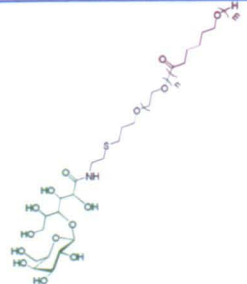
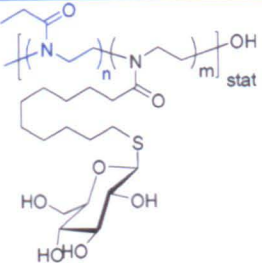
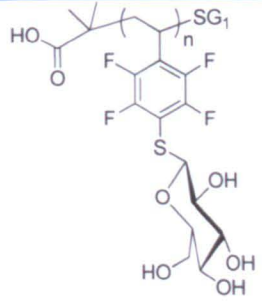


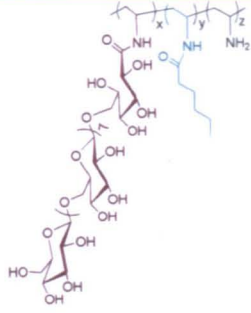
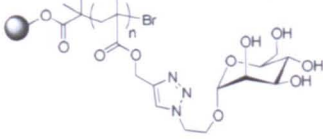
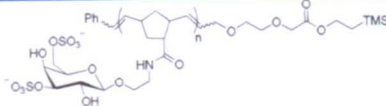
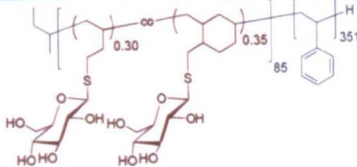
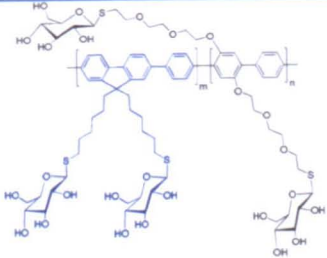
	ATRP	Linear and comb like glycopolymers grafted to poly(ethyleneterephthalate) tracketched membrane surface	91
 <p>a: R = H, X = O b: R = MO<sub>3</sub>S, X = O c: R = H, X = CH<sub>2</sub> d: R = MO<sub>3</sub>S, X = CH<sub>2</sub></p>	ROMP	Sulfated glycopolymers as P-selectin or L-selectin inhibitors	92-94
 <p>R = H, Ac</p>	NMP	Lactose-substituted polystyrene	95
	FRP*	Mannose copolymers examined in HeLa cells.	96
	FRP*	Thermoresponsive glucose glycopolymers	97
	FRP*	Cross-linked glycopolymers grafted to gold surface to interact with Con A	98

	SGP <sup>#</sup>	Well-defined fluorescent glycopolymers	99
---	------------------	--	----

\*Free radical polymerisation; # Palladium-catalysed Sonogashira coupling step-growth polymerisation.

Table 1.2 Post-functionalisation of precursor polymers.

Structure	Properties	Ref.
	Block galactose copolymer micelles for hepatoma-targeting delivery of paclitaxel and cancer chemotherapy	100
	Thermo-responsive copolymers containing glucose	101
	Homoglycopolymers and glyco-copolymers from block and random copolymers of styrene and pentafluorostyrene by NMP	102

	Amphiliphilic copolymers containing dextran	103
	Glycosylated polymeric resin beads containing mannose	104
	End-functional sulphated galactose glycopolymers to interact with L-selectin	93
	Glucose-grafted polybutadiene-block-polystyrene glycopolymers	105
	Fluorescent glycopolymers	99

### 1.3.2 Hyperbranched glycopolymers

Müller and co-workers<sup>106-109</sup> combined self-condensing vinyl copolymerisation and ATRP to synthesise glycopolymers from various glycomonomers with 2-(2-bromopropionyloxy)ethyl acrylate (BPEA) as comonomer, **Figure 1.9**. The resulting hyperbranched glycopolymers were grafted onto a silicon wafer, multi-walled carbon nanotubes, and poly(divinylbenzene) (PDVB) microspheres respectively for the



investigation of lectin-carbohydrate interactions. Molecular weight and composition of the glycopolymers and, thickness and roughness of the surfaces were adjusted by the ratio of the comonomers.

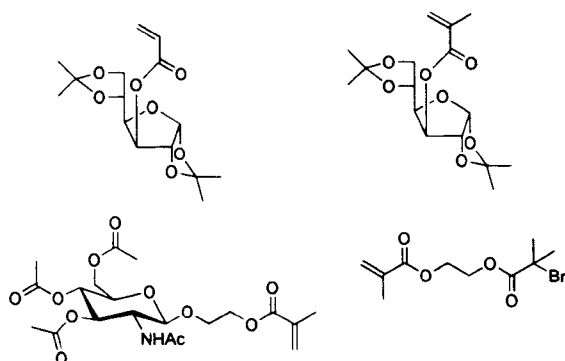


*Figure 1.9 Monomers used for the preparation of hyperbranched glycopolymers via combination of self-condensing vinyl copolymerisation and ATRP. Ref.106–109.*

Perrier and co-workers<sup>110</sup> prepared highly branched and hyperbranched glycopolymers using RAFT and click chemistry. By deprotection and post-functionalisation of the precursor copolymers of 50 equiv. of TMSPA and 1 equiv. of EGDMA with an excess of glucothiose sodium salt or 2-azidoethyl- $\beta$ -D-galactopyranoside, highly branched glycopolymers were generated by thiol-yne click or CuAAC reactions, **Figure 1.10**. The hyperbranched glycopolymers were prepared by thiol-ene click reactions with glucothiose sodium salt following RAFT polymerisation of EGDMA which was stopped at 25% conversion so as to avoid the formation of microgels.

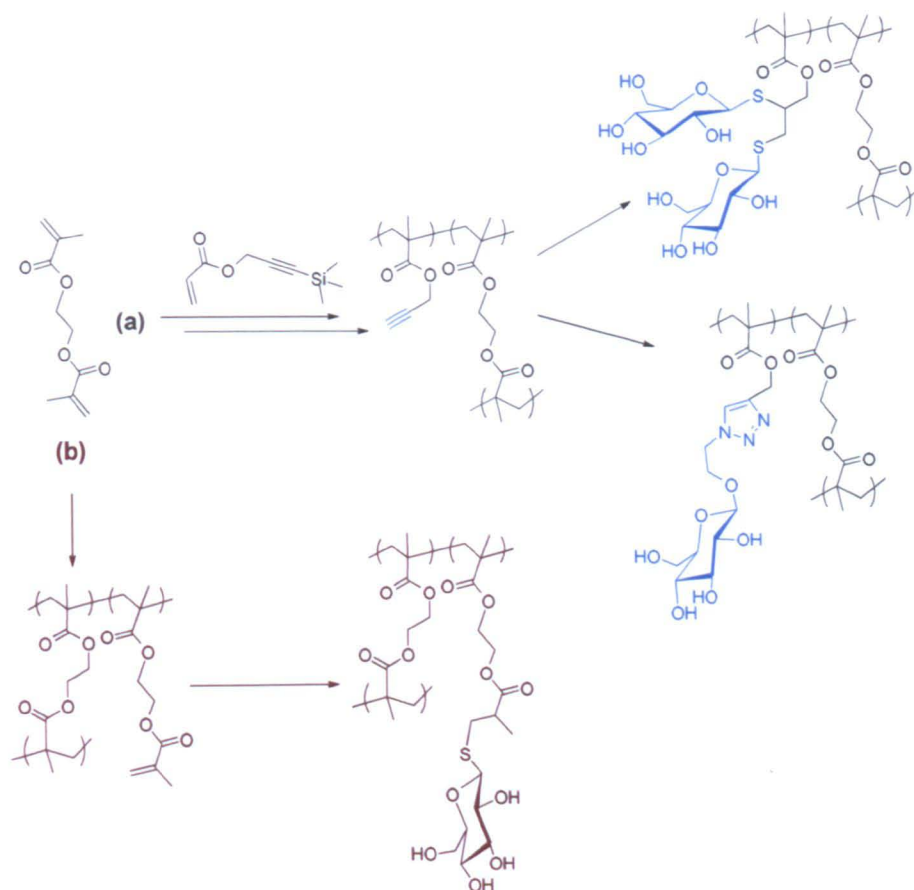


Figure 1.10 Synthesis of (a) highly branched and (b) hyperbranched glycopolymers by RAFT polymerisation and click chemistry. Ref. 110.

Hyperbranched polyglycerols (HPG) were modified to prepare hyperbranched glycopolymers by Kizhakkedathu *et al.* due to their biocompatibility,<sup>111</sup> **Figure 1.11**. A range of glycopolymers of various molecular weight, size, and mannose density (22-303 per HPG) were synthesised using HPG scaffolds (106 kDa, 200 kDa, or 500 kDa). The HPG-mannose conjugates exhibited a greatly enhanced potency in inhibition of Con A induced agglutination of fresh human red blood cells compared to methyl  $\alpha$ -D-mannopyranoside, which depended on both the size and ligand density.

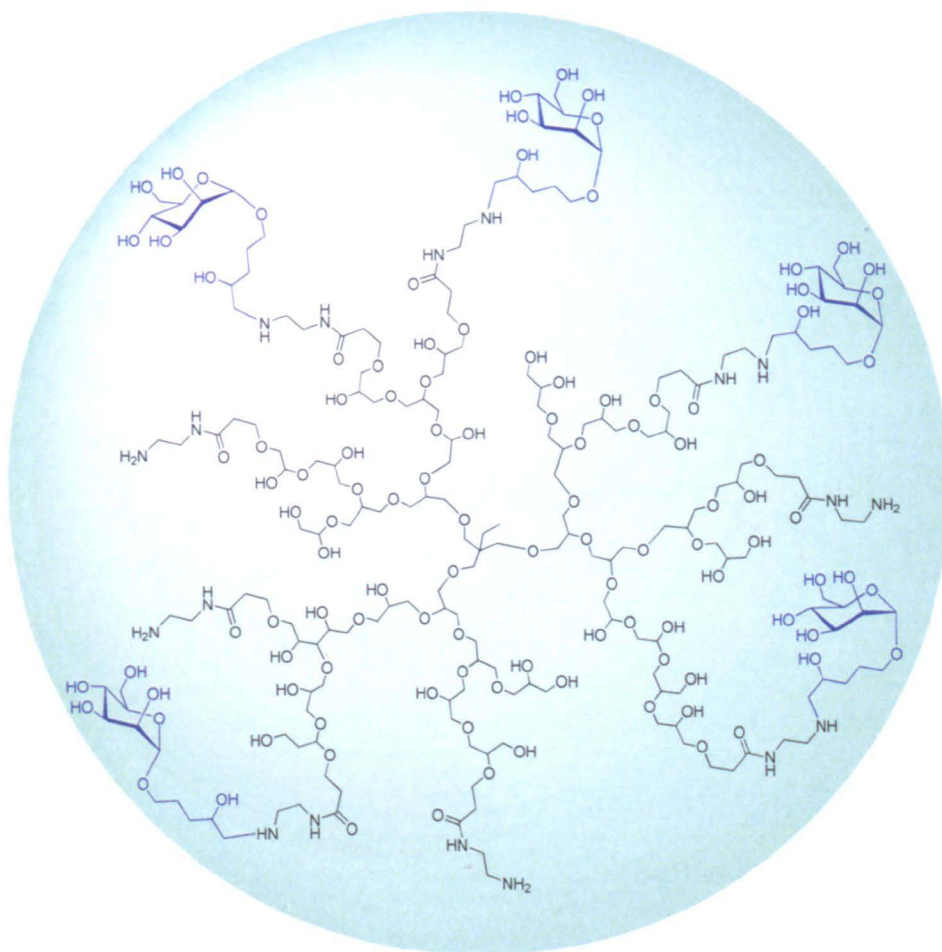


Figure 1.11 Mannose conjugates based on hyperbranched polyglycerols. Ref. 111.

### 1.3.3 Glycodendrimers

Glycodendrimers have been prepared due to their specific architectures by Wolfenden and Cloninger,<sup>112</sup> Pieters *et al.*,<sup>113</sup> Zhu and Marchant.<sup>114</sup> The synthesis of glycodendrimers has been reviewed by Roy and Baek in 2002,<sup>115</sup> Chabre and Roy in 2008,<sup>116</sup> Imbert, Chabre and Roy in 2008,<sup>117</sup> and Xu, *et al.* in 2011.<sup>118</sup> Unsymmetrical fluorescent mannose glycodendrimers were synthesised stepwise by Sharpless and co-workers using click chemistry, **Figure 1.12**, which showed potency in the hemagglutination assay using Con A and rabbit red blood cells.<sup>119</sup>

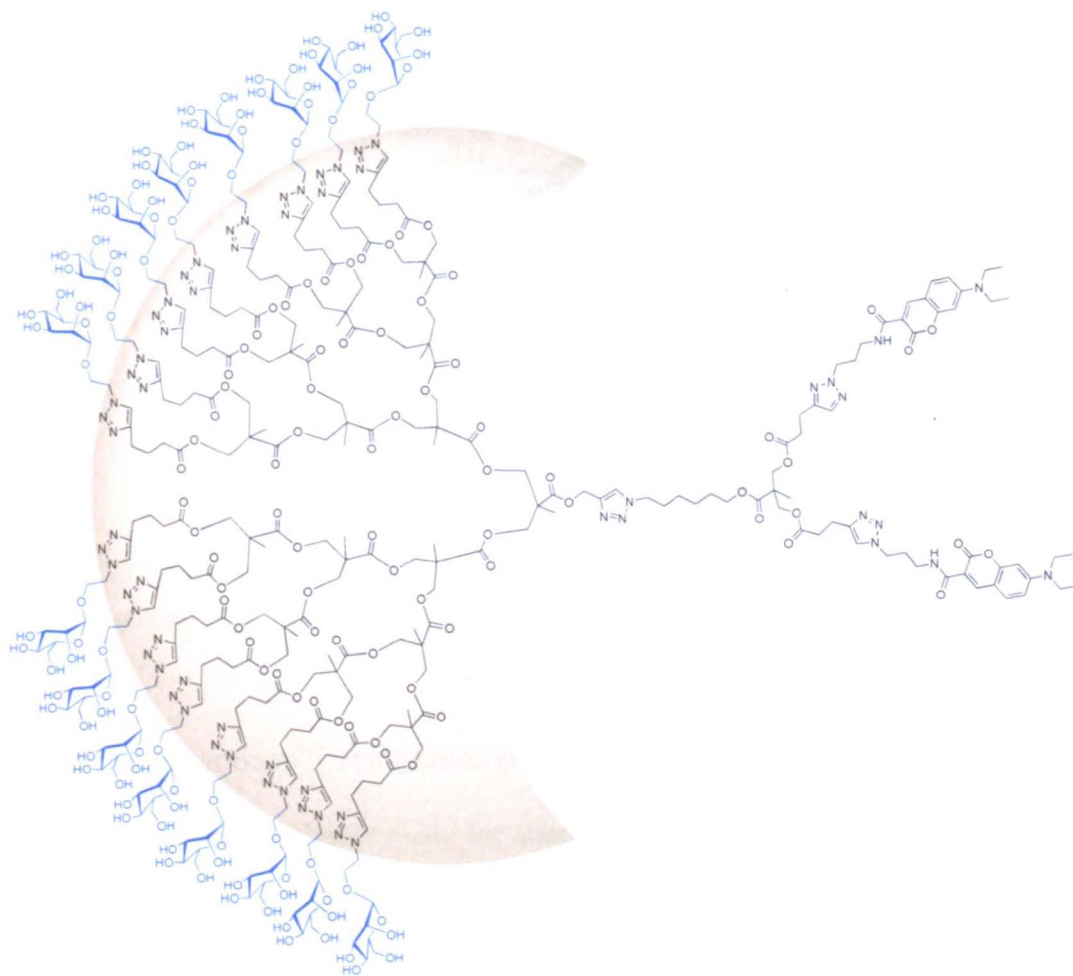


Figure 1.12 Unsymmetrical fluorescent mannose glycodendrimers synthesised by click chemistry. Ref. 119.

Polysulfated poly(ethylene oxide) (PEO) dendrimer-like glycopolymers bearing sulfated lactose were generated by Chaikof *et al.*,<sup>120</sup> **Figure 1.13**. The 1<sup>st</sup> generation of PEO stars (three arm,  $M_n \sim 5200$  mu; four arm,  $M_n \sim 5100$  mu) were synthesised by anionic polymerisation using core-first approach while the preparation of 2<sup>nd</sup> generation of dendrimers based on the phosphazene core ( $M_n \sim 52$  kD). Glycopolymers were then generated by glycosylations using trichloroacetimidate glycosidation methodology and lactose sulfation resulting in terminal sulphated oligosaccharides. These complex branched PEO heparinoid mimics exhibited *in vivo* anti-inflammatory activity.

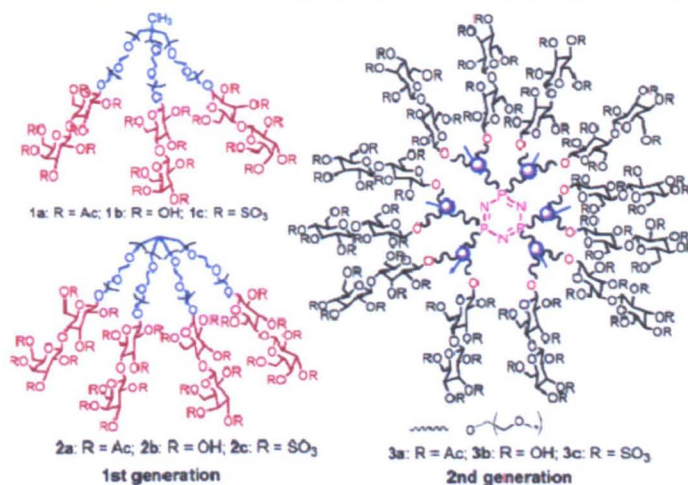


Figure 1.13 Polysulfated poly(ethylene oxide) (PEO) dendrimer-like glycopolymers bearing sulfated lactose. Ref. 120.

Davis and co-workers<sup>121</sup> synthesised dendritic glycopolymers with pyridyl disulfide (PDS) in the end of polymer chain for attachment of biomolecules, **Figure 1.14**. The well-defined glycopolymers were prepared by RAFT and click chemistry in a versatile way to control the sugar functionalities, which bore multivalent biorecognition groups, *in vivo* bioavailability, and the ability for conjugation to any therapeutic molecules containing free thiols or -ene groups. A short interfering RNA (siRNA) was attached to the glycopolymer in this work as a demonstration for the conjugation.

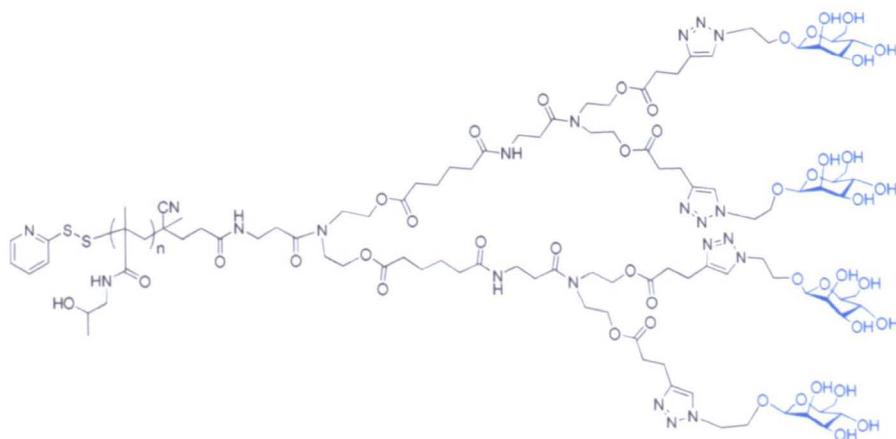


Figure 1.14 Dendritic glycopolymer synthesised by RAFT and click chemistry. Ref. 121.



Click chemistry was employed by Riguera *et al.* to prepare glycodendrimers,<sup>122</sup>

**Figure 1.15.** Three generations of azide-terminated gallic acid — triethylene glycol dendrimers were synthesised from 3,4,5-tri-(2-(2-(2-azidoethoxy)ethoxy)ethyl)benzoic acid. 2-Propynyl  $\alpha$ -L-fucopyranoside, 2-propynyl  $\alpha$ -D-mannopyranoside and 2-propynyl  $\beta$ -D-lactopyranoside were prepared from protected sugars. Efficient click reactions of the three generation dendrimers with different sugar alkynes in the presence of  $\text{CuSO}_4$  and sodium ascorbate in *t*-BuOH- $\text{H}_2\text{O}$  gave rise to glycodendrimers with high yields (85-92%).

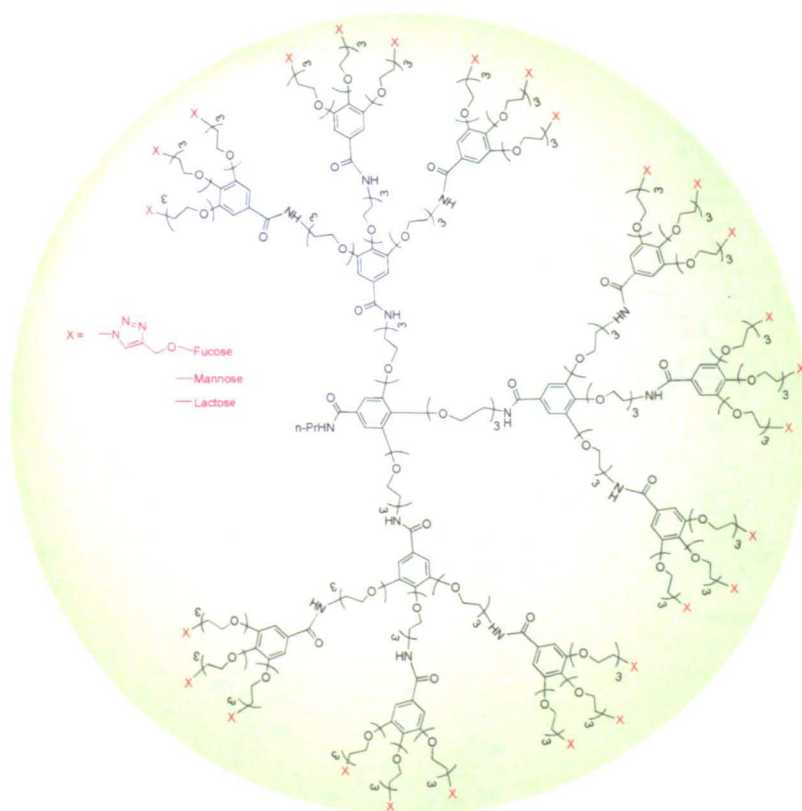


Figure 1.15 Glycodendrimers obtained by click chemistry. Ref. 122.

Supramolecular architectures based on the use of cyclodextrins (CDs) have also been reported, which are able to encapsulate other molecules within their hydrophobic cavities.<sup>123-124</sup> Supramolecular glycodendrimers were generated by Seeberger *et al.*,<sup>125</sup> which were comprised of a fluorescent ruthenium(II) core surrounded by

heptamannosylated  $\beta$ -cyclodextrin ( $\beta$ CDMan) scaffolds, **Figure 1.16**. Surface plasmon resonance (SPR) studies showed the interactions of Con A with RuCDMan2 **1** and RuCDMan4 **2** complexes, indicating the equilibrium constant of **1** was lower than that of **2**. However, complex **3** did not bind to Con A due to inherent bulkiness. Confocal microscopy was used to explore distinct interactions between mannosylated complex **3** and *E. coli* strain ORN178 and ORN208 taking advantage of the fluorescent properties of ruthenium(II). The specific binding of complex **3** with ORN178 indicated that these supramolecular multivalent probes can be used as the biosensors and bacterial sensing tools.

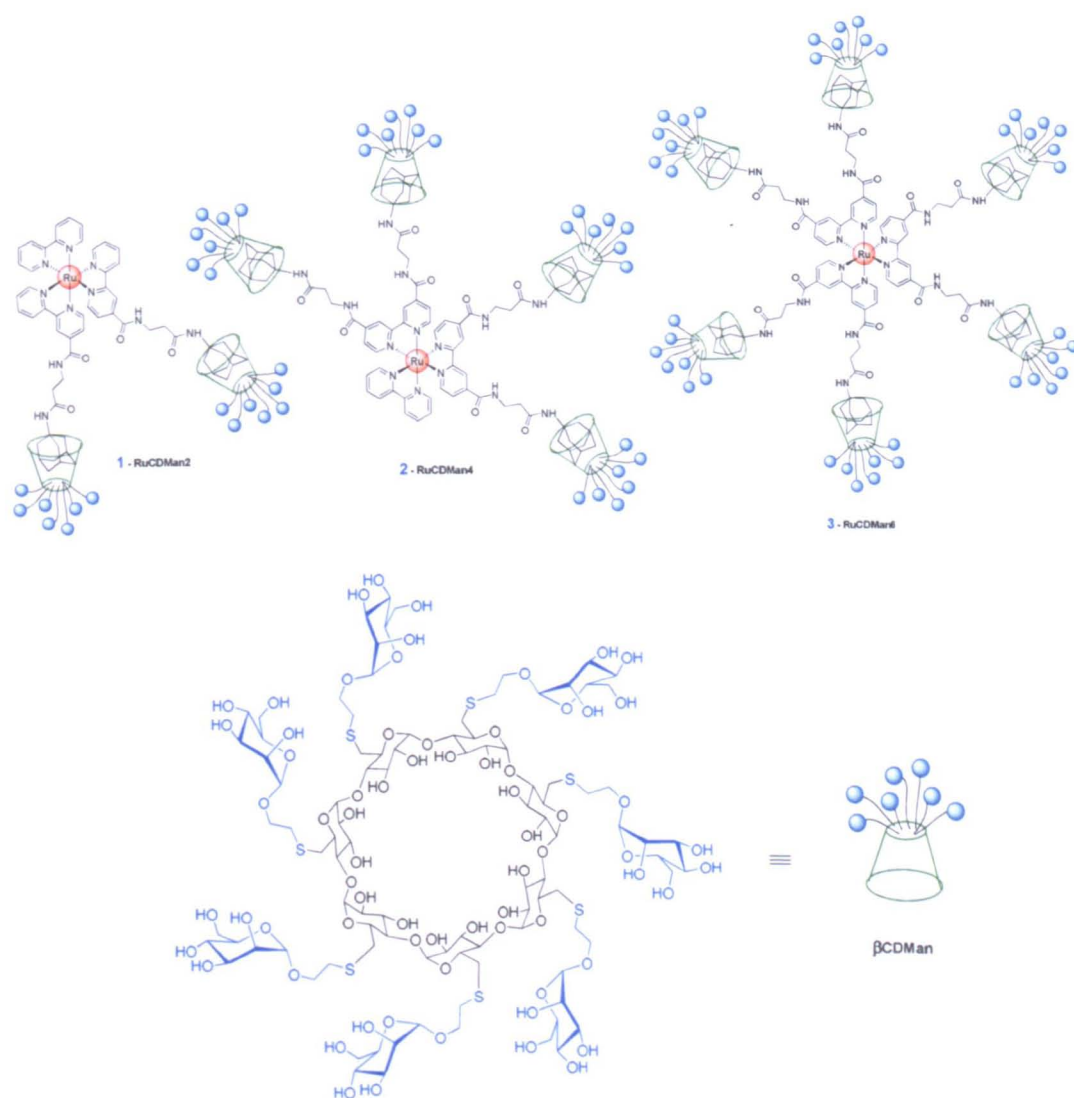


Figure 1.16 Supramolecular glycodendrimers based on the use of cyclodextrin. Ref. 125.

Benito, *et al.*<sup>126</sup> prepared cyclodextrin (CD) conjugates with glycodendrimers of various valency and geometry and glycodendritic CD dimmers *via* the reactions between isothiocyanate and amine functionalities of different building blocks,

**Figure 1.17.** The effects of valency, density and host on Con A binding efficiency and drug carrier capability were investigated. The highest capacity of hexavalents in inhibition of Con A-yeast mannan binding reflected the existence of cluster effect. Although with similar binding affinities toward Con A, the dimeric host exhibited larger docetaxel carrier capability than the monomeric host as docetaxel interacted simultaneously with two  $\beta$ CD cavities. The corresponding docetaxel complexes had 2-fold increased affinity in the interaction with Con A due to the sandwich-type supramolecular organisation.

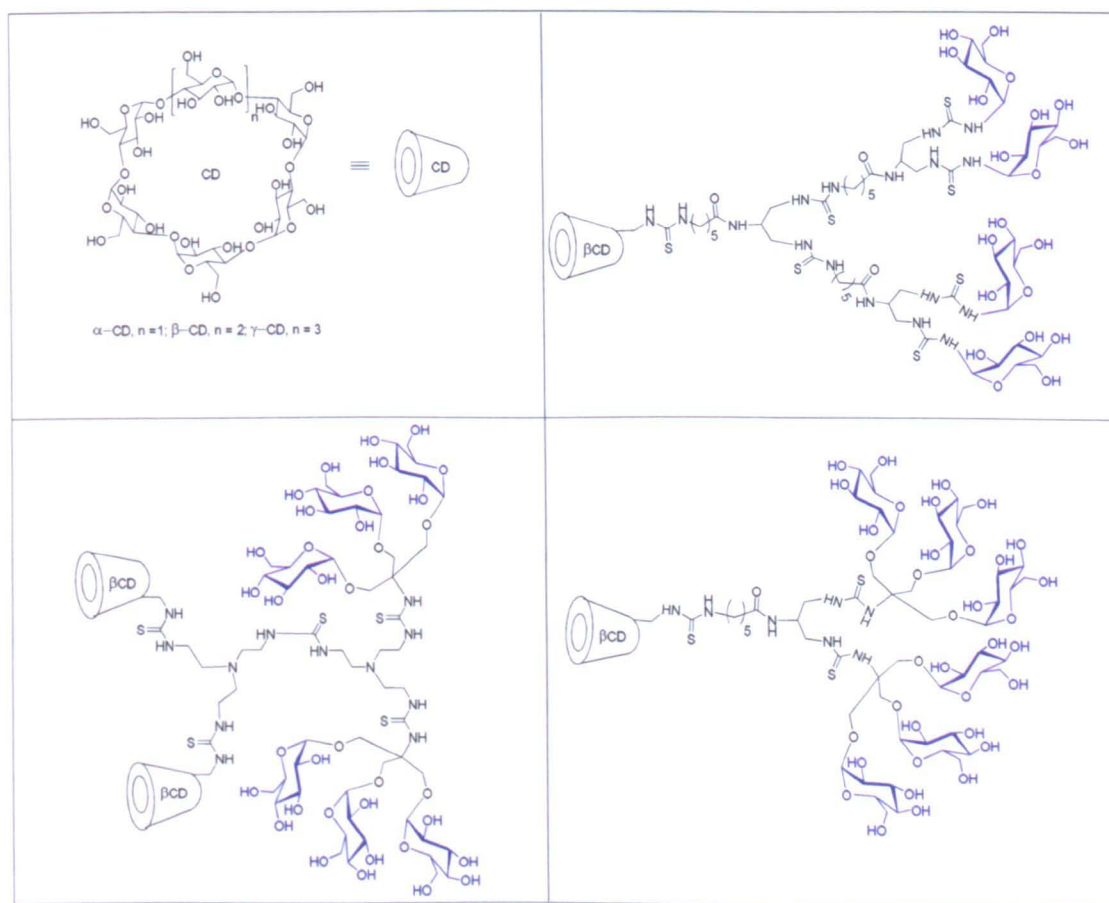


Figure 1.17 Glycodendrimer-cyclodextrin conjugates. Ref. 126.



### 1.3.4 Star glycopolymers

Sleiman *et al.*<sup>127</sup> showed that star-shaped multivalent ligands exhibited high inhibition potencies of Con A-induced hemagglutination. The unexpectedly increased inhibition amplification was attributed to the semi-rigid structures which mediated in the kinetic aggregation process of Con A cross-linking, **Figure 1.18**.

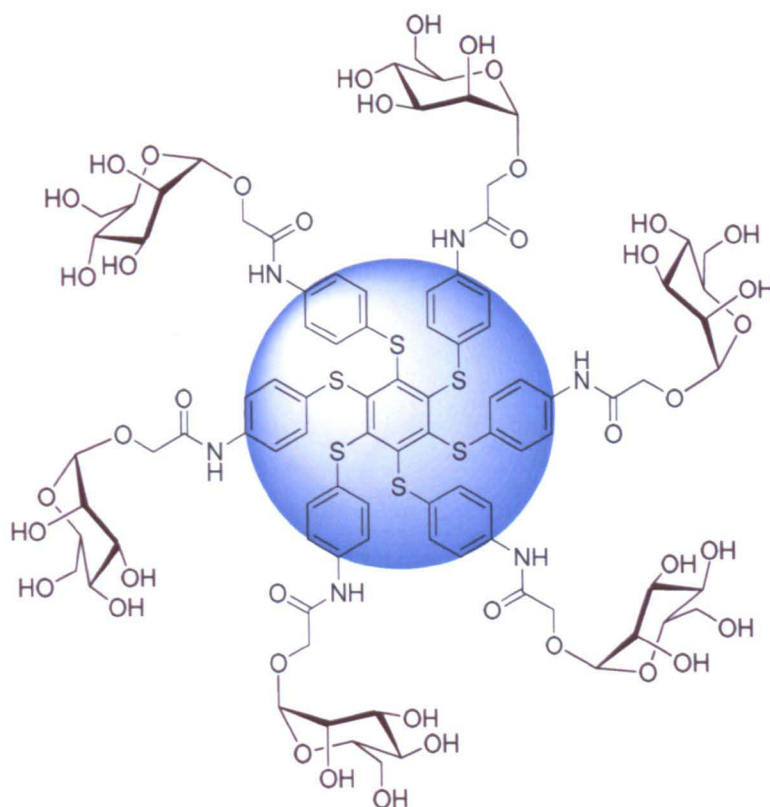


Figure 1.18 Star-shaped multivalent ligands with low valency. Ref. 127.

Amphiphilic A<sub>3</sub>B mikto-arm star glyco-copolymers based on a sugar core were generated by Dubois and co-workers, using polymerisation of  $\epsilon$ -caprolactone and ATRP of diisopropylidene galactose methacrylate.<sup>128</sup> Star-shaped glycopolymers were also synthesised by Dong *et al.*,<sup>129</sup> **Figure 1.19**, using ring-opening polymerisation (ROP) of  $\gamma$ -benzyl-L-glutamate *N*-carboxyanhydride (BLG-NCA) and the direct ATRP of unprotected D-gluconamidoethyl methacrylate (GAMA) glycomonomer. The resulting polypeptide/glycopolymer amphiphilic biohybrids

exhibited pH-sensitive self-assembly behaviour in aqueous solution and specific biomolecular recognition with Con A. Moreover, as the star-shaped copolymers showed higher efficiency in doxorubicin loading and longer drug-release time than their linear counterparts, they have potential application in anticancer drug delivery system. Similarly, star-shaped diblock copolymers poly( $\epsilon$ -caprolactone)-b-poly(D-gluconamidoethyl methacrylate) (PCL-PGAMA) starting from pentaerythritol,<sup>130</sup> and Star poly(amido amine)-b-poly( $\epsilon$ -caprolactone)-b-poly(D-gluconamidoethyl methacrylate) (PAMAM-PCL-PGAMA) triblock copolymers with a dendrimer core<sup>131</sup> were synthesised.

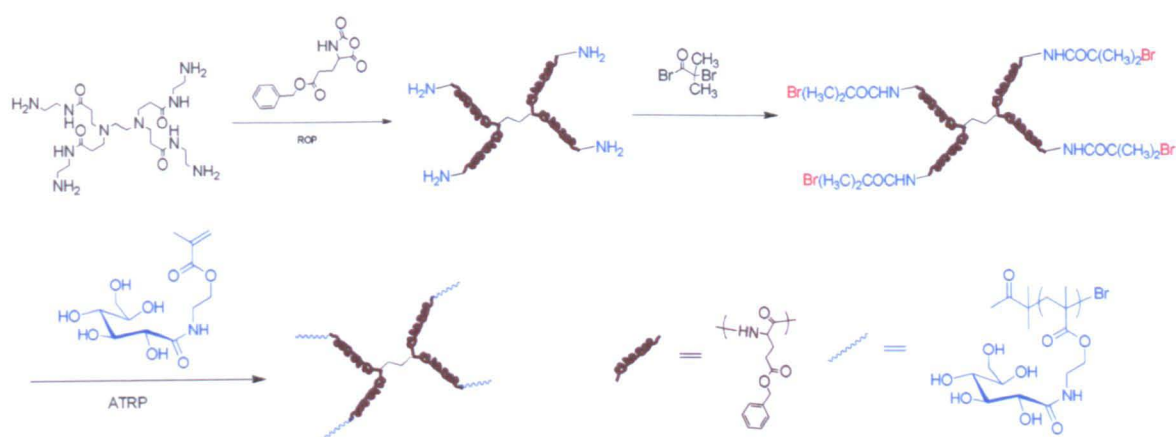


Figure 1.19 Synthesis of star-shaped SPBLG-PGAMA biohybrids. Ref.129.

RAFT polymerisation was used by Stenzel *et al.* to generate different star glycopolymers.<sup>76, 132</sup> They prepared a library of star glycopolymers of different molecular weights by post-functionalisation of reactive scaffolds with 1-thio- $\beta$ -D-glucose sodium salt.<sup>133</sup> The precursor polymers were synthesised *via* RAFT from vinyl benzyl chloride (VBC) using 1,2,4,5-tetrakis(thiobenzoylthiomethyl)benzene as RAFT agent, **Figure 1.20**. The interaction of these glycopolymers with

Concanavalin A (ConA) was investigated through turbidity assays and precipitation assays. They found that the stoichiometry and rate of these star glycopolymers in clustering Con A were comparable with linear glycopolymers. The star glycopolymer with medium molecular weight ( $n = 360$ ) was the most effective reagent to bind Con A among all the glycopolymers of different molecular weights.

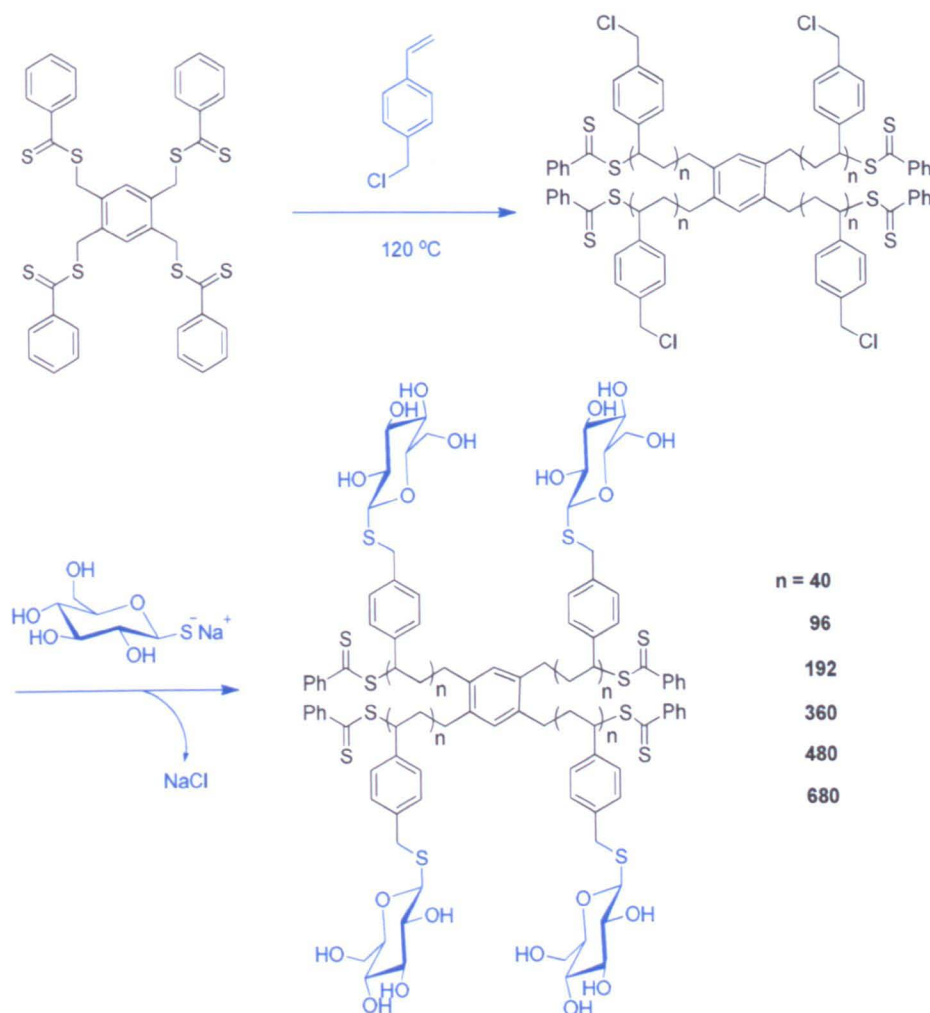


Figure 1.20 Synthesis of star glycopolymer by RAFT. Ref.133.

Zhang and Stenzel synthesised glycopolymers with a seven-arm star architecture using the core-first technique with a multifunctional RAFT agent based on a  $\beta$ -cyclodextrin core,<sup>134</sup> **Figure 1.21**. However, the core-first technique did not work

when it was used to make similar star glycopolymers copolymerised with *N*-isopropyl acrylamide (NIPAAm). Therefore, the arm-first technique was employed to prepare the thermo-responsive unimolecular micelles with core-crosslinking using hexamethylene diacrylate.

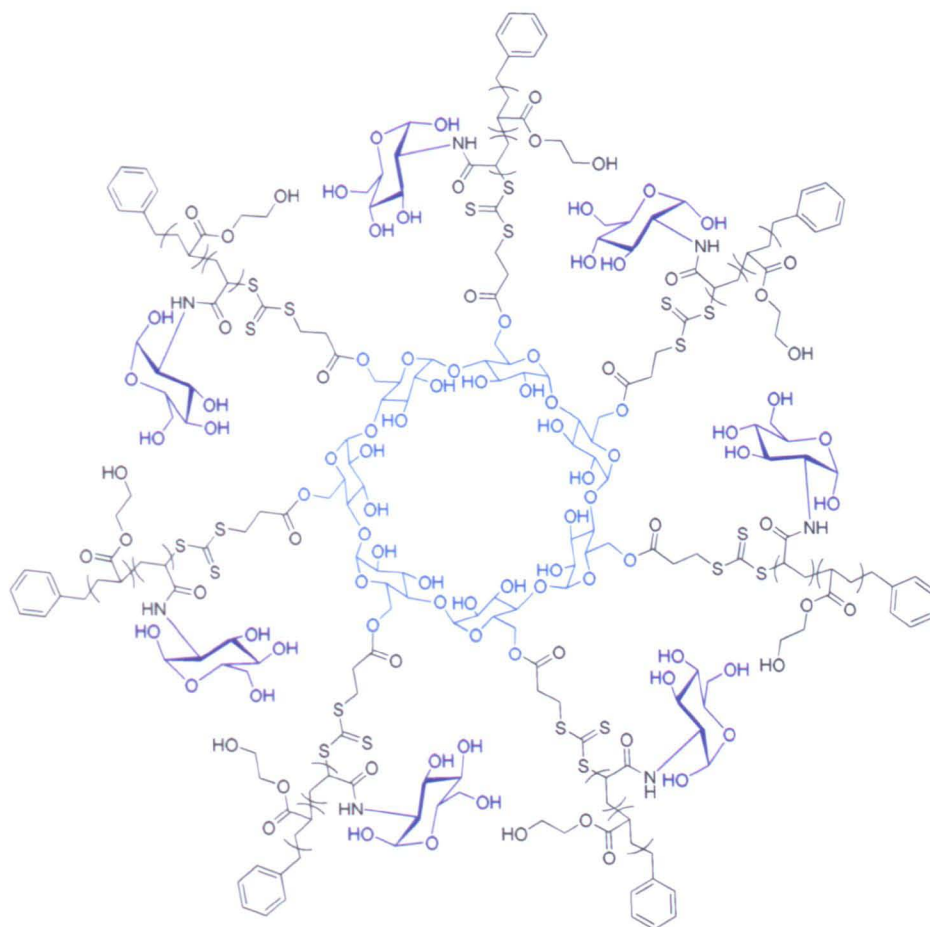


Figure 1.21 Structure of seven-arm  $\beta$ -CD-(PHEA<sub>10</sub>-b-PAGAx). Ref. 134.

## 1.4 Biological application of glycopolymers

Much attention has been drawn to the development of glycopolymers, which can intermediate various biological processes as inhibitors or effectors. As excellent protein-binding multivalent carbohydrate mimics, they have been applied in many

areas, including macromolecular drugs,<sup>135</sup> drug delivery systems,<sup>136-137</sup> hydrogels,<sup>138-139</sup> microfabrication<sup>140</sup> and surface modifiers,<sup>141-143</sup> *etc.* The biological applications of carbohydrate-based materials and glycopolymers in human health and disease have been reported in several reviews.<sup>117, 144-147</sup>

Since the first inhibitor of influenza haemagglutinin based on a glycopolymer was synthesised by Bovin and co-workers in 1990,<sup>148</sup> many glycopolymeric treatments of influenza viruses have been developed.<sup>149-152</sup> Not only the inhibition of influenza viruses was studied, the treatments of other viruses were also targeted. The interaction of glycopolymers containing mannose moiety with human DC-SIGN was investigated by Haddleton *et al.*<sup>69</sup> These glycopolymers can inhibit the interactions between DC-SIGN and the highly glycosylated HIV envelope glycoprotein gp120. In order to understand genetic and epigenetic mechanisms associated with human health and disease, the effective delivery of pDNA and siRNA by synthetic amphiphilic glycopolymers was studied by Reineke and co-workers.<sup>73</sup> They also screened the delivery of siRNA to cultured U-87 (glioblastoma) cells.

## 1.5 References

1. Blow, N., *Nature* **2009**, *457*, 617-620.
2. Dwek, R. A., *Chem. Rev.* **1996**, *96*, 683-720.
3. Kiessling, L. L.; Splain, R. A., *Annu. Rev. Biochem.* **2010**, *79*, 619-653.
4. Lowe, J. B., *Curr. Opin. Cell Biol.* **2003**, *15*, 531-538.



5. Lowe, J. B., *Cell* **2001**, *104*, 809-812.
6. Helenius, A.; Aebi, M., *Science* **2001**, *291*, 2364-2369.
7. Blomme, B.; Van Steenkiste, C.; Callewaert, N.; Van Vlierberghe, H., *J. Hepatol.* **2009**, *50*, 592-603.
8. Nimrichter, L.; Gargir, A.; Gortler, M.; Altstock, R. T.; Shtevi, A.; Weisshaus, O.; Fire, E.; Dotan, N.; Schnaar, R. L., *Glycobiology* **2004**, *14*, 197-203.
9. Zachara, N. E.; Hart, G. W., *Biochimica. et Biophysica Acta.* **2006**, *1761*, 599-617.
10. Disney, M. D.; Seeberger, P. H., *Chem. Biol.* **2004**, *11*, 1701-1707.
11. Mody, R.; Joshi, S.; Chaney, W., *J. Pharmacol. Toxicol. Methods* **1995**, *33*, 1-10.
12. Gorelik, E.; Galili, U.; Raz, A., *Cancer Metastasis Rev.* **2001**, *20*, 245-277.
13. Ofek, I.; Hasty, D. L.; Sharon, N., *FEMS Immunol. Med. Microbiol.* **2003**, *38*, 181-191.
14. Sharon, N.; Lis, H., *Science* **1989**, *246*, 227-234.
15. Sharon, N.; Lis, H., *Scientific American* **1993**, *268*, 82-89.
16. Dove, A., *Nat. Biotech.* **2001**, *19*, 913-917.
17. Bertozzi, C. R.; Kiessling, L. L., *Science* **2001**, *291*, 2357-2364.
18. Campbell, C.; Yarema, K., *Genome Biol.* **2005**, *6*, 236.
19. Kiessling, L. L.; Cairo, C. W., *Nat. Biotech.* **2002**, *20*, 234-235.
20. Garegg, P. J.; Derek, H., *Adv. Carbohydr. Chem. Biochem.*, **1997**, *52*, 179-205.

21. Koeller, K. M.; Wong, C.-H., *Chem. Rev.* **2000**, *100*, 4465-4494.
22. Seeberger, P. H.; Haase, W.-C., *Chem. Rev.* **2000**, *100*, 4349-4394.
23. Kahne, D., *Curr. Opin. Chem. Biol.* **1997**, *1*, 130-135.
24. Roberge, J.; Beebe, X.; Danishefsky, S., *Science* **1995**, *269*, 202-204.
25. Crich, D.; Sun, S., *J. Am. Chem. Soc.* **1998**, *120*, 435-436.
26. Danishefsky, S.; McClure, K.; Randolph, J.; Ruggeri, R., *Science* **1993**, *260*, 1307-1309.
27. Flitsch, S. L., *Curr. Opin. Chem. Biol.* **2000**, *4*, 619-625.
28. Palcic, M. M., *Curr. Opin. Biotechnol.* **1999**, *10*, 616-624.
29. David, S.; Aug, C.; Gautheron, C.; Derek, H., *Adv. Carbohydr. Chem. Biochem.*, **1991**, *49*, 175-237.
30. Wong, C.-H.; Halcomb, R. L.; Ichikawa, Y.; Kajimoto, T., *Angew. Chem. Int. Edit. Engl.* **1995**, *34*, 412-432.
31. Koeller, K. M.; Wong, C.-H., *Nature* **2001**, *409*, 232-240.
32. Schuster, M.; Wang, P.; Paulson, J. C.; Wong, C.-H., *J. Am. Chem. Soc.* **1994**, *116*, 1135-1136.
33. Schuerch, C.; Frechet, J. M., *J. Am. Chem. Soc.* **1971**, *93*, 492-496.
34. Plante, O. J.; Palmacci, E. R.; Seeberger, P. H., *Science* **2001**, *291*, 1523-1527.
35. Pashkuleva, I.; Reis, R. L., *J. Mater. Chem.* **2010**, *20*, 8803-8818.
36. Raghavan, S.; Kahne, D., *J. Am. Chem. Soc.* **1993**, *115*, 1580-1581.

- 
37. Takahashi, T.; Adachi, M.; Matsuda, A.; Doi, T., *Tetrahedron Lett.* **2000**, *41*, 2599-2603.
38. Zhang, Z.; Ollmann, I. R.; Ye, X.-S.; Wischnat, R.; Baasov, T.; Wong, C.-H., *J. Am. Chem. Soc.* **1999**, *121*, 734-753.
39. Burkhart, F.; Zhang, Z.; Wacowich-Sgarbi, S.; Wong, C.-H., *Angew. Chem. Int. Ed.* **2001**, *40*, 1274-1277.
40. Witte, K.; Seitz, O.; Wong, C.-H., *J. Am. Chem. Soc.* **1998**, *120*, 1979-1989.
41. Ando, H.; Manabe, S.; Nakahara, Y.; Ito, Y., *Angew. Chem. Int. Ed.* **2001**, *40*, 4725-4728.
42. Bergbreiter, D. E.; Case, B. L.; Liu, Y.-S.; Caraway, J. W., *Macromolecules* **1998**, *31*, 6053-6062.
43. Sears, P.; Wong, C.-H., *Science* **2001**, *291*, 2344-2350.
44. Stallforth, P.; Lepenies, B.; Adibekian, A.; Seeberger, P. H., *J. Med. Chem.* **2009**, *52*, 5561-5577.
45. Hořejší, V.; Smolek, P.; Kocourek, J., *J. Biochim. Biophys. Acta-Gen. Subj.* **1978**, *538*, 293-298.
46. Slavin, S.; Burns, J.; Haddleton, D. M.; Becer, C. R., *Eur. Polym. J.* **2011**, *47*, 435-446.
47. Ladmiral, V.; Melia, E.; Haddleton, D. M., *Eur. Polym. J.* **2004**, *40*, 431-449.
48. Ting, S. R. S.; Chen, G.; Stenzel, M. H., *Polym. Chem.* **2010**, *1*, 1392-1412.
49. Miura, Y., *J. Polym. Sci., Part A: Polym. Chem.* **2007**, *45*, 5031-5036.
50. Okada, M., *Prog. Polym. Sci.* **2001**, *26*, 67-104.
51. Satoh, T.; Kakuchi, T., *Macromol. Biosci.* **2007**, *7*, 999-1009.
-



- 
52. Spain, S. G.; Gibson, M. I.; Cameron, N. R., *J. Polym. Sci., Part A: Polym. Chem.* **2007**, *45*, 2059-2072.
53. Le Droumaguet, B.; Nicolas, J., *Polym. Chem.* **2010**, *1*, 563-598.
54. Voit, B.; Appelhans, D., *Macromol. Chem. Phys.* **2010**, *211*, 727-735.
55. Narumi, A.; Kakuchi, T., *Polym. J.* **2008**, *40*, 383-397.
56. Kiessling, L. L.; Gestwicki, J. E.; Strong, L. E., *Angew. Chem. Int. Ed.* **2006**, *45*, 2348-2368.
57. Schatz, C.; Lecommandoux, S., *Macromol. Rapid Commun.* **2010**, *31*, 1664-1684.
58. Rawat, M.; Gama, C. I.; Matson, J. B.; Hsieh-Wilson, L. C., *J. Am. Chem. Soc.* **2008**, *130*, 2959-2961.
59. Ke, B.-B.; Wan, L.-S.; Zhang, W.-X.; Xu, Z.-K., *Polymer* **2010**, *51*, 2168-2176.
60. Godula, K.; Rabuka, D.; Nam, K. T.; Bertozzi, C. R., *Angew. Chem. Int. Ed.* **2009**, *48*, 4973-4976.
61. Ladmiral, V.; Mantovani, G.; Clarkson, G. J.; Cauet, S.; Irwin, J. L.; Haddleton, D. M., *J. Am. Chem. Soc.* **2006**, *128*, 4823-4830.
62. Geng, J.; Lindqvist, J.; Mantovani, G.; Haddleton, D. M., *Angew. Chem. Int. Ed.* **2008**, *47*, 4180-4183.
63. Geng, J.; Lindqvist, J.; Mantovani, G.; Chen, G.; Sayers, C. T.; Clarkson, G. J.; Haddleton, D. M., *QSAR. Comb. Sci.* **2007**, *26*, 1220-1228.
64. Vinson, N.; Gou, Y.; Becer, C. R.; Haddleton, D. M.; Gibson, M. I., *Polym. Chem.* **2011**, *2*, 107-113.
65. Nurmi, L.; Lindqvist, J.; Randev, R.; Syrett, J.; Haddleton, D. M., *Chem. Commun.* **2009**, 2727-2729.
-

66. Gou, Y.; Becer, C. R.; Gibson, M. I.; Haddleton, D. M., **Submitted.**
  
67. Gou, Y.; Geng, J.; Becer, C. R.; Gibson, M. I.; Haddleton, D. M., **Submitted.**
  
68. Gou, Y.; Slavin, S.; Geng, J.; Voorhaas, L.; Becer, C. R.; Haddleton, D. M., **Submitted.**
  
69. Becer, C. R.; Gibson, M. I.; Geng, J.; Ilyas, R.; Wallis, R.; Mitchell, D. A.; Haddleton, D. M., *J. Am. Chem. Soc.* **2010**, *132*, 15130-15132.
  
70. Albertin, L.; Stenzel, M. H.; Barner-Kowollik, C.; Foster, L. J. R.; Davis, T. P., *Macromolecules* **2005**, *38*, 9075-9084.
  
71. Cameron, N. R.; Spain, S. G.; Kingham, J. A.; Weck, S.; Albertin, L.; Barker, C. A.; Battaglia, G.; Smart, T.; Blanz, A., *Faraday Discuss.* **2008**, *139*, 359-368.
  
72. Spain, S. G.; Albertin, L.; Cameron, N. R., *Chem. Commun.* **2006**, 4198-4200.
  
73. Smith, A. E.; Sizovs, A.; Grandinetti, G.; Xue, L.; Reineke, T. M., *Biomacromolecules* **2011**, *12*, 3015-3022.
  
74. Escale, P.; Ting, S. R. S.; Khoukh, A.; Rubatat, L.; Save, M.; Stenzel, M. H.; Billon, L., *Macromolecules* **2011**, *44*, 5911-5919.
  
75. Abdelkader, O.; Moebs-Sanchez, S.; Queneau, Y.; Bernard, J.; Fleury, E., *J. Polym. Sci., Part A: Polym. Chem.* **2011**, *49*, 1309-1318.
  
76. Bernard, J.; Hao, X.; Davis, T. P.; Barner-Kowollik, C.; Stenzel, M. H., *Biomacromolecules* **2005**, *7*, 232-238.
  
77. Pearson, S.; Allen, N.; Stenzel, M. H., *J. Polym. Sci., Part A: Polym. Chem.* **2009**, *47*, 1706-1723.
  
78. Ting, S. R. S.; Min, E. H.; Zetterlund, P. B.; Stenzel, M. H., *Macromolecules* **2010**, *43*, 5211-5221.
  
79. Granville, A. M.; Quémener, D.; Davis, T. P.; Barner-Kowollik, C.; Stenzel, M. H., *Macromol. Symp.* **2007**, *255*, 81-89.

- 
80. Hetzer, M.; Chen, G.; Barner-Kowollik, C.; Stenzel, M. H., *Macromol. Biosci.* **2010**, *10*, 119-126.
81. Özyürek, Z.; Komber, H.; Gramm, S.; Schmaljohann, D.; Müller, A. H. E.; Voit, B., *Macromol. Chem. Phys.* **2007**, *208*, 1035-1049.
82. Liu, L.; Zhang, J.; Lv, W.; Luo, Y.; Wang, X., *J. Polym. Sci., Part A: Polym. Chem.* **2010**, *48*, 3350-3361.
83. Gody, G.; Boullanger, P.; Ladavière, C.; Charreyre, M.-T.; Delair, T., *Macromol. Rapid Commun.* **2008**, *29*, 511-519.
84. Xiao, N.-Y.; Li, A.-L.; Liang, H.; Lu, J., *Macromolecules* **2008**, *41*, 2374-2380.
85. Vazquez-Dorbatt, V.; Tolstyka, Z. P.; Chang, C.-W.; Maynard, H. D., *Biomacromolecules* **2009**, *10*, 2207-2212.
86. Narain, R.; Armes, S. P., *Macromolecules* **2003**, *36*, 4675-4678.
87. Narain, R.; Armes, S. P., *Biomacromolecules* **2003**, *4*, 1746-1758.
88. Gupta, S. S.; Raja, K. S.; Kaltgrad, E.; Strable, E.; Finn, M. G., *Chem. Commun.* **2005**, 4315-4317.
89. Ladmiral, V.; Monaghan, L.; Mantovani, G.; Haddleton, D. M., *Polymer* **2005**, *46*, 8536-8545.
90. León, O.; Bordegé, V.; Muñoz-Bonilla, A.; Sánchez-Chaves, M.; Fernández-García, M., *J. Polym. Sci., Part A: Polym. Chem.* **2010**, *48*, 3623-3631.
91. Yang, Q.; Ulbricht, M., *Macromolecules* **2011**, *44*, 1303-1310.
92. Manning, D. D.; Hu, X.; Beck, P.; Kiessling, L. L., *J. Am. Chem. Soc.* **1997**, *119*, 3161-3162.
93. Gordon, E. J.; Gestwicki, J. E.; Strong, L. E.; Kiessling, L. L., *Chem. Biol.* **2000**, *7*, 9-16.
-

- 
94. Cairo, C. W.; Gestwicki, J. E.; Kanai, M.; Kiessling, L. L., *J. Am. Chem. Soc.* **2002**, *124*, 1615-1619.
95. Miura, Y.; Koketsu, D.; Kobayashi, K., *Polym. Advan. Technol.* **2007**, *18*, 647-651.
96. Obata, M.; Shimizu, M.; Ohta, T.; Matsushige, A.; Iwai, K.; Hirohara, S.; Tanihara, M., *Polym. Chem.* **2010**, *2*, 651-658.
97. Shinde, V. S.; Pawar, V. U., *J. Appl. Polym. Sci.* **2009**, *111*, 2607-2615.
98. Yu, L.; Huang, M.; Wang, P. G.; Zeng, X., *Anal. Chem.* **2007**, *79*, 8979-8986.
99. Xue, C.; Donuru, V. R. R.; Liu, H., *Macromolecules* **2006**, *39*, 5747-5752.
100. Yang, R.; Meng, F.; Ma, S.; Huang, F.; Liu, H.; Zhong, Z., *Biomacromolecules* **2011**, *12*, 3047-3055.
101. Kempe, K.; Neuwirth, T.; Czaplewska, J.; Gottschaldt, M.; Hoogenboom, R.; Schubert, U. S., *Polym. Chem.* **2011**, *2*, 1737-1743.
102. Becer, C. R.; Babiuch, K.; Pilz, D.; Hornig, S.; Heinze, T.; Gottschaldt, M.; Schubert, U. S., *Macromolecules* **2009**, *42*, 2387-2394.
103. Zhu, J.; Gosen, C.; Marchant, R. E., *J. Polym. Sci., Part A: Polym. Chem.* **2006**, *44*, 192-199.
104. Chen, G.; Tao, L.; Mantovani, G.; Geng, J.; Nystrom, D.; Haddleton, D. M., *Macromolecules* **2007**, *40*, 7513-7520.
105. You, L.; Schlaad, H., *J. Am. Chem. Soc.* **2006**, *128*, 13336-13337.
106. Muthukrishnan, S.; Erhard, D. P.; Mori, H.; Müller, A. H. E., *Macromolecules* **2006**, *39*, 2743-2750.
107. Pfaff, A.; Müller, A. H. E., *Macromolecules* **2011**, *44*, 1266-1272.
-

- 
108. Muthukrishnan, S.; Jutz, G.; André, X.; Mori, H.; Müller, A. H. E., *Macromolecules* **2004**, *38*, 9-18.
109. Gao, C.; Muthukrishnan, S.; Li, W.; Yuan, J.; Xu, Y.; Muller, A. H. E., *Macromolecules* **2007**, *40*, 1803-1815.
110. Semsarilar, M.; Ladmiral, V.; Perrier, S., *Macromolecules* **2010**, *43*, 1438-1443.
111. Kizhakkedathu, J. N.; Creagh, A. L.; Shenoi, R. A.; Rossi, N. A. A.; Brooks, D. E.; Chan, T.; Lam, J.; Dandepally, S. R.; Haynes, C. A., *Biomacromolecules* **2010**, *11*, 2567-2575.
112. Wolfenden, M. L.; Cloninger, M. J., *Bioconjugate Chem.* **2006**, *17*, 958-966.
113. Appeldoorn, C. C. M.; Joosten, J. A. F.; Ait el Maate, F.; Dobrindt, U.; Hacker, J.; Liskamp, R. M. J.; Khan, A. S.; Pieters, R. J., *Tetrahedron: Asymmetry* **2005**, *16*, 361-372.
114. Zhu, J.; Marchant, R. E., *Biomacromolecules* **2006**, *7*, 1036-1041.
115. Roy, R.; Baek, M.-G., *Rev. Mol. Biotechnol.* **2002**, *90*, 291-309.
116. Chabre, Y. M.; Roy, R., *Current Topics Med. Chem.* **2008**, *8*, 1237-1285.
117. Imberty, A.; Chabre, Y. M.; Roy, R., *Chem. Eur. J.* **2008**, *14*, 7490-7499.
118. Cheng, Y.; Zhao, L.; Li, Y.; Xu, T., *Chem. Soc. Rev.* **2011**, *40*, 2673-2703.
119. Wu, P.; Malkoch, M.; Hunt, J. N.; Vestberg, R.; Kaltgrad, E.; Finn, M. G.; Fokin, V. V.; Sharpless, K. B.; Hawker, C. J., *Chem. Commun.* **2005**, 5775-5777.
120. Rele, S. M.; Cui, W.; Wang, L.; Hou, S.; Barr-Zarse, G.; Tatton, D.; Gnanou, Y.; Esko, J. D.; Chaikof, E. L., *J. Am. Chem. Soc.* **2005**, *127*, 10132-10133.
121. Xu, J.; Boyer, C.; Bulmus, V.; Davis, T. P., *J. Polym. Sci., Part A: Polym. Chem.* **2009**, *47*, 4302-4313.
-

- 
122. Fernandez-Megia, E.; Correa, J.; Rodríguez-Meizoso, I.; Riguera, R., *Macromolecules* **2006**, *39*, 2113-2120.
123. Smiljanic, N.; Moreau, V.; Yockot, D.; Benito, J. M.; García Fernández, J. M.; Djedaïni-Pilard, F., *Angew. Chem.* **2006**, *118*, 5591-5594.
124. Ooya, T.; Eguchi, M.; Yui, N., *J. Am. Chem. Soc.* **2003**, *125*, 13016-13017.
125. Grünstein, D.; Maglinao, M.; Kikkeri, R.; Collot, M.; Barylyuk, K.; Lepenies, B.; Kamena, F.; Zenobi, R.; Seeberger, P. H., *J. Am. Chem. Soc.* **2011**, *133*, 13957-13966.
126. Benito, J. M.; Gómez-García, M.; Ortiz Mellet, C.; Baussanne, I.; Defaye, J.; Fernández, J. M. G., *J. Am. Chem. Soc.* **2004**, *126*, 10355-10363.
127. Sleiman, M.; Varrot, A.; Raimundo, J.-M.; Gingras, M.; Goekjian, P. G., *Chem. Commun.* **2008**, 6507-6509.
128. Suriano, F.; Coulembier, O.; Dubois, P., *J. Polym. Sci., Part A: Polym. Chem.* **2010**, *48*, 3271-3280.
129. Qiu, S.; Huang, H.; Dai, X.-H.; Zhou, W.; Dong, C.-M., *J. Polym. Sci., Part A: Polym. Chem.* **2009**, *47*, 2009-2023.
130. Dai, X.-H.; Dong, C.-M., *J. Polym. Sci., Part A: Polym. Chem.* **2008**, *46*, 817-829.
131. Dai, X.-H.; Zhang, H.-D.; Dong, C.-M., *Polymer* **2009**, *50*, 4626-4634.
132. Bernard, J.; Favier, A.; Zhang, L.; Nilasaroya, A.; Davis, T. P.; Barner-Kowollik, C.; Stenzel, M. H., *Macromolecules* **2005**, *38*, 5475-5484.
133. Chen, Y.; Chen, G.; Stenzel, M. H., *Macromolecules* **2010**, *43*, 8109-8114.
134. Zhang, L.; Stenzel, M. H., *Aust. J. Chem.* **2009**, *62*, 813-822.
135. Fleming, C.; Maldjian, A.; Da Costa, D.; Rullay, A. K.; Haddleton, D. M.; St John, J.; Penny, P.; Noble, R. C.; Cameron, N. R.; Davis, B. G., *Nat. Chem. Biol.* **2005**, *1*, 270-274.
-

136. Kim, A. P.; Yellen, P.; Yun, Y. H.; Azeloglu, E.; Chen, W., *Biomaterials* **2005**, *26*, 1585-1593.
137. Roche, A. C.; Fajac, I.; Grosse, S.; Frison, N.; Rondanino, C.; Mayer, R.; Monsigny, M., *Cell. Mol. Life Sci.* **2003**, *60*, 288-297.
138. Novick, S. J.; Dordick, J. S., *Chem. Mater.* **1998**, *10*, 955-958.
139. Miyata, T.; Uragami, T.; Nakamae, K., *Adv. Drug Delivery Rev.* **2002**, *54*, 79-98.
140. Sato, H.; Miura, Y.; Saito, N.; Kobayashi, K.; Takai, O., *Biomacromolecules* **2007**, *8*, 753-756.
141. Wulff, G.; Zhu, L.; Schmidt, H., *Macromolecules* **1997**, *30*, 4533-4539.
142. Wulff, G.; Schmidt, H.; Zhu, L., *Macromol. Chem. Phys.* **1999**, *200*, 774-782.
143. Chen, G.; Tao, L.; Mantovani, G.; Ladmiral, V.; Burt, D. P.; Macpherson, J. V.; Haddleton, D. M., *Soft Matter* **2007**, *3*, 732-739.
144. Ghazarian, H.; Idoni, B.; Oppenheimer, S. B., *Acta Histochem.* **2011**, *113*, 236-247.
145. Spain, S. G.; Cameron, N. R., *Polym. Chem.* **2011**, *2*, 60-68.
146. Seeberger, P. H.; Werz, D. B., *Nature* **2007**, *446*, 1046-1051.
147. Kulkarni, A. A.; Weiss, A. A.; Iyer, S. S., *Med. Res. Rev.* **2010**, *30*, 327-393.
148. Matrosovich, M. N.; Mochalova, L. V.; Marinina, V. P.; Byramova, N. E.; Bovin, N. V., *FEBS Lett.* **1990**, *272*, 209-212.
149. Gambaryan, A. S.; Karasin, A. I.; Tuzikov, A. B.; Chinarev, A. A.; Pazynina, G. V.; Bovin, N. V.; Matrosovich, M. N.; Olsen, C. W.; Klimov, A. I., *Virus Res.* **2005**, *114*, 15-22.

150. Matsuoka, K.; Takita, C.; Koyama, T.; Miyamoto, D.; Yingsakmongkon, S.; Hidari, K. I. P. J.; Jampangern, W.; Suzuki, T.; Suzuki, Y.; Hatano, K.; Terunuma, D., *Bioorg. Med. Chem.* **2007**, *17*, 3826-3830.
151. Sakamoto, J.-I.; Koyama, T.; Miyamoto, D.; Yingsakmongkon, S.; Hidari, K. I. P. J.; Jampangern, W.; Suzuki, T.; Suzuki, Y.; Esumi, Y.; Nakamura, T.; Hatano, K.; Terunuma, D.; Matsuoka, K., *Bioorg. Med. Chem.* **2009**, *17*, 5451-5464.
152. Papp, I.; Sieben, C.; Sisson, A. L.; Kostka, J.; Böttcher, C.; Ludwig, K.; Herrmann, A.; Haag, R., *Chembiochem.* **2011**, *12*, 887-895.



# **Chapter 2.**

## **Lectin-Carbohydrate Interactions**

---

## 2.1 Background

During recent years attention has been drawn to the lectin-carbohydrate interactions since the pioneering work was conducted by Kurt Drickamer.<sup>1-3</sup> Lectin-carbohydrate interactions modulate many biological processes such as cellular recognition adhesion, cancer cell metastasis, infection of pathogens to host cells, inflammation and autoimmunity, *etc.*<sup>4-9</sup> The infection of some viruses, influenza viruses and HIV for example, is through their initial interactions with host cells by binding to oligosaccharides on the surface of the cells.<sup>10</sup>

Lectins, known as carbohydrate-binding proteins excluding enzymes and antibodies,<sup>11</sup> have been widely studied since they were first described by Peter Hermann Stillmark in 1888.<sup>12-13</sup> A wide varieties of lectins have been identified and isolated from plants, animals, virus, microbes, fungi and other micro-organisms.<sup>14-17</sup> The lectins from plants employed commonly in studies, the classification of animal lectins and examples of other lectins from toxin and bacteria are summarised in **Table 2.1**. While little is known about the functions of plant lectins,<sup>18</sup> the functions of animal lectin include<sup>6</sup> (1) binding, uptake, and killing of cells, (2) control, differentiation and organ formation (3) migration of lymphocytes from the bloodstream into the lymphoid organs and (4) tumor metastasis and invasion.

Table 2.1 Examples of lectins and their binding carbohydrates.

Source	Lectin		Carbohydrate	Ref.
Plant	Concanavalin A (ConA)		Man/Glc	17
	Peanut agglutinin (PNA)		Gal/Gal(1 → 3)GalNAc	19-20
	Wheat germ agglutinin (WGA)		GlcNAc	6
	Lens culinaris agglutinin (LCA)		Man/Glc	21
	Ricin		Gal/Lac	22
	lentil		MeαMan, MeαGlc	23
	Jacalin		Galβ3GalNAc	5
Animal	C-Type	MHL	Gal/GalNAc	24
		CHL	GlcNAc	25
		MBL	Man/ManNAc/GlcNAc/L-Fuc	26
		AHL	Man/L-fucose	27
	S-Type (Galectin)	Galectin1-15	Gal-β(1→4)GlcNAc	28-30
	P-Type	IGF-II/MPR, CD-MPR	Mannose	31-32
	I-Type (Siglecs)	CD33, Sialoadhesin	Sialic acid-containing glycans	7
Other	Cholera toxin		Galactose/ganglioside GM1	33
	Shiga toxin		Globotriaosyl ceramide	34
	Bacteria <i>FimH</i>		Mannose/Glucose	35

**MHL:** Mammalian hepatic lectin. **CHL:** Chicken hepatic lectin. **MBL:** Mannose-binding lectin.

**AHL:** Alligator hepatic lectin. **Man:** mannose. **Gal:** galactose. **Glc:** glucose. **GlcNAc:** *N*-acetylglucosamine. **CD-MPR:** cation-dependent mannose 6-phosphate receptor. **IGF-II/CI-MPR:** insulin-like growth factor II/cation-independent mannose 6-phosphate receptor.

The C-type lectins are so named due to the requirement of calcium in their binding events. The carbohydrate recognition domain (CRD), the minimum polypeptide

structure that is required for binding carbohydrate ligands (about 135 amino acids for C-type and about 130 amino acids for S-type), exhibits specific recognition with terminal monosaccharides residues depending mainly on their chelation to the  $\text{Ca}^{2+}$  ion *via* the 3- and 4-hydroxyl groups.<sup>36</sup> The use of metal ions,  $\text{Ca}^{2+}$  and  $\text{Mn}^{2+}$  for example, is essential for the interaction as these ions help shaping the binding sites of lectins, **Figure 2.1**.

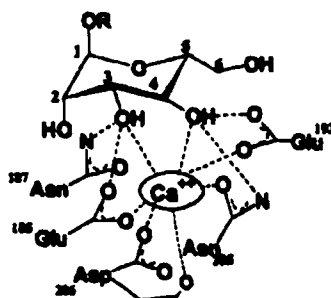


*Figure 2.1 An example of hydrogen-bonding and calcium coordination bonding patterns in the binding of a mannoside to the MBL binding sites. Ref. 26.*

The interactions between lectins and carbohydrates are mainly derived by extensive formation of hydrogen binding between the hydroxyl groups of sugars and the polar groups in the amino acid residues of the lectins. The stabilisation of the resulting complexes is generated by many possible factors in the binding processes such as Van der Waals, metal co-ordinations, hydrophobic interactions and hydrations. Hydration plays an essential role in the lectin-carbohydrate interactions as in the biological environment both lectins and carbohydrates are heavily hydrated. Besides increasing the surface area at the binding sites, water is also very important in involving the overall energy changes during the interactions.<sup>37-40</sup> The specificity of the lectin-carbohydrate interactions is achieved through the complementarity of the binding surfaces, which is related to the directional properties of the hydrogen bonding acting in the binding processes.

## 2.2 Glycoside cluster effect

The interactions of lectins with monovalent carbohydrate ligands are usually with low binding constants (for example, the affinity constant of Con A with  $\alpha$ -D-mannopyranoside is  $8.2 \times 10^3 \text{ M}^{-1}$ ),<sup>41</sup> which are too weak to produce any useful biological responses. These low affinities can be attributed to many factors in the binding processes such as the amount of water removed from lectin and ligand surfaces, the conformational changes of binding sites, and the topologies of binding sites as shallow depressions on the lectin surface instead as deep binding pockets.<sup>37</sup> However, the binding affinities can be amplified by using multivalent carbohydrate ligands. The enhancement of the affinities is normally more than that induced by the sum of binding affinities of all the individual interactions. This phenomenon was termed as the "glycoside cluster effect", which was reported first by Lee and Lee.<sup>26</sup>

The occurrence of significant affinity enhancement demands multivalent ligands with proper presentation (orientation, linker, and spacing) of binding elements interact with lectins with clustered binding sites. Although it is still very difficult to explain the exact mechanism lying behind this phenomenon using limited investigations, the origin of the enhancement of binding affinity can be related to several aspects of the multivalent interactions including intermolecular aggregation, intramolecular chelation, stability of the clustering complexes and the internal dynamic diffusion of the bound lectins, *etc.*<sup>37</sup>

In most lectin-carbohydrate interactions, the predominant reaction would be the entropically favoured intermolecular aggregation. Although a loss of entropy will be induced by constraining multiple binding elements in a closer proximity through

binding with the lectins, it will be compensated by the favourable enthalpic changes. An intramolecular chelation process can happen following the initial intermolecular interaction when no deformation or strain is generated by the interaction. This second binding will be dependent on not only the thermodynamic changes but also the nature and length of the linkers between the binding elements. The rigid and short linkers will hinder the second binding to the available binding sites, while linkers with long length and spatial distribution will allow the intramolecular interaction happen with maximum possibility. The internal dynamic diffusion of the bound lectins was recently proposed by Brewer, *et al.*,<sup>42-44</sup> which was referred as the "bind and slide" mechanism. The dynamic diffusion of bound lectin from one ligand to another can be used to explain the formation of the cross-linked complexes of lectin and multivalent carbohydrate ligands.

Further analysis on the possible mechanism involved in the lectin-carbohydrate interactions and the glycoside cluster effect can be found in several good reviews by Mammen, Choi and Whitesides in 1998,<sup>45</sup> Lundquist and Toone in 2002,<sup>46</sup> Ambrosi, Cameron and Davis in 2005,<sup>18</sup> Kiessling, Gestwicki and Strong in 2006,<sup>47</sup> Jayaraman in 2009,<sup>37</sup> Dam and Brewer in 2010.<sup>48</sup>

## 2.3 Investigation of lectin-carbohydrate interactions

The bindings between lectins and carbohydrates depend on the accessibility, valency and precise geometry of recognition elements, which are reversible and highly specific. The interactions are very complicated as any fine changes in the architectures and orientation of the ligands may influence the binding strength and selectivity of the corresponding lectin. The investigation of these interactions has

been hindered by the complexity and heterogeneity of the components on cell surfaces and by the inherent structure complexity of all kinds of carbohydrates. However, with fast development of various techniques the assays employed in studies of lectin-carbohydrate interactions become much more sophisticated and accurate. These assays vary from traditional methods such as hemagglutination inhibition assay (HIA), turbidimetry, quantitative precipitation assay (QPA), enzyme-linked lectin assay (ELLA), fluorescence titration assay (FTA), isothermal titration microcalorimetry (ITC), *etc.* to quartz crystal microbalance (QCM) and surface plasmon resonance (SPR). The improvements in the binding assays will greatly facilitate the investigation of the interactions between lectins and carbohydrates and will promote thorough understanding of various binding events.

Due to the weak binding affinities in the interactions of monovalent ligands, multivalent glycoconjugates are commonly used instead for exploration of various aspects of the corresponding interactions. The magnitude of the "glycoside cluster effect" is not directly proportional to the valency of multivalent ligands showing dependency on the assays employed. Therefore, it is necessary to update and summarise development of the studies in the lectin-carbohydrate interactions using various chemical assays, which have once been carried out by Lundquist and Toone in 2002.<sup>46</sup> The subsequent subsections will mainly focus on the screening of typical investigations into the interactions between various lectins and multivalent glycoconjugates using different binding assays in the past several years after 2002.

---

### 2.3.1 Traditional methods

The traditional assays commonly used in the evaluation of various aspects of the lectin-carbohydrate interactions are hemagglutination inhibition assay (HIA), turbidimetry, quantitative precipitation assay (QPA), enzyme-linked lectin assay (ELLA), solid-phase binding assay (SBA) and fluorescence titration assay (FTA), isothermal titration microcalorimetry (ITC) and so forth.

Red blood cells are usually aggregated in HIA.<sup>49</sup> This method reports the minimum concentration of the carbohydrate ligand which can fully inhibit the hemagglutination reaction and also reports  $IC_{50}$  values. QPA involves in the precipitation of a lectin by the interested inhibitor and generates the minimum concentration of the carbohydrate ligand that can induce fully precipitation of the lectin. Therefore, QPA can give the stoichiometry information of the resulting lectin-carbohydrate complexes.<sup>50</sup> Turbidimetry is used to investigate the rate of the interaction between lectins and their specific ligands.<sup>51</sup>

ELLA is a typical assay in the studies of lectin-carbohydrate interactions. The polymeric saccharide-coated microtiter plate wells are usually used, into which lectin-enzyme conjugates and carbohydrate ligands are added. After incubation and evacuation the wells are refilled with a prodye compound to conjugate with the enzyme for the development of colour, which is proportional to the lectin remained in the well.<sup>52</sup> SBA is similar to ELLA. Instead of using lectin-enzyme conjugates in ELLA, fluorescently labelled lectin is commonly used in SBA for the development of colour, fluorescein isothiocyanate-conjugated concanavalin A (FITC-ConA), for example.<sup>53</sup>  $IC_{50}$  values can be obtained by curve fitting from both experiments which



can show the potency of the carbohydrate ligand in inhibition reactions. As the interaction with multivalent ligand can change the average inter-receptor distances of the lectin, FTA is usually carried out for the evaluation of proximity of the lectin receptors in their conjugates with carbohydrate ligand.<sup>54</sup>

ITC is the only method for direct measurement of thermodynamic parameters such as binding constant ( $K$ ), free energy change ( $\Delta G$ ), enthalpy change ( $\Delta H$ ), entropy change ( $\Delta S$ ) and reaction stoichiometry ( $n$ ) involved in the lectin-carbohydrate interactions.<sup>55</sup> Although so much information can be obtained from ITC, only few studies employed ITC in the investigations of lectin binding events, which was mainly limited to small or dendritic glycoconjugates with valency less than six.<sup>56</sup> This is due to the relatively high amount of materials needed to conduct such an experiment and the difficulty in analysing and elucidating experimental data. It will be more complicated for the interactions between multivalent ligands and lectins due to the intrinsic structural complexity of multivalent ligands and their cross-linked precipitates with lectins. The first calorimetric study involving synthetic polymeric glycoconjugates with lectin PNA was carried out by Ambrosi, *et al.* in 2005.<sup>19</sup>

Several studies of lectin-carbohydrate interactions using different traditional assays in recent years are included in the **Table 2.2**. As mentioned above, an assay is only capable to measure one aspect of the interaction between lectin and their multivalent ligands. Usually not a single assay would be enough for the full evaluation of lectin-carbohydrate interactions. So several of these assays often needs to be combined together to obtain a useful conclusion on a specific interaction.

Polizzotti and Kiick exploited ELLA and FTA to investigate the inhibition of a bacterial lectin cholera toxin by polypeptide-based linear glycopolymers.<sup>33</sup> By modification of the carboxylic acid residues of a poly(L-glutamic acid) (PGA) backbone with amino-functionalised saccharides ( $\beta$ -D-galactosylamine or *N*-( $\epsilon$ -aminocaproyl)- $\beta$ -D-galactosylamine), a series of PGA-based glycopolymers were synthesised varying in valency and linker arm length. ELLA showed there was a decrease of the glycopolymer potency in inhibiting the adhesion of cholera toxin B<sub>5</sub> subunit to ganglioside GD1b with an increase of the valency. The glycopolymers with the 6-aminohexanoic acid linker arm exhibited better inhibition up to 3 times than those modified with  $\beta$ -D-galactosylamine. The combination of both assays was used to draw the conclusion that the interaction of cholera toxin with these glycopolymers was through a chelate effect mechanism but not through the steric or other mechanisms.

ELLA and ITC measurements were employed by Roy and co-workers for evaluation of lectin-carbohydrate interactions using a series of monovalent ligands and monodisperse synthetic glycodendrimers against bacterial adhesion.<sup>57</sup> The multivalent inhibitors of bacterial lectin PA-IL from *Pseudomonas aeruginosa* were synthesised by CuAAC click reactions using *C*-galactopyranosides, which contained 3 to 27 epitopes per ligand. A representative example of the glycodendrimers involved in the work is shown in **Figure 2.2**. However, because of the poor solubility of the ligands with high valencies in water, only di-, tri-, hexa- and nonavalent glycocusters were tested by these assays, showing up to 400-fold enhancement in avidity when compared with the monovalent reference. More analysis indicated that these well-defined *C*-galacto-conjugates were excellent

inhibitor of PA-IL and the aromatic moiety in the architectures played an important role in the recognition processes.

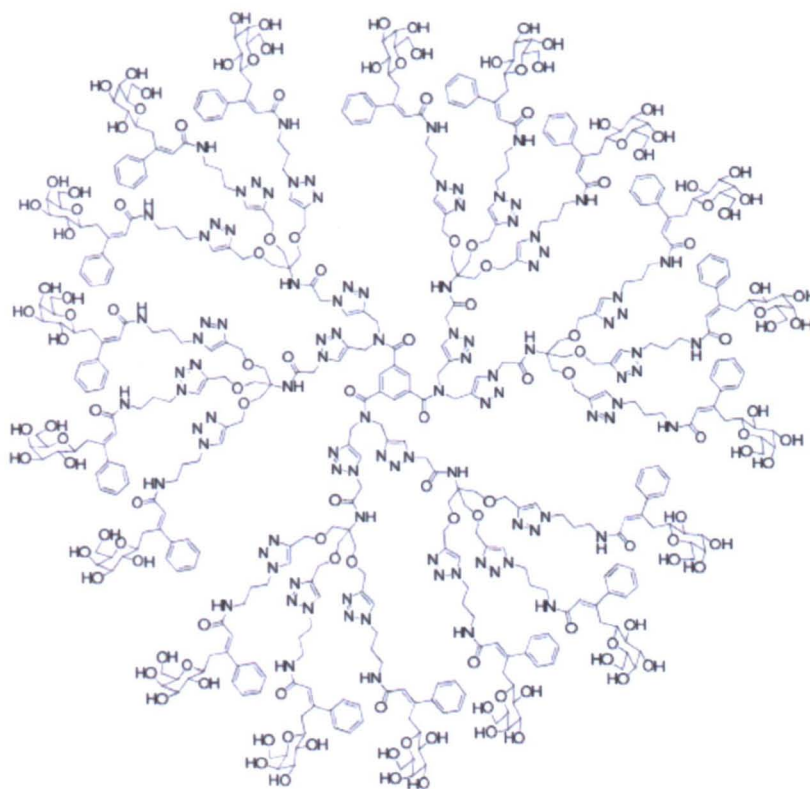


Figure 2.2 Representative glycodendrimer involved in the study against bacterial adhesion. Ref. 57.

Table 2.2 Studies of the lectin-carbohydrate interactions by traditional methods.

Lectin	Ligand	Assay	Aim	Ref.
Shiga-like toxin	P <sup>k</sup> -trisaccharide tethered dimers	ELLA	Optimisation of Tether Length	58
Shiga toxin	Heterobifunctional ligands	ELLA	Design of inhibitors	59

Pathogen <i>Actinomyces naeslundii</i>	Gal-presenting glycodendriprotein	ELLA	Inhibition of bacterial aggregation	60
Cholera toxin	Bivalent ligands	ELLA	Design of inhibitors	61
Cholera toxin	Cyclic peptide-core-based pentavalent ligands	ELLA	Multivalent ligand design	62
Cholera toxin	Monodisperse protein-Based glycopolymers	ELLA	Synthesis of monodisperse glycosylated polymers and their efficient binding	63
Cholera toxin and human serum amyloid P component	Heterobifunctional ligand	ELLA	Design of high-affinity protein ligands	64
Cholera toxin	Glycopolypeptides	ELLA	Toxin inhibition	65
Cholera toxin	Glycopolypeptides	ELLA	Evaluation of the effects of spacing and conformation in inhibition.	66
Hemagglutinin	Sialic acid-mimic peptides	ELLA	Anti-influenza therapy	67
WGA	Cyclic neoglycopeptide	ELLA	Structural basis for well-defined multivalent ligand	68
Con A	Nanoparticles obtained from multivalent polycationic glyco-	ELLA	Generation of polycationic glycoclusters as new ligands	69

	amphiphilic CDs and pDNA			
Sialoadhesin	Paucivalent synthetic sialosides	ELLA	Design of multivalent ligands.	70
PA-IIL	DNA-based glycoclusters	ELLA	Preparation of new ligands	71
galectin-1	CD-based pseudopolyrotaxanes	HIA	Inhibition of galectin-1- mediated T-cell agglutination.	72
<i>Sambucus sieboldiana</i>	Spacer- <i>N</i> -linked glycopolymers	HIA	Inhibitors of influenza virus	73
Influenza A virus	Glyconanoparticles	HIA	Inhibition of influenza virus	74
Con A  PNA	Maltose- and lactose- cyclodextrin vesicles	Turbidimetry	Study the multivalent interactions at interfaces	75
Con A	Carbohydrate- functionalised oligothiophenes	Turbidimetry	Design of electronically active inhibitors	76
RCA120, ConA, Jacalin	Multifunctional glyconanoparticles	Turbidimetry	Synthesis of multifunctional ligands	77
Con A	Carbohydrate- functionalised catanionic vesicles	Turbidimetry	Investigation of multivalent interaction at the bilayer interface	78
Con A, <i>fimH</i>	Cross-linked glycoparticles	Turbidimetry	Novel synthetic technique for glycoparticles	35
PNA	Amphiphilic diblock glycopolymers	Turbidimetry	Development of ligands in the form of micelles and porous films	79

Con A	Dendritic glycopolymer	Turbidimetry , QPA	Design of amphiphilic inhibitors	80
Con A	Amphiphilic block and triblock glycopolymers	QPA	Design of amphiphilic inhibitors	81
Galectin	Multivalent pseudopolyrotaxanes	QPA	Investigation of supramolecular ligands	82
FITC-ConA	Hyperbranched polysaccharides	FTA	Investigation of the bioactivity of hyperbranched polysaccharides	83
FITC-WGA	Sulfated glycopolymers	FTA	Design of a novel inhibitor	84
FITC-ConA FITC-RCA <sub>120</sub>	Glycopolymers with poly(vinyl alcohol) backbone	FTA	Chemoenzymatical synthesis of a new multivalent ligand	85
Galectin	Carbamate-linked lactose compounds	SBA	New lectin-binding ligands	86
Con A	Various multivalent ligands	SBA, Turbidimetry , QPA, FTA	Investigation of influences of ligand architectures on the interactions with lectin	53
Con A	Mono-, di- and tri- aromatic disulfide glycosides	ITC	Novel carbohydrate derivatives for mechanism study	87
Con A	Ferrocene-mannose conjugates	ITC	Development of electrochemical sensors	88
Con A	Unnatural monosaccharides	ITC	Study of lectin interaction with unnatural saccharides	89



Con A, PNA	Azobenzene containing glycoclusters	ITC	Design of photoswitchable multivalent ligands	90
Calreticulin	Trisaccharides	ITC	Determination of the role of various hydroxyl groups of the sugar substrates in the interaction	91
BclA lectin	Mannosylated PEO-b- PCL diblock copolymer	ITC	Drug targeting and vaccine delivery	92
Shiga-like toxin	Oligovalent carbohydrate ligands	ITC, ELLA	Design and maximisation of the avidity of ligands	93
WGA, ECA, and PA-IL	Glycosylated poly(phenylacetylene)s	ITC, HIA	Enhancement of binding affinities by three-dimensional organisation of the ligands	94
Con A	Hyperbranched polyglycerol (HPG)- based high molecular glycojugates	ITC, HIA	Synthesis of HPG- glycojugates	95

### 2.3.2 Quartz crystal microbalance biosensor with dissipation monitoring (QCM-D)

Quartz crystal microbalance biosensor with dissipation monitoring (QCM-D) technique is based on phenomenon of the piezoelectricity discovered in 1880 by the Curie brothers, that is electrical charges will be formed on the surface of some solids by pushing, pulling or torsion.<sup>96</sup> According to Sauerbrey equation (in 1959), there

exists a linear relationship between the mass adsorbed on the piezoelectric crystal surface and the crystal's resonant frequency for the formation of rigid, evenly distributed thin layers in air or vacuum without any interface slip and internal friction.<sup>97</sup> At the early stage of the microbalance biosensor, this technique was used to measure mass binding from gas phase to the quartz crystal surface.<sup>98-100</sup>

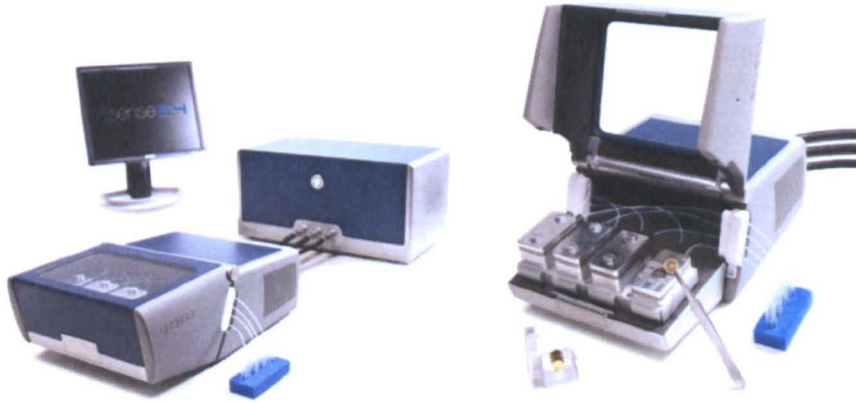


Figure 2.3 QCM-D instrument images obtained from Q-Sense website.

In QCM-D setup, **Figure 2.3**, by applying a voltage across the electrodes which are deposited on both sides of the crystal, the crystal is excited to oscillate in thickness shear mode at the fundamental resonant frequency. The frequency shift  $\Delta f$  and the coupled mass  $\Delta m$  on the crystal surface have a relationship following the Sauerbrey equation,

$$\Delta m = - \frac{C \times \Delta f}{n}$$

where  $C = 17.7 \text{ ng Hz}^{-1} \text{ cm}^{-2}$  for a 5 MHz AT-cut quartz crystal and  $n$  is the overtone number ( $n = 1, 3, 5, 7, 9, 11$ ).



By disconnecting the oscillating crystal periodically from the driver circuit, the amplitude of the crystal oscillation will decay exponentially with the following function,

$$U(t) = U_0 \exp\left(\frac{-t}{\tau}\right) \sin(2\pi ft + \varphi)$$

$U$  is the voltage over the crystal,  $\tau$  is the decay time constant and  $\varphi$  is the phase. So the energy dissipation  $D$  can be measured in this specific oscillating system<sup>101</sup> by

$$D = \frac{E_{\text{dissipated}}}{2\pi E_{\text{stored}}} = (\pi f \tau)^{-1}$$

$E_{\text{dissipated}}$  is the lost energy in the oscillation and  $E_{\text{stored}}$  is the stored energy in the system. Therefore, both of the frequency shift and energy dissipation can be monitored simultaneously.

In the 1980s solution based quartz crystal microbalance biosensor was developed.<sup>102-104</sup> However, the Sauerbrey equation needs to be modified for the system in liquid media due to the influences of viscosity and density of the liquid and the viscoelastic properties of the adsorbed film need to be taken into account.<sup>105</sup> The frequency shift will not be directly proportional to the coupled mass on the surface because of the propagation and damping of the acoustic wave through the viscoelastic film. On the other hand, the coupled water (or other liquid) by hydration, viscous drag or entrapment in cavities inside the film may contribute to the deviation from the Sauerbrey equation as well.<sup>106-107</sup> The causes of energy dissipation shift ( $D = 0$  for rigid film consistent with Sauerbrey relation) can be attributed to the ultrasonically

induced structural or conformational changes in the absorbed films, the concerted liquid, or possible interfacial processes (including slip, friction or roughness effects at the film-substrate interface or the film-liquid interface).<sup>108</sup> In this case, Voight model of viscoelastic solids,<sup>109-110</sup> Maxwell model of relaxation in highly viscous fluids,<sup>111-112</sup> and a model developed by Voinova, *et al.*<sup>113</sup> can be used to model the corresponding QCM-D responses. Therefore the simultaneous measurements of  $\Delta f$  and  $\Delta D$  in QCM-D technique can provide information not only about the mass and thickness of the absorbed films, but also the structure, conformation and dynamic viscoelastic properties of the films deposited on the crystal surface.<sup>114</sup>

The quartz crystal microbalance biosensor technique has been extensively developed and employed for many applications in recent years. As a simple, sensitive, label-free tool, it is especially suitable for the real-time investigation of biomolecular interactions such as antibody-antigen interactions,<sup>115</sup> nucleotide-protein interactions,<sup>116</sup> and biotin-avidin interactions.<sup>117</sup> The studies of biomolecular interactions using the biosensor from 2001 to 2005 have been reviewed by Cooper and Singleton.<sup>118</sup>

With the measurement of frequency shift and energy dissipation at the same time, quartz crystal microbalance with dissipation monitoring is a very attractive approach in exploration of lectin-carbohydrate interactions. Some typical investigations over the past decade are summarised in **Table 2.3**.

Table 2.3 QCM-D measurements of the lectin-carbohydrate interactions.

Lectin	Carbohydrate	Avidity constant $K_a / M^{-1}$	Ref.
Con A	Enzyme: carboxypeptidase Y	$2.17 \times 10^6$	119
Con A	Glyconanoparticles with mannoside	$1.6 \times 10^7$	41
	Glyconanoparticles with maltoside	$7.2 \times 10^7$	
Con A, HSA	Glycodendrimeric porphyrins	$(0.18 - 1.67) \times 10^5$ $(0.62 - 1.26) \times 10^5$	120
Con A, Jacalin	Maltose Fetuin	$(4.5 \pm 0.1) \times 10^2$ $(6.4 \pm 0.2) \times 10^4$	121
Con A, ECL	Self-assembled mannose monolayers Self-assembled lactose monolayers	$(8.7 \pm 2.8) \times 10^5$ $(4.6 \pm 2.4) \times 10^6$	122
Con A	Immobilised biotinylated mannotriose	$(4 - 14) \times 10^6$	123
Con A	Cross-linked glycopolymer layer	$(2.5 - 3.2) \times 10^6$	124
Shiga toxin	Biotinylated branched globotriaosyl saccharides	$(6 - 600) \times 10^6$	125

The QCM-D biosensor has also been exploited for screening the combinatorial carbohydrate libraries to determine their potential binding affinities by Pei, *et al.*<sup>126</sup> The libraries were constructed with 14 different thiols on the basis of thiol-disulfide exchanges, **Figure 2.4**. The gold-plated quartz crystals were modified with polystyrene and mannan. Con A was used as the model lectin and the inhibitory potencies of the libraries were investigated by monitoring the competition of their interactions with Con A against mannan.

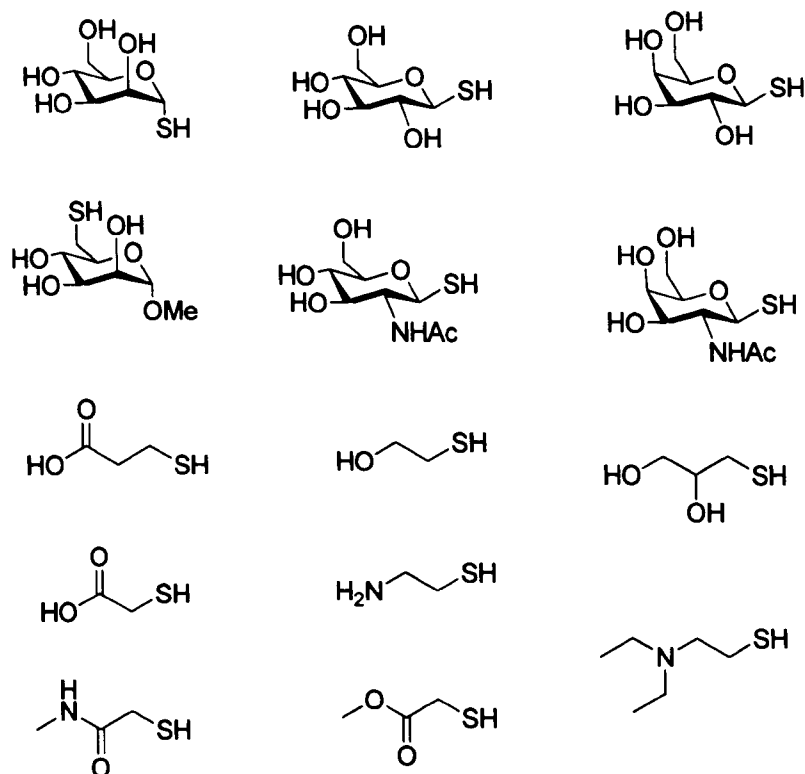


Figure 2.4 Different thiols used for the construction of carbohydrate libraries. Ref. 126.

Wang, *et al.*<sup>127</sup> prepared self-assembled monolayers (SAMs) by immobilising synthetic glycopolymer on the clean Au electrodes for screening different lectins. The glycopolymer is shown in **Figure 2.5**. The polymeric backbone was prepared by radical polymerisation of *N*-(acryloyloxy) succinimide and the ratio of mannose units, alkanethiol units and acrylamide was 1:1:1 calculated by <sup>1</sup>H NMR spectra. While the alkanethiol groups served as the linkers with gold surface, mannose units of the polymer interacted with Con A. The avidity constant of the interaction of this glycopolymer monolayer with Con A was  $1.4 \times 10^6 \text{ M}^{-1}$ .

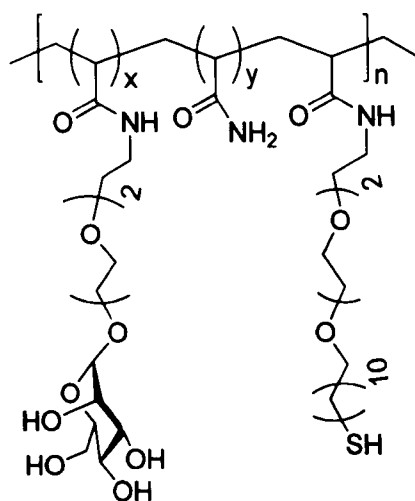


Figure 2.5 Synthetic functional glycopolymer to be immobilised on Au surface for screening different lectins. Ref. 127.

Danielsson and co-workers<sup>128</sup> investigated the interaction of various lectins with different glycoproteins. By using 10 mM PBS containing 1 mM  $\text{Ca}^{2+}$ , 1 mM  $\text{Mg}^{2+}$ , 1 mM  $\text{Mn}^{2+}$  salts, they employed 4 different lectins, which were sialic acid binding lectin *Triticum vulgaris* (WGA), fucose binding lectin *Ulex europaeus* (UEA) and mannose binding lectin *Lens culinaris* (LCA) and Concanavalin A (Con A), and 6 different serum glycoproteins, transferrin, fetuin, asialofetuin, ribonuclease A (RNase), thyroglobulin and fibrinogen. The gold-coated quartz crystal chips were modified with an alcohol solution of 1 mM 11-mercaptoundecanoic acid (MUA) overnight and then with an aqueous solution of 0.4 M 1-[3-(Dimethylamino)propyl]-3-ethyl carbodiimide (EDC) hydrochloride and 0.1 M *N*-hydroxysuccinimide NHS (1:1, v/v). The lectins were injected into the QCM-D system (0.1 mg/mL) to be immobilised on the modified gold chip surface respectively, followed by passing through different glycoproteins (1 mg/mL) over the immobilised lectin. The changes of frequencies are shown in **Figure 2.6**.

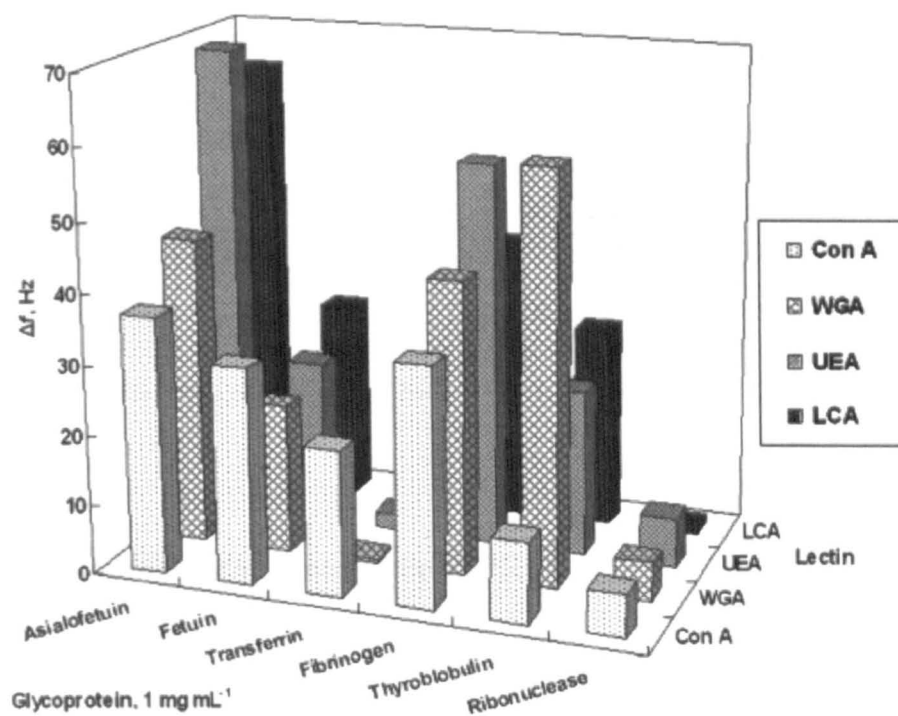


Figure 2.6 Frequency changes by binding glycoproteins onto immobilised lectin surface in the investigation of various lectins and different glycoproteins. Ref. 128.

A QCM-D biosensor was employed by Wang, *et al.*<sup>129</sup> for bacterial detection through the lectin-carbohydrate interactions, **Figure 2.7**. The binding of Con A to O-antigen on the surface of *Escherichia coli* W1485 bacteria strain facilitated adhesion of the bacteria to the self-assembled mannose monolayer immobilised on quartz crystal surface, acting as bridges to increase the contact area between the cell and the chip surface. The limit of bacterial detection by QCM-D increased greatly from  $7.5 \times 10^2$  to  $7.5 \times 10^7$ . The application of the interactions of Con A with the immobilised mannose layers enhanced significantly the sensitivity and specificity of QCM-D biosensors for detection and screening of bacteria.

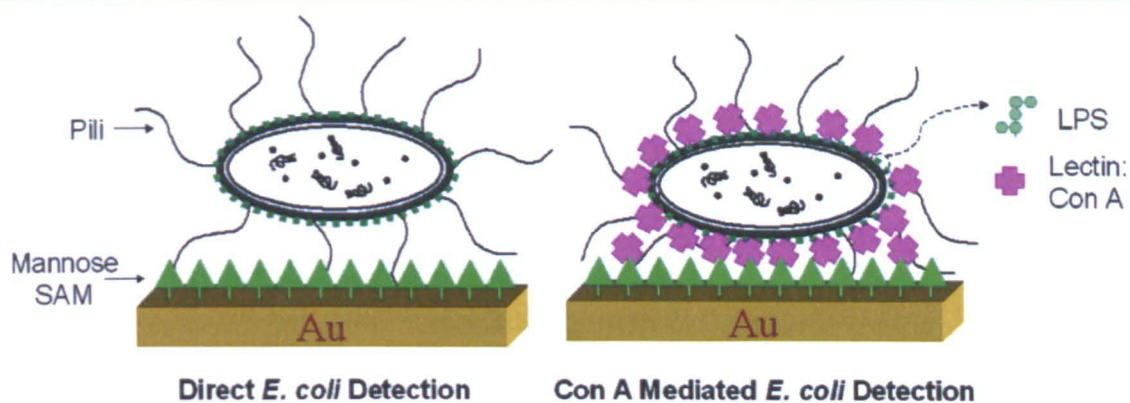


Figure 2.7 Schematic presentation of bacterial detection mediated by Con A. Ref. 129.

### 2.3.3 Surface plasmon resonance (SPR)

Although the diffraction of surface plasma waves was first described in 1902 by Wood,<sup>130</sup> it was until 1980s that SPR was first applied as the biosensor for gas detection.<sup>131-132</sup> A schematic representation of a typical SPR-sensing configuration is shown in **Figure 2.8**, in which the surface plasmon resonance is excited by attenuated total reflection (ATR) as demonstrated by Kretschmann and Raether.<sup>133</sup> The resonance of the longitudinal propagating wave along the interface of the metal and dielectric will cause energy loss, resulting in the change in density of the reflected light recorded by detectors. A variety of materials such as dextran matrix, lipid bilayer, polymer and protein can be immobilised on the silver or gold coated glass surface. During the interaction of analytes with the deposited materials on the silver/gold surface, the refractive index of the dielectric medium will change with time, which will induce a change of the angle of the convergent light in order to excite a surface plasmon resonance. By recording the changes of angle and reflectivity with time, kinetic parameters of the interaction, association and dissociation constant for example, can be obtained.<sup>134</sup> The detailed information with respect to SPR and its instrumental design can be founded in several excellent



reviews by Homola, *et al.* in 1999,<sup>135</sup> Pattnaik in 2005,<sup>136</sup> Minunni, *et al.* in 2010,<sup>137</sup> Cheng, *et al.* in 2011.<sup>138</sup>

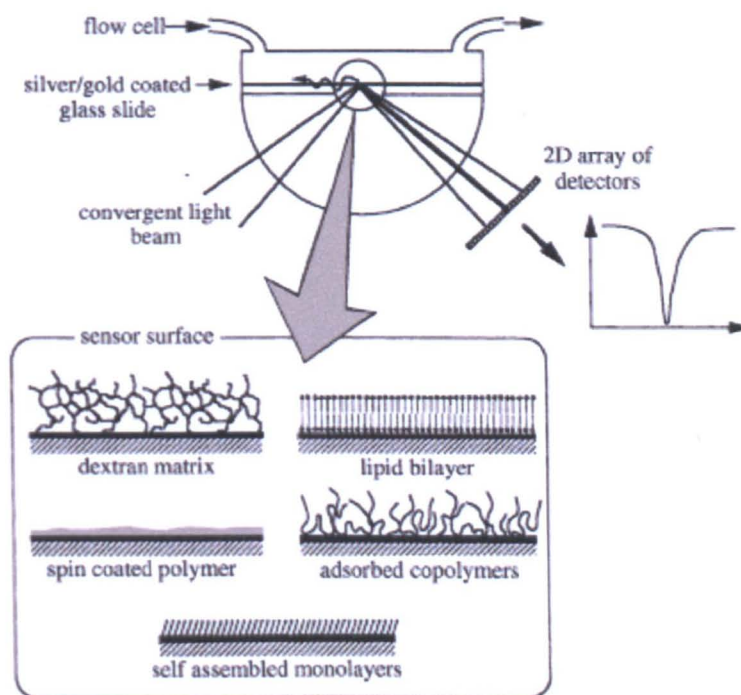


Figure 2.8 A schematic representation of a typical SPR-sensing configuration. Ref. 134.

As a similar technique to QCM-D, SPR facilitates the investigation of biological interactions with real-time, label-free, sensitive and flexible measurements. SPR has been mainly used for the analysis of various biological interactions and for the detection of many biomolecular analytes.<sup>139-143</sup> A variety of investigations of lectin-carbohydrate interactions based on SPR approach are summarised in **Table 2.4**.

Table 2.4 Investigations of lectin-carbohydrate interactions based on SPR approach.

Lectin	ligand	Technique	Aim	Ref.
L- and P-selectin	Gold colloids with carbohydrate	SPR	Effects of different ring size, polarity, configuration,	144



	mimetics.		flexibility and spacer length on the interactions	
DC-SIGN	Linear glycopolymers	SPR	Inhibition of DC-SIGN binding to the HIV envelope glycoprotein gp120	145
Con A, Lentil, WGA, <i>V. album</i> I-agglutinin, <i>Ulex</i> <i>europaeus</i> I- agglutinin, <i>Helix</i> pomatia- agglutinin	Starch and mannan, fucoidan, hyaluronic acid, <i>N</i> -acetyl- $\beta$ -D- galactosamine	SPR	Screening on lectins by SPR bio-chips	146
Con A, jacalin	Carbohydrate arrays	SPR	A new approach to study lectin- carbohydrate interactions	147
<i>E. coli</i> PapG <sub>J96</sub>	Multivalent galabiose dendrimers	HIA, SPR	Evaluation of inhibition potency by SPR	148
Con A	Mono- and bivalent ligands	ITC, SPR	Kinetic study of the interactions	149
Con A	Glycopolymers based on hyperbranched polyglycerols	QPA, turbidimetry, SPR	Synthetic approach for potential multivalent ligands	150
RCA <sub>120</sub>	Glycopolymer	ITC, SPR	Investigation of the glycoside cluster effect	151
Bacterial lectin PA-IL	Calix[4]arene Glycoconjugates	ITC, SPR	Design of inhibitor with high affinity	152

In some cases, several assays or techniques were conducted together with SPR using the same lectin and multivalent ligands in order to get a comprehensive understanding about the mechanisms involved in the interactions. HIA, ITC and SPR were employed by Vidal and co-workers<sup>153</sup> to explore the effects such as topology, flexibility and multivalency of galactose-based glycoclusters in their interactions with lectin PA-IL from *Pseudomonas aeruginosa* and lectin *Erythrina cristagalli* (ECA) respectively. QCM and SPR spectroscopy were exploited by Azzaroni, *et al.* to monitor the layer-by-layer self-assembly processes of enzyme glucose oxidase (GOx) onto the Con A modified gold electrodes.<sup>154</sup>

ELLA, ITC and SPR were exploited by Blanco, *et al.* to investigate the lectin-carbohydrate interactions using homo- and heteroglycocluster ligands and model lectin Con A,<sup>155</sup> **Figure 2.9.** By synthesising various glycodendrons from fully homogeneous  $\alpha$ -D-mannopyranoside residues to fully homogeneous  $\beta$ -D-glucopyranoside residues, they prepared a series of low-density and high-density glycoclusters with different valencies by conjugating the glycodendrons to  $\alpha$ -D-glucopyranoside and  $\beta$ CD scaffolds. While the experimental results from ELLA were in agreement with the expected affinity enhancement by an increase in the valency of the binding element, ITC results showed a heterocluster effect and the entropy-enthalpy compensation in the interactions of horseradish peroxidase (HPR) labelled Con A with  $\beta$ CD-based glycoclusters. SPR results further confirmed the heterocluster effect observed in ELLA and ITC experiments.

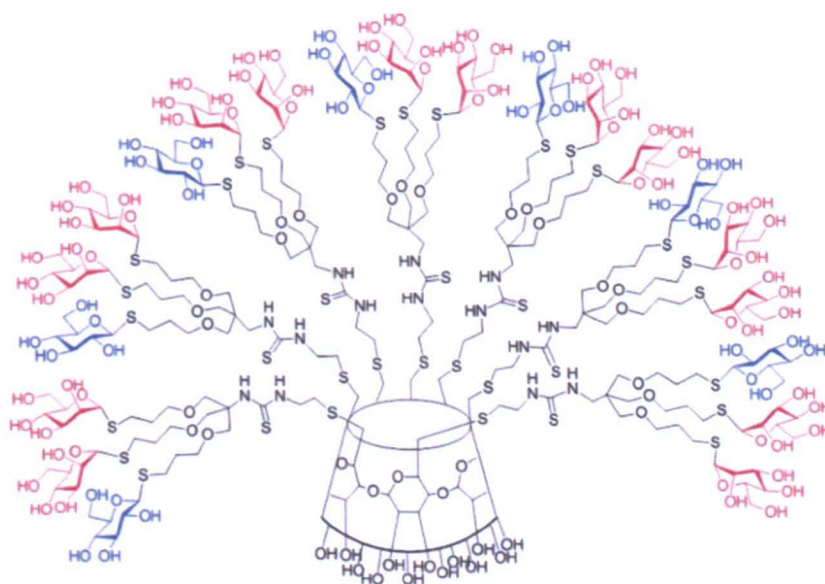


Figure 2.9 Representative heteroglycocluster based on  $\beta$ CD. Ref. 155.

Very special dodecavalent ligands on the basis of a fullerene molecule were synthesised by Vidal and co-workers,<sup>156</sup> as shown in **Figure 2.10**. Three different glycoclusters were prepared *via* CuAAC click reactions using carbohydrate-based azides or alkynes. The biological activities of these multivalent ligands were compared in their interactions with the galactose-specific bacterial lectin PA-IL from the opportunistic pathogen *Pseudomonas aeruginosa*. Different results were obtained by HIA, ELLA and SPR measurements. The results from HIA and ELLA were in a very good agreement except that the glycocluster **2** with pendant glucose showed a bigger relative potency in HIA than that in ELLA. However, in both experiments the potencies of the dodecavalent galactosylated glycoclusters increased greatly than the monovalent reference ligands due to the "glycoside cluster effect" and glycocluster **3** was better than **1** in binding. SPR results also showed the enhancement in the potencies of the galactosylated glycoclusters to inhibit the adhesion of the bacterial lectin to a galactosylated surface, although the relative potency of glycocluster **1** was larger than that of **3**. In summary, a more comprehensive understanding of the

interactions was obtained from these three combined assays than any single assay and the fullerene-based glycoclusters showed binding properties up to 12000-fold better than the monovalent references.

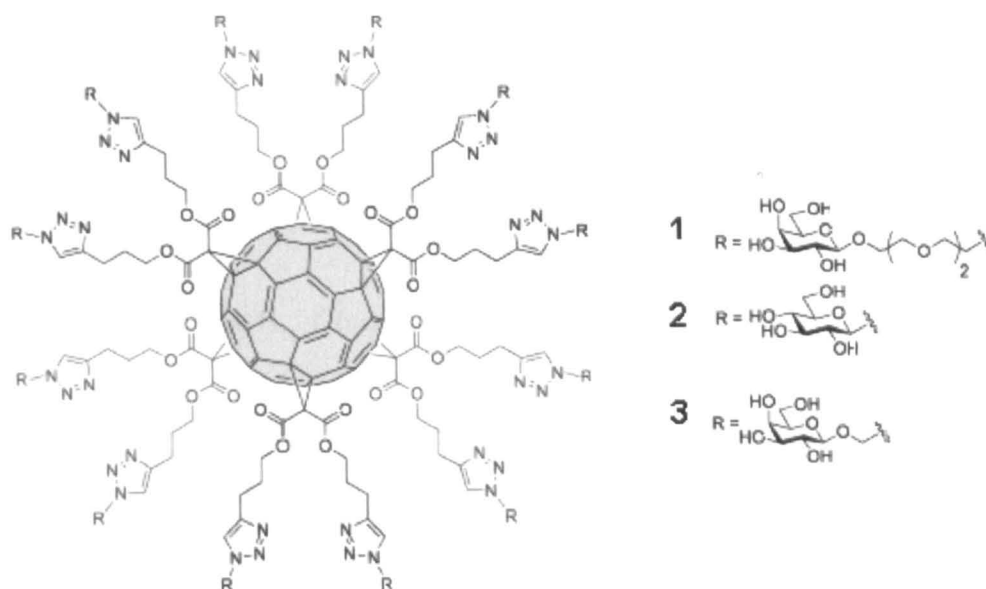


Figure 2.10 Synthesis of dodecavalent fullerene-based glycocluster. Ref. 156.

## 2.4 References

1. Drickamer, K., *J. Biol. Chem.* **1988**, 263, 9557-9560.
2. Drickamer, K., *Nature* **1992**, 360, 183-186.
3. Weis, W. I.; Drickamer, K., *Annu. Rev. Biochem.* **1996**, 65, 441-473.
4. Dwek, R. A., *Chem. Rev.* **1996**, 96, 683-720.
5. Lis, H.; Sharon, N., *Chem. Rev.* **1998**, 98, 637-674.
6. Sharon, N.; Lis, H., *Science* **1989**, 246, 227-234.

- 
7. van Kooyk, Y.; Rabinovich, G. A., *Nat. Immunol.* **2008**, *9*, 593-601.
  8. Paulson, J. C.; Blixt, O.; Collins, B. E., *Nat. Chem. Biol.* **2006**, *2*, 238-248.
  9. Nakahara, S.; Raz, A., *Anticancer Agents Med. Chem.* **2008**, *8*, 22-36.
  10. Ji, X.; Gewurz, H.; Spear, G. T., *Mol. Immunol.* **2005**, *42*, 145-152.
  11. Samuel H, B., *Trends Biochem. Sci.* **1988**, *13*, 480-482.
  12. Sharon, N.; Lis, H., *Trends Biochem. Sci.* **1987**, *12*, 488-491.
  13. Sharon, N.; Lis, H., *Glycobiology* **2004**, *14*, 53R-62R.
  14. Ting, S. R. S.; Chen, G.; Stenzel, M. H., *Polym. Chem.* **2010**, *1*, 1392-1412.
  15. David C, K., *Biochim. Biophys. Acta* **2002**, *1572*, 187-197.
  16. Loris, R.; Hamelryck, T.; Bouckaert, J.; Wyns, L., *Biochim. Biophys. Acta* **1998**, *1383*, 9-36.
  17. Gabius, H.-J.; Siebert, H.-C.; Andre, S.; Jimenez-Barbero, J.; Rudiger, H., *Chembiochem.* **2004**, *5*, 740 - 764.
  18. Ambrosi, M.; Cameron, N. R.; Davis, B. G., *Org. Biomol. Chem.* **2005**, *3*, 1593-1608.
  19. Ambrosi, M.; Cameron, N. R.; Davis, B. G.; Stolnik, S., *Org. Biomol. Chem.* **2005**, *3*, 1476-1480.
  20. Baek, M.-G.; Roy, R., *Macromol. Biosci.* **2001**, *1*, 305-311.
  21. Nagahori, N.; Nishimura, S.-I., *Biomacromolecules* **2000**, *2*, 22-24.
  22. Nagatsuka, T.; Uzawa, H.; Ohsawa, I.; Seto, Y.; Nishida, Y., *Acs Appl. Mater. Inter.* **2010**, *2*, 1081-1085.

- 
23. Loris, R.; van Overberge, D.; Dao-Thi, M.-H.; Poortmans, F.; Maene, N.; Wyns, L., *Proteins Struct. Funct. Genet.* **1994**, *20*, 330-346.
24. Hudgin, R. L. P., W. E.; Ashwell, G.; Stocked, R. J.; Morell A. G. , *J. Biol. Chem.* **1974**, *249*, 5536-5543.
25. Lunney, J.; Ashwell, G., *Proc. Natl. Acad. Sci.* **1976**, *73*, 341-343.
26. Lee, Y. C.; Lee, R. T., *Acc. Chem. Res.* **1995**, *28*, 321-327.
27. Lee, R. T.; Yang, G. C.; Kiang, J.; Bingham, J. B.; Golgher, D.; Lee, Y. C., *J. Biol. Chem.* **1994**, *269*, 19617-19625.
28. Leffler, H.; Carlsson, S.; Hedlund, M.; Qian, Y.; Poirier, F., *Glycoconjugate J.* **2002**, *19*, 433-440.
29. Hirabayashi, J.; Hashidate, T.; Arata, Y.; Nishi, N.; Nakamura, T.; Hirashima, M.; Urashima, T.; Oka, T.; Futai, M.; Muller, W. E. G.; Yagi, F.; Kasai, K.-i., *Biochim. Biophys. Acta* **2002**, *1572*, 232-254.
30. Di Lella, S.; Sundblad, V.; Cerliani, J. P.; Guardia, C. M.; Estrin, D. A.; Vasta, G. R.; Rabinovich, G. A., *Biochemistry* **2011**, *50*, 7842-7857.
31. Dahms, N. M.; Hancock, M. K., *Biochim. Biophys. Acta* **2002**, *1572*, 317-340.
32. Rini, J. M.; Lobsanov, Y. D., *Curr. Opin. Struct. Biol.* **1999**, *9*, 578-584.
33. Polizzotti, B. D.; Kiick, K. L., *Biomacromolecules* **2006**, *7*, 483-490.
34. Gargano, J. M.; Ngo, T.; Kim, J. Y.; Acheson, D. W. K.; Lees, W. J., *J. Am. Chem. Soc.* **2001**, *123*, 12909-12910.
35. Ting, S. R. S.; Min, E. H.; Zetterlund, P. B.; Stenzel, M. H., *Macromolecules* **2010**, *43*, 5211-5221.
36. Weis, W. I.; Drickamer, K.; Hendrickson, W. A., *Nature* **1992**, *360*, 127-134.
-

37. Jayaraman, N., *Chem. Soc. Rev.* **2009**, *38*, 3463-3483.
38. Elgavish, S.; Shaanan, B., *J. Mol. Biol.* **1998**, *277*, 917-932.
39. Eric J, T., *Curr. Opin. Struct. Biol.* **1994**, *4*, 719-728.
40. Chervenak, M. C.; Toone, E. J., *J. Am. Chem. Soc.* **1994**, *116*, 10533-10539.
41. Mahon, E.; Aastrup, T.; Barboiu, M., *Chem. Commun.* **2010**, *46*, 5491-5493.
42. Dam, T. K.; Brewer, C. F., *Biochemistry* **2008**, *47*, 8470-8476.
43. Dam, T. K.; Gabius, H.-J.; André, S.; Kaltner, H.; Lensch, M.; Brewer, C. F., *Biochemistry* **2005**, *44*, 12564-12571.
44. Dam, T. K.; Roy, R.; Pagé, D.; Brewer, C. F., *Biochemistry* **2001**, *41*, 1351-1358.
45. Mammen, M.; Choi, S.-K.; Whitesides, G. M., *Angew. Chem. Int. Ed.* **1998**, *37*, 2754-2794.
46. Lundquist, J.; Toone, E., *Chem. Rev.* **2002**, *102*, 555 - 578.
47. Kiessling, L. L.; Gestwicki, J. E.; Strong, L. E., *Angew. Chem. Int. Ed.* **2006**, *45*, 2348-2368.
48. Dam, T. K.; Brewer, C. F., *Glycobiology* **2010**, *20*, 270-279.
49. Osawa, T.; Matsumoto, I.; Victor, G., *Methods Enzymol.* **1972**, *28*, 323-327.
50. Islam Khan, M.; Mandal, D. K.; Brewer, C. F., *Carbohydr. Res.* **1991**, *213*, 69-77.
51. Roy, R.; Page, D.; Figueroa Perez, S.; Verez Bencomo, V., *Glycoconjugate J.* **1998**, *15*, 251-263.
52. McCoy Jr, J. P.; Varani, J.; Goldstein, I. J., *Anal. Biochem.* **1983**, *130*, 437-444.

- 
53. Gestwicki, J. E.; Cairo, C. W.; Strong, L. E.; Oetjen, K. A.; Kiessling, L. L., *J. Am. Chem. Soc.* **2002**, *124*, 14922-14933.
54. Burke, S. D.; Zhao, Q.; Schuster, M. C.; Kiessling, L. L., *J. Am. Chem. Soc.* **2000**, *122*, 4518-4519.
55. Friere, E.; Mayorga, O. L.; Straume, M., *Anal. Chem.* **1990**, *61*, 950A-959A.
56. Corbell, J. B.; Lundquist, J. J.; Toone, E. J., *Tetrahedron: Asymmetry* **2000**, *11*, 95-111.
57. Chabre, Y. M.; Giguère, D.; Blanchard, B.; Rodrigue, J.; Rocheleau, S.; Neault, M.; Rauthu, S.; Papadopoulos, A.; Arnold, A. A.; Imberty, A.; Roy, R., *Chem. Eur. J.* **2011**, *17*, 6545-6562.
58. Kitov, P. I.; Shimizu, H.; Homans, S. W.; Bundle, D. R., *J. Am. Chem. Soc.* **2003**, *125*, 3284-3294.
59. Solomon, D.; Kitov, P. I.; Paszkiewicz, E.; Grant, G. A.; Sadowska, J. M.; Bundle, D. R., *Org. Lett.* **2005**, *7*, 4369-4372.
60. Rendle, P. M.; Seger, A.; Rodrigues, J.; Oldham, N. J.; Bott, R. R.; Jones, J. B.; Cowan, M. M.; Davis, B. G., *J. Am. Chem. Soc.* **2004**, *126*, 4750-4751.
61. Pickens, J. C.; Mitchell, D. D.; Liu, J.; Tan, X.; Zhang, Z.; Verlinde, C. L. M. J.; Hol, W. G. J.; Fan, E., *Chem. Biol.* **2004**, *11*, 1205-1215.
62. Zhang, Z.; Liu, J.; Verlinde, C. L. M. J.; Hol, W. G. J.; Fan, E., *J. Org. Chem.* **2004**, *69*, 7737-7740.
63. Wang, Y.; Kiick, K. L., *J. Am. Chem. Soc.* **2005**, *127*, 16392-16393.
64. Liu, J.; Zhang, Z.; Tan, X.; Hol, W. G. J.; Verlinde, C. L. M. J.; Fan, E., *J. Am. Chem. Soc.* **2005**, *127*, 2044-2045.
65. Polizzotti, B. D.; Maheshwari, R.; Vinkenburg, J.; Kiick, K. L., *Macromolecules* **2007**, *40*, 7103-7110.
66. Liu, S.; Kiick, K. L., *Macromolecules* **2008**, *41*, 764-772.
-



- 
67. Matsubara, T.; Onishi, A.; Saito, T.; Shimada, A.; Inoue, H.; Taki, T.; Nagata, K.; Okahata, Y.; Sato, T., *J. Med. Chem.* **2010**, *53*, 4441-4449.
68. Schwefel, D.; Maierhofer, C.; Beck, J. G.; Seeberger, S.; Diederichs, K.; Möller, H. M.; Welte, W.; Wittmann, V., *J. Am. Chem. Soc.* **2010**, *132*, 8704-8719.
69. Díaz-Moscoso, A.; Guilloteau, N.; Bienvenu, C.; Méndez-Ardoy, A.; Jiménez Blanco, J. L.; Benito, J. M.; Le Gourriérec, L.; Di Giorgio, C.; Vierling, P.; Defaye, J.; Ortiz Mellet, C.; García Fernández, J. M., *Biomaterials* **2011**, *32*, 7263-7273.
70. Kalovidouris, S. A.; Blixt, O.; Nelson, A.; Vidal, S.; Turnbull, W. B.; Paulson, J. C.; Stoddart, J. F., *J. Org. Chem.* **2003**, *68*, 8485-8493.
71. Morvan, F.; Meyer, A.; Jochum, A.; Sabin, C.; Chevolot, Y.; Imberty, A.; Praly, J.-P.; Vasseur, J.-J.; Souteyrand, E.; Vidal, S., *Bioconjugate Chem.* **2007**, *18*, 1637-1643.
72. Nelson, A.; Belitsky, J. M.; Vidal, S.; Joiner, C. S.; Baum, L. G.; Stoddart, J. F., *J. Am. Chem. Soc.* **2004**, *126*, 11914-11922.
73. Ogata, M.; Hidari, K. I. P. J.; Kozaki, W.; Murata, T.; Hiratake, J.; Park, E. Y.; Suzuki, T.; Usui, T., *Biomacromolecules* **2009**, *10*, 1894-1903.
74. Papp, I.; Sieben, C.; Sisson, A. L.; Kostka, J.; Böttcher, C.; Ludwig, K.; Herrmann, A.; Haag, R., *ChemBiochem.* **2011**, *12*, 887-895.
75. Voskuhl, J.; Ravoo, B. J., *Langmuir* **2011**, *27*, 1391-1397.
76. Schmid, S.; Mishra, A.; Bauerle, P., *Chem. Commun.* **2011**, *47*, 1324-1326.
77. Deng, Z.; Li, S.; Jiang, X.; Narain, R., *Macromolecules* **2009**, *42*, 6393-6405.
78. Thomas, G. B.; Rader, L. H.; Park, J.; Abezgauz, L.; Danino, D.; DeShong, P.; English, D. S., *J. Am. Chem. Soc.* **2009**, *131*, 5471-5477.
79. Ting, S. R. S.; Min, E. H.; Escalé, P.; Save, M.; Billon, L.; Stenzel, M. H., *Macromolecules* **2009**, *42*, 9422-9434.
-

- 
80. Kumar, J.; Bousquet, A.; Stenzel, M. H., *Macromol. Rapid Commun.* **2011**, n/a-n/a.
81. León, O.; Muñoz-Bonilla, A.; Bordegé, V.; Sánchez-Chaves, M.; Fernández-García, M., *J. Polym. Sci., Part A: Polym. Chem.* **2011**, *49*, 2627-2635.
82. Belitsky, J. M.; Nelson, A.; Hernandez, J. D.; Baum, L. G.; Stoddart, J. F., *Chem. Biol.* **2007**, *14*, 1140-1151.
83. Hoai, N. T.; Sasaki, A.; Sasaki, M.; Kaga, H.; Kakuchi, T.; Satoh, T., *Biomacromolecules* **2011**, *12*, 1891-1899.
84. Miura, Y.; Yasuda, K.; Yamamoto, K.; Koike, M.; Nishida, Y.; Kobayashi, K., *Biomacromolecules* **2007**, *8*, 2129-2134.
85. Miura, Y.; Ikeda, T.; Kobayashi, K., *Biomacromolecules* **2003**, *4*, 410-415.
86. André, S.; Specker, D.; Bovin, N. V.; Lensch, M.; Kaltner, H.; Gabius, H.-J.; Wittmann, V., *Bioconjugate Chem.* **2009**, *20*, 1716-1728.
87. Murthy, B. N.; Sinha, S.; Surolia, A.; Jayaraman, N.; Szilágyi, L.; Szabó, I.; Kövér, K. E., *Carbohydr. Res.* **2009**, *344*, 1758-1763.
88. Casas-Solvas, J. M.; Ortiz-Salmeron, E.; Garcia-Fuentes, L.; Vargas-Berenguel, A., *Org. Biomol. Chem.* **2008**, *6*, 4230-4235.
89. Castro, S.; Duff, M.; Snyder, N. L.; Morton, M.; Kumar, C. V.; Peczuh, M. W., *Org. Biomol. Chem.* **2005**, *3*, 3869-3872.
90. Srinivas, O.; Mitra, N.; Surolia, A.; Jayaraman, N., *Glycobiology* **2005**, *15*, 861-873.
91. Gupta, G.; Gemma, E.; Oscarson, S.; Surolia, A., *Glycoconjugate J.* **2008**, *25*, 797-802.
92. Rieger, J.; Stoffelbach, F.; Cui, D.; Imberty, A.; Lameignere, E.; Putaux, J.-L.; Jérôme, R.; Jérôme, C.; Auzély-Velty, R., *Biomacromolecules* **2007**, *8*, 2717-2725.
93. Kitov, P. I.; Bundle, D. R., *J. Am. Chem. Soc.* **2003**, *125*, 16271-16284.
-

- 
94. Otsuka, I.; Blanchard, B.; Borsali, R.; Imberty, A.; Kakuchi, T., *Chembiochem.* **2010**, *11*, 2399-2408.
95. Kizhakkedathu, J. N.; Creagh, A. L.; Shenoi, R. A.; Rossi, N. A. A.; Brooks, D. E.; Chan, T.; Lam, J.; Dandepally, S. R.; Haynes, C. A., *Biomacromolecules* **2010**, *11*, 2567-2575.
96. J. Curie, P. C., *Comptes rendus* **1880**, *91*, 294-297.
97. Sauerbrey, G., *Z Physics* **1959**, *155*, 206-222.
98. King, W. H., *Anal. Chem.* **1964**, *36*, 1735-1739.
99. Guilbault, G. G., *Anal. Chem.* **1983**, *55*, 1682-1684.
100. Konash, P. L.; Bastiaans, G. J., *Anal. Chem.* **1980**, *52*, 1929-1931.
101. Hemmersam, A. G.; Rechendorff, K.; Besenbacher, F.; Kasemo, B.; Sutherland, D. S., *J. Phys. Chem. C* **2008**, *112*, 4180-4186.
102. Ward, M. D.; Buttry, D. A., *Science* **1990**, *249*, 1000-1007.
103. Nomura, T.; Okuhara, M., *Anal. Chim. Acta* **1982**, *142*, 281-284.
104. Nomura, T.; Watanabe, M.; West, T. S., *Anal. Chim. Acta* **1985**, *175*, 107-116.
105. K.K. Kanazawa, J. G. G., *Anal. Chem.* **1985**, *175*, 99-105
106. Höök, F.; Kasemo, B.; Nylander, T.; Fant, C.; Sott, K.; Elwing, H., *Anal. Chem.* **2001**, *73*, 5796-5804.
107. Bingen, P.; Wang, G.; Steinmetz, N. F.; Rodahl, M.; Richter, R. P., *Anal. Chem.* **2008**, *80*, 8880-8890.
108. Höök, F.; Rodahl, M.; Brzezinski, P.; Kasemo, B., *Langmuir* **1998**, *14*, 729-734.
-

- 
109. Voinova, M. V.; Rodahl, M.; Jonson, M.; Kasemo, B., *Phys. Scr.* **1999**, *59*, 391.
110. Johannsmann, D., *Macromol. Chem. Phys.* **1999**, *200*, 501-516.
111. Zhang, Y.; Du, B.; Chen, X.; Ma, H., *Anal. Chem.* **2008**, *81*, 642-648.
112. Razumovitch, J.; de Franca, K.; Kehl, F.; Wiki, M.; Meier, W.; Vebert, C., *J. Phys. Chem. B* **2009**, *113*, 8383-8390.
113. Voinova, M. V.; Jonson, M.; Kasemo, B., *Biosens. Bioelectron.* **2002**, *17*, 835-841.
114. Rodahl, M.; Kasemo, B., *Sensor Actuat. B-Chem.* **1996**, *37*, 111-116.
115. Zhang, J.; Su, X. D.; O'Shea, S. J., *Biophys. Chem.* **2002**, *99*, 31-41.
116. Niikura, K.; Matsuno, H.; Okahata, Y., *J. Am. Chem. Soc.* **1998**, *120*, 8537-8538.
117. Slavin, S.; De Cuendias, A.; Ladmiral, V.; Haddleton, D. M., *J. Polym. Sci., Part A: Polym. Chem.* **2010**, *49*, 1163-1173.
118. Cooper, M. A.; Singleton, V. T., *J. Mol. Recognit.* **2007**, *20*, 154-184.
119. Lebed, K.; Kulik, A. J.; Forr, L.; Lekka, M., *J. Colloid Interf. Sci.* **2006**, *299*, 41-48.
120. Makky, A.; Michel, J. P.; Kasselouri, A.; Briand, E.; Maillard, P.; Rosilio, V., *Langmuir* **2010**, *26*, 12761-12768.
121. Pedroso, M. M.; Watanabe, A. M.; Roque-Barreira, M. C.; Bueno, P. R.; Faria, R. C., *Microchem. J.* **2008**, *89*, 153-158.
122. Zhang, Y.; Luo, S.; Tang, Y.; Yu, L.; Hou, K.-Y.; Cheng, J.-P.; Zeng, X.; Wang, P. G., *Anal. Chem.* **2006**, *78*, 2001-2008.
123. Mori, T.; Toyoda, M.; Ohtsuka, T.; Okahata, Y., *Anal. Biochem.* **2009**, *395*, 211-216.
-

- 
124. Yu, L.; Huang, M.; Wang, P. G.; Zeng, X., *Anal. Chem.* **2007**, *79*, 8979-8986.
125. Mori, T.; Ohtsuka, T.; Okahata, Y., *Langmuir* **2010**, *26*, 14118-14125.
126. Pei, Z.; Larsson, R.; Aastrup, T.; Anderson, H.; Lehn, J.-M.; Ramström, O., *Biosens. Bioelectron.* **2006**, *22*, 42-48.
127. Huang, M.; Shen, Z.; Zhang, Y.; Zeng, X.; Wang, P. G., *Biorg. Med. Chem. Lett.* **2007**, *17*, 5379-5383.
128. Yakovleva, M. E.; Safina, G. R.; Danielsson, B., *Anal. Chim. Acta* **2010**, *668*, 80-85.
129. Shen, Z.; Huang, M.; Xiao, C.; Zhang, Y.; Zeng, X.; Wang, P. G., *Anal. Chem.* **2007**, *79*, 2312-2319.
130. Wood, R. W., *Phil. Mag.* **1902**, *4*, 396-402.
131. Nylander, C.; Liedberg, B.; Lind, T., *Sens. Actuators* **1982**, *3*, 79-88.
132. Liedberg, B.; Nylander, C.; Lunström, I., *Sens. Actuators* **1983**, *4*, 299-304.
133. Kretschmann, E.; Raether, H., *Z. Naturforsch.* **1968**, *23A*, 2135-2136.
134. Green, R. J.; Frazier, R. A.; Shakesheff, K. M.; Davies, M. C.; Roberts, C. J.; Tendler, S. J. B., *Biomaterials* **2000**, *21*, 1823-1835.
135. Homola, J.; Yee, S. S.; Gauglitz, G., *Sensor Actuat. B-Chem.* **1999**, *54*, 3-15.
136. Pattnaik, P., *Appl. Biochem. Biotechnol.* **2005**, *126*, 79-92.
137. Scarano, S.; Mascini, M.; Turner, A. P. F.; Minunni, M., *Biosens. Bioelectron.* **2010**, *25*, 957-966.
138. Abbas, A.; Linman, M. J.; Cheng, Q., *Biosens. Bioelectron.* **2011**, *26*, 1815-1824.
139. Homola, J., *Anal. Bioanal. Chem.* **2003**, *377*, 528-539.
-

- 
140. de la Fuente, J.; Penadés, S., *Glycoconjugate J.* **2004**, *21*, 149-163.
141. Boozer, C.; Kim, G.; Cong, S.; Guan, H.; Londergan, T., *Curr. Opin. Biotechnol.* **2006**, *17*, 400-405.
142. Berggård, T.; Linse, S.; James, P., *Proteomics* **2007**, *7*, 2833-2842.
143. Campbell, C. T.; Kim, G., *Biomaterials* **2007**, *28*, 2380-2392.
144. Roskamp, M.; Enders, S.; Pfrengle, F.; Yekta, S.; Dekaris, V.; Dervede, J.; Reissig, H.-U.; Schlecht, S., *Org. Biomol. Chem.* **2011**.
145. Becer, C. R.; Gibson, M. I.; Geng, J.; Ilyas, R.; Wallis, R.; Mitchell, D. A.; Haddleton, D. M., *J. Am. Chem. Soc.* **2010**, *132*, 15130-15132.
146. Vornholt, W.; Hartmann, M.; Keusgen, M., *Biosens. Bioelectron.* **2007**, *22*, 2983-2988.
147. Smith, E. A.; Thomas, W. D.; Kiessling, L. L.; Corn, R. M., *J. Am. Chem. Soc.* **2003**, *125*, 6140-6148.
148. Salminen, A.; Loimaranta, V.; Joosten, J. A. F.; Khan, A. S.; Hacker, J.; Pieters, R. J.; Finne, J., *J. Antimicrob. Chemother.* **2007**, *60*, 495-501.
149. Murthy, B.; Sinha, S.; Surolia, A.; Indi, S.; Jayaraman, N., *Glycoconjugate J.* **2008**, *25*, 313-321.
150. Papp, I.; Dervede, J.; Enders, S.; Riese, S. B.; Shiao, T. C.; Roy, R.; Haag, R., *Chembiochem.* **2011**, *12*, 1075-1083.
151. Spain, S. G.; Cameron, N. R., *Polym. Chem.* **2011**, *2*, 1552-1560.
152. Cecioni, S.; Lalor, R.; Blanchard, B.; Praly, J.-P.; Imberty, A.; Matthews, S. E.; Vidal, S., *Chem. Eur. J.* **2009**, *15*, 13232-13240.
153. Cecioni, S.; Faure, S.; Darbost, U.; Bonnamour, I.; Parrot-Lopez, H.; Roy, O.; Taillefumier, C.; Wimmerová, M.; Praly, J.-P.; Imberty, A.; Vidal, S., *Chem. Eur. J.* **2011**, *17*, 2146-2159.
-

154. Pallarola, D.; Queralto, N.; Battaglini, F.; Azzaroni, O., *Phys. Chem. Chem. Phys.* **2010**, *12*, 8071-8083.
155. Gomez-Garcia, M.; Benito, J. M.; Gutierrez-Gallego, R.; Maestre, A.; Mellet, C. O.; Fernandez, J. M. G.; Blanco, J. L. J., *Org. Biomol. Chem.* **2010**, *8*, 1849-1860.
156. Cecioni, S.; Oerthel, V.; Iehl, J.; Holler, M.; Goyard, D.; Praly, J.-P.; Imberty, A.; Nierengarten, J.-F.; Vidal, S., *Chem. Eur. J.* **2011**, *17*, 3252-3261.

## **Chapter 3.**

# **Synthesis of Glycopolymers *via* the Combination of CCTP and Click Chemistry**



### 3.1 Introduction

Synthetic glycopolymers containing pendant saccharide moieties have been employed as multivalent natural oligosaccharide mimics in many biological and biomedical applications such as macromolecular drugs and drug delivery systems.<sup>1-6</sup> In order to develop novel glycopolymeric drugs and therapeutic agents, numerous efforts have been devoted to the synthesis of glycopolymers.<sup>7-11</sup> With the development of synthetic technologies in recent years, it is now possible to prepare well-defined glycopolymers either by polymerisation of glycomonomers<sup>12-16</sup> or by post-functionalisation of precursor polymers.<sup>17-19</sup>

Narain, *et al.* reported the first synthesis of glycopolymers by atom transfer radical polymerisation (ATRP) without any protection of the carbohydrate hydroxyl groups.<sup>20-21</sup> Although a few papers also showed the polymerisation of unprotected monomer afterwards,<sup>12, 14, 22</sup> most ATRP requires the protection of glycomonomers.<sup>13, 15, 23</sup> Kiessling and co-workers synthesised a series of glycopolymers by ring-opening metathesis polymerisation (ROMP) using mannose- and galactose-substituted monomers.<sup>24</sup> Whilst Stenzel, *et al.* employed radical addition-fragmentation chain-transfer (RAFT) polymerisation to prepare glycopolymers from a glucose-substituted glycomonomer.<sup>25</sup> RAFT has been a useful tool to prepare glycopolymers<sup>26-30</sup> since Lowe and co-workers successfully did the polymerisation of 2-methacryloxyethyl glucoside *via* RAFT in aqueous media in 2003<sup>31</sup>.

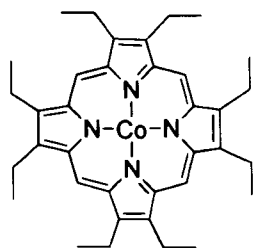
However, direct polymerisation often needs additional steps for the synthesis and purification of glycomonomers which have tendency to self-polymerise. In this case,

the post-functionalisation strategy shows a promising way to the synthesis of glycopolymers, especially when modern synthetic techniques make it possible to synthesise a wide range of well-defined reactive polymer scaffolds from simple monomers. One of the most attractive methods involved in the synthesis of glycopolymers is post-functionalisation of a *clickable* precursor polymer *via* click chemistry which are prepared by controlled/living radical polymerisation.<sup>32</sup> In this present work, catalytic chain transfer polymerisation (CCTP) was employed to prepare the clickable polymer scaffolds, which were then used to synthesise glycopolymers *via* post-modification by click chemistry.

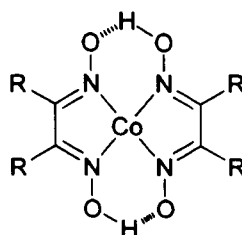
### 3.1.1 Catalytic chain transfer polymerisation (CCTP)

As a controlled radical polymerisation technique, catalytic chain transfer was first discovered in 1975 by Boris Smirnov and Alexander Marchenko working on cobalt porphyrin chemistry for the polymerisation of methacrylates.<sup>33</sup> Unlike porphyrins, cobaloximes (with a similar structure to coenzyme B<sub>12</sub>) were found to be much more effective catalysts for CCTP.<sup>34</sup> Moreover, the properties of cobaloxime mediated polymerisation such as low levels of colour and toxicity, good solubility and tunable ligand structure made them the most developed chain transfer agents for CCTP,<sup>35-38</sup>

**Figure 3.1.** Although some complexes of chromium and molybdenum also show chain transfer activity, the control of molecular weight and polydispersity by these compounds is limited.<sup>39-40</sup>



Cobalt Porphyrin



Cobaloximes

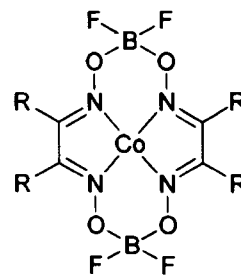


Figure 3.1 Catalysts commonly used in CCTP. Ref. 33 ~ 38.

The widely accepted mechanism<sup>41-42</sup> for CCTP catalysed by cobalt<sup>(II)</sup> chelates is shown in **Figure 3.2**. The cobalt(II) complex can abstract one hydrogen from the growing polymer chain to give abstraction product and cobalt hydride. The cobalt hydride can then reinitiate the vinyl group of the monomer or the abstraction product and result in the regeneration of the cobalt(II) catalyst. Hence, the concentration of cobalt(II) remains steady during the polymerisation. In fact, the carbon-centred radicals can act as the reducing agent to give cobalt(II) form continuously during the polymerisation even if cobalt(III) chelates is employed to start with the reaction.<sup>35</sup> However, the cobalt(III) complexes cannot be the catalysts in CCTP as they are not able to abstract a hydrogen from the growing polymer chain. Besides oxidation to cobalt(III), the cobalt(II) catalyst can also be poisoned *via* reduction to cobalt(I) complex by a proton acceptor such as an amine, OH<sup>-</sup>, or an aprotic solvent. Therefore, CCTP is not suitable for basic monomers (*i.e.* amino methacrylates).<sup>33</sup>

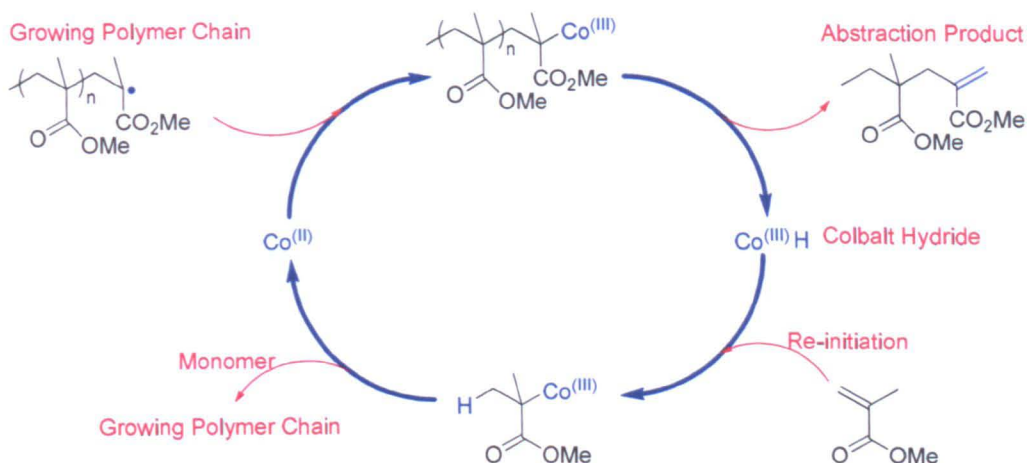


Figure 3.2 Proposed mechanism for CCTP of methacrylates catalysed by cobalt chelates. Ref. 41 and 42.

The catalytic chain transfer constant  $C_S$  (the ratio of chain transfer and propagation rate coefficients,  $k_{tr}/k_p$ ) is used to define the efficiency of the catalyst. The magnitude of  $C_S$  value depends on the structure of both the chain transfer agent and the attacking radicals. The higher the  $C_S$  value, the lower concentration of the catalyst required for a certain molecular weight. Although a chain length distribution (CLD) procedure<sup>43-47</sup> has been employed in the measurement of chain transfer constant, the most commonly used method is the use of Mayo equation,<sup>48-50</sup>

**Equation 3.1.1.** As the equation is based on the assumption of long chain and steady-state, so it is applicable for polymerisations with small conversions and the rate constants are chain length independent. The number average degree of polymerisation ( $\text{DP}_n$ ) is usually obtained from SEC analysis of the number average molecular weight ( $M_n$ ) or the weight average molecular weight ( $M_w$ ). The straight line of  $1/\text{DP}_n$  vs  $[\text{Chain transfer agent}]/[\text{Monomer}]$  gives the  $C_S$  value as the slope. The chain transfer constants of cobaloximes in CCTP can reach up to  $10^9$ , which indicates their catalytic activities are even comparable with those of enzymes.<sup>33</sup>

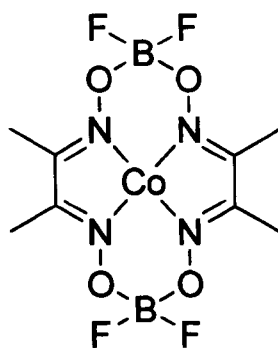
$$\frac{1}{DP_n} = \frac{1}{DP_n^0} + C_s \frac{[\text{Transfer agent}]}{[\text{Monomer}]} \quad (3.1.1)$$

$DP_n$  = degree of polymerisation with transfer agent

$DP_n^0$  = degree of polymerisation without transfer agent

$C_s$  = chain transfer constant

The appearance of bis(boron difluorodimethylglyoximate) cobalt(II) (CoBF) as the chain transfer agent was a great achievement towards the commercial application of CCTP.<sup>51</sup> Usually the cobaloximes complexes can be very sensitive to oxidation and hydrolysis, However, this is reduced by the introduction of the  $BF_2$  bridges in the structure of CoBF, **Figure 3.3**. Thus, CoBF is air-stable in the solid state, although anaerobic conditions are usually required to keep the catalytic activity in CoBF solutions with the stability being very solvent dependant.<sup>52</sup> The chain transfer constant of the CoBF catalysed CCTP of various monomers are shown in **Table 3.1**.



CoBF

Figure 3.3 CoBF as the catalyst in CCTP. Ref. 51.

Table 3.1  $C_S$  Values of CCTP at 60 °C using CoBF as the chain transfer agent.

Monomer	Solvent	$C_S$ value	Ref.
MMA	bulk	20700 - 40900	53,54, 55-56
	toluene	41000 - 59600	57
	methanol	10100	55
EMA	bulk	27000	54
BMA	bulk	16000	54
MA	bulk	8	58
BA	bulk	650	57
STY	bulk	290 – 6900	56, 57

Besides controlling molecular weight, CCTP has other advantages over traditional chain transfer in radical polymerisation. Very small amount (*i.e.* ppm) of chain transfer agents is needed to prepare polymers of low molecular weights, which can greatly simplify purification procedures to remove catalyst from the product. The unsaturated vinyl bond at the end of every polymer chain remains available for post-reactions.<sup>57</sup> The macromonomers obtained by CCTP have been used for copolymerisation with monomers such as methacrylates,<sup>59-61</sup> acrylates and styrene.<sup>62</sup>

### 3.1.2 Click chemistry

Since the term “click chemistry” was defined in 2001 by Sharpless and co-workers,<sup>63</sup> there has been a huge development of this synthetic philosophy in polymer chemistry,<sup>64-67</sup> nanomaterials,<sup>68-69</sup> drug discovery<sup>70</sup>, bioconjugation,<sup>71-74</sup> *etc.*. Several

reviews are very useful for a comprehensive understanding of click chemistry.<sup>75-79</sup> In order to be included in the toolbox of click chemistry, such requirements need to be fulfilled by the reaction:

- Modular, readily available starting materials, wide in scope;
- Stereoselective, high yields, simple reaction condition;
- No solvent or only benign solvent, simple product purification without any need of chromatography.

Huisgen copper-catalysed azide–alkyne cycloaddition (CuAAC) is an extremely successful example among all the click reactions.<sup>80-83</sup> CuAAC is a straightforward, efficient, robust, orthogonal ligation tool for the covalent connections of various functional groups. It has been utilised in a wide range of fields such as design of novel polymer materials, macromolecular engineering, bioconjugation, synthesis of functional nanomaterials, synthesis of lead discovery libraries, tagging of live organisms and proteins, activity-based protein profiling and labeling of DNA.<sup>84-90</sup>

The 1,3-dipolar cycloaddition of azides and terminal alkynes without catalyst was discovered in 1893 by Arthur Michael<sup>91</sup> and then developed by Rolf Huisgen.<sup>92-93</sup> In the original cycloaddition process, both 1,4- and 1,5-triazole regioisomers can be generated simultaneously, **Figure 3.4**.

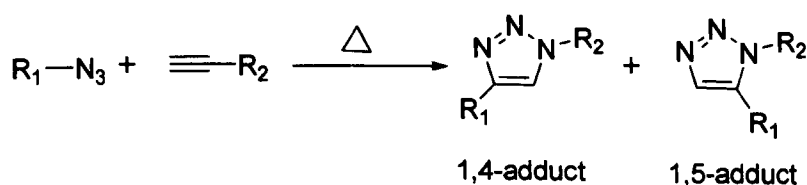


*Figure 3.4 The preliminary 1,3-dipolar cycloaddition of azides and alkynes. Ref. 92 and 93.*

However, in 2002 K. Barry Sharpless<sup>94</sup> and Morten Meldal<sup>95</sup> independently discovered that with addition of copper(I) catalysts, the reaction could be highly efficient and regioselective at ambient temperature in organic media or even in polar media, such as ethanol or pure water. Only 1,4-disubstituted 1,2,3-triazole heterocycles are generated in the CuAAC reaction, **Figure 3.5**.

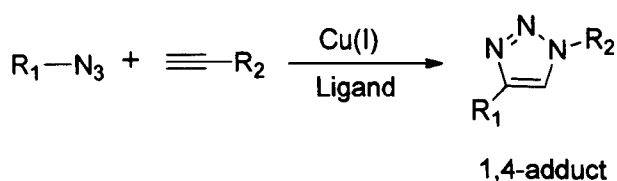


*Figure 3.5 Copper(I)-catalysed azide–alkyne cycloadditions (CuAAC). Ref. 94 and 95.*

Since its discovery, CuAAC has been employed in various reaction conditions, solvents, additives, functional groups and catalysts. For the improvement and expansion of CuAAC, different catalyst systems (Copper(I) salts or coordination complexes) and various ligands have been investigated.<sup>96</sup> Cu(I) is the most reactive oxidation state of copper in CuAAC while element copper is less efficient in catalysing this reaction. Though Cu(II) cannot catalyse the reaction directly, it can be used with combination of an ascorbate reducing agent.<sup>94</sup> The use of ligands can stabilise the Cu(I) oxidation state in the reaction media and accelerate the CuAAC reaction. While bipyridine,<sup>64</sup> tris(benzyltriazolylmethyl) amine (TBTA)<sup>7</sup> and phosphine complexes<sup>97-98</sup> such as Cu(P(OMe)<sub>3</sub>)<sub>3</sub>Br and Cu(PPh<sub>3</sub>)<sub>2</sub>OAc were used for CuAAC in organic solvents, ligands for use in aqueous solution have also been discovered.<sup>80</sup>



Despite the simple reaction conditions, the mechanism of CuAAC is quite complicated and has not yet been well understood. The proposed mechanism is shown in **Figure 3.6**.<sup>80, 83</sup> The efficiency of CuAAC is based on the reactivity of the *in situ* formed copper(I) acetylides. The presence of organic azides can prevent the formation of unreactive aggregated Cu(I) acetylides.<sup>99</sup>

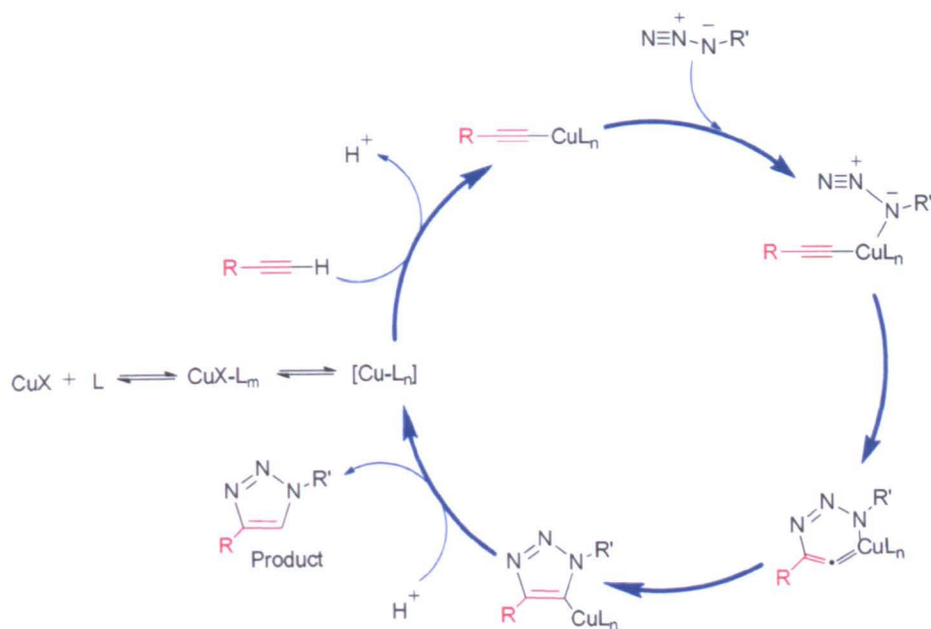


Figure 3.6 The proposed mechanism of CuAAC. Ref. 80.

The broad applications of the facile CuAAC reactions have inspired chemists' efforts to search for other reactions that meet the click chemistry requirements. Therefore, in recent years click reactions have been extended to metal-free dipolar cycloadditions,<sup>100-101</sup> hetero-Diels-Alder reactions<sup>102-104</sup> and thiol-based reactions<sup>105</sup> such as thiol-ene,<sup>106-108</sup> thiol-yne,<sup>109-112</sup> thiol-bromo<sup>113-114</sup> and thiol-isocyanate<sup>115-116</sup> reaction, *etc.*. Among all these reactions, thiol-ene click reaction is an efficient technique which has attracted massive investigation.<sup>117-118</sup>

Although thiol-ene reactions have been used originally for preparing films and networks for many years,<sup>117</sup> only recently it was taken as one of the most efficient click reactions.<sup>107</sup> Ever since, it has been extensively employed as a facile way for the post-functionalisation of polymers, modification of substrate surfaces, production of high-energy absorbing materials, hydrogels and biomaterials, *etc.*<sup>118</sup> Thiol-ene click reactions have mostly been conducted mostly under a radical mechanism<sup>119-120</sup> to give an anti-Markovnikov-oriented thioether which are initiated photochemically or thermally, **Figure 3.7**. The thiyl radical  $R_1-S\cdot$  is generated by irradiation (at near-visible wavelengths,<sup>121-122</sup>  $\lambda = 365 - 405$  nm) of a thiol with photoinitiator, followed by formation of the intermediate carbon-centred radical. The intermediate can react with another thiol to give the click product and produce a new thiyl radical. The efficiency of thiol-ene click reactions depends on the structure properties of both the thiols and the alkenes.<sup>117</sup>

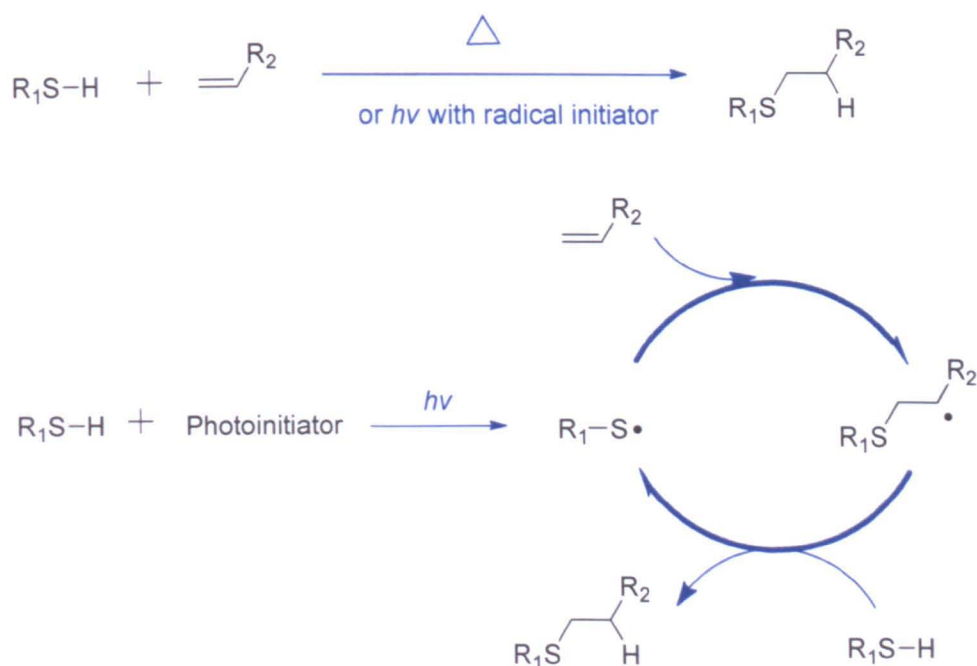


Figure 3.7 The mechanism of thiol-ene radical reaction. Ref. 107.

However, high UV irradiation will cause problems especially for the *in vivo* application of thiol-ene click reaction. Fortunately, this thiol-click reaction can also work with catalysts for activated alkenes *via* Michael addition,<sup>106</sup> as shown in **Figure 3.8**. The nucleophilic-catalysed addition of thiols to activated alkenes can be conducted using primary/secondary amines or certain phosphines, dimethylphenylphosphine (DMPP), for example.<sup>65, 123</sup> The proposed mechanism of the thiol-Michael addition to acrylates is shown in **Figure 3.9**.

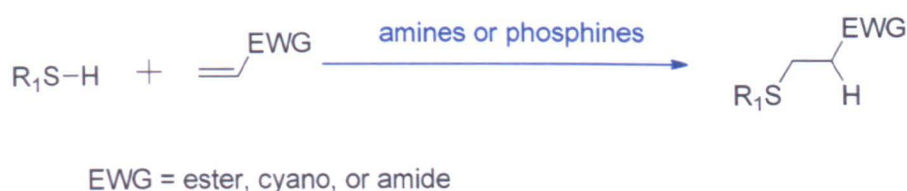


Figure 3.8 The thiol-Michael addition to various enes bearing electron-withdrawing (EWG) moiety.

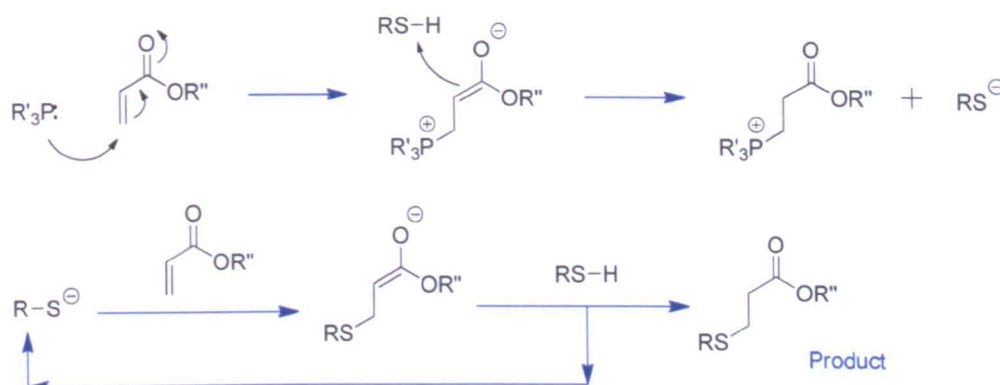


Figure 3.9 The proposed mechanism of the thiol-ene Michael addition catalysed by phosphines. Ref. 106.

### 3.1.3 Conclusions

With the versatile CuAAC click reactions, glycopolymers can be synthesised by the reactions either between sugar azides and alkyne-containing polymers<sup>124</sup> or between

alkyne-containing sugars and azide terminated polymers.<sup>125-126</sup> In our group, we employed a facile approach to synthesise glycopolymers *via* the combination of ATRP and CuAAC. Alkyne-containing polymer scaffolds were prepared by ATRP, followed by post-modification of the polymer scaffolds with sugar azides.<sup>64, 84-85, 127</sup> However, preliminary work<sup>66</sup> showed that by changing ATRP to CCTP we could obtain double functionality in the resulting polymer scaffolds, which can be further modified by CuAAC or thiol-ene click chemistry. Therefore, with considerations of the advantages of CCTP synthetic technique, in this work we combined CCTP and CuAAC to generate well-defined glycopolymers, **Figure 3.10**.

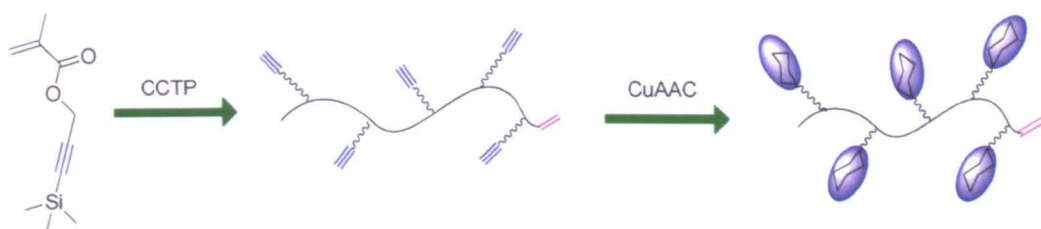


Figure 3.10 Preparation of glycopolymers by CCTP and CuAAC.

By using CoBF as the catalyst, the polymerisations of methyl methacrylate were carried out firstly for determination of catalyst reactivity and comparison of the CCTP reaction processes. Then the chain transfer polymerisation of the monomer TMS-protected propargyl methacrylate was investigated and precursor polymer scaffolds with double functionality were synthesised. After preliminary study of CuAAC and thiol-ene click reaction features of the polymer scaffolds, a series of glycopolymers were prepared *via* CuAAC of the clickable polymer scaffolds with sugar azides which were from direct one-step synthesis without any protection of the hydroxyl groups.

### 3.2.1.1 Determination of the chain transfer constant of CoBF

$$\text{CH}_2=\text{C}(\text{CH}_3)\text{C}(=\text{O})\text{OC}(\text{CH}_3)_3 \xrightarrow[\text{AIBN}]{\text{CoBF}_4} \text{H}-(\text{CH}_2-\text{C}(\text{CH}_3)(\text{C}(=\text{O})\text{OC}(\text{CH}_3)_2))_n-\text{C}(\text{CH}_3)=\text{CH}_2$$

Distilled methyl ethyl ketone (MEK) was used as the solvent to fully dissolve the catalyst CoBF. Two stock solutions were freshly prepared under nitrogen:

**S2: AIBN (115 mg) in MMA (23 mL) and mesitylene (1 mL).**

Five experiments (**A – E**) were performed using different proportion of the two stock solutions, as shown in **Table 3.2**. The reaction mixtures were stirred at 60 °C for 15 minutes before being cooled down using ice bath and bubbled through with air. The molecular weight and PDI of the resulting polymers were obtained using gel permeation chromatography (GPC) with a mixture of chloroform and triethylamine

(95:5, v/v) as the eluent. The conversion of the reaction was calculated by comparing the vinyl peaks and mesitylene peaks in  $^1\text{H}$  NMR spectrum.

Table 3.2 Determination of the chain transfer constant in CCTP of MMA.

No.	S1/mL	S2/mL	MEK/mL	$M_n$ /Da	PDI	Conv./%
A	0	4	1	154500	1.50	4.93
B	0.2	4	0.8	900	1.62	1.53
C	0.4	4	0.6	600	1.45	1.35
D	0.6	4	0.4	400	1.28	0.81
E	0.8	4	0.2	300	1.23	0.66

As the conversion of each polymerisation is low ( $< 5\%$ ) the Mayo equation can be applied to this situation, **Equation 3.2.1**, the chain transfer constant  $C_S$  is obtained by a linear fit to the data, **Figure 3.12**. The  $C_S$  value of CoBF used in these experiments was obtained as  $1.2 \times 10^4$ , which is comparable with the data in literature (20700 ~ 40900).<sup>43, 55-56</sup>

$$\frac{1}{DP_n} = \frac{1}{DP_n^0} + C_S \frac{[\text{CoBF}]}{[\text{MMA}]} \quad (3.2.1)$$

$DP_n$  = degree of polymerisation with transfer agent

$DP_n^0$  = degree of polymerisation without transfer agent

$C_S$  = chain transfer constant



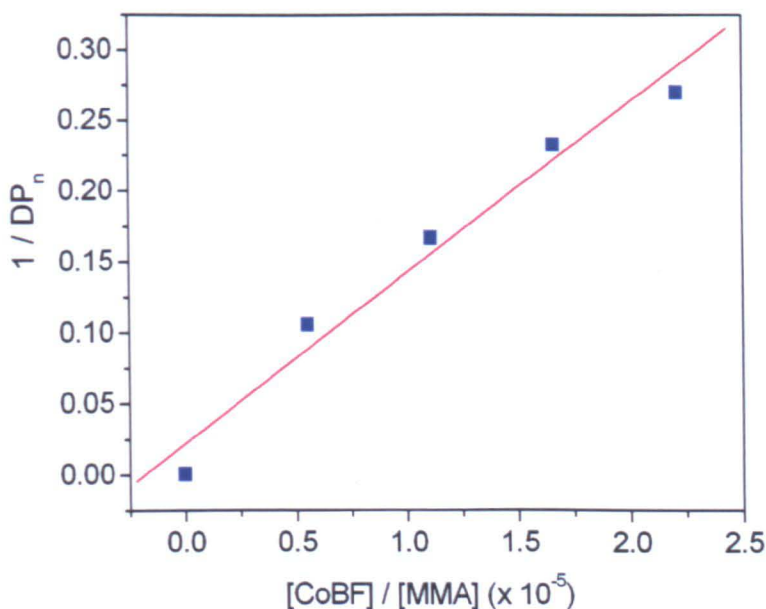


Figure 3.12 Mayo plot of the CCTP of MMA at 60 °C.

### 3.2.1.2 Bulk catalytic chain transfer polymerisation of MMA

As CoBF is soluble in MMA, no solvent is required in the polymerisation. CoBF was dissolved in the monomer to make CoBF stock solution. Two different concentrations of CoBF were employed for the bulk catalytic chain transfer polymerisation of MMA. When the concentration of CoBF was high enough, the polymerisation mixture was mainly consisted of oligomers such as dimers, trimers, tetramers, and pentamers, **Figure 3.13 (a)**. However, the amount of oligomers decreased and that of polymers increased during the polymerisation process if the concentration of CoBF was lower, **Figure 3.13 (b)**.

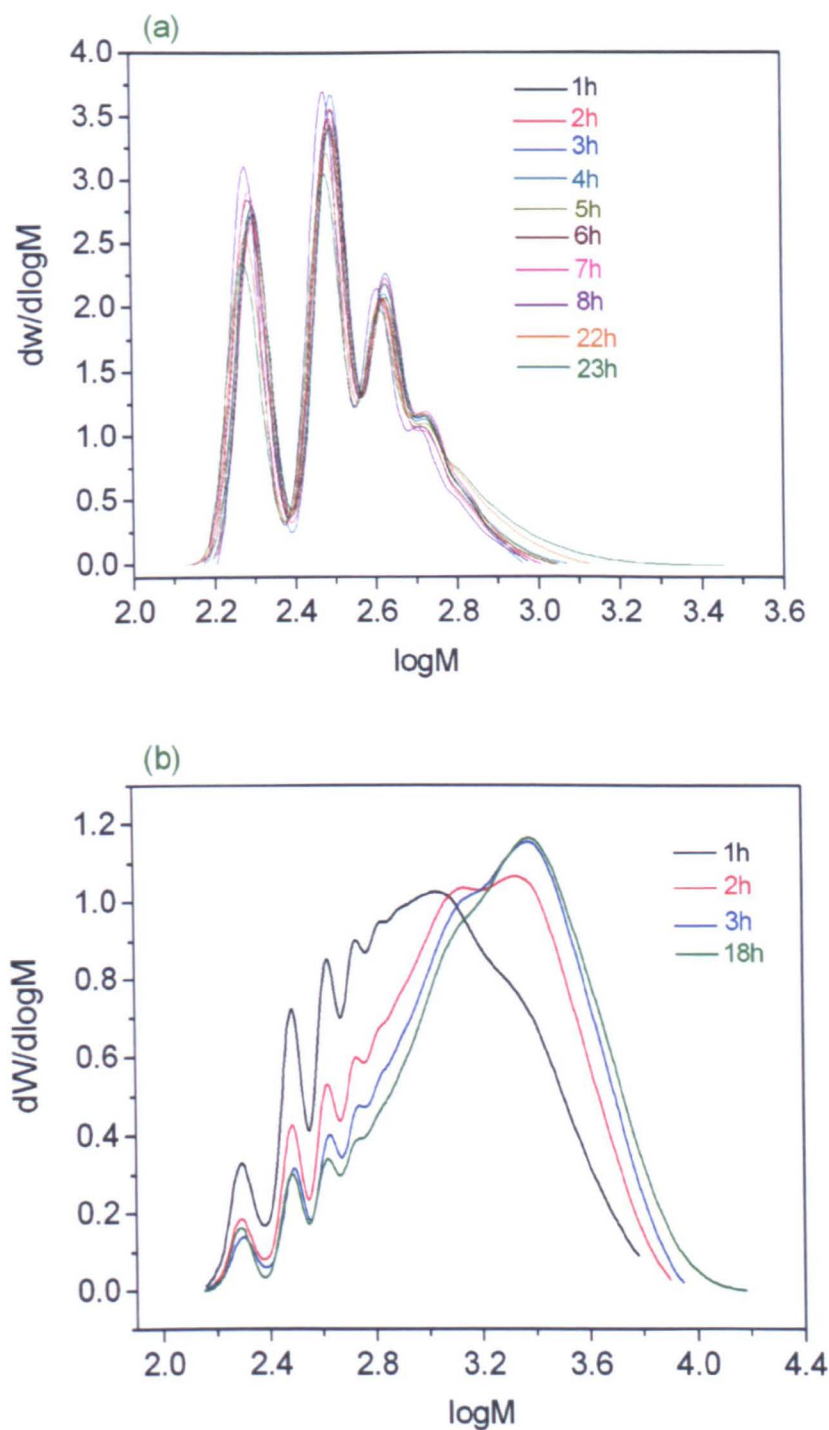


Figure 3.13 SEC spectra of samples obtained from the CCTP of MMA at 60 °C. (a) High concentration of CoBF (0.1 mg/mL). (b) Low concentration of CoBF (0.05 mg/mL).

These trends of molecular weight distribution during the CCTP of MMA indicated that the rate of chain transfer to monomer would be equivalent with the rate of



propagation if the concentration of CoBF was high enough. Therefore, the ratio of dimers, trimers and other oligomers kept nearly the same during the polymerisation from 1 h to 23 h, **Figure 3.13 (a)**. In one extreme case, polymerisation cannot even proceed if the concentration of CoBF is too high, which will result in remaining of MMA monomer during the process. However, with low concentration of CoBF, the oligomers generated by the chain transfer process at the beginning of the polymerisation can also be reinitiated by AIBN or cobalt hydride and can propagate to give polymers of high molecular weight. That is the reason why the amount of oligomers decreased and that of polymers increased in **Figure 3.13 (b)**.

This point of view is confirmed by the analysis of the number average molecular weights and the polydispersity indexes of samples obtained from the polymerisation. The molecular weights of samples in first case remained almost the same during the polymerisation when the ratio  $[\text{CoBF}] / [\text{MMA}]$  was high, **Figure 3.14 (a)**, while there was an increase of  $M_n$  in the second case when the ratio  $[\text{CoBF}] / [\text{MMA}]$  was low, **Figure 3.14 (b)**. The molecular weight distributions were relatively narrow comparing with the samples from the polymerisation with low value of  $[\text{CoBF}] / [\text{MMA}]$ . Although the number average molecular weights remained nearly unchanged, the conversion of the monomer increased up to 60% with time during the polymerisation, **Figure 3.15 (a)**. The conversion of MMA reached up to 80% when the concentration of the catalyst was low, **Figure 3.15 (b)**.

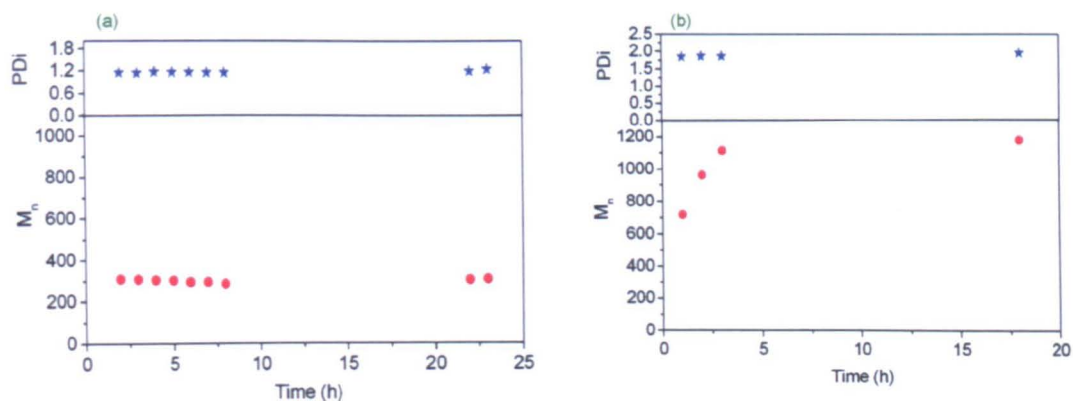


Figure 3.14 The changes of molecular weight  $M_n$  and polydispersity PDI during the CCTP of MMA. (a) High concentration of CoBF (0.1 mg/mL). (b) Low concentration of CoBF (0.05 mg/mL).

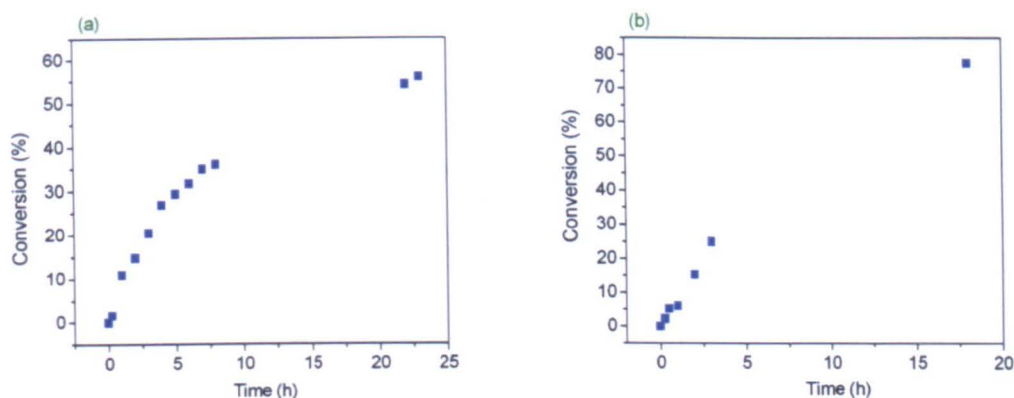


Figure 3.15 The conversion vs. time during the CCTP of MMA calculated from  $^1\text{H}$  NMR spectra. (a) High concentration of CoBF (0.1 mg/mL). (b) Low concentration of CoBF (0.05 mg/mL).

## 3.2.2 Preparation of clickable polymer scaffolds

### 3.2.2.1 Polymerisation of propargyl methacrylate (PMA) via CCTP

In order to prepare the clickable precursor polymer scaffolds, PMA was employed as the monomer for the CCTP, **Figure 3.16**. PMA was synthesised using propargyl alcohol and methacryloyl chloride. A mixture of AIBN, mesitylene (internal NMR standard) and PMA in MEK was freeze-pump-thawed for 4 times to remove air,

followed by addition of the CoBF stock solution. The resulting reaction mixture was stirred at 60 °C and samples were taken every hour.

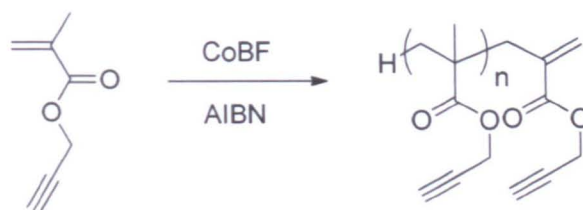


Figure 3.16 Cctp of propargyl methacrylate.

Analysis of the samples using SEC showed the conversion of monomer increased with time during the polymerisation, **Figure 3.17**. The conversion of PMA was about 10% at 2 hours after the reaction started and increased faster with time with a jump to over 40% after 4 hours. The reaction mixture started to slightly turn to gel after 2 hours and became gel after 4 hours.

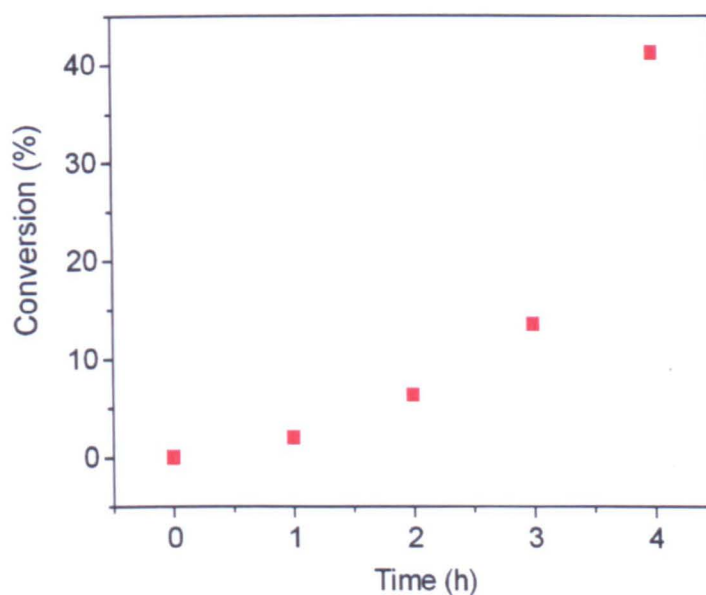


Figure 3.17 The conversion vs. time during the Cctp of PMA calculated from SEC results.

The selected zones in the  $^1\text{H}$  NMR spectrum of the sample taken at 4 h indicated the appearance of polymers in the reaction mixture, **Figure 3.18**. However, it was too diluted to see the expected peaks related to the double bonds in the end of polymer chains.

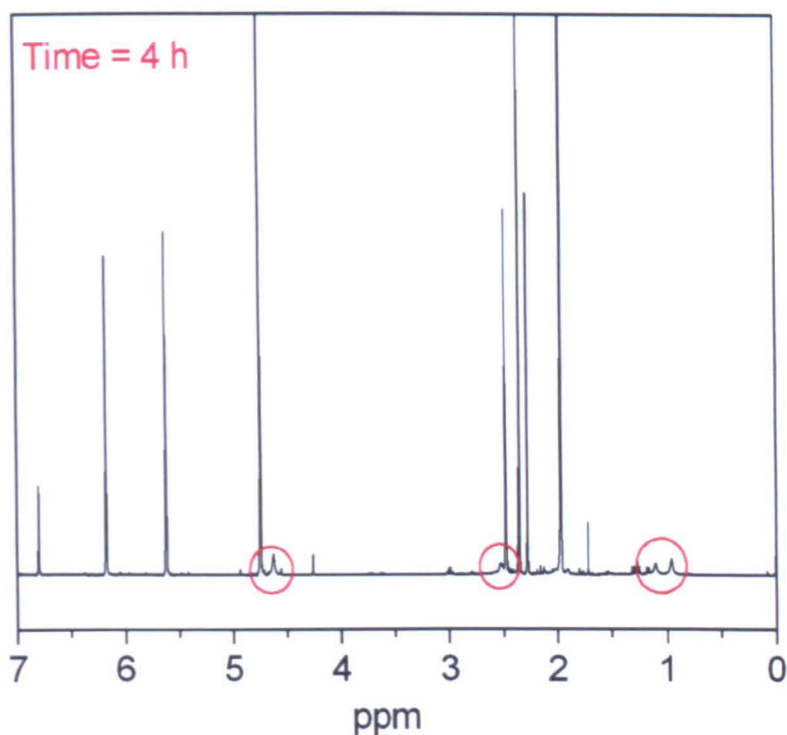


Figure 3.18  $^1\text{H}$  NMR spectrum of one sample during the CCTP of PMA.

The SEC result of the sample taken at 2 h is shown in **Figure 3.19**. The number average molecular weight was as high as 9000 with  $\text{PDI} = 2.00$ . In this case, the CCTP of PMA can only be controlled when the conversion is really low ( $< 10\%$ ). Therefore, in order to prepare the clickable polymer scaffolds in large scale with high monomer conversion, TMS-protected propargyl methacrylate was used instead.

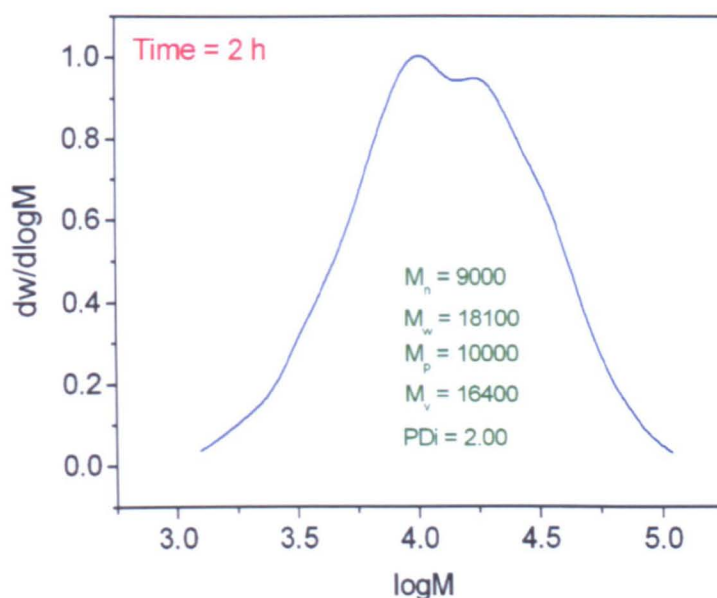


Figure 3.19 SEC result of the sample taken at  $t = 2$  h during the CCTP of PMA.

### 3.2.2.2 Synthesis of TMS-protected propargyl methacrylate

The monomer TMS-protected propargyl methacrylate (TMS-PMA) was synthesised using a procedure as described previously<sup>64</sup> with a modification of the purification step, **Figure 3.20**.

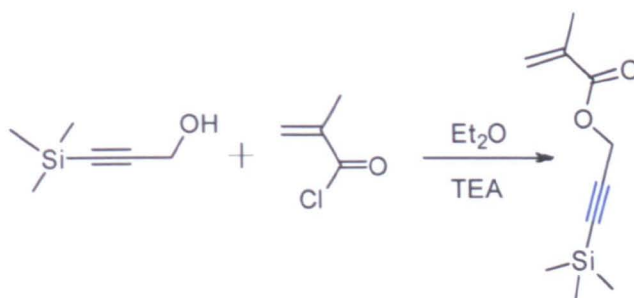
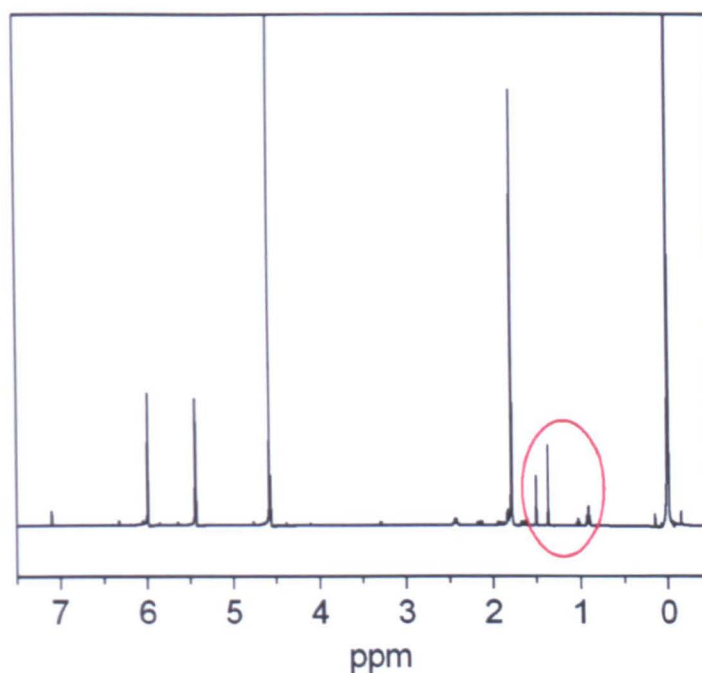


Figure 3.20 Synthesis of TMS-PMA.

A mixture of 3-trimethylsilylpropyn-1-ol, triethylamine (TEA) and methacryloyl chloride in dry diethyl ether was stirred at ambient temperature overnight. After removal of the excess methacryloyl chloride, TEA and solvent, the remaining oil was

pale yellow. The  $^1\text{H}$  NMR spectrum of this crude oil product is shown in **Figure 3.21**.



*Figure 3.21  $^1\text{H}$  NMR spectrum of the crude pale yellow oil in  $\text{CDCl}_3$ .*

Two relatively large impurity peaks were found in the  $^1\text{H}$  NMR spectrum, as shown in the selected zone. It has been proved that these impurities are Diels-Alder adducts of methacryloyl chloride which can kill the activity of the chain transfer agent CoBF in CCTP processes. The impurities were finally separated by Kugelrohr distillation as brown viscous liquid, **Figure 3.22**.

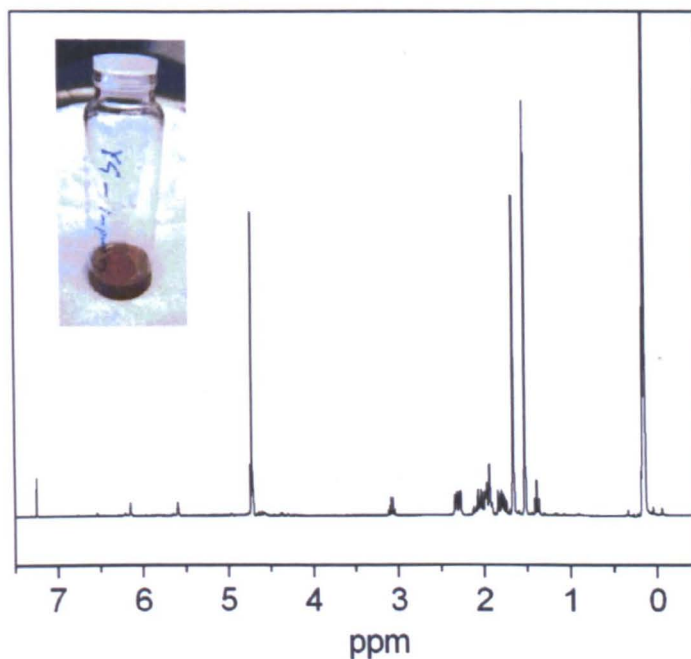


Figure 3.22  $^1\text{H}$  NMR spectrum of impurities from the process in  $\text{CDCl}_3$ .

Pure monomer was obtained as colourless oil in 77.4% yield, **Figure 3.23**.

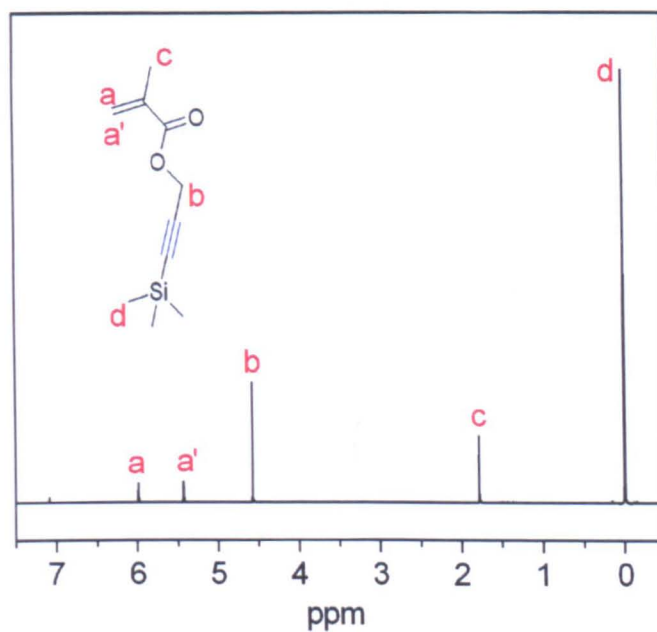


Figure 3.23  $^1\text{H}$  NMR spectrum of pure TMS-PMA in  $\text{CDCl}_3$ .



### 3.2.2.3 CCTP of TMS-protected propargyl methacrylate

The clickable polymers were synthesised by CCTP of TMS-protected propargyl methacrylate (TMS-PMA) and following deprotection to remove TMS protecting groups, **Figure 3.24**.

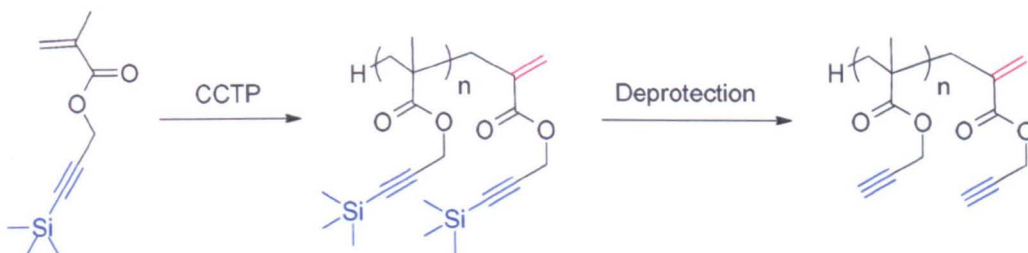


Figure 3.24 Preparation of clickable polymer scaffolds by CCTP of TMS-PMA and deprotection.

The chain transfer agent CoBF was dissolved in MEK to make a stock solution. The solution was freeze-pump-thawed for 3 times to remove air and then refilled with nitrogen. The CoBF solution of calculated volume was added by a syringe into a mixture of TMS-PMA, AIBN and mesitylene (internal NMR standard) which was previously freeze-pump-thawed for 3 times and filled with nitrogen. The reaction mixture was stirred under nitrogen at 60 °C overnight, **Figure 3.25**.

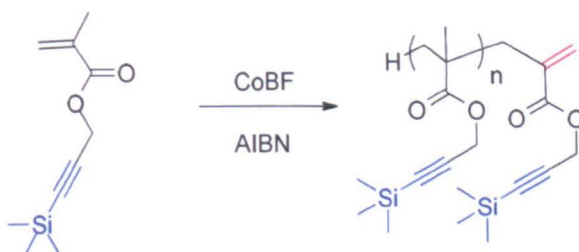


Figure 3.25 CCTP of the monomer TMS-PMA.

When the reaction finished, the solution was cooled to ambient temperature and bubbled through with air for several hours. The polymers were purified by removal



of the monomer and volatile solvent under reduced pressure at 80°C.  $^1\text{H}$  NMR spectrum of the TMS-protected polymers is shown in **Figure 3.26**. The appearance of the two peaks at around 6.1 ppm and 5.5 ppm is unique to the CCTP of the monomer, which is from the double bond in the end of every polymer chain.

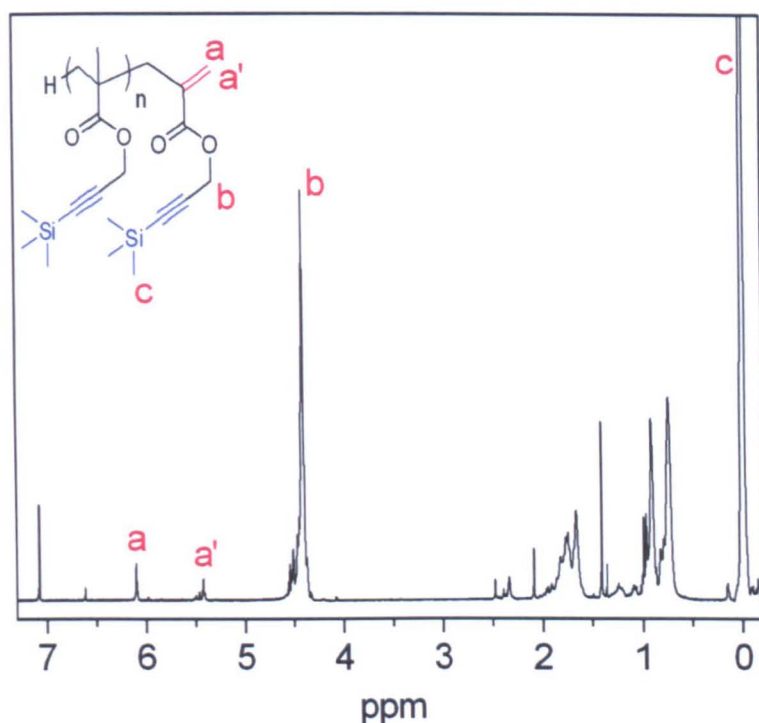


Figure 3.26  $^1\text{H}$  NMR spectrum of TMS-protected polymers in  $\text{CDCl}_3$ .

SEC analysis of the samples taken from the polymerisation reaction mixture is shown respectively in **Figure 3.27** and **Figure 3.28**. The evolution of molecular weight distribution during the polymerisation process was monitored. The amount of dimers and trimers decreased slightly with time during the polymerisation, which was similar to the CCTP of MMA with low concentration of  $\text{CoBF}_4$ .

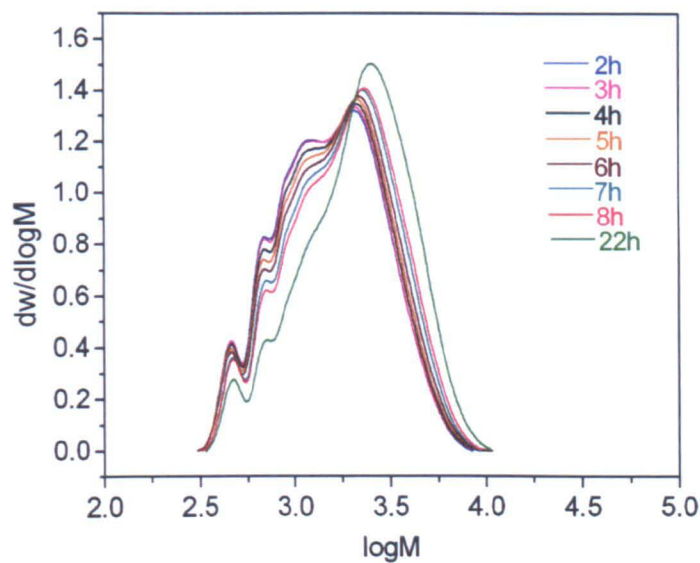


Figure 3.27 SEC spectra of samples obtained from the CCTP of TMS-PMA.

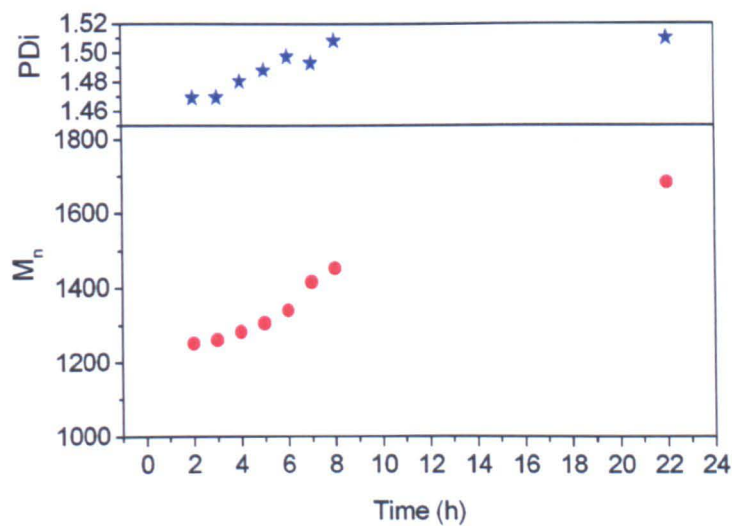


Figure 3.28 The changes of molecular weight  $M_n$  and polydispersity  $PDI$  with time during the CCTP of TMS-PMA.

Theoretically, different polymers of targeted molecular weights can be prepared by addition of different amount of CoBF, by which CCTP is a controlled polymerisation technique widely used in industry. One of the outstanding features of CCTP is preparing polymers of low molecular weight using only low level amount of catalyst,

which can greatly reduce the toxicity, colour or odour of the final products. Furthermore, the relatively broad molecular weight distribution can be the appealing target in certain applications, for example, high solid coatings.<sup>37</sup>

Therefore, a series of polymers with different molecular weights were synthesised in this work, **Table 3.3**. Slightly varying the ratio of [CoBF]/[Monomer], polymers of low molecular weight were easily prepared. Their molecular weight distributions had PDI from 1.34 to 2.14. The magnitudes of the molecular weights obtained by <sup>1</sup>H NMR spectra and by SEC analysis were matched very well. The conversions of the CCTP of TMS-PMA reached up to 95% after 22 hours. Hence, only very small amounts of the chain transfer agent are needed to get a good control on the molecular weights of the resulting polymers with relatively high conversions.

*Table 3.3 Polymers of different  $M_n$  and PDI obtained by CCTP of TMS-PMA.*

No.	[CoBF] / [M]	Time (h)	Conv. (%) <sup>a</sup>	$M_n(\text{Da})^a$	$M_n(\text{Da})^b$	PDI
1	$1.59 \times 10^{-4}$	23	75	700	600	1.34
2	$1.24 \times 10^{-4}$	22	86	1200	1100	2.14
3	$8.64 \times 10^{-5}$	22	95	1600	1600	1.53
4	$4.52 \times 10^{-5}$	23	88	3100	3400	1.74

<sup>a</sup>Obtained by NMR. <sup>b</sup>Obtained by SEC.

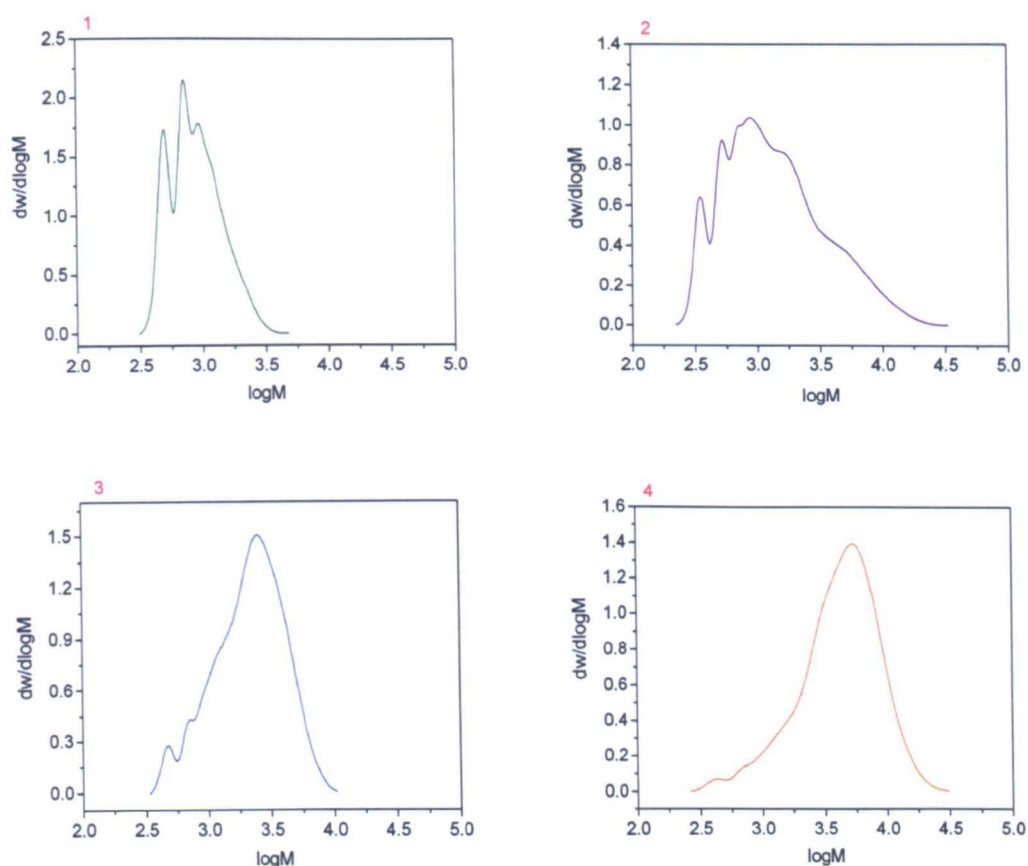


Figure 3.29 SEC traces of polymers prepared by CCTP of TMS-PMA.

SEC plots of the four polymers with different molecular weights are shown in **Figure 3.29**. For the chain transfer polymerisation of the monomer TMS-PMA, when ratio of  $[\text{CoBF}] / [\text{TMS-PMA}]$  was  $1.59 \times 10^{-4}$ , the composition of the product was a mixture of dimers, trimers, tetramers and other oligomers. It is obvious that the proportions of oligomers decreased with reduction of the ratio of  $[\text{CoBF}]/[\text{Monomer}]$ . When the ratio was as low as  $4.52 \times 10^{-5}$ , the product was mainly composed of polymers of relatively high molecular weight. Although CCTP is an especially useful synthetic tool to prepare oligomers, polymers with very high molecular weights can also be obtained using this technique.

By analysing the conversion of monomer during the CCTP polymerisation process, we found that the results from  $^1\text{H}$  NMR spectra and those from SEC analysis are different, as shown in **Figure 3.30**. The conversion values of samples from SEC analysis are larger than those calculated by comparing integrations of relative peaks in the  $^1\text{H}$  NMR spectra.

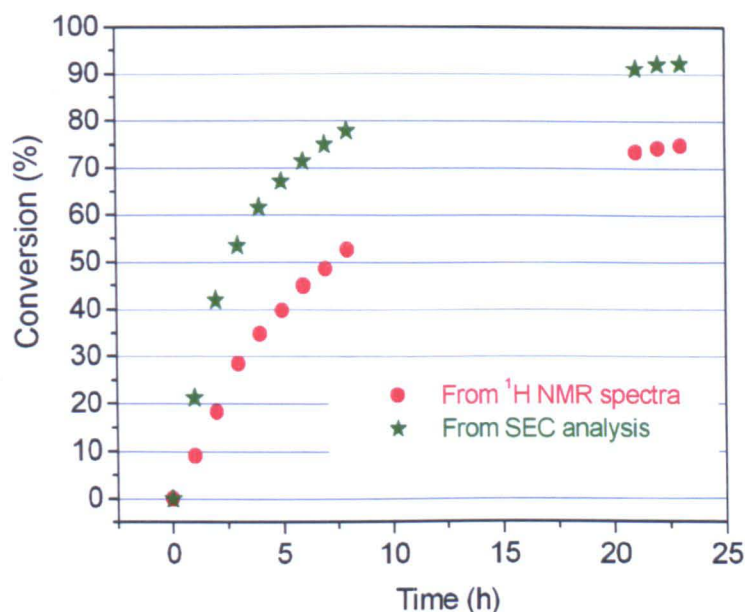


Figure 3.30 The difference of conversions from  $^1\text{H}$  NMR spectra and those from SEC analysis.

Therefore, in order to compare systematically the changes of conversion during the polymerisation reaction, the conversion results calculated from  $^1\text{H}$  NMR spectra are employed, **Figure 3.31**. The conversion of monomer increased with time during the polymerisation of TMS-PMA, which could reach up to quite high levels. Comparing the conversions obtained with different ratios of  $[\text{CoBF}] / [\text{Monomer}]$ , we can conclude that the amount of transfer agent CoBF in the reaction mixture influences the conversion of the monomer in the polymerisation. In general, the conversion can be reduced if a large amount of CoBF is applied.



This phenomenon can be explained using the mechanism of CCTP. When a large amount of CoBF is used, the rate of chain transfer of the growing chain in the polymerisation will increase, which will reduce their propagation with monomer. Although the chain transfer product of the growing polymer chain can be reinitiated in the regeneration of Cobalt(II) and can consume more monomer, it will take longer time to reach as high conversion as in the polymerisation with small amount of CoBF because there is a chain transfer step added into the propagation process.

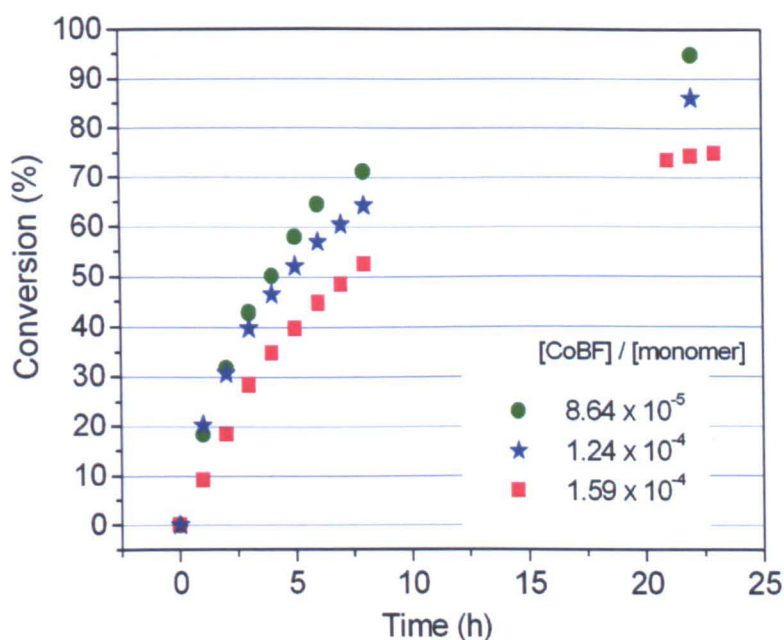


Figure 3.31 The changes of conversions with time in CCTP of TMS-PMA.

The clickable polymer scaffolds can be obtained by deprotection to remove TMS groups of the polymers prepared by CCTP. The deprotection was conducted following a procedure as described early,<sup>64</sup> using tetra-*n*-butylammonium fluoride (TBAF) and acetic acid at ambient temperature, **Figure 3.32**.

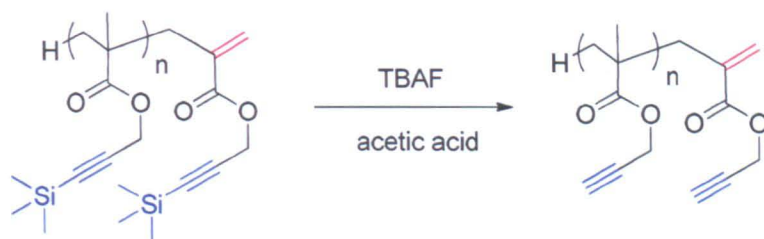


Figure 3.32 Deprotection of polymers prepared by CCTP of TMS-PMA.

The successful removal of the protective groups was indicated by the appearance of alkyne peak at 2.5 ppm and disappearance of TMS peak at 0.2 ppm, **Figure 3.33**. MALDI-TOF spectra also confirmed the structures of polymers before and after deprotection, **Figure 3.34**. The clickable polymers with pendant alkyne groups and a double bond at the end of every polymer chain have been prepared.

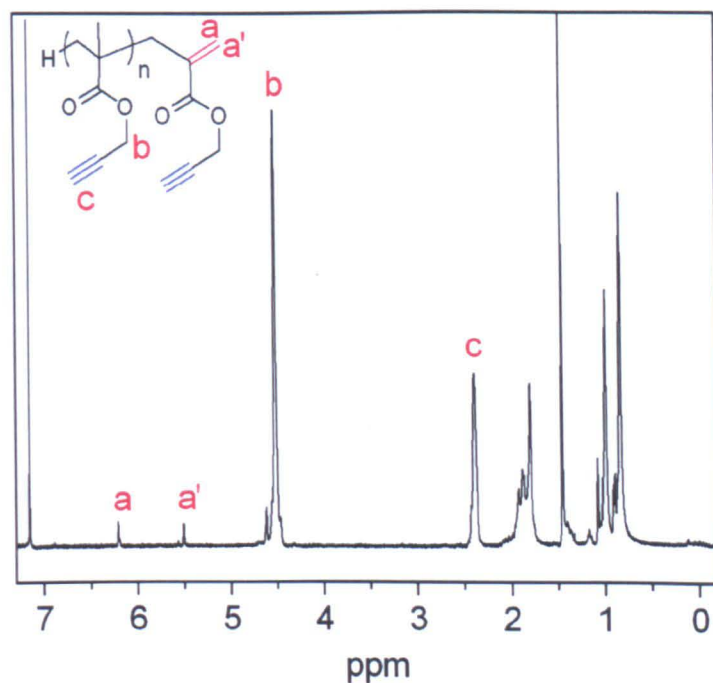


Figure 3.33  $^1\text{H}$ NMR spectrum of polymers after deprotection.

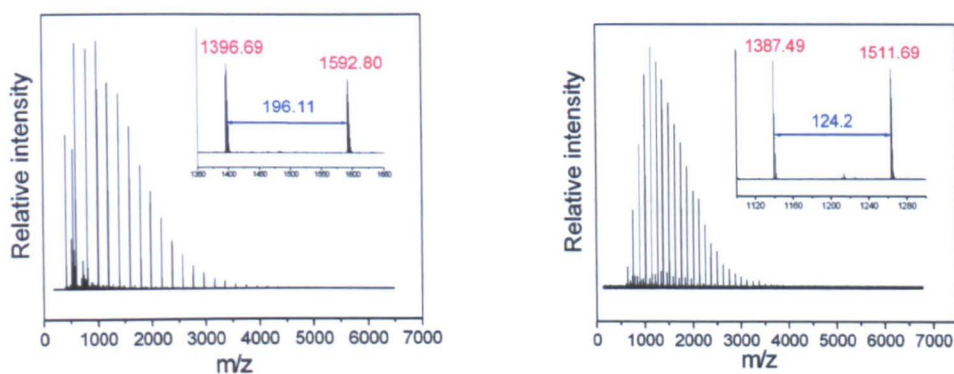


Figure 3.34 MALDI-TOF spectra of polymers before (left) and after (right) deprotection.

### 3.2.3 Post-modification of polymers *via* click reactions

As the precursor polymers contain both alkyne groups and vinyl bond in the polymer chain, they can be further modified by Cu(I)-catalysed azide-alkyne cycloaddition (CuAAC), thiol-ene or thiol-yne click reaction depending on what kinds of functional groups are needed. Here we demonstrate two different click reactions of the precursor polymer scaffolds and explore their properties in the click reactions.

#### 3.2.3.1 CuAAC click reaction with poly(ethylene glycol) (PEG) azide

The click reaction between the precursor polymers and PEG azide was catalysed by CuBr with bipyridine as the ligand. The experiments were carried out in DMSO- $d_6$  with mesitylene as internal NMR standard, **Figure 3.35**.

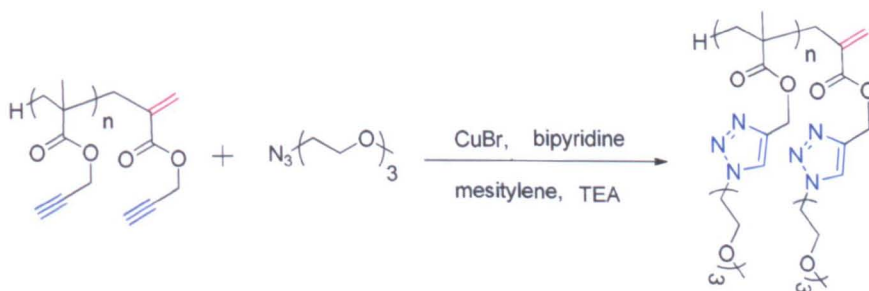
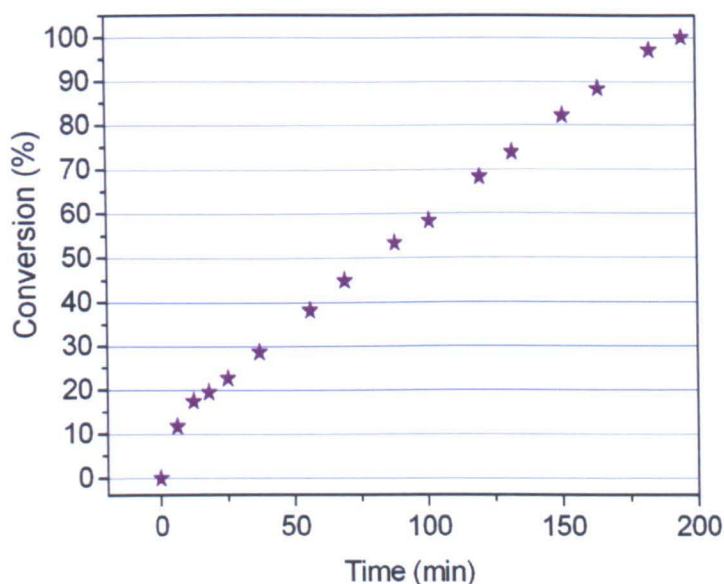


Figure 3.35 CuAAC click reaction with PEG azide.



The reaction was performed in a Young's-tap NMR tube filled with nitrogen. After all the reagents had been put into the tube, the NMR tube was immediately put into the NMR spectrometer with temperature controlled at 60 °C. The reaction was monitored by  $^1\text{H}$  NMR at regular intervals of time (5 minutes). Conversion of the alkyne groups of the polymer were calculated from the relative peaks in the  $^1\text{H}$  NMR spectra, **Figure 3.36**. The click reaction was very efficient and was completely finished within 4 hours. The conversion of the clickable alkyne groups increased linearly with reaction time and reached up to 100%.



*Figure 3.36 Conversion vs. time in CuAAC click reaction with PEG azide.*

The reaction mixture was passed through a short neutral alumina pad to remove copper and other residues and then placed into a dialysis tube. After dialysing against water for 2 days, the product of the click reaction was obtained as white solid by freeze-drying. The  $^1\text{H}$  NMR spectrum of the product is shown in **Figure 3.37**. The peak at 8.0 ppm from the triazole groups of the polymers confirmed the successful click reactions.

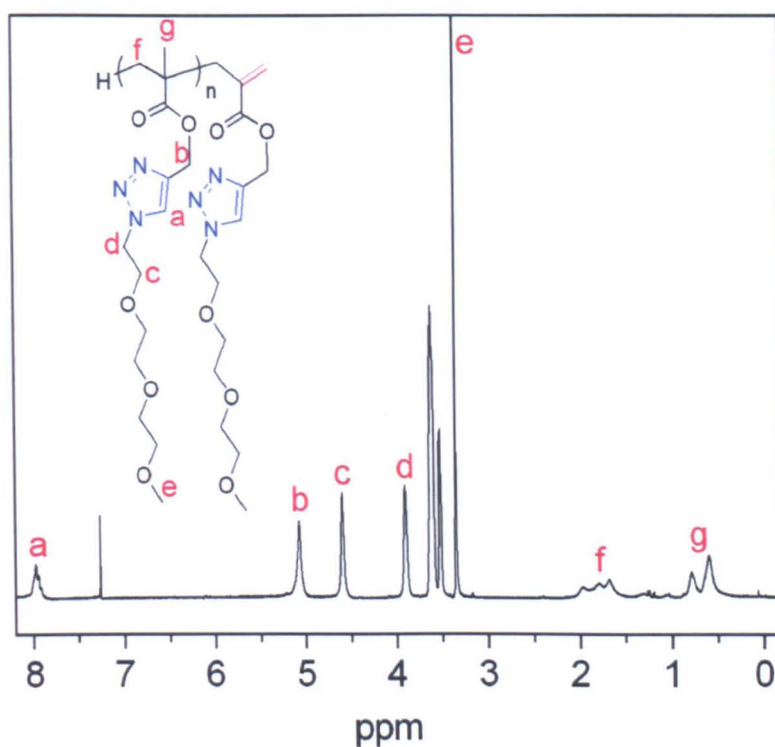


Figure 3.37  $^1\text{H}$  NMR spectrum of CuAAC click product with PEG azide.

### 3.2.3.2 Thiol-ene click reaction with benzyl mercaptan

In order to demonstrate that the clickable polymers prepared by CCTP and deprotection can be functionalised *via* thiol-ene click reaction, benzyl mercaptan was chosen to react with the polymer scaffolds using dimethylphenylphosphine (DMPP) as the catalyst, **Figure 3.38**.



Figure 3.38 Thiol-ene click reaction with benzyl mercaptan.

Similar to the CuAAC click reaction, the thiol-ene click experiment was also performed in a Young's-tap NMR tube with deuterated acetone as the solvent. The reaction was monitored by  $^1\text{H}$  NMR at regular intervals of time (5 minutes) at ambient temperature. The conversions of the vinyl bond at the end of polymer chain were obtained from a series of  $^1\text{H}$  NMR spectra, **Figure 3.39**.

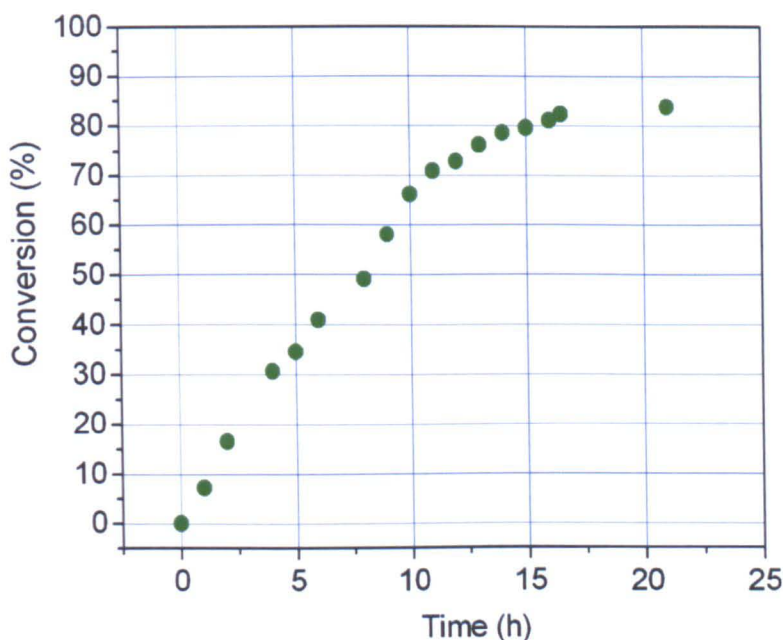


*Figure 3.39 Conversion vs. time of the thiol-ene click reaction.*

The thiol-ene click reaction was relatively slow and the conversion increased with time during the reaction. After 20 hours, the conversion reached up to 85%. The product of the click reaction was purified by precipitation of the reaction mixture in petroleum ether. The  $^1\text{H}$  NMR and MALDI-TOF spectra (**Figure 3.40** and **Figure 3.41**) indicated the success of this reaction and confirmed the structure of the final product.

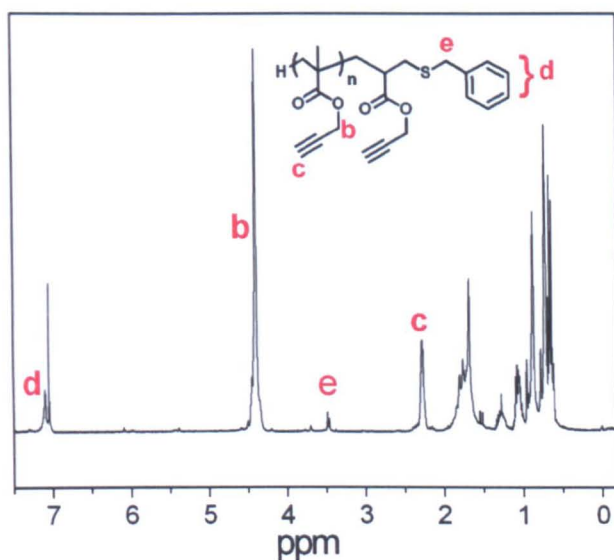


Figure 3.40  $^1\text{H}$  NMR spectrum of the thiol-ene click product in  $\text{CDCl}_3$ .

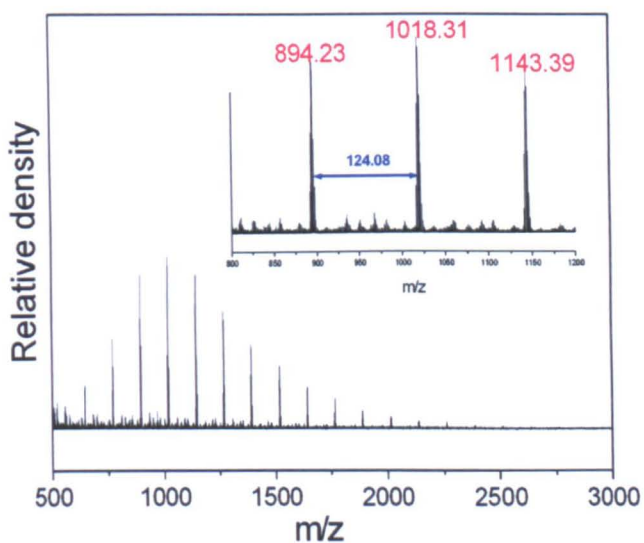


Figure 3.41 MALDI-TOF spectrum of the thiol-ene click product.

### 3.2.4 Synthesis of glycopolymers *via* CuAAC with sugar azides

#### 3.2.4.1 Synthesis of sugar azides

Shoda and co-workers<sup>128</sup> published a new route for the one-step synthesis of sugar azides in 2009. They prepared 21 different kinds of sugar azides *via* the reactions

between unprotected sugars and sodium azide in water mediated by 2-chloro-1,3-dimethylimidazolidinium chloride (DMC). Thus the synthesis of sugar azides has become much easier without the processes of protection and deprotection of hydroxyl groups, **Figure 3.42**.

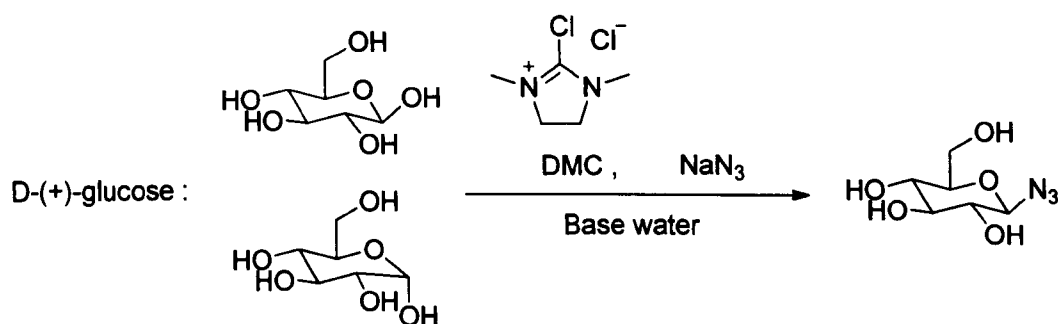


Figure 3.42 One-step synthesis of  $\beta$ -D-glucopyranosyl azide.

As it is an excellent dehydrating agent, DMC has been employed in many synthetic applications.<sup>129-133</sup> The proposed mechanism<sup>129</sup> for the one-step synthesis of sugar azides is shown in **Figure 3.43**. The nucleophilic attack of  $\beta$ -D-glucose to DMC is promoted by a base such as triethylamine (TEA) or *N,N*-diisopropylethylamine (DIPEA) to form the intermediate **2β**. The intermediate **2β** is not stable and can react with the neighbouring 2-hydroxy group to form the 1,2-anhydro intermediate **3** and 1,3-dimethyl-2-imidazolidinone (DMI). The anomeric carbon of the resulting intermediate **3** reacts with sodium azide to give the  $\beta$ -D-glucopyranosyl azide. Moreover, the  $\alpha$ -D-glucose can also react with DMC and NaN<sub>3</sub> similarly to form the  $\beta$ -D-glucopyranosyl azide.

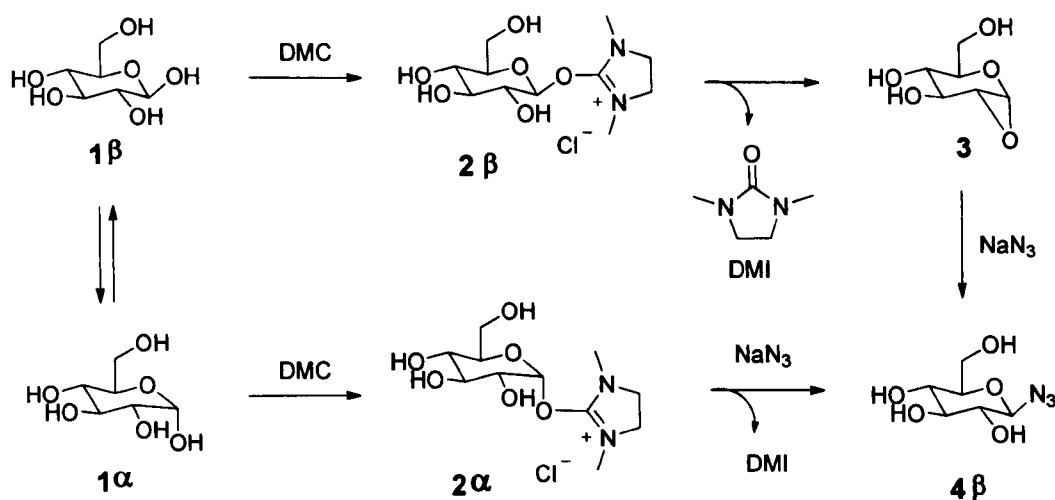


Figure 3.43 The proposed mechanism for the one-step synthesis of sugar azide.

However, in the original work the synthesis was only conducted on a small scale (< 50 mg) and HPLC was employed for the purification. Therefore, we scaled up the synthesis to prepare multigram sugar azides and to make it generally applicable. We also modified the purification protocol of the procedure to remove the requirement for chromatography.<sup>7</sup>

A mixture of D-(+)-mannose, diisopropylethylamine (DIPEA), sodium azide and DMC in water was stirred for 5 h at 0 °C. The excess of sodium azide was removed by precipitating in ethanol. Instead of HPLC, the solution was passed through an acidic ion-exchange column to remove the HCl salts of the base.  $\alpha$ -D-Mannopyranosyl azide was obtained by freeze-drying as an off-white solid.  $^1\text{H}$  NMR was used to assign the anomeric azide as either  $\alpha$  (axial) or  $\beta$  (equatorial). Higher chemical shifts (*i.e.* downfield, > 5 ppm) and smaller coupling constants for the anomeric carbon are typical for  $\alpha$ -linked glycosides relative to their  $\beta$ -isomers.  $^1\text{H}$  NMR and  $^{13}\text{C}$  NMR spectra were shown in **Figure 3.44** and **Figure 3.45**.

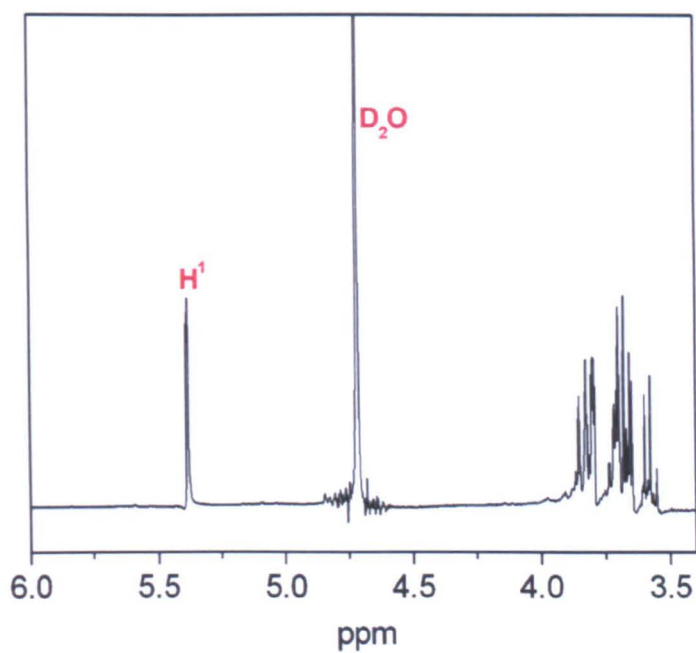


Figure 3.44  $^1\text{H}$  NMR spectrum of  $\alpha$ -D-mannopyranosyl azide in  $\text{D}_2\text{O}$ .

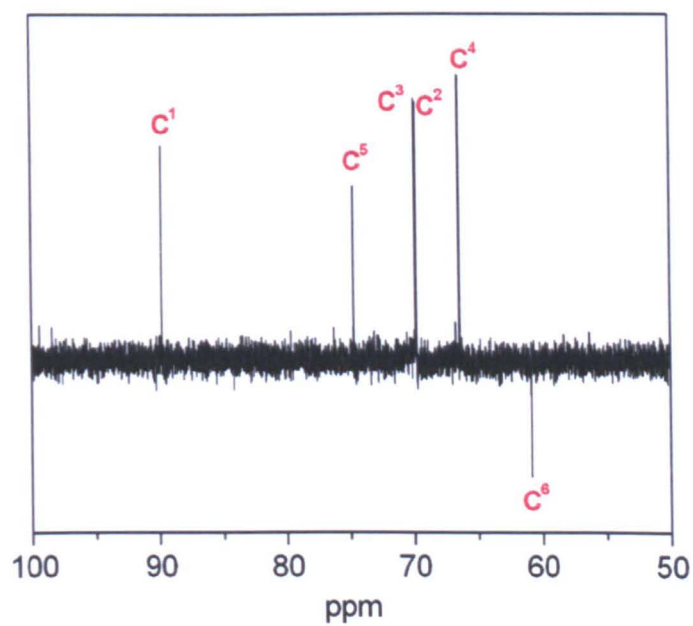


Figure 3.45  $^{13}\text{C}$  NMR spectrum of  $\alpha$ -D-mannopyranosyl azide in  $\text{D}_2\text{O}$ .



FTIR spectrum confirmed the product with appearance of the peak at  $2120\text{ cm}^{-1}$  which was caused by a single azide stretch, **Figure 3.46**. The spectrum also indicated that there was no residual sodium azide (the peak at  $2015\text{ cm}^{-1}$ ) in the product.

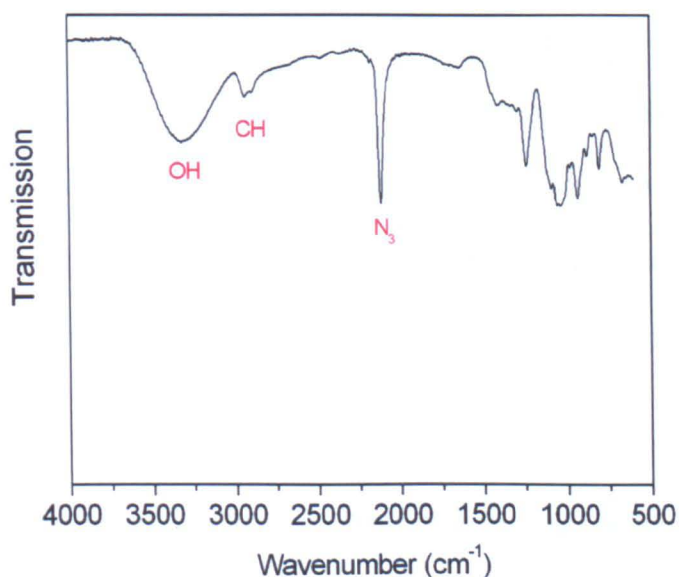


Figure 3.46 FTIR spectrum of  $\alpha$ -D-mannopyranosyl azide.

Besides D-(+)-mannose, four other sugar were used to prepare sugar azides following the modified procedure, **Figure 3.47**.

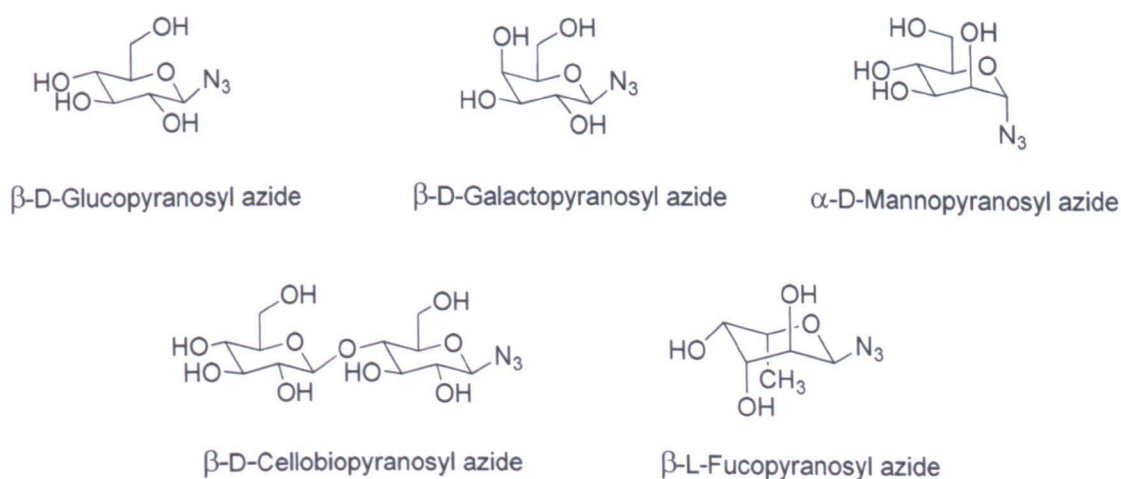


Figure 3.47 Glycosyl azides prepared in the work.



All of the investigated carbohydrates gave rise to the  $\beta$ -anomers apart from D-(+)-mannose which had a stereochemistry.<sup>7</sup> These observations agree with the possible aforementioned mechanism *via* a 1,2-anhydro intermediate from the 2-hydroxyl group directing the product stereochemistry. The ratio of the  $\beta$  :  $\alpha$  peaks showed over 80% anomeric purity in all cases, as confirmed by the presence of a single peak between 85 and 100 ppm in  $^{13}\text{C}$  NMR. This method represents a significant improvement over the traditional Koenigs–Knorr type glycosylation which is atom inefficient due to the need for protecting groups, additional purification and rigorously dry organic solvents and catalysts.<sup>64</sup>

### 3.2.4.2 CuAAC reaction of precursor polymers with sugar azides.

Employing the precursor polymers which were prepared by CCTP and deprotection, glycopolymers can be synthesised *via* the copper(I)-catalysed azide-alkyne cycloaddition with various sugar azides. As shown in **Figure 3.48**, fucose glycopolymer was generated by CuAAC click reaction between the clickable polymers and  $\beta$ -L-fucose azide using Cu(I)Br as the catalyst and bipyridine as the ligand. Following a procedure as described previously,<sup>84</sup> the reactants were dissolved in DMSO and stirred under nitrogen at ambient temperature for three days. The product was purified by dialysing against water and then freeze-drying.

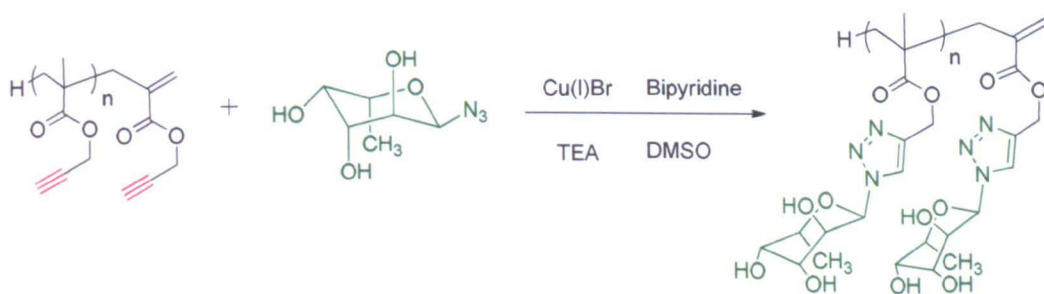


Figure 3.48 Synthesis of fucose glycopolymers via CuAAC reaction.

$^1\text{H}$ NMR spectrum (**Figure 3.49**) indicated that the click reaction was successful with appearance of the new peak at about 8.3 ppm from triazole groups and several peaks (the selected red zone) from fucose. The conversion of this CuAAC click reaction was up to 100% by comparing integrations of the peak **a** and peak **b** in the  $^1\text{H}$  NMR spectrum. The structure of the click product was also confirmed by MALDI-TOF spectrum, **Figure 3.50**.

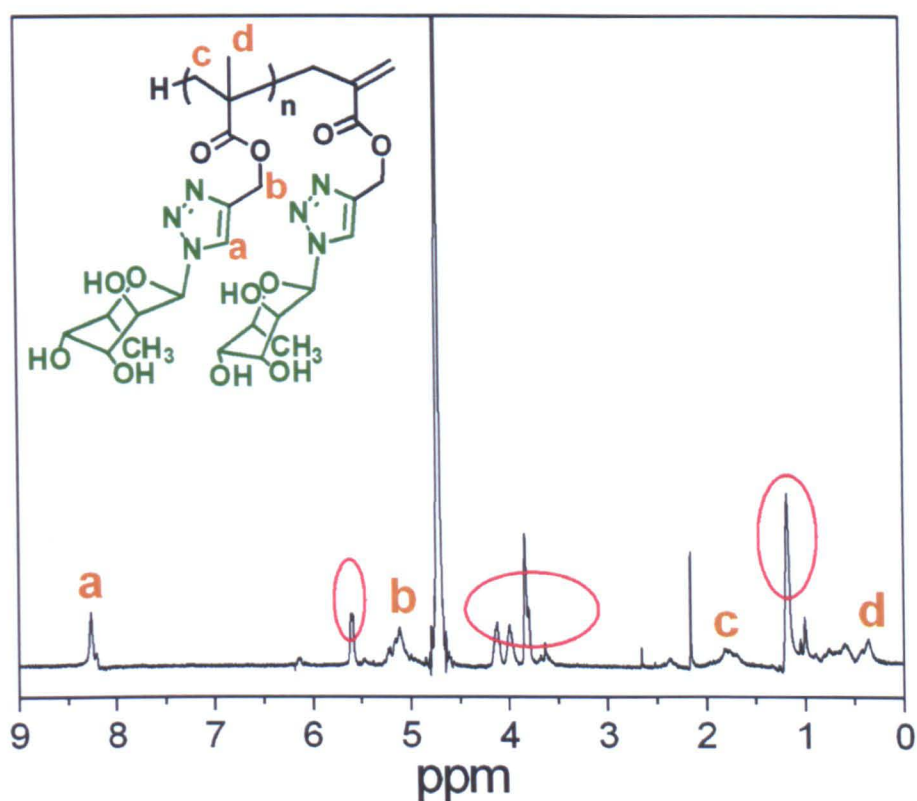


Figure 3.49  $^1\text{H}$  NMR spectrum of fucose glycopolymer in  $\text{D}_2\text{O}$ .

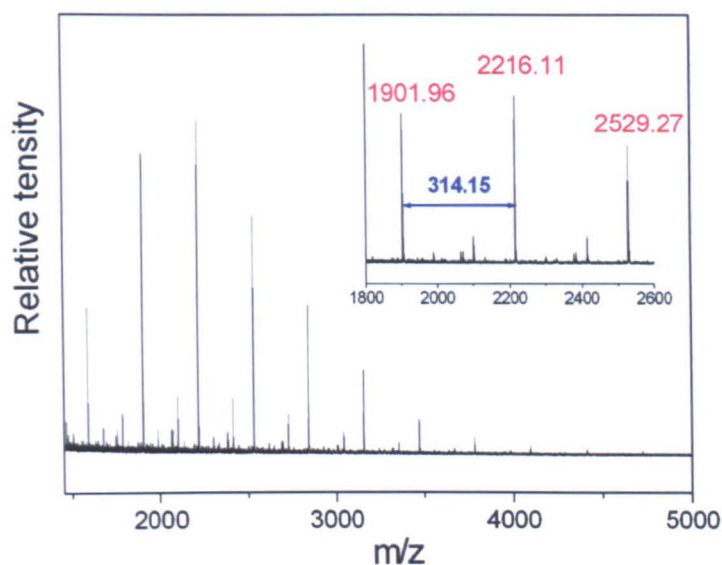


Figure 3.50 MALDI-TOF spectrum of fucose glycopolymer.

The number average molecular weight  $M_n$  of the polymer increased from 5700 Da to 8500 Da after CuAAC reaction according to SEC results using DMF as the eluent. **Figure 3.51.** However, the polydispersity index PDI of the polymer reduced from 1.36 to 1.26, which was caused by the different solubility properties of the precursor polymer and the resulting glycopolymer in DMF eluent.

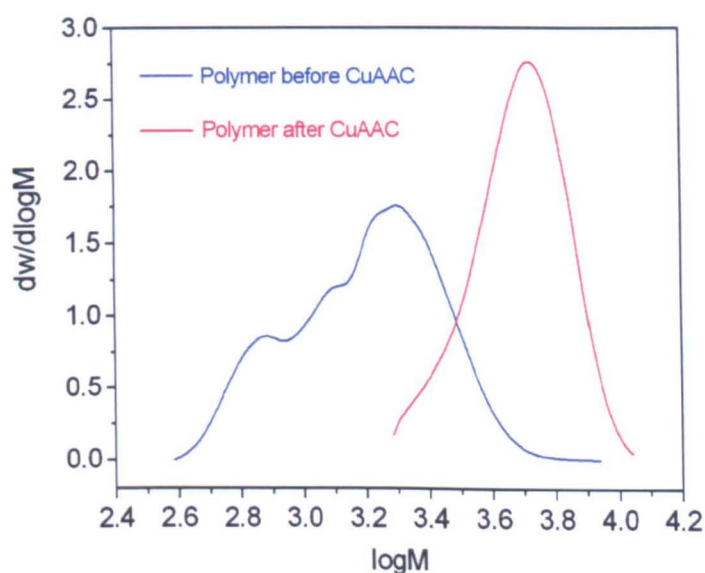


Figure 3.51 SEC results of polymers before and after CuAAC reaction.

Mannose glycopolymer and galactose glycopolymer were also prepared in this work. The CuAAC of the clickable polymers with related sugar azides were also confirmed by comparison of their FTIR spectra, **Figure 3.52**. The peak of  $\text{—C}\equiv\text{C—}$  stretching at around  $2300\text{ cm}^{-1}$  disappeared after reaction with appearance of the large peak of  $\text{—OH}$  stretching at about  $3300\text{ cm}^{-1}$ .

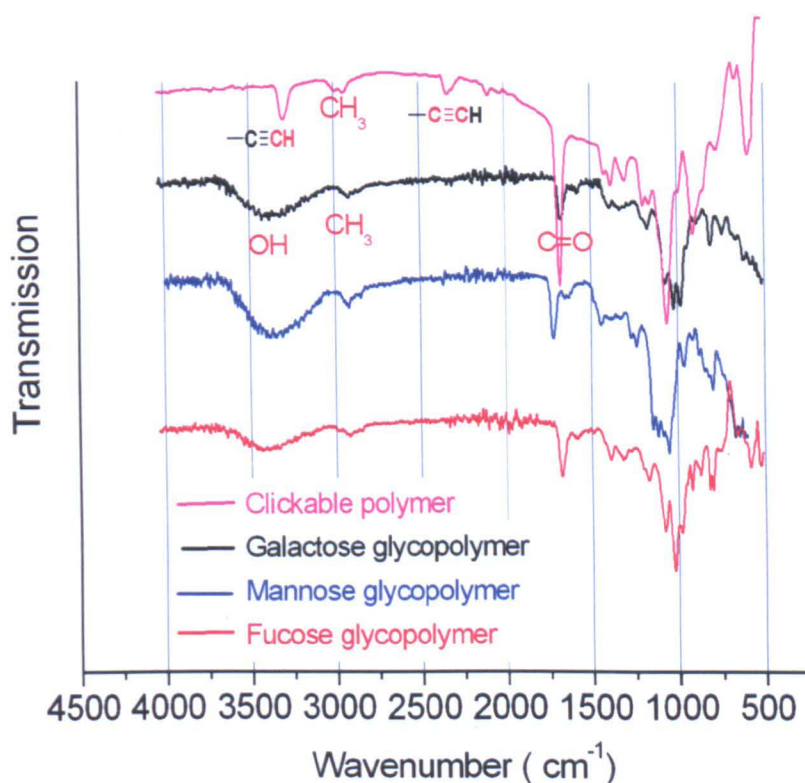


Figure 3.52 FTIR spectra of polymers before and after CuAAC reaction.

The glycopolymers of different molecular weights prepared by CuAAC of clickable precursor polymer **1** and polymer **2** with different sugar azides are shown in **Table 3.4**. Molecular weight,  $M_n$ , and polydispersity PDI of all the polymers were obtained from SEC analysis using DMF as the eluent.

Table 3.4 The glycopolymer prepared by CuAAC.

Polymer	Mannose (%)	Galactose (%)	Fucose (%)	$M_n$	PDI
<b>1</b>	0	0	0	3000	1.23
<b>1a</b>	100	0	0	6500	1.21
<b>1b</b>	0	100	0	8300	1.14
<b>1c</b>	0	0	100	4600	1.12
<b>2</b>	0	0	0	5700	1.36
<b>2a</b>	100	0	0	11200	1.21
<b>2b</b>	0	100	0	11900	1.21
<b>2c</b>	0	0	100	8500	1.26
<b>3*</b>	100	0	0	14000	1.38
<b>4*</b>	100	0	0	25600	1.34

\*Their clickable precursor polymers were prepared by ATRP.

### 3.3 Conclusions

Glycopolymers play an important role in many biological and biomedical applications as multivalent natural oligosaccharide mimics. They can be synthesised by post-functionalisation of precursor polymer scaffolds *via* click chemistry. This method is especially valuable to prepare a library of well-defined glycopolymers only differing in the pendant sugars. CCTP was used to prepare the clickable polymer scaffolds. The advantage of CCTP is that it can be used to prepare polymers of low molecular weight with only low level amount of catalyst, which can greatly

reduce the toxicity, colour or odour of the final products. Furthermore, the broad molecular weight distribution of the resulting polymers can be the appealing target in certain applications.

By using CoBF as the catalyst, the polymerisations of MMA were carried out firstly for determination of the catalyst reactivity. The chain transfer constant was obtained *via* Mayo equation method, which was comparable with the record in literature. The bulk CCTP processes of MMA were also investigated with two different concentration of CoBF to show the general CCTP features. In order to prepare clickable polymer scaffolds, propargyl methacrylate (PMA) was employed as the monomer. However, the CCTP of PMA led to formation of gel even with low conversion. So the monomer TMS-protected propargyl methacrylate (TMS-PMA) was used instead. The synthetic TMS-PMA crude product needed to be purified by Kugelrohr distillation to remove the impurities coming from the original starting chemicals as they could destroy the activity of the catalyst in the polymerisation. CCTP process of TMS-PMA was well studied and polymers with different molecular weights were prepared by varying the amount of CoBF. The precursor polymer scaffolds with double functionality were synthesised by deprotection of the CCT polymers.

After preliminary study of CuAAC and thiol-ene click reaction features of the polymer scaffolds with PEG azide and benzyl mercaptan respectively, a series of glycopolymers were prepared *via* CuAAC of the clickable polymer scaffolds with sugar azides. The one-step synthesis of sugar azide involved in this work represented a significant improvement over the traditional Koenigs–Knorr type glycosylation.

## 3.4 References

1. Kiessling, L. L.; Gestwicki, J. E.; Strong, L. E., *Angew. Chem. Int. Ed.* **2006**, *45*, 2348-2368.
2. Bertozzi, C. R.; Kiessling, L., *Science* **2001**, *291*, 2357-2364.
3. Becer, C. R.; Gibson, M. I.; Geng, J.; Ilyas, R.; Wallis, R.; Mitchell, D. A.; Haddleton, D. M., *J. Am. Chem. Soc.* **2010**, *132*, 15130-15132.
4. Dove, A., *Nat. Biotech.* **2001**, *19*, 913-917.
5. Spain, S. G.; Cameron, N. R., *Polym. Chem.* **2011**, *2*, 60-68.
6. Fleming, C.; Maldjian, A.; Da Costa, D.; Rullay, A. K.; Haddleton, D. M.; St John, J.; Penny, P.; Noble, R. C.; Cameron, N. R.; Davis, B. G., *Nat. Chem. Biol.* **2005**, *1*, 270-274.
7. Vinson, N.; Gou, Y.; Becer, C. R.; Haddleton, D. M.; Gibson, M. I., *Polym. Chem.* **2011**, *2*, 107-113.
8. Godula, K.; Rabuka, D.; Nam, K. T.; Bertozzi, C. R., *Angew. Chem. Int. Ed.* **2009**, *48*, 4973-4976.
9. Benito, J. M.; Gómez-García, M.; Ortiz Mellet, C.; Baussanne, I.; Defaye, J.; Fernández, J. M. G., *J. Am. Chem. Soc.* **2004**, *126*, 10355-10363.
10. Cerrada, M. L.; Ruiz, C.; Sanchez-Chaves, M.; Fernandez-Garcia, M., *Polym. J.* **2011**, *43*, 205-213.
11. Ruff, Y.; Buhler, E.; Candau, S.-J.; Kesselman, E.; Talmon, Y.; Lehn, J.-M., *J. Am. Chem. Soc.* **2010**, *132*, 2573-2584.
12. Vazquez-Dorbatt, V.; Tolstyka, Z. P.; Chang, C.-W.; Maynard, H. D., *Biomacromolecules* **2009**, *10*, 2207-2212.
13. Muthukrishnan, S.; Erhard, D. P.; Mori, H.; Müller, A. H. E., *Macromolecules* **2006**, *39*, 2743-2750.



- 
14. Vazquez-Dorbatt, V.; Maynard, H. D., *Biomacromolecules* **2006**, *7*, 2297-2302.
  15. Gao, C.; Muthukrishnan, S.; Li, W.; Yuan, J.; Xu, Y.; Muller, A. H. E., *Macromolecules* **2007**, *40*, 1803-1815.
  16. Kempe, K.; Weber, C.; Babiuch, K.; Gottschaldt, M.; Hoogenboom, R.; Schubert, U. S., *Biomacromolecules* **2011**, *12*, 2591-2600.
  17. Xu, N.; Wang, R.; Du, F.-S.; Li, Z.-C., *J. Polym. Sci., Part A: Polym. Chem.* **2009**, *47*, 3583-3594.
  18. Kumar, J.; McDowall, L.; Chen, G.; Stenzel, M. H., *Polym. Chem.* **2011**, *2*, 1879-1886.
  19. Xu, J.; Boyer, C.; Bulmus, V.; Davis, T. P., *J. Polym. Sci., Part A: Polym. Chem.* **2009**, *47*, 4302-4313.
  20. Narain, R.; Armes, S. P., *Biomacromolecules* **2003**, *4*, 1746-1758.
  21. Narain, R.; Armes, S. P., *Macromolecules* **2003**, *36*, 4675-4678.
  22. Gupta, S. S.; Raja, K. S.; Kaltgrad, E.; Strable, E.; Finn, M. G., *Chem. Commun.* **2005**, 4315-4317.
  23. Dong, C.-M.; Sun, X.-L.; Faucher, K. M.; Apkarian, R. P.; Chaikof, E. L., *Biomacromolecules* **2003**, *5*, 224-231.
  24. Cairo, C. W.; Gestwicki, J. E.; Kanai, M.; Kiessling, L. L., *J. Am. Chem. Soc.* **2002**, *124*, 1615-1619.
  25. Ting, S. R. S.; Min, E. H.; Zetterlund, P. B.; Stenzel, M. H., *Macromolecules* **2010**, *43*, 5211-5221.
  26. Jiang, X.; Ahmed, M.; Deng, Z.; Narain, R., *Bioconjugate Chem.* **2009**, *20*, 994-1001.
  27. Pearson, S.; Allen, N.; Stenzel, M. H., *J. Polym. Sci., Part A: Polym. Chem.* **2009**, *47*, 1706-1723.
-



- 
28. Albertin, L.; Stenzel, M. H.; Barner-Kowollik, C.; Foster, L. J. R.; Davis, T. P., *Macromolecules* **2005**, *38*, 9075-9084.
29. Bernard, J.; Hao, X.; Davis, T. P.; Barner-Kowollik, C.; Stenzel, M. H., *Biomacromolecules* **2005**, *7*, 232-238.
30. Cameron, N. R.; Spain, S. G.; Kingham, J. A.; Weck, S.; Albertin, L.; Barker, C. A.; Battaglia, G.; Smart, T.; Blanz, A., *Faraday Discuss.* **2008**, *139*, 359-368.
31. Lowe, A. B.; Sumerlin, B. S.; McCormick, C. L., *Polymer* **2003**, *44*, 6761-6765.
32. Slavin, S.; Burns, J.; Haddleton, D. M.; Becer, C. R., *Eur. Polym. J.* **2011**, *47*, 435-446.
33. Gridnev, A., *J. Polym. Sci., Part A: Polym. Chem.* **2000**, *38*, 1753-1766.
34. Gridnev, A. A., *Polym. Sci. U.S.S.R.* **1989**, *31*, 2369-2376.
35. Krstina, J.; Moad, C. L.; Moad, G.; Rizzardo, E.; Berge, C. T.; Fryd, M., *Macromol. Symp.* **1996**, *111*, 13-23.
36. Gridnev, A. A.; Ittel, S. D., *Chem. Rev.* **2001**, *101*, 3611-3660.
37. Heuts, J. P. A.; Roberts, G. E.; Biasutti, J. D., *Aust. J. Chem.* **2002**, *55*, 381-398.
38. Debuigne, A.; Poli, R.; Jérôme, C.; Jérôme, R.; Detrembleur, C., *Prog. Polym. Sci.* **2009**, *34*, 211-239.
39. Abramo, G. P.; Norton, J. R., *Macromolecules* **2000**, *33*, 2790-2792.
40. Le Grogne, E.; Claverie, J.; Poli, R., *J. Am. Chem. Soc.* **2001**, *123*, 9513-9524.
41. Karmilova, L. V.; et al., *Russ. Chem. Rev.* **1984**, *53*, 132.
42. Enikolopyan, N. S.; Smirnov, B. R.; Ponomarev, G. V.; Belgovskii, I. M., *J. Polym. Sci. Polym. Chem. Ed.* **1981**, *19*, 879-889.
-

43. Heuts, J. P. A.; Davis, T. P.; Russell, G. T., *Macromolecules* **1999**, *32*, 6019-6030.
44. Moad, G.; Moad, C. L., *Macromolecules* **1996**, *29*, 7727-7733.
45. Clay, P. A.; Gilbert, R. G., *Macromolecules* **1995**, *28*, 552-569.
46. Whang, B.; Ballard, M.; Napper, D.; Gilbert, R., *Aust. J. Chem.* **1991**, *44*, 1133-1137.
47. Christie, D. I.; Gilbert, R. G., *Macromol. Chem. Phys.* **1996**, *197*, 403-412.
48. Haddleton, D. M.; Depaquis, E.; Kelly, E. J.; Kukulj, D.; Morsley, S. R.; Bon, S. A. F.; Eason, M. D.; Steward, A. G., *J. Polym. Sci., Part A: Polym. Chem.* **2001**, *39*, 2378-2384.
49. Mayo, F. R., *J. Am. Chem. Soc.* **1943**, *65*, 2324-2329.
50. Bon, S. A. F.; Morsley, D. R.; Waterson, J.; Haddleton, D. M., *Macromol. Symp.* **2001**, *165*, 29-42.
51. Janowicz, A. H. U.S. Patent 4,694,054, 1987.
52. McEwan, K. A.; Haddleton, D. M., *Polym. Chem.* **2011**.
53. Kukulj, D.; Davis, T. P., *Macromol. Chem. Phys.* **1998**, *199*, 1697-1708.
54. Heuts, J. P. A.; Forster, D. J.; Davis, T. P., *Macromolecules* **1999**, *32*, 3907-3912.
55. Haddleton, D. M.; Maloney, D. R.; Suddaby, K. G.; Muir, A. V. G.; Richards, S. N., *Macromol. Symp.* **1996**, *111*, 37-46.
56. Suddaby, K. G.; Maloney, D. R.; Haddleton, D. M., *Macromolecules* **1997**, *30*, 702-713.
57. Pierik, S. C. J. Shining a Light on Catalytic Chain Transfer. Eindhoven University of Technology, Eindhoven, 2002.

- 
58. Pierik, B.; Masclee, D.; van Herk, A., *Macromol. Symp.* **2001**, *165*, 19-28.
59. Haddleton, D. M.; Maloney, D. R.; Suddaby, K. G., *Macromolecules* **1996**, *29*, 481-483.
60. Haddleton, D. M.; Topping, C.; Hastings, J. J.; Suddaby, K. G., *Macromol. Chem. Phys.* **1996**, *197*, 3027-3042.
61. Haddleton, D. M.; Topping, C.; Kukulj, D.; Irvine, D., *Polymer* **1998**, *39*, 3119-3128.
62. Abbey, K. J.; Trumbo, D. L.; Carlson, G. M.; Masola, M. J.; Zander, R. A., *J. Polym. Sci., Part A: Polym. Chem.* **1993**, *31*, 3417-3424.
63. Kolb, H. C.; Finn, M. G.; Sharpless, K. B., *Angew. Chem. Int. Ed.* **2001**, *40*, 2004-2021.
64. Ladmiral, V.; Mantovani, G.; Clarkson, G. J.; Cauet, S.; Irwin, J. L.; Haddleton, D. M., *J. Am. Chem. Soc.* **2006**, *128*, 4823-4830.
65. Li, G.-Z.; Randev, R. K.; Soeriyadi, A. H.; Rees, G.; Boyer, C.; Tong, Z.; Davis, T. P.; Becer, C. R.; Haddleton, D. M., *Polym. Chem.* **2010**, *1*, 1196-1204.
66. Nurmi, L.; Lindqvist, J.; Randev, R.; Syrett, J.; Haddleton, D. M., *Chem. Commun.* **2009**, 2727-2729.
67. Johnson, J. A.; Finn, M. G.; Koberstein, J. T.; Turro, N. J., *Macromol. Rapid Commun.* **2008**, *29*, 1052-1072.
68. Li, H.; Cheng, F.; Duft, A. M.; Adronov, A., *J. Am. Chem. Soc.* **2005**, *127*, 14518-14524.
69. Liu, J.; Nie, Z.; Gao, Y.; Adronov, A.; Li, H., *J. Polym. Sci., Part A: Polym. Chem.* **2008**, *46*, 7187-7199.
70. Kolb, H. C.; Sharpless, K. B., *Drug Discov. Today* **2003**, *8*, 1128-1137.
71. Gramlich, P.; Warncke, S.; Gierlich, J.; Carell, T., *Angew. Chem. Int. Ed.* **2008**, *47*, 3442-3444.
-

- 
72. Jones, M. W.; Mantovani, G.; Ryan, S. M.; Wang, X.; Brayden, D. J.; Haddleton, D. M., *Chem. Commun.* **2009**, 5272-5274.
73. Wang, Q.; Chan, T. R.; Hilgraf, R.; Fokin, V. V.; Sharpless, K. B.; Finn, M. G., *J. Am. Chem. Soc.* **2003**, *125*, 3192-3193.
74. Agard, N. J.; Prescher, J. A.; Bertozzi, C. R., *J. Am. Chem. Soc.* **2004**, *126*, 15046-15047.
75. Mamidyala, S. K.; Finn, M. G., *Chem. Soc. Rev.* **2010**, *39*, 1252-1261.
76. Moses, J. E.; Moorhouse, A. D., *Chem. Soc. Rev.* **2007**, *36*, 1249-1262.
77. Binder, W. H.; Sachsenhofer, R., *Macromol. Rapid Commun.* **2007**, *28*, 15-54.
78. Becer, C. R.; Hoogenboom, R.; Schubert, U. S., *Angew. Chem. Int. Ed.* **2009**, *48*, 4900-4908.
79. Sumerlin, B. S.; Vogt, A. P., *Macromolecules* **2009**, *43*, 1-13.
80. Hein, J. E.; Fokin, V. V., *Chem. Soc. Rev.* **2010**, *39*, 1302-1315.
81. Hein, J. E.; Tripp, J. C.; Krasnova, L. B.; Sharpless, K. B.; Fokin, V. V., *Angew. Chem. Int. Ed.* **2009**, *48*, 8018-8021.
82. Kappe, C. O.; Van der Eycken, E., *Chem. Soc. Rev.* **2010**, *39*, 1280-1290.
83. Binder, W. H.; Sachsenhofer, R., *Macromol. Rapid Commun.* **2008**, *29*, 952-981.
84. Geng, J.; Mantovani, G.; Tao, L.; Nicolas, J.; Chen, G.; Wallis, R.; Mitchell, D. A.; Johnson, B. R. G.; Evans, S. D.; Haddleton, D. M., *J. Am. Chem. Soc.* **2007**, *129*, 15156-15163.
85. Geng, J.; Lindqvist, J.; Mantovani, G.; Chen, G.; Sayers, C. T.; Clarkson, G. J.; Haddleton, D. M., *QSAR. Comb. Sci.* **2007**, *26*, 1220-1228.
86. El-Sagheer, A. H.; Brown, T., *Chem. Soc. Rev.* **2010**, *39*, 1388-1405.
-

- 
87. Jones, M. W.; Gibson, M. I.; Mantovani, G.; Haddleton, D. M., *Polym. Chem.* **2011**, *2*, 572-574.
88. Holub, J. M.; Kirshenbaum, K., *Chem. Soc. Rev.* **2010**, *39*, 1325-1337.
89. Meldal, M., *Macromol. Rapid Commun.* **2008**, *29*, 1016-1051.
90. Devaraj, N. K.; Collman, J. P., *QSAR. Comb. Sci.* **2007**, *26*, 1253-1260.
91. Michael, A., *J. Prakt. Chem.* **1893**, *48*, 94-95.
92. Huisgen, R., *Angew. Chem. Int. Ed. Engl.* **1963**, *2*, 565-598.
93. Huisgen, R., *Angew. Chem. Int. Ed. Engl.* **1963**, *2*, 633-645.
94. Rostovtsev, V. V.; Green, L. G.; Fokin, V. V.; Sharpless, K. B., *Angew. Chem. Int. Ed.* **2002**, *41*, 2596-2599.
95. Tornøe, C. W.; Christensen, C.; Meldal, M., *J. Org. Chem.* **2002**, *67*, 3057-3064.
96. Meldal, M.; Tornøe, C. W., *Chem. Rev.* **2008**, *108*, 2952-3015.
97. Pérez-Balderas, F.; Ortega-Muñoz, M.; Morales-Sanfrutos, J.; Hernández-Mateo, F.; Calvo-Flores, F. G.; Calvo-Asín, J. A.; Isac-García, J.; Santoyo-González, F., *Org. Lett.* **2003**, *5*, 1951-1954.
98. Gonda, Z.; Novak, Z., *Dalton T.* **2010**, *39*, 726-729.
99. Mykhalichko, B. M.; Temkin, O. N.; Mys'kiv, M. G., *Russ. Chem. Rev.* **2000**, *69*, 957.
100. Lutz, J.-F., *Angew. Chem. Int. Ed.* **2008**, *47*, 2182-2184.
101. Codelli, J. A.; Baskin, J. M.; Agard, N. J.; Bertozzi, C. R., *J. Am. Chem. Soc.* **2008**, *130*, 11486-11493.
102. Li, M.; De, P.; Gondi, S. R.; Sumerlin, B. S., *J. Polym. Sci., Part A: Polym. Chem.* **2008**, *46*, 5093-5100.
-

103. Inglis, A. J.; Sinnwell, S.; Davis, T. P.; Barner-Kowollik, C.; Stenzel, M. H., *Macromolecules* **2008**, *41*, 4120-4126.
104. Bousquet, A.; Boyer, C.; Davis, T. P.; Stenzel, M. H., *Polym. Chem.* **2010**, *1*, 1186-1195.
105. Hoyle, C. E.; Lowe, A. B.; Bowman, C. N., *Chem. Soc. Rev.* **2010**, *39*, 1355-1387.
106. Lowe, A. B., *Polym. Chem.* **2010**, *1*, 17-36.
107. Dondoni, A., *Angew. Chem. Int. Ed.* **2008**, *47*, 8995-8997.
108. Kade, M. J.; Burke, D. J.; Hawker, C. J., *J. Polym. Sci., Part A: Polym. Chem.* **2010**, *48*, 743-750.
109. Chan, J. W.; Hoyle, C. E.; Lowe, A. B., *J. Am. Chem. Soc.* **2009**, *131*, 5751-5753.
110. Fairbanks, B. D.; Sims, E. A.; Anseth, K. S.; Bowman, C. N., *Macromolecules* **2010**, *43*, 4113-4119.
111. Naik, S. S.; Chan, J. W.; Comer, C.; Hoyle, C. E.; Savin, D. A., *Polym. Chem.* **2011**, *2*, 303-305.
112. Hoogenboom, R., *Angew. Chem. Int. Ed.* **2010**, *49*, 3415-3417.
113. Rosen, B. M.; Lligadas, G.; Hahn, C.; Percec, V., *J. Polym. Sci., Part A: Polym. Chem.* **2009**, *47*, 3931-3939.
114. Rosen, B. M.; Lligadas, G.; Hahn, C.; Percec, V., *J. Polym. Sci., Part A: Polym. Chem.* **2009**, *47*, 3940-3948.
115. Li, H.; Yu, B.; Matsushima, H.; Hoyle, C. E.; Lowe, A. B., *Macromolecules* **2009**, *42*, 6537-6542.
116. Shin, J.; Matsushima, H.; Chan, J. W.; Hoyle, C. E., *Macromolecules* **2009**, *42*, 3294-3301.

- 
117. Hoyle, C. E.; Lee, T. Y.; Roper, T., *J. Polym. Sci., Part A: Polym. Chem.* **2004**, *42*, 5301-5338.
118. Hoyle, C. E.; Bowman, C. N., *Angew. Chem. Int. Ed.* **2010**, *49*, 1540-1573.
119. Morgan, C. R.; Magnotta, F.; Ketley, A. D., *J. Polym. Sci. Polym. Chem. Ed.* **1977**, *15*, 627-645.
120. Griesbaum, K., *Angew. Chem. Int. Ed. Engl.* **1970**, *9*, 273-287.
121. ten Brummelhuis, N.; Diehl, C.; Schlaad, H., *Macromolecules* **2008**, *41*, 9946-9947.
122. Uygun, M.; Tasdelen, M. A.; Yagci, Y., *Macromol. Chem. Phys.* **2009**, *211*, 103-110.
123. Chan, J. W.; Yu, B.; Hoyle, C. E.; Lowe, A. B., *Chem. Commun.* **2008**, 4959-4961.
124. Wu, P.; Malkoch, M.; Hunt, J. N.; Vestberg, R.; Kaltgrad, E.; Finn, M. G.; Fokin, V. V.; Sharpless, K. B.; Hawker, C. J., *Chem. Commun.* **2005**, 5775-5777.
125. Sumerlin, B. S.; Tsarevsky, N. V.; Louche, G.; Lee, R. Y.; Matyjaszewski, K., *Macromolecules* **2005**, *38*, 7540-7545.
126. Correa, J.; Rodriguez-Meizoso, I.; Riguera, R., *Macromolecules* **2006**, *39*, 2113-2120.
127. Geng, J.; Lindqvist, J.; Mantovani, G.; Haddleton, D. M., *Angew. Chem. Int. Ed.* **2008**, *47*, 4180-4183.
128. Tanaka, T.; Nagai, H.; Noguchi, M.; Kobayashi, A.; Shoda, S.-i., *Chem. Commun.* **2009**, 3378-3379.
129. Tanaka, T.; Matsumoto, T.; Noguchi, M.; Kobayashi, A.; Shoda, S.-i., *Chem. Lett.* **2009**, *38*, 458-459.
130. Tanaka, T.; Huang, W. C.; Noguchi, M.; Kobayashi, A.; Shoda, S.-i., *Tetrahedron Lett.* **2009**, *50*, 2154-2157.
-

131. Isobe, T.; Ishikawa, T., *J. Org. Chem.* **1999**, *64*, 6984-6988.
132. Isobe, T.; Ishikawa, T., *J. Org. Chem.* **1999**, *64*, 6989-6992.
133. Isobe, T.; Ishikawa, T., *J. Org. Chem.* **1999**, *64*, 5832-5835.



## **Chapter 4.**

# **Well-defined Multivalent Glycopolymers for the Lectin-Carbohydrate Interaction**

## 4.1 Introduction

Synthetic glycopolymers are important natural oligosaccharides mimics for many biological applications.<sup>1-5</sup> As multivalent ligands, the potencies of glycopolymers acting as inhibitors or effectors depend on the mechanism by which they operate.<sup>6-7</sup> As the multi-protein complexes caused by subcellular localisation<sup>8</sup> is the dominant signalling units for signal transductions such as the immune synapses<sup>9</sup> and eukaryotic cell adhesion,<sup>10</sup> synthetic glycopolymers are valuable tools to reveal the mystery of these sophisticated receptor complexes in signal transduction.<sup>11</sup> Meanwhile, in order to develop glycopolymeric drugs and therapeutic agents, factors that control the receptor-ligand interactions also need to be investigated.

### 4.1.1 The interaction mechanisms of ligands with receptors

The binding mechanisms for monovalent ligands (monosaccharides such as mannose and galactose) are relatively simple. The ligand can only either bind to a single receptor or dimerise two receptors, **Figure 4.1**. However, the binding mechanisms are more complicated for multivalent ligands due to the influences of both the macromolecular features and binding elements. The structural complexities enable multivalent ligands to bind with receptors in many possible different ways.

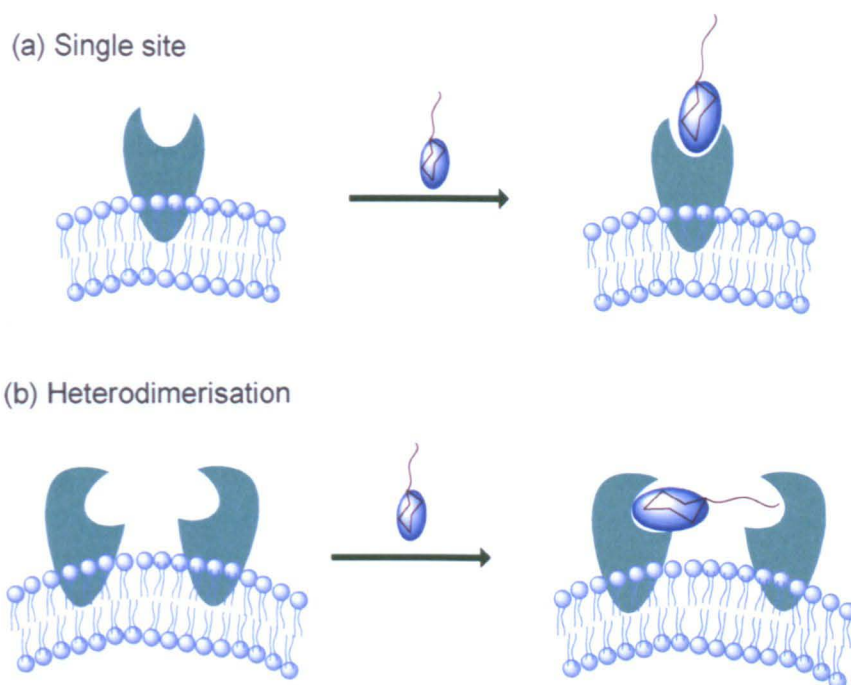
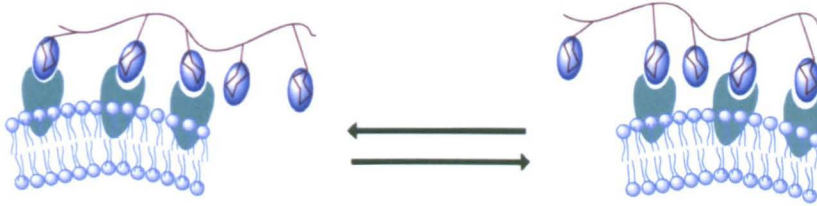


Figure 4.1 Binding mechanisms of monovalent ligands with receptors.

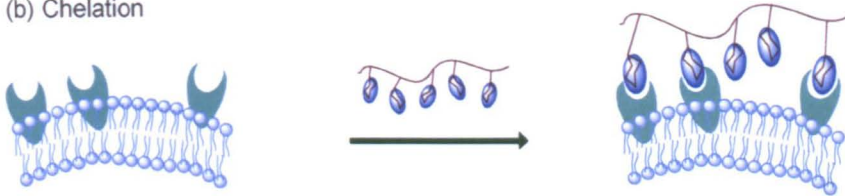
The proposed binding mechanisms<sup>11-14</sup> of multivalent ligands with receptors include the statistical rebinding effect, chelation, receptor clustering, subsite binding, and steric stabilisation, **Figure 4.2**. High local concentration of the binding elements can enable the statistical rebinding of the multivalent ligands to the receptors, **(a)**. When multiple binding epitopes of a multivalent ligand bind to many binding sites on one oligomeric receptor, the entropic penalty<sup>15-16</sup> is only paid by the first binding of the ligand with the receptor, not by the subsequent binding interactions of the ligand. The affinity of multivalent ligands with the receptors is much higher than that of a monovalent ligand, **(b)**. The binding of multivalent ligands can change the orientation and proximity of the relevant receptors, which is important in signal transduction, **(c)**. In a similar way to the chelation effect, multivalent ligands can contact with both primary binding sites and adjacent subsites of receptors through the binding elements or the other parts of the ligands, **(d)**. Due to the steric blockage,

the receptors bound to multivalent ligands can rarely have further interactions with other ligands, viral particles, or cells. This mechanism is particular important for the application of multivalent ligands as the inhibitors, (e).

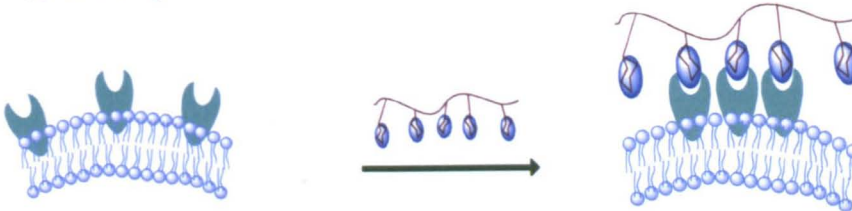
(a) Statistical effect



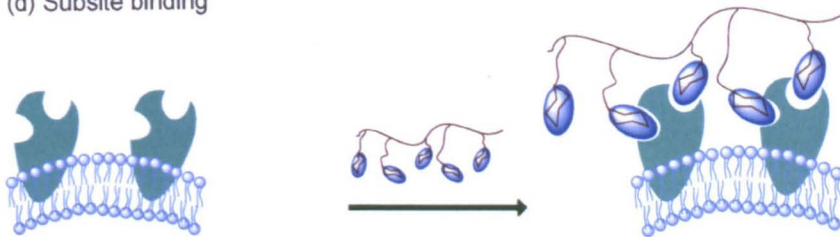
(b) Chelation



(c) Clustering



(d) Subsite binding



(e) Steric stabilisation

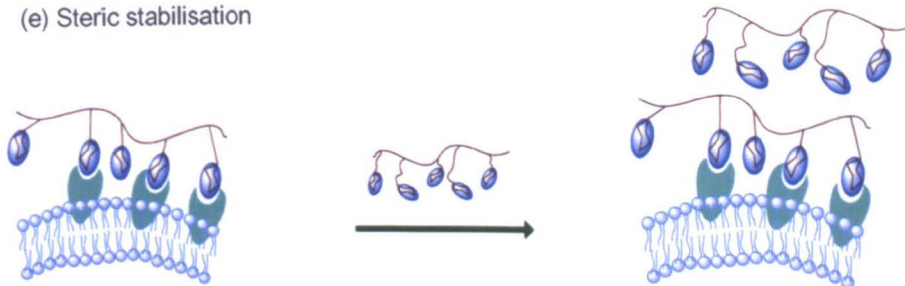


Figure 4.2 Proposed binding mechanisms of multivalent ligands with receptors.

### 4.1.2 Investigation into lectin-glycopolymer interactions

Unlike monovalent ligands, glycopolymers are involved in quite complicated interactions with lectins as multivalent ligands. The various shapes, sizes, flexibilities, orientations, valencies and densities of the binding epitopes can affect the formation of receptor complexes and thus ultimately, influence biological activities of the relevant glycopolymers.<sup>17-18</sup> To address the effects of different variables on the lectin-glycopolymer interactions, experiments have been performed using multiple methods. Although modern techniques such as quartz crystal microbalance (QCM),<sup>19-20</sup> surface plasmon resonance (SPR),<sup>21-23</sup> have been employed to explore the lectin-glycopolymer interactions, traditional high throughput methods (quantitative precipitation, turbidity, fluorescence quenching assays, *etc.*) provide more straightforward but important information about the inhibition and clustering of receptors.<sup>24-27</sup>

Kiessling, *et al.*<sup>17</sup> investigated the influence of the binding epitope density of multivalent ligands on the clustering of a model receptor, concanavalin A (Con A). By using different ratios of mannose- and galactose-substituted monomers in the polymerisation reactions, they prepared a series of glycopolymers *via* ROMP, which were similar in polymeric length, polarity, and steric properties differing only in their proportion of binding epitopes. They studied the stoichiometry of Con A within the cluster *via* quantitative precipitation, the rate of cluster formation *via* turbidity assays and the receptor proximity *via* fluorescence resonance energy transfer (FRET) experiments. They found that the ligands with most binding epitopes clustered the most Con A units per polymer chain. However, on a mannose residue basis, the most efficient ligands are those with the lowest density of binding epitopes. By increasing

the binding epitope density to 70% there was no additional increase in the number of receptors bound per multivalent ligand. The rate of clustering is directly related to binding epitope density. The highest density ligands showed the fastest rates of complex assembly. They indicated that the increases of binding epitope density from 20 to 70% resulted in decreases of the average inter-receptor distances. However, there were no significant changes in FRET by increasing the binding epitope density from 70% to 100%.

They also investigated the influence of the multivalent ligand architecture.<sup>28</sup> By employing 28 multivalent ligands of 5 different structural classes to be tested by solid-phase binding assay and the clustering assays including quantitative precipitation, turbidimetry and fluorescence quenching assay, they showed that the polydisperse polymers with relatively high molecular weight and the protein conjugates were very effective inhibitors which bound many copies of Con A, but the rate of their clustering Con A was slow and the average distances of Con A tetramers within the clusters were quite large. Ligands with low molecular weight were poor as the clustering agents for Con A. However, some could inhibit and cluster Con A which can be used as the leads for the potent effectors or inhibitors. Generally, the highly substituted glycopolymers prepared by ROMP showed the highest activities in promoting receptor clustering and fluorescence quenching.

Stenzel and co-workers<sup>29-30</sup> showed that the binding was more efficient with the formation of micelles as the glycopolymer in the micelle took on a more brush-like conformation. They also showed that the distance of galactose from the polymer backbone of the glycopolymers also played an important role in the lectin-

glycopolymer binding.<sup>18</sup> They synthesised block copolymers of DEGMA and HEMA, DEGMA and PEGMA *via* RAFT polymerisation, followed by clicking galactose azide to the copolymers by CuAAC. With investigation of the interaction between the glycopolymers and galactose-specific plant toxin, ricin *via* asialofetuin competition assays, they showed that P(DEGMA-*b*-PEGMA) glycopolymers had the highest degree of binding with shorter glycopolymeric chain having a better inhibition of ricin as compared to monovalent galactose. They established the order for ricin inhibition which was  $P(\text{HEMA-Gal}) < P(\text{PEGMA-Gal}) < P(\text{DEGMA}_{43}\text{-b-P(HEMA-Gal)}) \leq P(\text{DEGMA}_{43}\text{-b-P(PEGMA-Gal)})$ .

### 4.1.3 Conclusions

In summary, the interactions between multivalent ligands and receptors have a range of possible mechanisms. More than one mechanism may involve in a single interaction. The change of parameters of glycopolymers can significantly influence their binding patterns with lectins and eventually affect their biological applications.

Preliminary studies<sup>31</sup> of the lectin-glycopolymer interaction in our research group showed that linear glycopolymers prepared by ATRP and CuAAC with different epitope densities occupied excellent clustering properties to the lectin Con A. Therefore, in this study similar linear glycopolymers were synthesised by a combination of ATRP and CuAAC, which bear the same macromolecular features differing only in the nature and proportions of the pendant binding units. The binding properties of these multivalent ligands introduced by not only the epitope densities but also the different nature of sugars will be investigated, **Figure 4.3**.

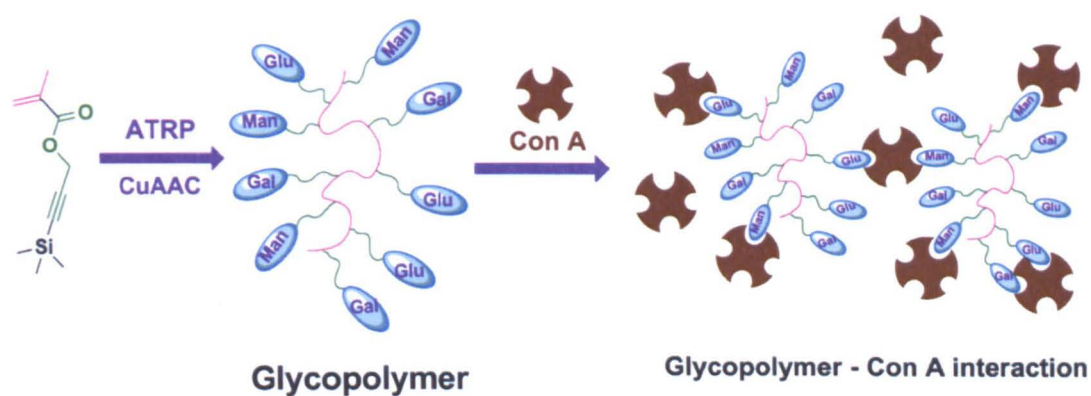


Figure 4.3 The strategy used in this study.

Concanavalin A (Con A) was employed as the model lectin as it is structurally similar to many animal and bacterial lectins in cell communication events.<sup>32-33</sup> Con A is extracted from jack beans and exists as a homotetramer at neutral pH with four binding units which can bind specifically to  $\alpha$ -linked mannopyranosides and glucopyranosides, **Figure 4.4**. Con A is an excellent model for the lectin-glycopolymer interaction as it can be clustered by various multivalent ligands.<sup>28, 34</sup>

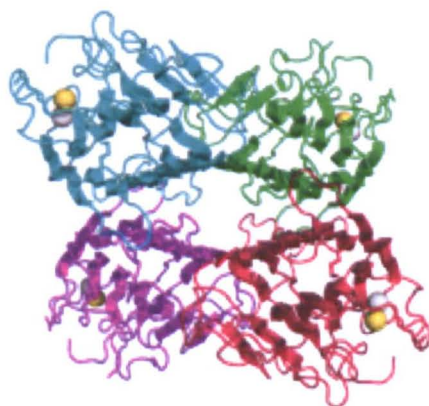


Figure 4.4 The crystallographic structure of concanavalin A (Con A): The four subunits are coloured with cyan, magenta, red, green. The gold and grey spheres represent calcium and manganese cations respectively.



## 4.2 Results and discussion

### 4.2.1 Synthesis of glycopolymers

The synthesis was carried out by a former PhD student in the group, Dr. Jin Geng.

The general procedures are shown in **Figure 4.5**.

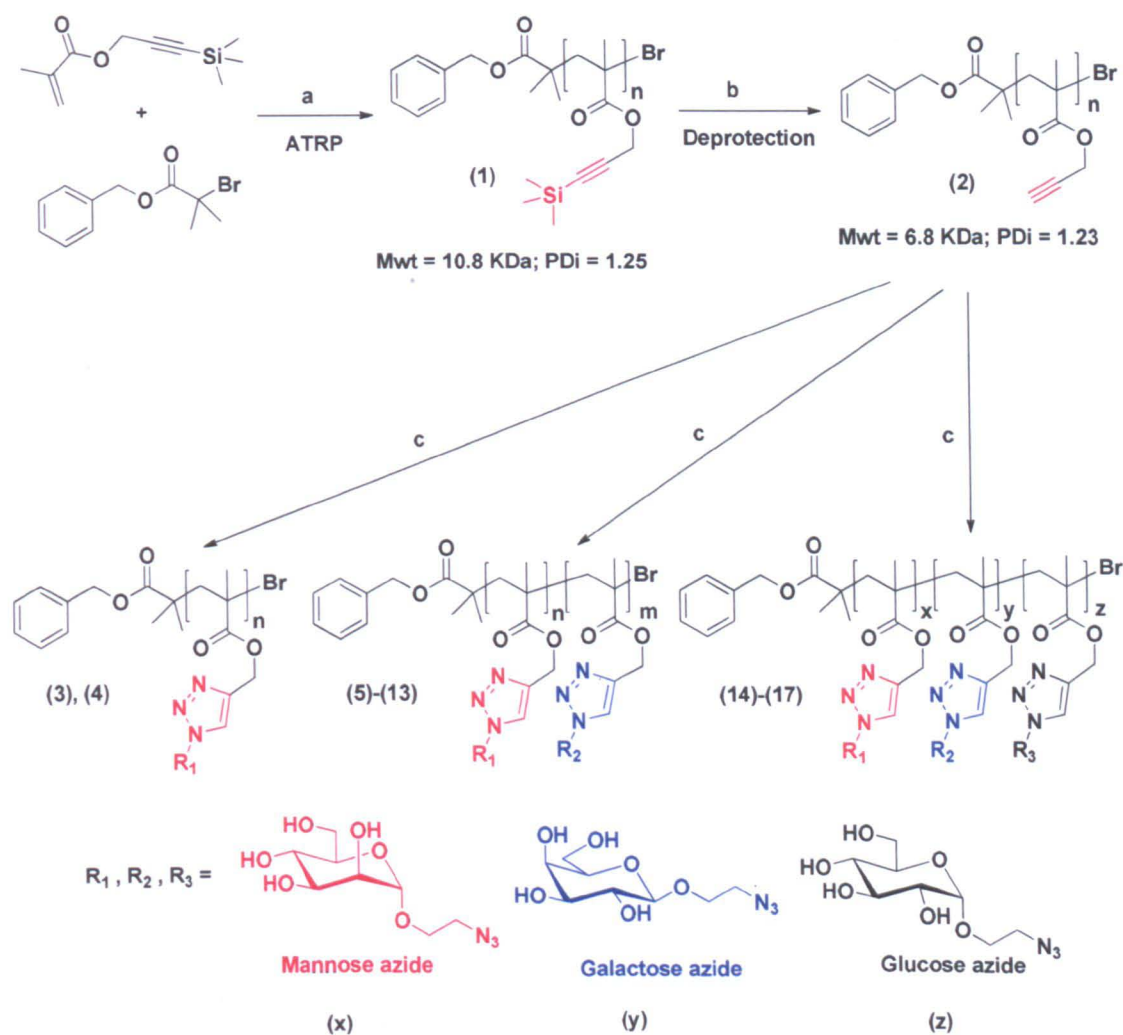


Figure 4.5 Synthesis of glycopolymers by ATRP and CuAAC click reaction. Reagents and conditions: (a) *N*-(ethyl)-2-pyridylmethanimine/CuBr, toluene, 70 °C; (b) TBAF, acetic acid, THF; (c) RN<sub>3</sub>, CuBr, bipyridine, Et<sub>3</sub>N.

The monomer TMS-protected propargyl methacrylate was prepared from commercially available 3-trimethylsilylpropyn-1-ol and methacryloyl chloride.<sup>31</sup> The polymerisation was catalysed by a Cu(I)Br/*N*-(ethyl)-2-pyridylmethanimine catalyst system.<sup>35</sup> The alkyne-containing polymers were generated by removal of the TMS protecting groups using TBAF with acetic acid as buffering agent. The sugar azides were made as previously described.<sup>36</sup> 2'-Azidoethyl-O- $\alpha$ -D-mannopyranoside (**x**) 2'-azidoethyl-O- $\beta$ -D-galactopyranoside (**y**) and 2'-azidoethyl-O- $\alpha$ -D-glucopyranoside (**z**) were used to click with the precursor polymers.

A library of well-defined glycopolymers was prepared *via* CuAAC by simultaneously attaching different sugar moieties (mannose, galactose or glucose) onto the same alkyne-containing polymer scaffolds (DP = 58), **Table 4.1**. 15 different glycopolymers were generated with single type of sugars, two types of sugar with different densities or all three types of sugars with different concentrations. These glycopolymers were then used in the investigation into different aspects of binding interactions with the model lectin Con A.

Table 4.1 Glycopolymers synthesised in this study.

Polymer	$\alpha$ -mannose (%)	$\beta$ -galactose (%)	$\alpha$ -glucose (%)	$M_n$ (kDa) <sup>b</sup>	$M_w / M_n$ <sup>a</sup>
(3)	100	0	0	22.1	1.31
(4)	0	100	0	22.1	1.29
(5)	75	25	0	22.5	1.34
(6)	50	50	0	22.2	1.33
(7)	25	75	0	22.1	1.31
(8)	0	25	75	22.2	1.31
(9)	0	50	50	22.3	1.34
(10)	0	75	25	22.1	1.32
(11)	75	0	25	22.0	1.31
(12)	50	0	50	22.0	1.35
(13)	25	0	75	22.1	1.30
(14)	50	25	25	22.1	1.32
(15)	33	33	33	22.2	1.31
(16)	25	25	50	22.0	1.30
(17)	25	50	25	22.1	1.32

<sup>a</sup>Obtained by SEC with DMF as the eluent; <sup>b</sup>Obtained by <sup>1</sup>H NMR.

#### 4.2.2 The stoichiometry of the glycopolymer–Con A complexes.

As a single assay often only elucidates one aspect of the lectin-glycopolymer clustering, so we employed four high throughput assays to fully explore the contributions of macromolecular structure and composition to the inhibition and clustering of Con A. HBS buffer (0.10 M HEPES, 0.9 M NaCl, 1 mM MgCl<sub>2</sub>, 1 mM

$\text{CaCl}_2$  and 1 mM  $\text{MnCl}_2$ , pH 7.4) was used in all of the experiments. The presence of metal ions  $\text{Ca}^{2+}$ ,  $\text{Mg}^{2+}$  and  $\text{Mn}^{2+}$  is essential for the binding activity of Con A.<sup>37</sup>

In order to investigate the stoichiometry of the glycopolymer–Con A aggregates, quantitative precipitation assays were employed,<sup>38</sup> **Figure 4.6 ~ Figure 4.9**. Con A was dissolved in HBS buffer to make a fresh stock solution (60  $\mu\text{M}$ , assuming Con A tetramers with a molecular weight of 106 kDa). A series of glycopolymer concentrations were used to precipitate Con A from the solution of the same concentration (30  $\mu\text{M}$ ). The precipitates of Con A were purified and then dissolved in HBS buffer solution (1 M) of methyl- $\alpha$ -D-mannopyranoside. The content of Con A in the solution was determined by measuring the absorbance at 280 nm. After fitting the data with a sigmoidal curve, the steepest point of the curve was taken as the half concentration required to fully precipitate Con A.

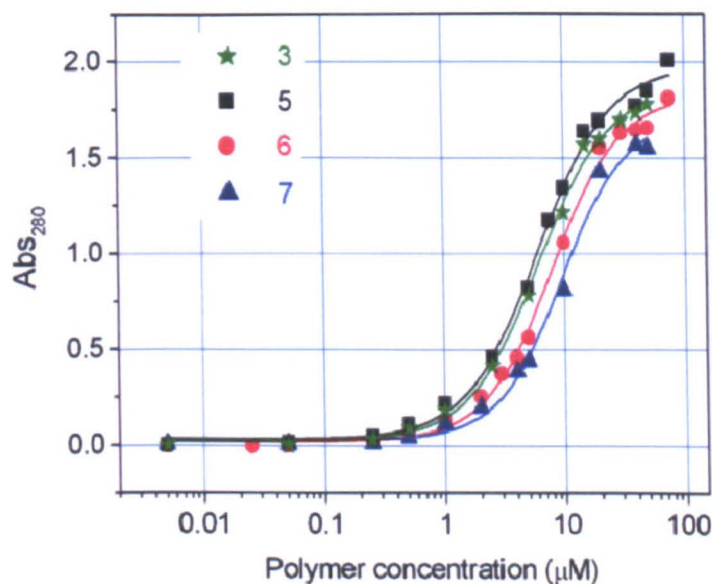


Figure 4.6 The sigmoidal curves fitted to the data from quantitative precipitation assays using glycopolymers (3 ~ 7) containing pendant mannose or galactose.

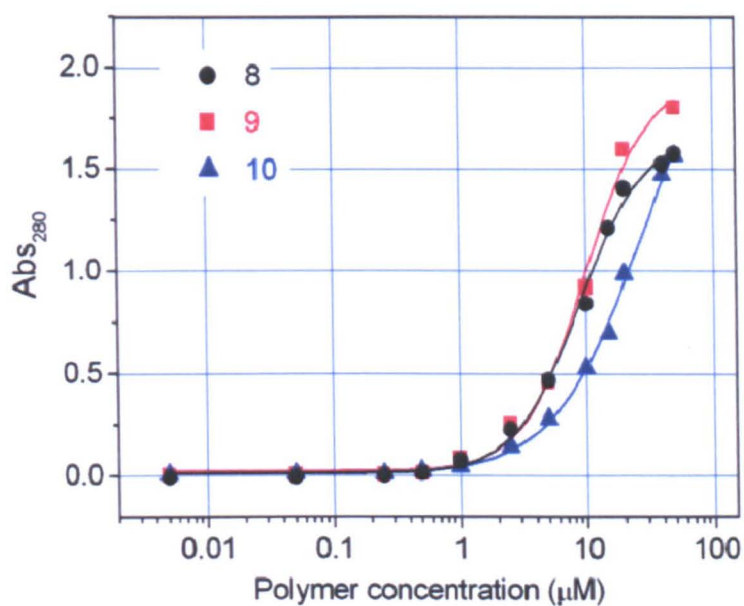


Figure 4.7 The sigmoidal curves fitted to the data from quantitative precipitation assays using glycopolymers (8 ~ 10) containing pendant galactose and glucose.

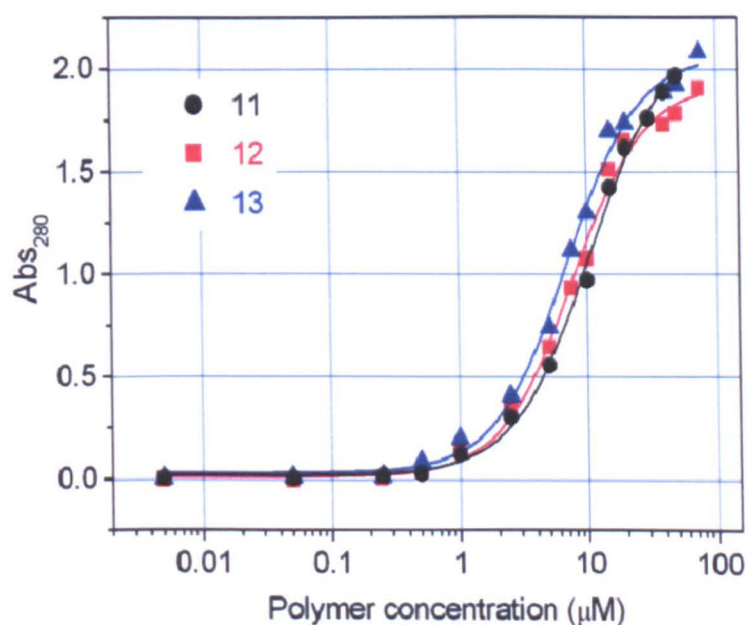


Figure 4.8 The sigmoidal curves fitted to the data from quantitative precipitation assays using glycopolymers (11 ~ 13) containing pendant mannose and glucose.

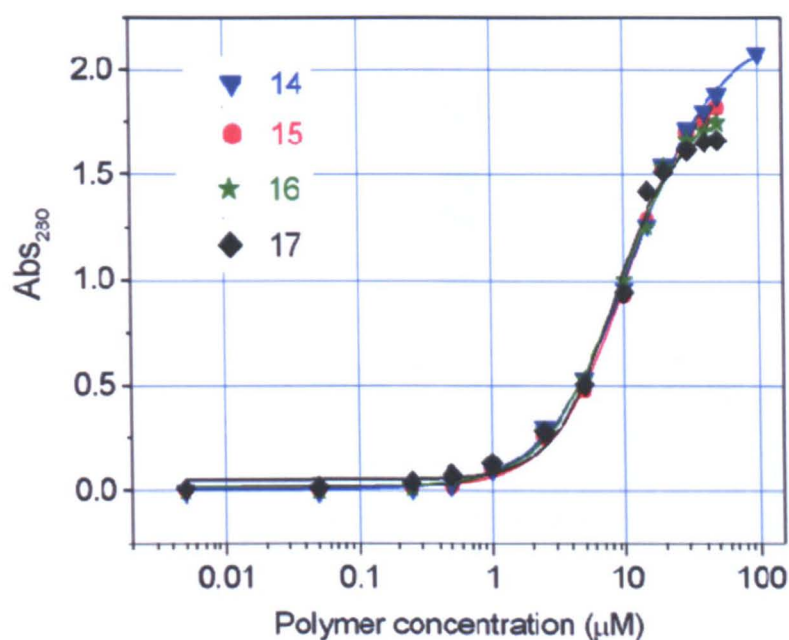


Figure 4.9 The sigmoidal curves fitted to the data from quantitative precipitation assays using glycopolymers (14 ~ 17) containing pendant mannose, galactose and glucose of different ratios.

These experiments assessed the glycopolymeric concentration required for half-maximal precipitation of Con A. For all glycopolymers 3 – 17, these concentrations are shown in **Figure 4.10 (a)**. By comparing with the concentration of Con A (30 μM), the numbers of Con A units bound to each glycopolymer chain were obtained, **Figure 4.10 (b)**.



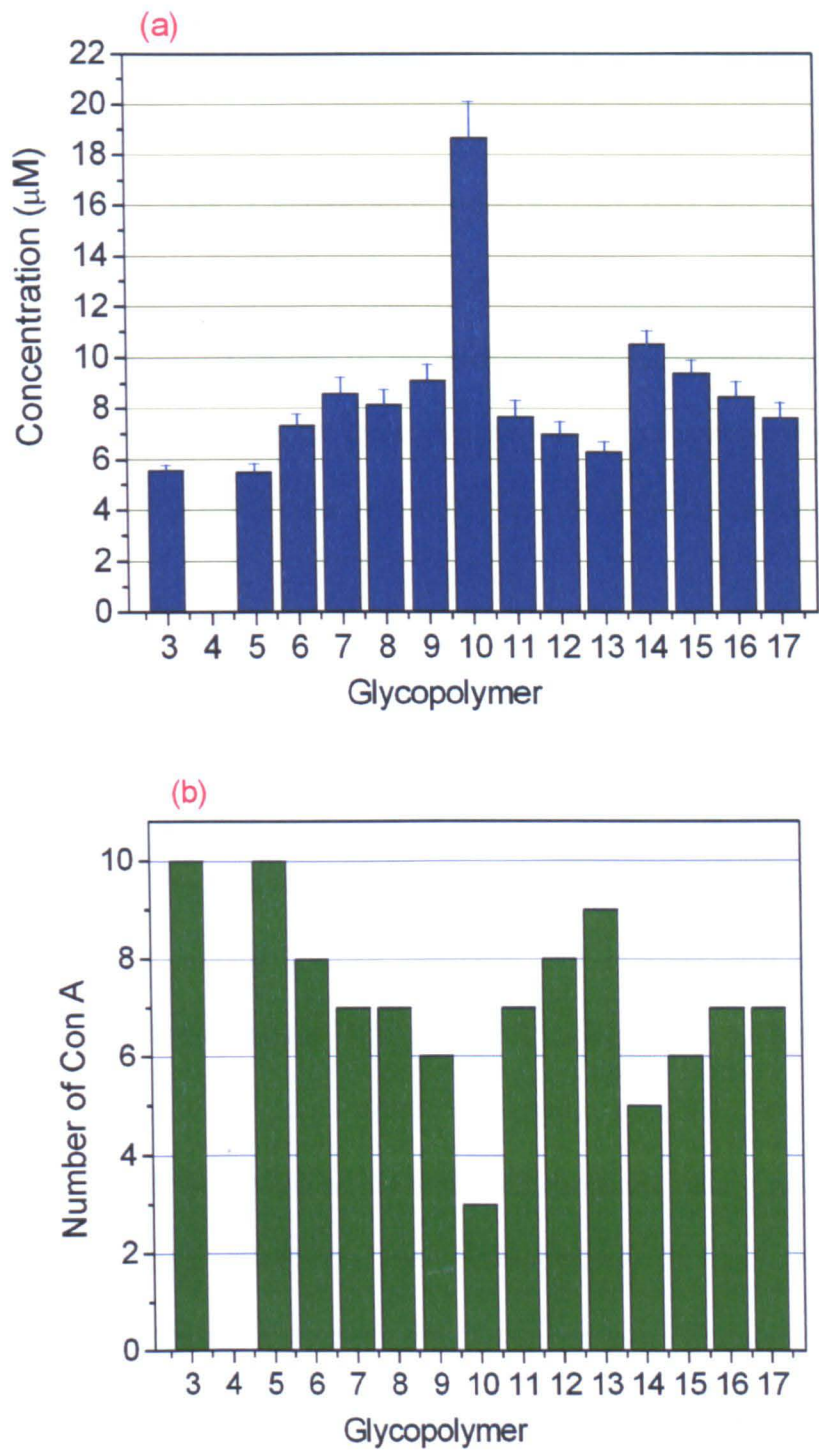


Figure 4.10 Quantitative precipitation results. (a) The concentration required for half-maximal precipitation. The error bars represent the standard deviation. (b) The number of Con A units bound per glycopolymer chain.

The results show that the mannose rich glycopolymer **3** bound the most Con A units amongst all of the glycopolymers while glycopolymer **4** containing only pendant galactose did not precipitate Con A from solution. The mannose-galactose glycopolymers **5, 6 and 7** bound more Con A units than the glucose-galactose glycopolymers **8, 9 and 10** with the same epitope densities. These results agreed well with the binding properties of the relative monosaccharides to Con A. The densities of binding elements of these glycopolymers influenced the clustering of Con A, however, this effect was decreasing as the densities increased to 75% or above.

Comparing to the mannose-glucose glycopolymers **11, 12 and 13**, we can conclude that the binding capability is greatly enhanced by grafting mannose instead of galactose to the polymer backbone containing pendant glucose. However, for all of the glycopolymers containing both mannose and glucose, glycopolymer **11** to glycopolymer **17**, the mannose density is the predominant control factor on the binding capability. With low mannose density of 25%, the corresponding glycopolymers bind more Con A. In summary, both the nature and the density of pendant sugars have effect on the stoichiometry of the clustering lectin-glycopolymer complexes. However, the homo-mannose glycopolymer **3** and the mannose-galactose glycopolymer **5** are the most effective at binding many copies of Con A per polymer chain.

#### **4.2.3 The rate of glycopolymer–Con A clustering.**

The rate of receptor clustering on the cell surface determines many signalling events, which can vary from seconds to hours.<sup>39-41</sup> In order to monitor the precipitation of



the glycopolymer–Con A clustering in real time, turbidimetry experiments were performed. The glycopolymer solution (5  $\mu\text{M}$ ) that can fully precipitate Con A was mixed with the lectin solution (5  $\mu\text{M}$ ). The absorbance of the mixture at 420 nm was measured for 10 min with intervals of 12 s, **Figure 4.11 ~ Figure 4.14**.

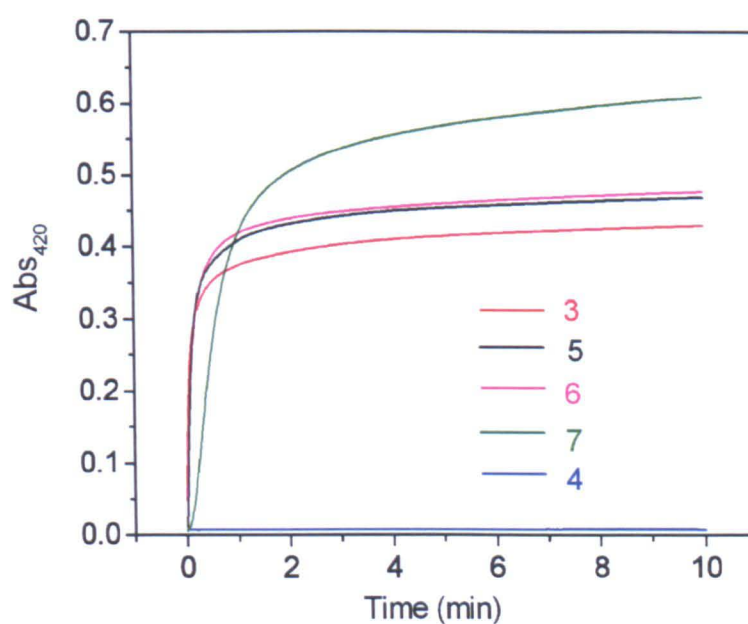


Figure 4.11 Plots of  $Abs_{420}$  vs. time in turbidimetry experiments of glycopolymers (3 ~ 7) containing pendant mannose or galactose.

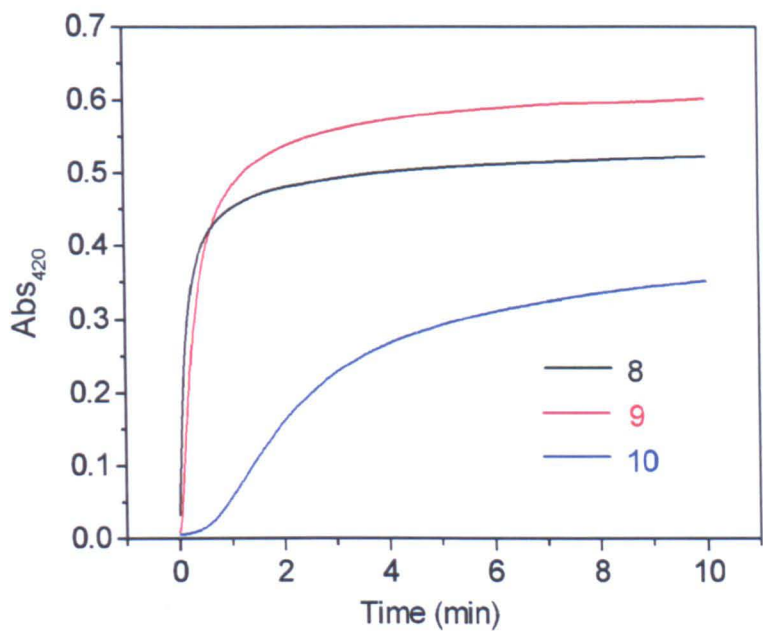


Figure 4.12 Plots of Abs<sub>420</sub> vs. time in turbidimetry experiments of glycopolymers (8 ~ 10) containing pendant galactose and glucose.

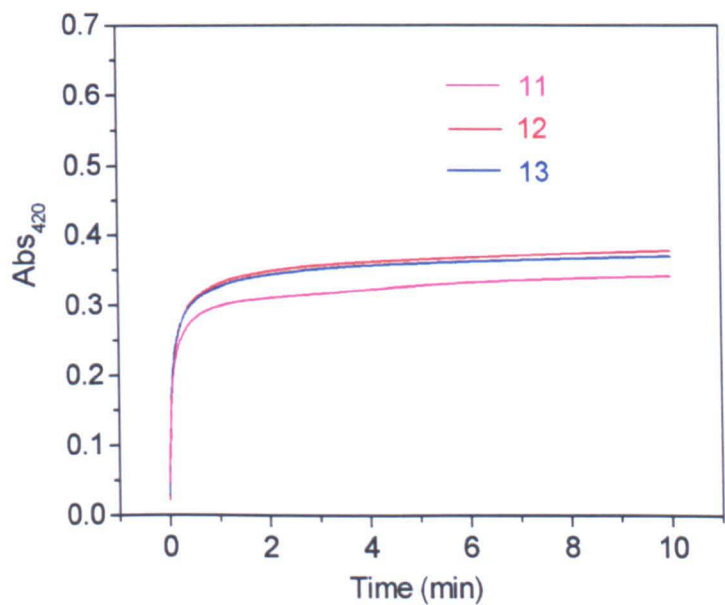


Figure 4.13 Plots of Abs<sub>420</sub> vs. time in turbidimetry experiments of glycopolymers (11 ~ 13) containing pendant mannose and glucose.

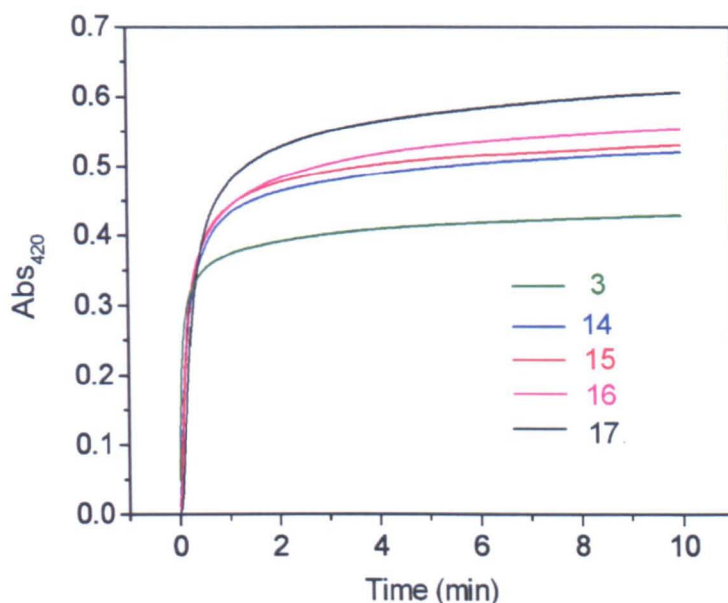


Figure 4.14 Plots of  $Abs_{420}$  vs. time in turbidimetry experiments of glycopolymers (14 ~ 17) containing pendant mannose, galactose and glucose of different ratios.

A linear fit to the initial part of the curve was used to determine the rate of the clustering, which is expressed as arbitrary units per minute ( $AU\ min^{-1}$ ), **Figure 4.15 (a)**. The endpoint of the curve was used to calculate the time for half-maximal precipitation of Con A, **Figure 4.15 (b)**.

The results revealed that the glycopolymers **3**, **5**, **6** and **7** that contain mannose moieties initiated the clustering of Con A more rapidly than glycopolymers **8**, **9** and **10** with pendant glucose of the same epitope densities. Galactose was the most effective sugar in regulating the rate of the clustering. For glycopolymers **11**, **12** and **13** containing both mannose and glucose moieties, the lower the mannose density the faster the rate of the clustering was observed. These tendencies were confirmed by the mannose-galactose-glucose glycopolymers **14** – **17**. Most of these

glycopolymers containing mannose moieties with no or low galactose residues promoted the very rapid precipitation ( $t_{1/2} < 10$  s).

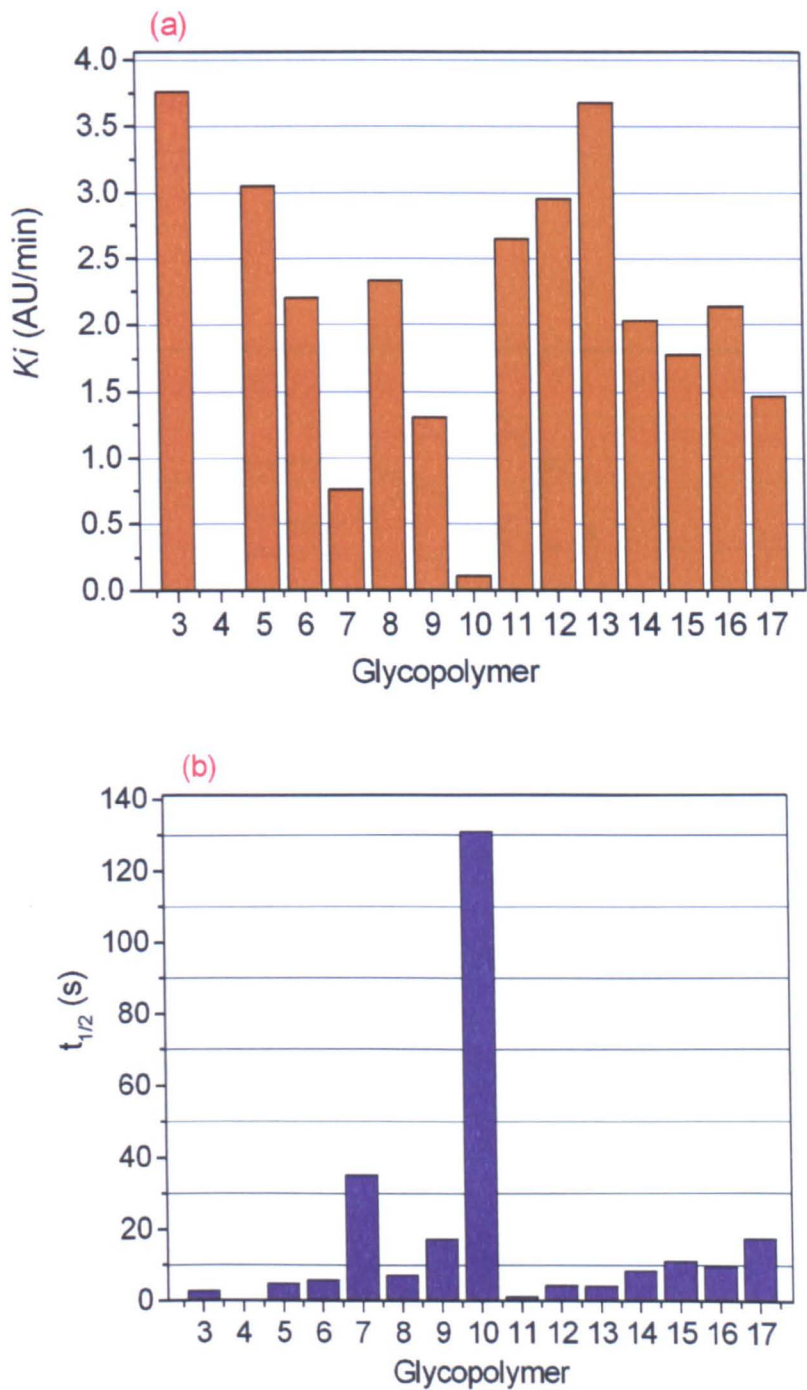


Figure 4.15 Results of turbidimetry experiments. (a) The initial rate of the clustering. (b) The time for half-maximum precipitation of Con A.

#### 4.2.4 Inhibitory potency of the glycopolymers.

The inhibitory potency of multivalent ligands is an important factor for them to be used to identify potent inhibitors.<sup>28</sup> Assays were performed by adding Con A to the mixture of glycopolymer and methyl- $\alpha$ -D-mannopyranoside ( $\alpha$ MeMan) and the absorbance measured at 420 nm of the resulting turbidity, **Figure 4.16 ~ Figure 4.19**.

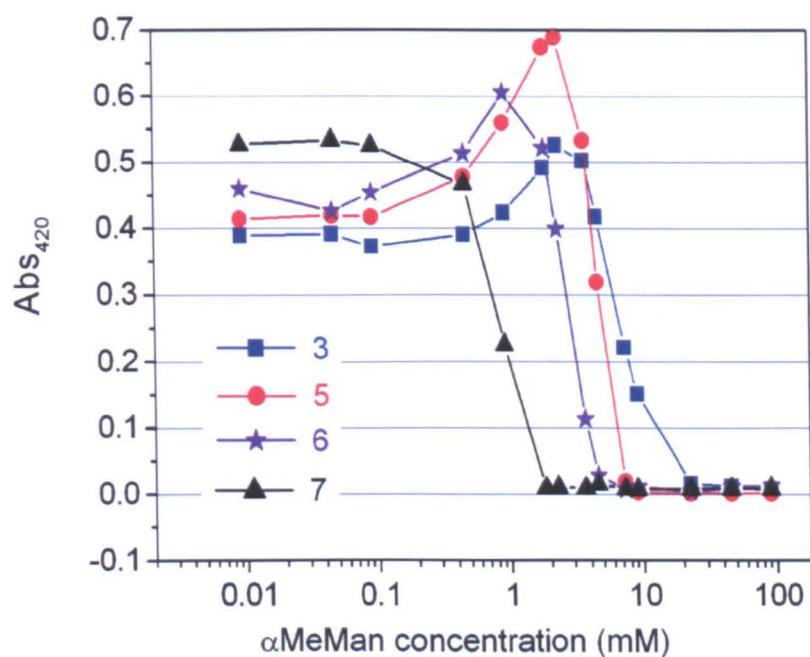


Figure 4.16 The absorbance of turbidities at 420 nm in the inhibitory potency experiments of glycopolymers (3 ~ 7) containing pendant mannose or galactose.

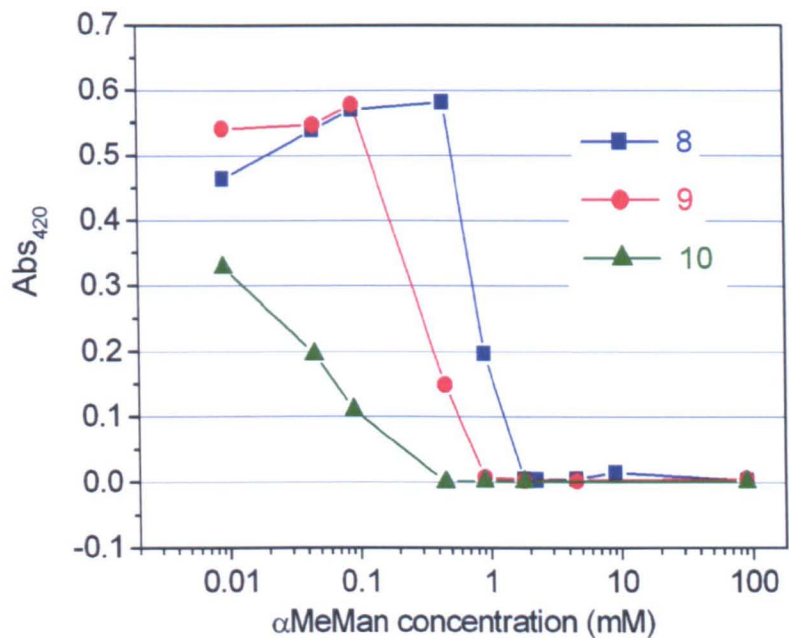


Figure 4.17 The absorbance of turbidities at 420 nm in the inhibitory potency experiments of glycopolymers (8 ~ 10) containing pendant galactose and glucose.

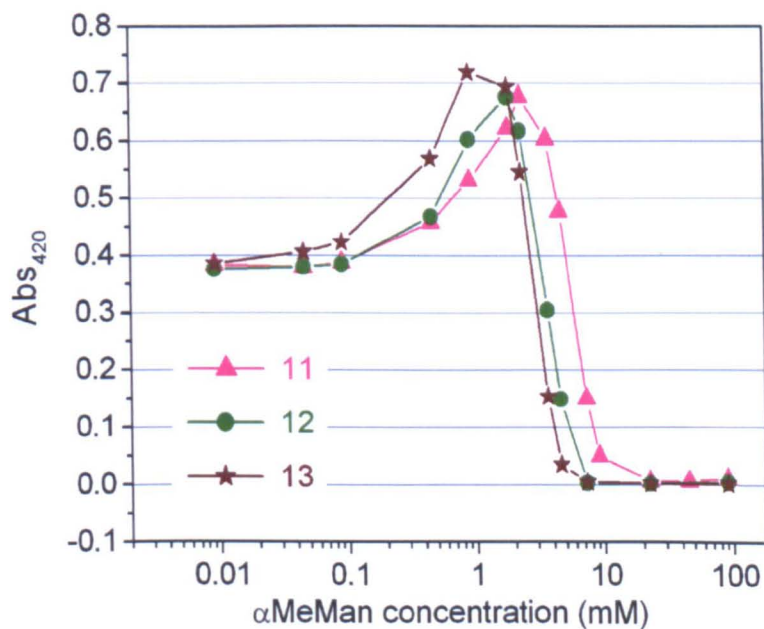


Figure 4.18 The absorbance of turbidities at 420 nm in the inhibitory potency experiments of glycopolymers (11 ~ 13) containing pendant mannose and glucose.



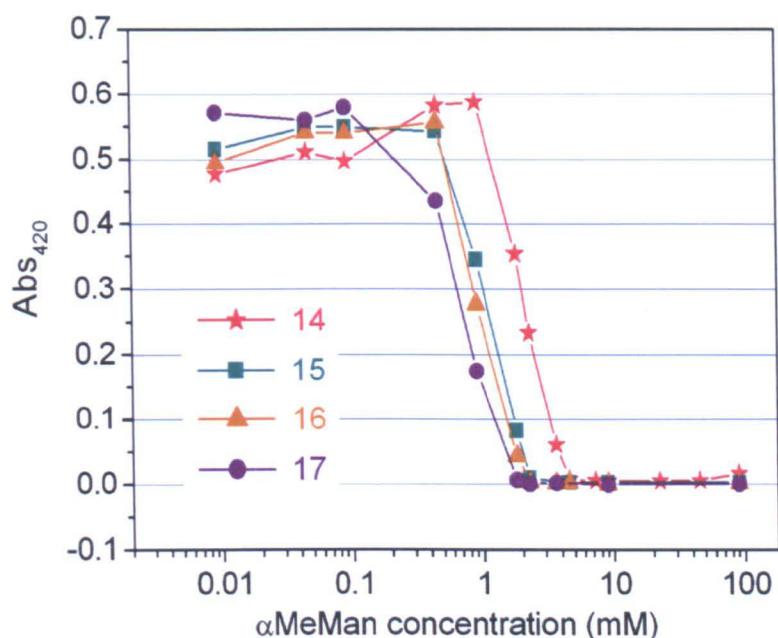


Figure 4.19 The absorbance of turbidities at 420 nm in the inhibitory potency experiments of glycopolymers (14 ~ 17) containing pendant mannose, galactose and glucose of different ratios.

Through only varying the concentration of the competitive monovalent ligand  $\alpha$ MeMan the minimum inhibitory concentration for half-maximum precipitation,  $MIC_{50}$  values, of  $\alpha$ MeMan were determined, **Figure 4.20 (a)**. Comparing the  $MIC_{50}$  values of  $\alpha$ MeMan for all glycopolymers, we see that the density of galactose residues has a big influence on the potency of all of the multivalent ligands and that glycopolymers with mannose residues are much better inhibitors of Con A than those of the same binding-element concentration but with pendant glucose and galactose residues. The inhibitory potencies of mannose-containing glycopolymers decrease by adding pendant glucose or galactose moieties onto the glycopolymer backbone. The mannose containing glycopolymer **3** and the mannose-glucose glycopolymer **11** are the most effective inhibitors of Con A under these conditions. Taking the rate of clustering and the inhibitory potency into considerations, the

mannose glycopolymer **3** is the most effective inhibitor amongst all of the multivalent ligands tested, **Figure 4.20 (b)**. However, with the diversity of the rate and the potency, a range of multivalent ligands are provided to be chosen for specific functions which would be expected to require different structures.

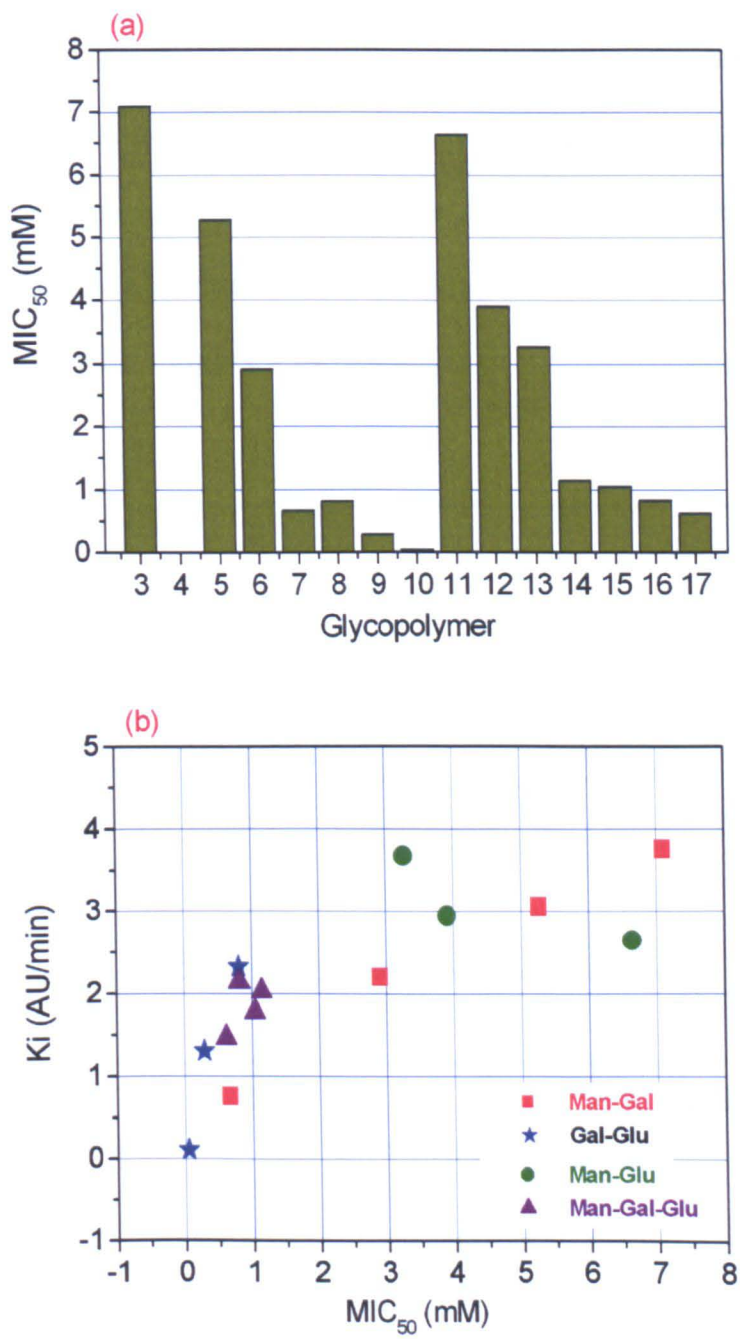


Figure 4.20 Results of inhibitory potency assays. (a) The  $MIC_{50}$  values of  $\alpha$ MeMan for all the glycopolymers. (b) The rate of clustering and inhibitory potency for all of the multivalent ligands tested.



4.2.5 Stability of the glycopolymer–Con A cluster.

As the lectin-carbohydrate interaction is reversible, the inhibitory potency assays measured the ability of these multivalent ligands in kinetic competition with the monovalent ligand  $\alpha$ MeMan for clustering of Con A. In order to investigate the stability of the glycopolymer-Con A complexes, reversal aggregation assays were employed.<sup>31</sup> Following the turbidimetry measurement, the absorbance  $A_{420}$  of the solution after 2 hours at ambient temperature was recorded as  $A_{420}(t=0)$ . Following the addition of monovalent ligand  $\alpha$ MeMan of the same concentration into the turbidity solution, the absorbance of the resulting solution at 420 nm was measured with time, **Figure 4.21 ~ Figure 4.24**.

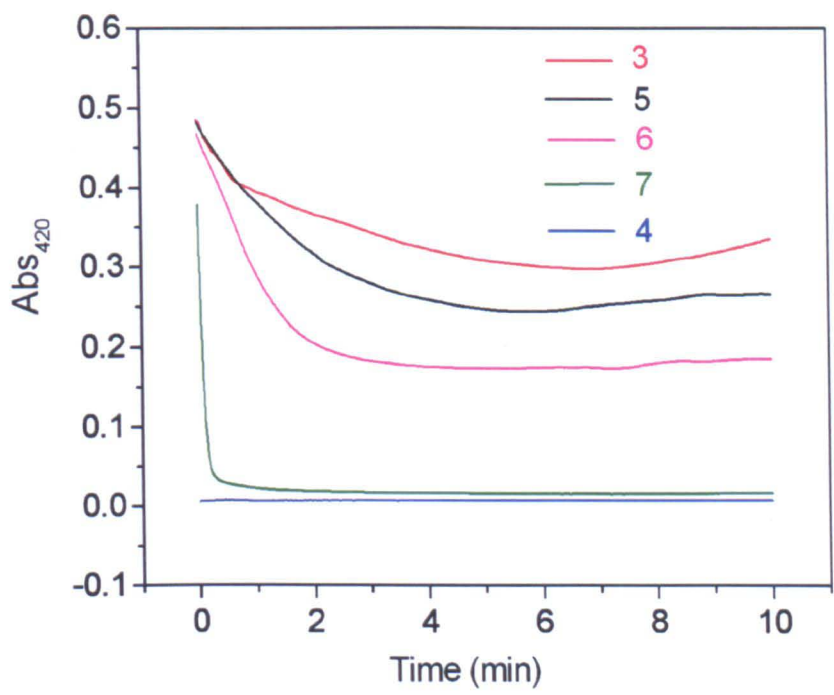


Figure 4.21 Plots of  $Abs_{420}$  vs. time in the reversal aggregation experiments of glycopolymers (3 ~ 7) containing pendant mannose or galactose.

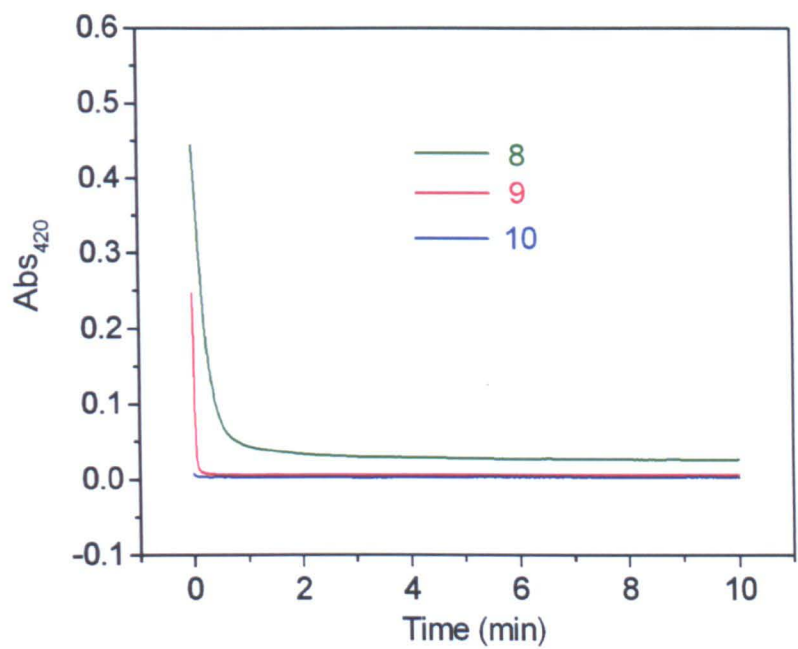


Figure 4.22 Plots of  $Abs_{420}$  vs. time in the reversal aggregation experiments of glycopolymers (8 ~ 10) containing pendant galactose and glucose.

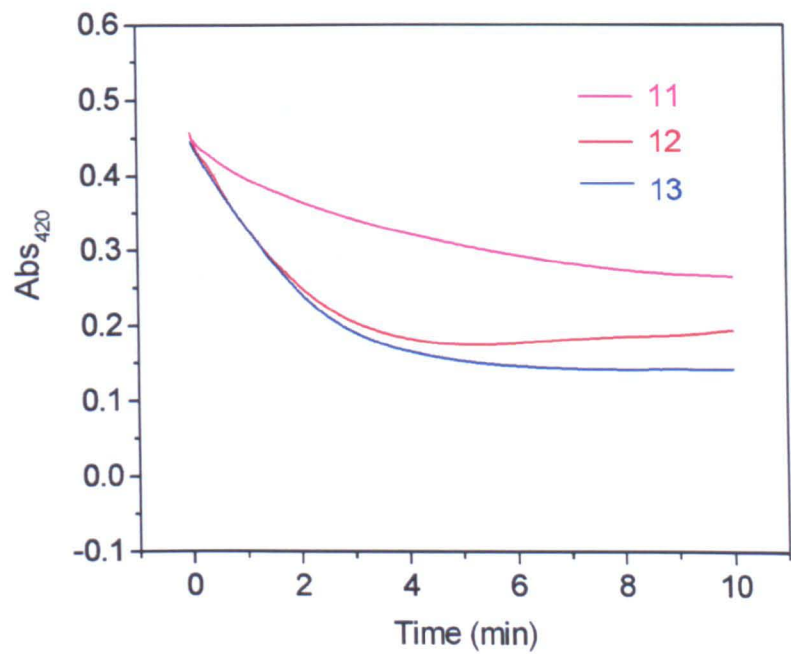


Figure 4.23 Plots of  $Abs_{420}$  vs. time in the reversal aggregation experiments of glycopolymers (11 ~ 13) containing pendant mannose and glucose.

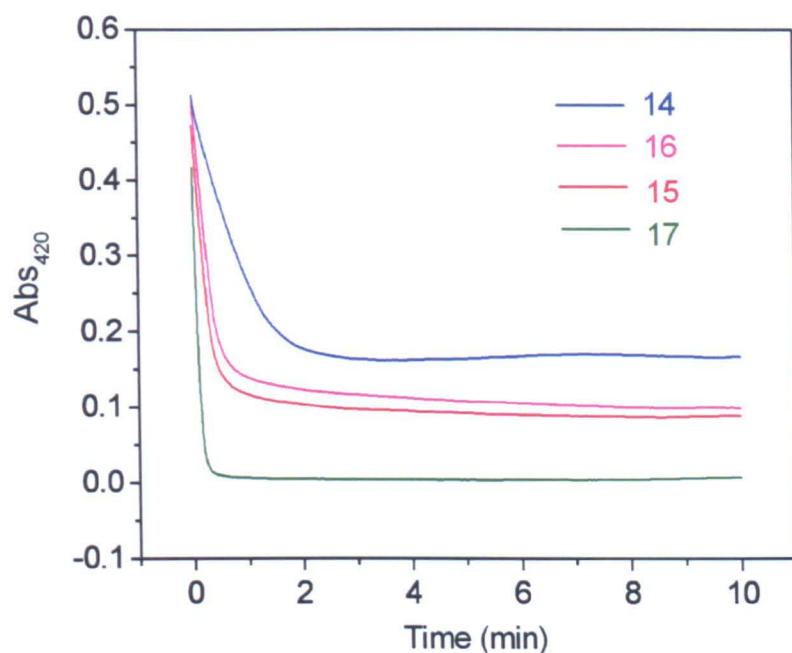


Figure 4.24 Plots of  $Abs_{420}$  vs. time in the reversal aggregation experiments of glycopolymers (14 ~ 17) containing pendant mannose, galactose and glucose of different ratios.

The rate of the reverse interaction was determined by a linear fit of the steepest portion of the data, **Figure 4.25 (a)**. The percent change of the turbidity after 10 min was calculated using  $(A_{420}(t=0)-A_{420}(t=10))/A_{420}(t=0)$ , **Figure 4.25 (b)**. The  $A_{420}(t=10)$  was calculated as an average of the last 10 seconds of each experiment.

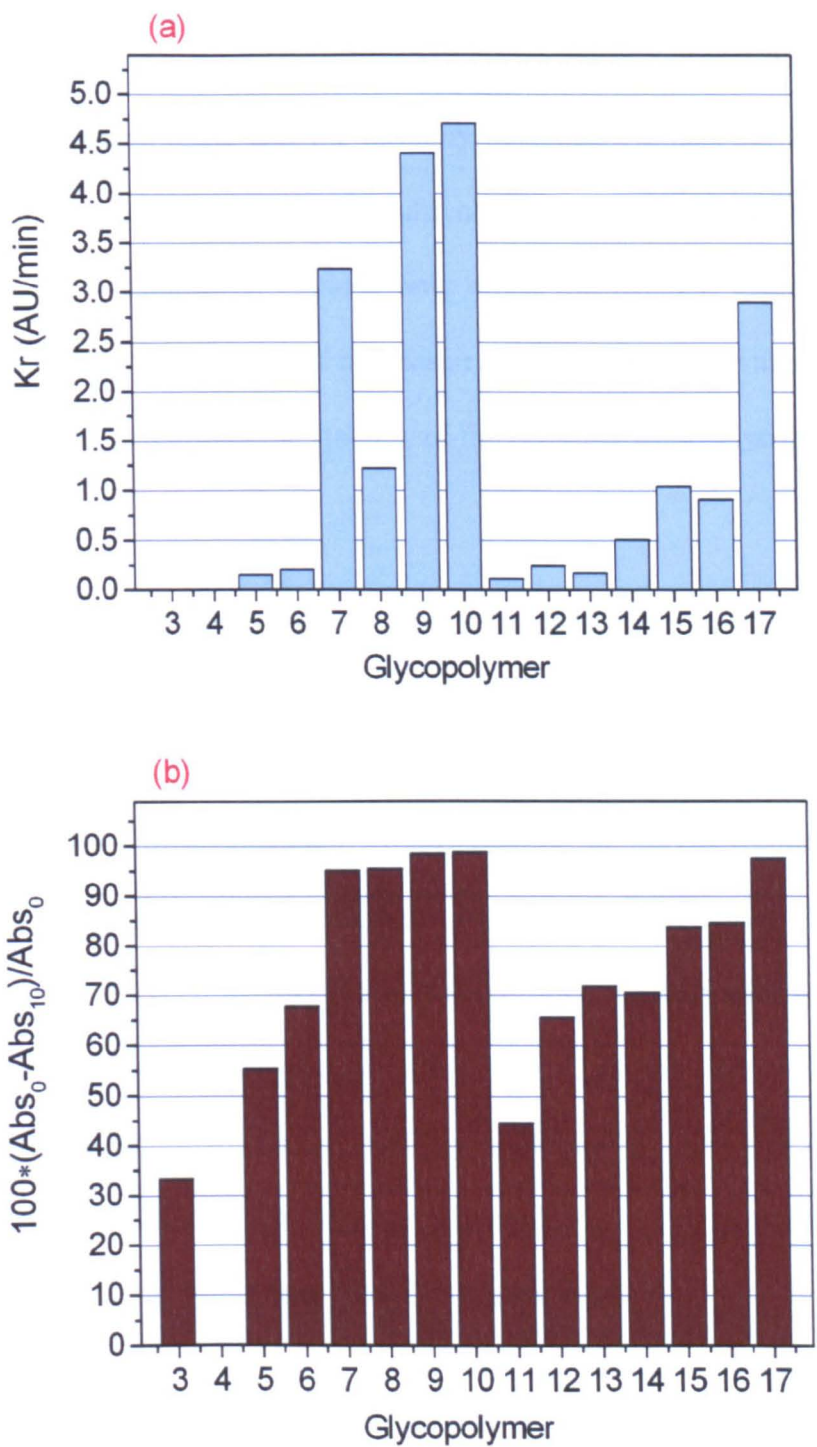


Figure 4.25 Results of reversal aggregation assays. (a) The rate of the reverse interaction between the Con A-glycopolymer aggregates and  $\alpha$ MeMan. (b) The percent change of the turbidity after 10 min with the addition of  $\alpha$ MeMan solution.

The cluster of Con A with mannose containing glycopolymer **3** was very stable with the reverse interaction being relatively slow. The results show that the lectin conjugates induced by glucose residues of glycopolymer **7**, **8** and **9** quickly interact with the monovalent sugar and the turbidity disappears almost completely after 10 minutes. A comparison of all of the multivalent ligands shows that the influence of galactose on the stability is obvious only when the pendant galactose density is greater than 50%. The density of mannose residues in the multivalent ligands is the key factor which determines the stability of the resulting lectin-glycopolymer cluster.

#### **4.2.5 The influence of polymer chain length.**

The chain length of glycopolymers is an essential factor that influences the clustering of lectins.<sup>17</sup> In this work, we also compared the binding properties of the glycopolymers of different chain lengths (degree of polymerisation, DP). Three mannose glycopolymers were employed. Using the same monomer, Glycopolymer **3** (DP = 58) was prepared by ATRP and CuAAC click reaction with 2'-azidoethyl-O- $\alpha$ -D-mannopyranoside, glycopolymer **18** (DP = 42) by ATRP and CuAAC click reaction with  $\alpha$ -azido-D-mannose, and glycopolymer **19** (DP = 23) by CCTP and CuAAC click with  $\alpha$ -azido-D-mannose. The molecular weights and polydispersities of these three glycopolymers are shown in **Figure 4.26**.

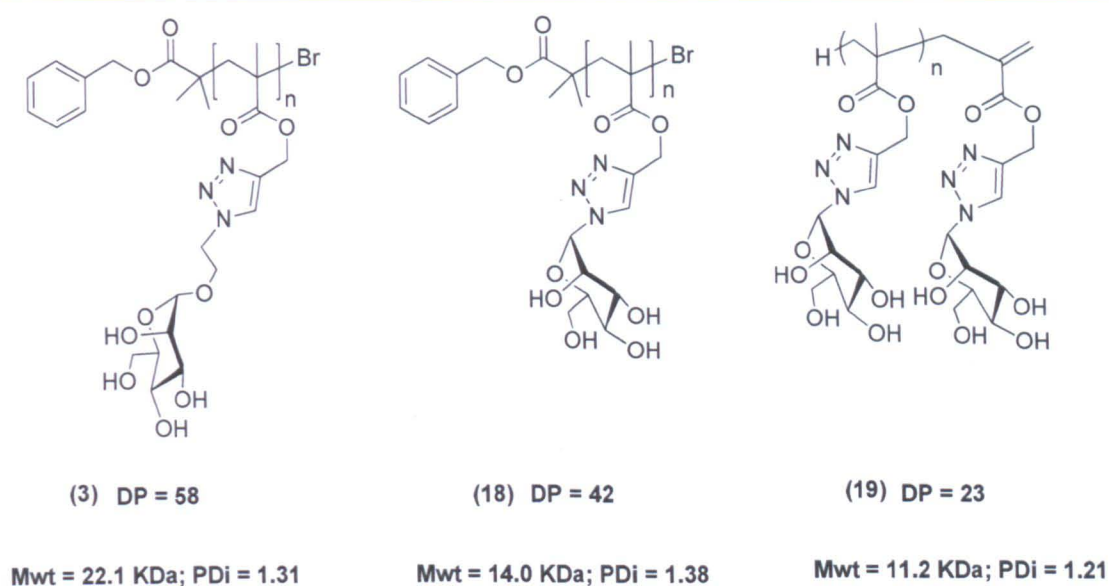


Figure 4.26 Mannose-containing glycopolymers with different chain lengths.

In order to fully investigate the influence of these three different chain lengths in the lectin-glycopolymer interactions, the experiments quantitative precipitation (**Figure 4.27**), turbidimetry (**Figure 4.28**), inhibitory potency assays (**Figure 4.29**), and reversal aggregation assays (**Table 4.2**) were performed.

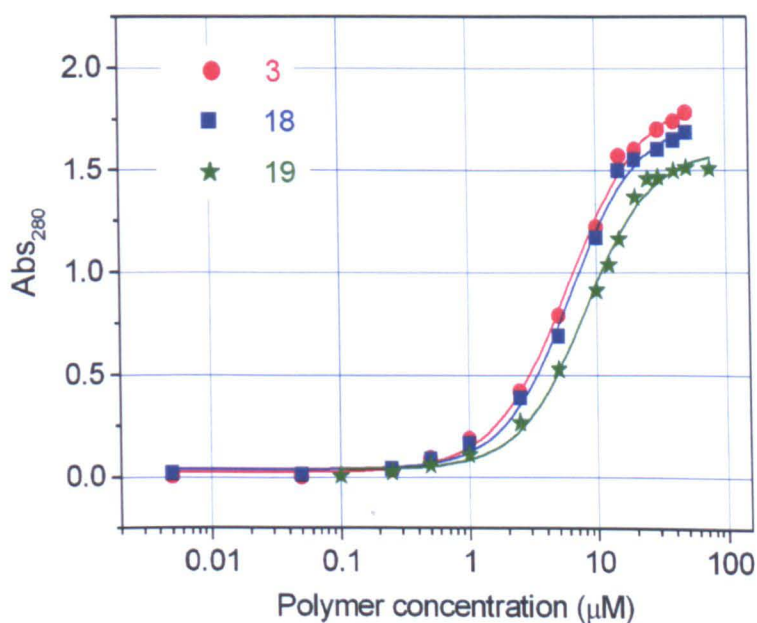


Figure 4.27 Sigmoidal curves fitted to quantitative precipitation data.

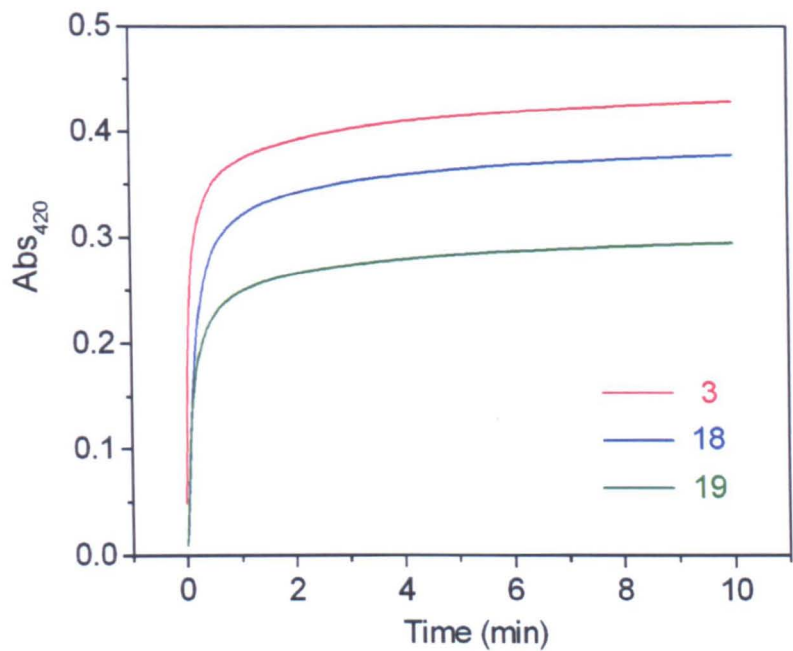


Figure 4.28 The results of turbidimetry experiments.

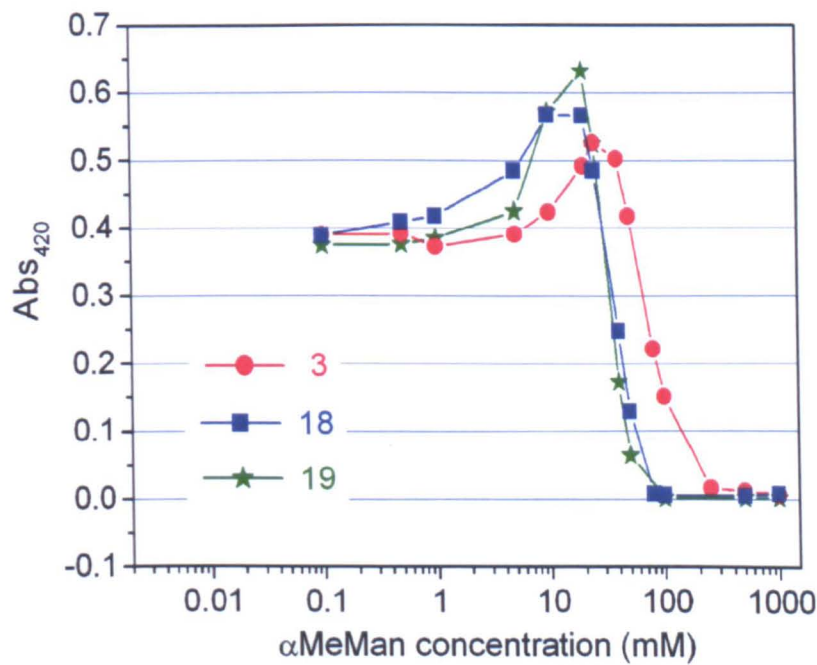


Figure 4.29 The data from inhibitory potency experiments.



Table 4.2 The results from four different assays.

Polymer	Con A units/ polymer chain	$k_i$ (AU/min)	MIC <sub>50</sub> (mM)	$(A_{420}(t=0)-A_{420}(t=10))/$ $A_{420}(t=0)$ (%)
<b>3</b>	<b>10</b>	3.76	78	33.38
<b>18</b>	<b>10</b>	3.75	43.3	71.48
<b>19</b>	<b>7</b>	1.31	38.5	73.48

The results indicate that the chain length has an influence on the clustering of Con A by the three mannose containing glycopolymers. Overall, glycopolymer **3** with DP = 58 showed to be the most effective in clustering Con A. Each polymer chain of glycopolymer **3** bound the most Con A units, the rate of the clustering was the highest and the affinity of this polymer to Con A was the strongest.

The stoichiometry of the Con A-glycopolymer complex and the rate of cluster formation were the same for glycopolymers **18** and **3**, although glycopolymer **18** was less effective than glycopolymer **3** and the resulting cluster was less stable.

Glycopolymer **19** was poor at promoting receptor clustering and also possessed the least potent activity. The conjugation of this glycopolymer with Con A was very weak towards the disruption of the competitive ligand  $\alpha$ MeMan. DP of 58 shows some benefits over DP = 42 but there is less difference between 42 and 58. Thus there seems to be less benefit in increasing the chain length after a certain length is achieved.



---

## 4.3 Conclusions

In summary, a series of glycopolymers have been prepared by the combination of controlled radical polymerisation and CuAAC. By post-functionalisation of the same alkyne-containing precursor polymers *via* clicking different sugar azides onto the polymeric backbone, the well-defined glycopolymers were generated featuring the same macromolecular properties (architecture, polydispersity, valency, polarity, *etc.*) with difference only in the densities of different sugars (mannose, galactose and glucose). This synthetic strategy is significantly important for the investigation of the influence of pendant various epitopes on the lectin-multivalent interactions.

Employing four different efficient assays, quantitative precipitation, turbidimetry, inhibitory potency assay and reversal aggregation assay, we explored the behaviours of the 15 different multivalent ligands in clustering receptors using Con A as the model lectin. The stoichiometry of the glycopolymer-Con A conjugates, the rate of the cluster formation, the inhibitory potency of these multivalent ligands and the stability of the glycopolymer-Con A turbidity were all investigated.

The glycopolymer **3** fully substituted with one mannose residue per repeat unit is the most efficient multivalent ligand for clustering Con A in all of the experiments. The mannose density is the dominant factor for the binding stoichiometry, the rate of binding, the potency and the stability of Con A clustering. However, the galactose residues of different density are effective in regulating the rate of cluster formation. Although the glucose-induced clusters are not very stable towards the disruption caused by the competitive monovalent ligand methyl- $\alpha$ -D-mannopyranoside, glucose

moieties of the glycopolymers are important for the stoichiometry and the rate of the interactions by co-working with mannose residues.

Besides the different sugar natures and their densities, we also explored the influence of chain lengths by employing three mannose glycopolymers with different degree of polymerisation. Glycopolymers with DP = 58 and 42 can bind the most copies of Con A and possess the quickest rate of clustering the lectin. However, glycopolymer with DP = 42 is less effective inhibitor than the one with DP = 58. Overall, Glycopolymer with DP = 23 is poor at promoting receptor clustering and also possesses the least potent activity.

Thus, the diversities of binding properties contributed by different clustering parameters can make it possible to define the structures of the multivalent ligands and densities of binding epitopes for specific functions in the lectin-ligand interactions. These conclusions can be employed as the springboard to develop new glycopolymeric drugs and therapeutic agents and to assess the mechanisms by which they work.

## 4.4 References

1. Miura, Y., *J. Polym. Sci., Part A: Polym. Chem.* **2007**, *45*, 5031-5036.
2. Kim, A. P.; Yellen, P.; Yun, Y. H.; Azeloglu, E.; Chen, W., *Biomaterials* **2005**, *26*, 1585-1593.
3. Roche, A. C.; Fajac, I.; Grosse, S.; Frison, N.; Rondanino, C.; Mayer, R.; Monsigny, M., *Cell. Mol. Life Sci.* **2003**, *60*, 288-297.

4. Roy, R.; Baek, M.-G., *Rev. Mol. Biotechnol.* **2002**, *90*, 291-309.
5. Fleming, C.; Maldjian, A.; Da Costa, D.; Rullay, A. K.; Haddleton, D. M.; St John, J.; Penny, P.; Noble, R. C.; Cameron, N. R.; Davis, B. G., *Nat. Chem. Biol.* **2005**, *1*, 270-274.
6. Lundquist, J.; Toone, E., *Chem. Rev.* **2002**, *102*, 555 - 578.
7. Bertozzi, C. R.; Kiessling, L., *Science* **2001**, *291*, 2357-2364.
8. Teruel, M. N.; Meyer, T., *Cell* **2000**, *103*, 181-184.
9. Matsuuchi, L.; Gold, M. R., *Curr. Opin. Immunol.* **2001**, *13*, 270-277.
10. van der Flier, A.; Sonnenberg, A., *Cell Tissue Res.* **2001**, *305*, 285-298.
11. Kiessling, L. L.; Gestwicki, J. E.; Strong, L. E., *Angew. Chem. Int. Ed.* **2006**, *45*, 2348-2368.
12. Mammen, M.; Choi, S.-K.; Whitesides, G. M., *Angew. Chem. Int. Ed.* **1998**, *37*, 2754-2794.
13. Kiessling, L. L.; Gestwicki, J. E.; Strong, L. E., *Curr. Opin. Chem. Biol.* **2000**, *4*, 696-703.
14. Kiessling, L. L.; Pohl, N. L., *Chem. Biol.* **1996**, *3*, 71-77.
15. Kitov, P. I.; Sadowska, J. M.; Mulvey, G.; Armstrong, G. D.; Ling, H.; Pannu, N. S.; Read, R. J.; Bundle, D. R., *Nature* **2000**, *403*, 669-672.
16. Zhang, Z.; Merritt, E. A.; Ahn, M.; Roach, C.; Hou, Z.; Verlinde, C. L. M. J.; Hol, W. G. J.; Fan, E., *J. Am. Chem. Soc.* **2002**, *124*, 12991-12998.
17. Cairo, C. W.; Gestwicki, J. E.; Kanai, M.; Kiessling, L. L., *J. Am. Chem. Soc.* **2002**, *124*, 1615-1619.
18. Kumar, J.; McDowall, L.; Chen, G.; Stenzel, M. H., *Polym. Chem.* **2011**, *2*, 1879-1886.

- 
19. Cooper, M. A.; Singleton, V. T., *J. Mol. Recognit.* **2007**, *20*, 154-184.
  20. Gou, Y.; Slavin, S.; Geng, J.; Voorhaar, L.; Becer, C. R.; Haddleton, D. M., *Submitted* **2011**.
  21. Becer, C. R.; Gibson, M. I.; Geng, J.; Ilyas, R.; Wallis, R.; Mitchell, D. A.; Haddleton, D. M., *J. Am. Chem. Soc.* **2010**, *132*, 15130-15132.
  22. Vila-Perelló, M.; Gutiérrez Gallego, R.; Andreu, D., *Chembiochem.* **2005**, *6*, 1831-1838.
  23. Smith, E. A.; Thomas, W. D.; Kiessling, L. L.; Corn, R. M., *J. Am. Chem. Soc.* **2003**, *125*, 6140-6148.
  24. Chen, Y.; Chen, G.; Stenzel, M. H., *Macromolecules* **2010**, *43*, 8109-8114.
  25. Gestwicki, J. E.; Kiessling, L. L., *Nature* **2002**, *415*, 81-84.
  26. Allen, J. R.; Harris, C. R.; Danishefsky, S. J., *J. Am. Chem. Soc.* **2001**, *123*, 1890-1897.
  27. Bruehl, R. E.; Dasgupta, F.; Katsumoto, T. R.; Tan, J. H.; Bertozzi, C. R.; Spevak, W.; Ahn, D. J.; Rosen, S. D.; Nagy, J. O., *Biochemistry* **2001**, *40*, 5964-5974.
  28. Gestwicki, J. E.; Cairo, C. W.; Strong, L. E.; Oetjen, K. A.; Kiessling, L. L., *J. Am. Chem. Soc.* **2002**, *124*, 14922-14933.
  29. Ting, S. R. S.; Min, E. H.; Zetterlund, P. B.; Stenzel, M. H., *Macromolecules* **2010**, *43*, 5211-5221.
  30. Hetzer, M.; Chen, G.; Barner-Kowollik, C.; Stenzel, M. H., *Macromol. Biosci.* **2010**, *10*, 119-126.
  31. Ladmiral, V.; Mantovani, G.; Clarkson, G. J.; Cauet, S.; Irwin, J. L.; Haddleton, D. M., *J. Am. Chem. Soc.* **2006**, *128*, 4823-4830.
  32. Lis, H.; Sharon, N., *Chem. Rev.* **1998**, *98*, 637-674.

33. Kogelberg, H.; Feizi, T., *Curr. Opin. Struct. Biol.* **2001**, *11*, 635-643.
34. Burke, S. D.; Zhao, Q.; Schuster, M. C.; Kiessling, L. L., *J. Am. Chem. Soc.* **2000**, *122*, 4518-4519.
35. Haddleton, D. M.; Jasieczek, C. B.; Hannon, M. J.; Shooter, A. J., *Macromolecules* **1997**, *30*, 2190-2193.
36. Geng, J.; Lindqvist, J.; Mantovani, G.; Chen, G.; Sayers, C. T.; Clarkson, G. J.; Haddleton, D. M., *QSAR. Comb. Sci.* **2007**, *26*, 1220-1228.
37. Ting, S. R. S.; Chen, G.; Stenzel, M. H., *Polym. Chem.* **2010**, *1*, 1392-1412.
38. Olsen, L. R.; Dessen, A.; Gupta, D.; Sabesan, S.; Sacchettini, J. C.; Brewer, C. F., *Biochemistry* **1997**, *36*, 15073-15080.
39. Germain, R. N.; Stefanova, I., *Annu. ReV. Immunol.* **1999**, *17*, 467-522.
40. Petrie, R. J.; Schnetkamp, P. M.; Patel, K. D.; Awasthi-Kalia, M.; Deans, J. P., *J. Immunol.* **2000**, *165*, 1220-1227.
41. Cochran, J. R.; Aivazian, D.; Cameron, T. O.; Stern, L. J., *TIBS* **2001**, *26*, 304-310.

## **Chapter 5.**

# **Controlled Interactions of Lectins and Glycopolymers Using QCM-D and SPR**

---

## 5.1 Layer-by-layer self-assembly by QCM-D

### 5.1.1 Introduction

There has been more and more attention drawn to layer-by-layer (LBL) self-assembly in recent years for successively depositing highly functional multilayer films from solutions onto solid surfaces. This technique allows for many choices of various substrates and gives very good control over the thickness, composition and molecular organization of the resulting films. LBL assembled multilayer films have been prepared using polymers,<sup>1</sup> nanoparticles,<sup>2</sup> proteins,<sup>3</sup> DNA,<sup>4</sup> enzyme,<sup>5</sup> or polypeptides<sup>6</sup> through the electrostatic force of polycationic and polyanionic materials,<sup>7-9</sup> hydrogen bonding,<sup>10</sup> or biological affinities through avidin-biotin,<sup>11-12</sup> lectin-carbohydrate,<sup>3</sup> and antigen-antibody<sup>13</sup> interactions. These films have multiple applications in biosensors,<sup>14</sup> nonlinear optics,<sup>15</sup> electrical devices,<sup>16</sup> drug delivery systems,<sup>17</sup> and so forth. The dynamic build-up and application of multilayer films by LBL has been fully summarised in several reviews.<sup>18-20</sup>

As a sensitive, *in situ* and label free analysis technique, with the ability for direct measurement of adsorbed mass, concentration assay, pH dependent measurements, thermodynamic and kinetic study of binding events, QCM-D has been widely used in the areas of protein-protein and protein-carbohydrate interactions, immunological systems,<sup>21-22</sup> biosensor techniques,<sup>23</sup> immunoassays<sup>24</sup> and DNA hybridisation.<sup>25</sup> QCM-D has been employed for the LBL self-assembly to prepare functional films as reviewed by Marx.<sup>26</sup>

Caruso and co-workers showed the assembly of DNA multilayer films from oligonucleotides composed of two homopolymeric diblocks (polyAnGn and polyTnCn) and studied the influence of salt concentration using QCM-D.<sup>27</sup> Lundin *et al.* investigated the effect of ionic strength and pH on the multilayer build-up process of natural positively charged polysaccharide chitosan (CH) and negatively charged polysaccharide heparin (HEP) for their potential application in medical implants.<sup>28</sup> Gleason and co-workers prepared thermally responsive polymer films by using homopolymer poly(N-isopropylacrylamide) (pNIPAAm) and copolymer poly(NIPAAm-co-di(ethylene glycol) divinylether) [p(NIPAAm-co-DEGDVE)] *via* initiated chemical vapour deposition (iCVD). The diffusion of protein bovine serum albumin (BSA) into the swollen p(NIPAAm-co-DEGDVE) film below its lower critical solution temperature (LCST) was monitored *via* QCM-D measurements.<sup>29</sup> Sequential assembly of biocompatible chitosan-graft-NIPAAm and alginate to prepare multilayer films responsible to both pH and temperature was conducted by Martins *et al.*<sup>30</sup> These films were also assessed by examining cellular morphology, adhesion, and detachment as the cell sheets. Lee and co-workers<sup>31</sup> used mannose-modified gold nanoparticles (NPs) to amplify the signals in QCM measurements. The gold electrodes were coated with thiolated mannose to form the self-assembled monolayer (SAM), followed by injection of Concanavalin A to bind to the SAM. The amplification was conducted by passing through mannose-stabilised gold NPs over the Con A layer. The sensitivity was enhanced about 13-fold by the NPs comparing with that of the original SAM. The amplification of sensitivity is especially important for the analysis of trace biological analytes.

Assembly of glycopolymers to prepare biologically active surfaces which employs



oligosaccharides as the recognition signals is important. In this current work, we made use of the biological affinities to demonstrate a novel method for *in-situ* alternate LBL assembly of lectin and glycopolymers controlled by QCM-D, **Figure 5.1**. In order to mimic the biological components on cell membrane surface which involve in the cell recognition processes, either lectins or carbohydrates can be immobilised onto the gold surface of the quartz crystal. The process of the LBL self-assembly of different lectins and glycopolymers to prepare multilayer films was investigated.

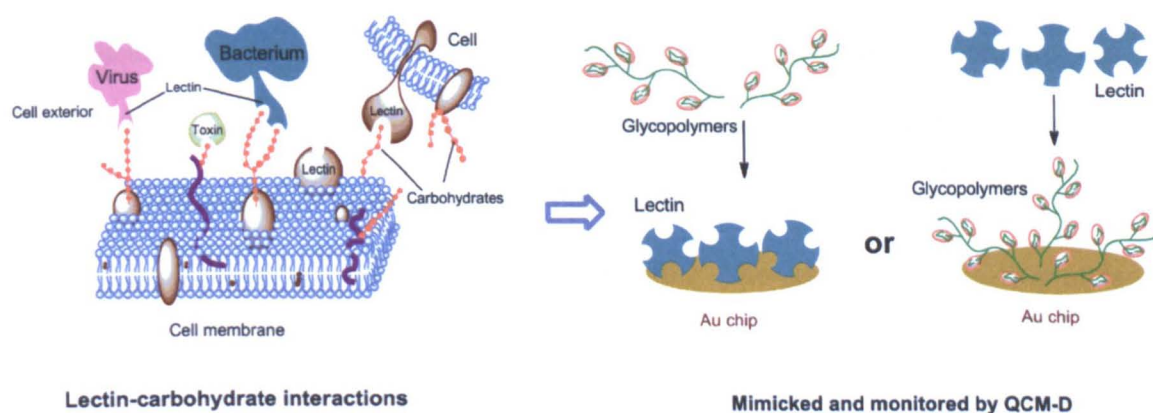


Figure 5.1 Schematic diagram of the self-assembly in this study.

All of the QCM-D experiments were carried out using the Q-Sense E4 system with four sensor chambers for four parallel measurements. In all QCM-D experiments, HBS buffer (10 mM HEPES, 150 mM NaCl, pH 7.4) containing 1 mM  $\text{Ca}^{2+}$ ,  $\text{Mg}^{2+}$  and  $\text{Mn}^{2+}$  was used as the presence of metal ions is essential for the activity of lectins.<sup>32</sup> The flow rate was set to  $50 \mu\text{Lmin}^{-1}$  to get efficient mass coverage over the quartz crystal surface and to reduce the time caused by the assay. The temperature was controlled at 25 °C for all the QCM-D experiments.

### 5.1.2 Immobilisation of lectin on an Au chip

It is desirable to immobilise lectin onto the Au chip surface. Concanavalin A (Con A) was selected as the model lectin. Con A, extracted from jack bean seeds, is a mannose-selective and well-studied homotetramer with four subunits (26.5 kDa each).

#### 5.1.2.1 Con A on bare Au chip surface

The Au chips were cleaned with a boiling mixture of 35 % of  $\text{NH}_3$ , 33 % of  $\text{H}_2\text{O}_2$  and Milli-Q water (1:1:5, v/v) for 10 min and dried by a stream of nitrogen. Subsequently, the chips were set up in the QCM chamber and the temperature was controlled at 25 °C. HBS was passed through the system to give flat baselines of frequency and energy dissipation. Con A buffer solution (1 mg/mL) was ejected into the system, followed by washing with HBS buffer. The resulting QCM-D plot is shown in **Figure 5.2**.

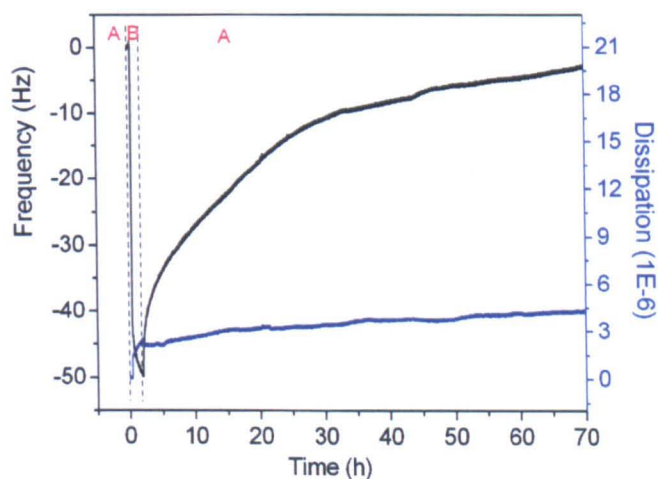


Figure 5.2 QCM-D plot of Con A on the Au chip surface. (A) HBS buffer; (B) Con A in HBS solution (1 mg/mL).

The large decrease of frequency after changing to Con A solution was due to the bulk effect of the solution on the surface, which was caused by the changes in composition of the injected Con A solution in this microbalance system. The increase of energy dissipation was not large indicating that the dynamic viscoelastic property of the Con A solution was similar to that of HBS buffer itself. However, the Con A binding to bare gold was not stable and it was washed off gradually with HBS buffer. Con A absorbed on the surface was removed completely after washing by the HBS buffer for 3 days.

#### 5.1.2.2 Con A on a modified Au chip surface

The Au chip surfaces need to be modified for immobilisation of Con A. The modification was carried out using 11-mercaptoundecanoic acid (MUA), 1-[3-(dimethylamino)propyl]-3-ethyl carbodiimide (EDC) hydrochloride and *N*-hydroxysuccinimide (NHS), **Figure 5.3**.

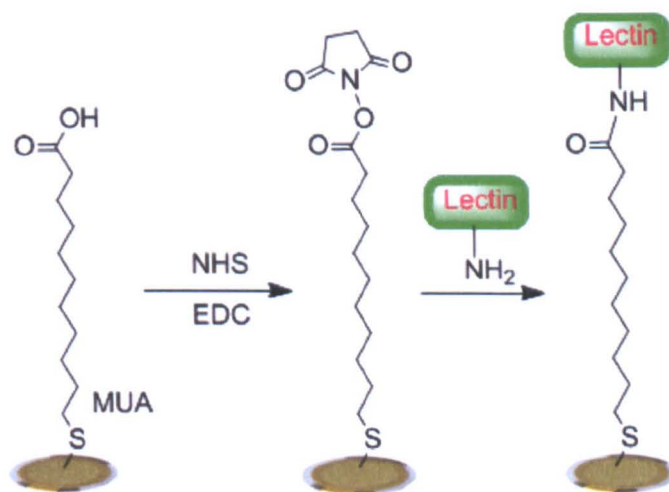


Figure 5.3 Modification of Au chip surface with MUA, EDC and NHS.

After being cleaned, the chips were immediately immersed into the solution of 10 mM MUA in ethanol and kept overnight at ambient temperature to obtain the thiol

self-assembled monolayer (SAM) on the gold surfaces. The chips were washed with ethanol and Milli-Q water sequentially and then immersed into a freshly prepared water solution of 0.4 M EDC and 0.1M NHS (1:1, v/v) to activate the carboxyl groups on the Au chip surface. After washed with Milli-Q water and dried with a stream of nitrogen, the quartz crystal chips were mounted in the QCM-D chambers. HBS buffer was running through the system until flat baselines of frequency and dissipation were achieved. The solution of Con A in HBS buffer (0.1 mg/mL) was passed over the system, **Figure 5.4**.

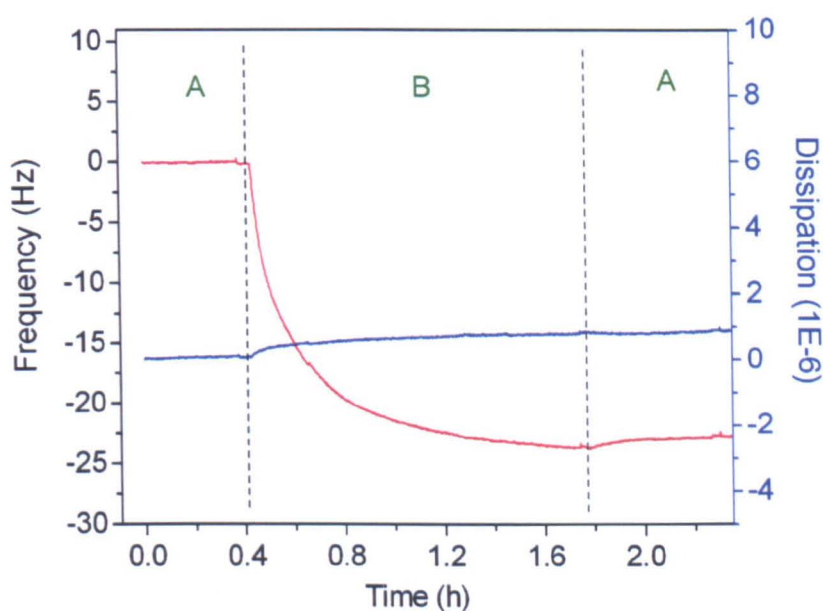


Figure 5.4 QCM-D plot of Con A on modified Au chip surface. (A) HBS buffer; (B) Con A solution (0.1 mg/mL).

Con A was bound to modified gold chip surface *via* nucleophilic substitution with lysine residues. In this case, the QCM-D data showed that Con A was stable on the modified quartz crystal surface and was not washed off with HBS buffer.



### 5.1.2.3 The self-assembly of lectin and glycopolymer

As Con A can bind to the modified Au chip surface, the self-assembly of the lectin with glycopolymer was then investigated. The glycopolymer was synthesised *via* a combination of transition-metal-mediated living radical polymerisation (often termed ATRP) and Cu(I) catalysed azide-alkyne cycloaddition (CuAAC) click reaction following a general procedure,<sup>33</sup> **Figure 5.5**. The mannose glycopolymer **P1** was selected as the model glycopolymer because the pendant mannose moieties of the polymer can interact with Con A.

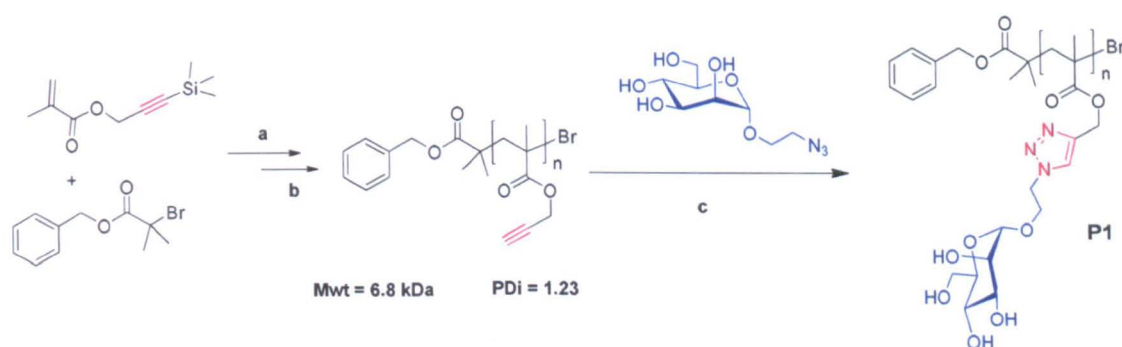


Figure 5.5 Synthesis of mannose glycopolymer **P1**. (a) *N*-(ethyl)-2-pyridylmethanimine/CuBr, toluene, 70 °C. (b) TBAF, acetic acid, THF. (c) mannose azide, CuBr, bipyridine, Et<sub>3</sub>N.

Con A solution (0.5 mg/mL) was passed through the system. After it reached a plateau, the surface needed to be rinsed by HBS buffer to exclude the bulk effect until another plateau was reached. Ethanolamine hydrochloride (1M, pH = 8.5) was then used to block unreacted NHS groups to prevent their binding to glycopolymers. Subsequently, the solution of mannose glycopolymer **P1** (0.5 mg/mL) was passed over the gold chip surface, followed by rinsing with HBS buffer. The changes of frequency and energy dissipation are shown in **Figure 5.6**.

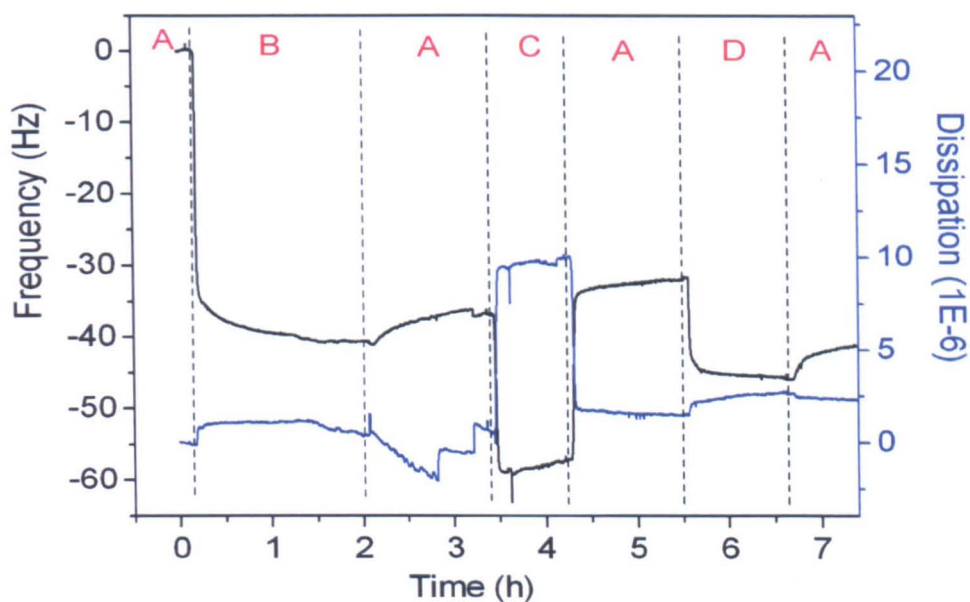


Figure 5.6 QCM-D plot of the self-assembly of Con A and mannose glycopolymer **P1**: (A) HBS buffer; (B) Con A in HBS buffer (0.5 mg/mL); (C) ethanolamine HCl in HBS buffer (1M, pH 8.5); (D) **P1** in HBS buffer (0.5 mg/mL).

As the pendant mannose interacted with immobilised Con A, **P1** on the surface was stable when washed by HBS buffer. The mass and thickness of the materials deposited on the quartz crystal surface over time was estimated by Sauerbrey's equation and also by Voigt modelling, **Figure 5.7**.

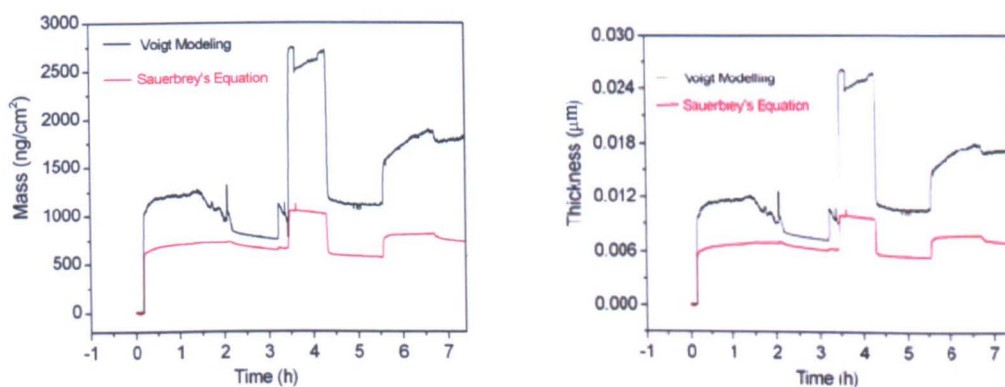


Figure 5.7 Estimated mass and thickness of materials deposited on the modified Au chip over time.

### 5.1.3 Immobilisation of glycopolymers on a Au chip

#### 5.1.3.1 Mannose glycopolymer on a bare gold chip surface

An alternative approach for the LBL self-assembly between Con A and mannose glycopolymer is to immobilise glycopolymer instead of Con A onto the Au chip surface. In nature, oligosaccharides presented on the cell membrane surface are important elements for many recognition processes. Thus it is reasonable to bind glycopolymers to the gold quartz crystal surface to investigate lectin-carbohydrate interactions. The mannose glycopolymer **P1** was passed over bare gold surface in QCM-D experiments, **Figure 5.8**. However, the polymer did not remain on the surface and it was washed off slowly by HBS buffer. This is probably due to the hydrophobic property of the Au surface, which cannot bind to glycopolymer non-valently at neutral pH.

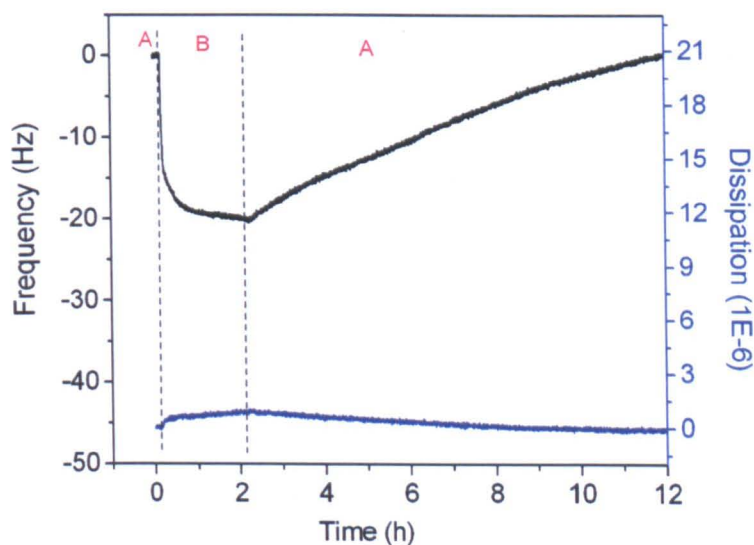


Figure 5.8 Glycopolymer on a bare gold chip surface. (A) HBS buffer; (B) glycopolymer **P1** solution.

### 5.1.3.2 Disulfide mannose glycopolymer on a bare gold chip surface

As the mannose glycopolymer **P1** did not remain bound to the Au chip surface, disulfide mannose glycopolymer **P2** was used instead following a literature procedure.<sup>34</sup> The glycopolymer **P2** was synthesised using a disulfide initiator in the polymerisation of TMS-protected propargyl methacrylate, followed by CuAAC click reactions with mannose azide, **Figure 5.9**.

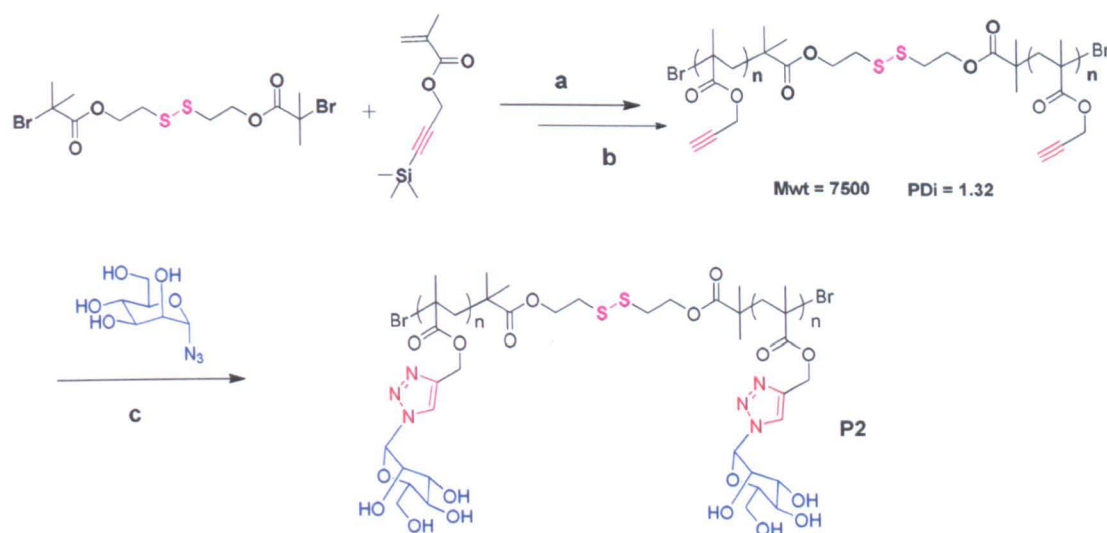


Figure 5.9 Synthesis of disulfide mannose glycopolymer **P2**. (a) *N*-(ethyl)-2-pyridylmethanimine/CuBr, [M]:[I]:[Cu(I)]:[L] = 141:1:1:2 in toluene, 90 °C (b) TBAF, acetic acid, THF. (c) mannose azide, CuBr, *N*-(ethyl)-2-pyridylmethanimine, Et<sub>3</sub>N.

The absorption of glycopolymer **P2** onto the gold surface was monitored by QCM-D as shown in **Figure 5.10**. In this case, the disulfide bond in the polymer chain stably attached on the gold surface. Thus the glycopolymer **P2** remained bound and stable on the surface when washed with HBS buffer for several hours.



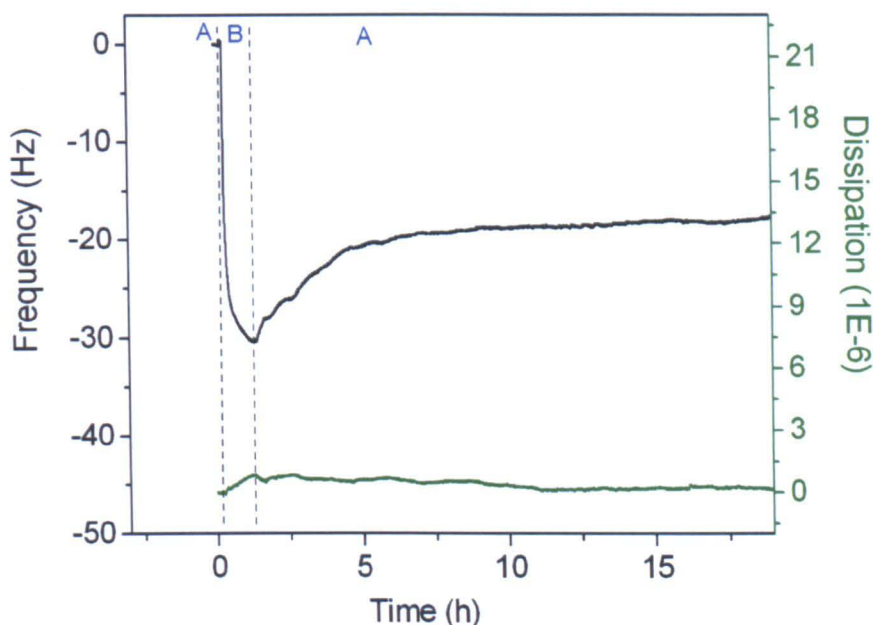


Figure 5.10 Absorption of glycopolymer **P2** onto the bare gold surface: (A) HBS buffer; (B) **P2** solution.

Therefore, bilayer assemblies were made by adsorbing disulfide mannose glycopolymer **P2** directly onto the Au chip surface and then passing Con A buffer solution over the chip. As Con A can bind to the mannose moieties of **P2**, it remained on the surface as the second layer when washed with HBS buffer. With the same concentration of glycopolymer **P2** (0.5 mg/mL), two concentrations of Con A in HBS buffer solution (0.1 mg/mL and 0.5 mg/mL, respectively) were investigated in this work, **Figure 5.11**.

The frequency change of the quartz crystal chip caused by Con A solution (0.1 mg/mL) is  $\Delta f = -108$  Hz, whilst that caused by using a higher concentration of Con A solution (0.5 mg/mL) is  $\Delta f = -185$  Hz. Thus, the mass and thickness of the two layers can be tuned by changing the concentration of **P2** and Con A. In this case, the factors

which affect the lectin-carbohydrate interaction such as concentration, pH value, temperature and ionic strength can be investigated systematically due to the advantages of QCM-D technique.

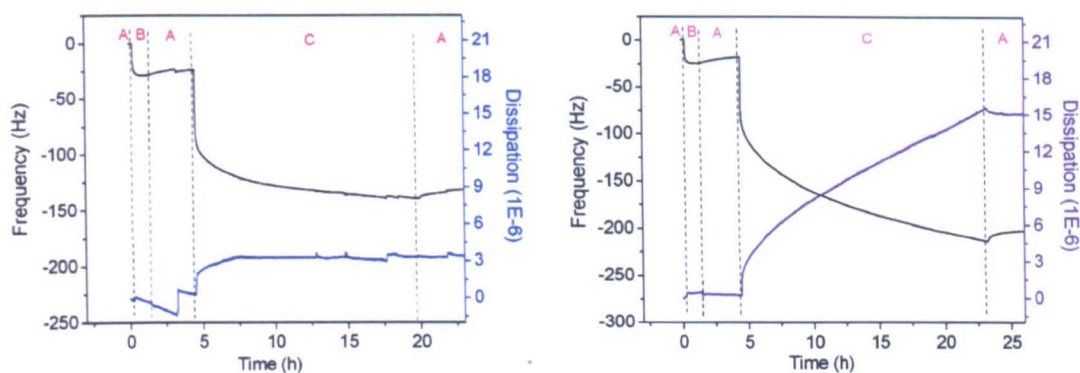


Figure 5.11 QCM-D plot of two self-assembled layers formed by interaction between P2 and Con A: (A) HBS buffer; (B) P2 in HBS buffer (0.5 mg/mL); (C) Con A in HBS buffer (left: 0.1 mg/mL; right: 0.5 mg/mL).

Besides the adsorption and interaction kinetics, information about the structure and dynamic viscoelastic properties of the absorbed layers can also be obtained from the Dissipation vs. Frequency plot ( $D$ - $f$  plot), **Figure 5.12**. For adsorption of glycopolymer P2, the dissipation changes for both concentrations were very small and the  $D$ - $f$  relations were nearly linear, which simply indicated that the two layers formed by P2 were rigid. However, the process of Con A adsorption was much more complicated. The slope of the  $D$ - $f$  plot for Con A binding increased gradually in both cases, signalling more dissipation per added molecule during the adsorption process. This showed that the binding of Con A to the glycopolymer P2 monolayer was not only kinetically controlled, but also influenced by the transport limitations such as the conformational rearrangement of Con A, trapped liquid in the layer or even the interfacial processes.<sup>35</sup> The influence on the layer of Con A with higher

concentration (0.5 mg/mL) was larger than that of the lower concentration (0.1 mg/mL) and the absorbed film was less rigid.

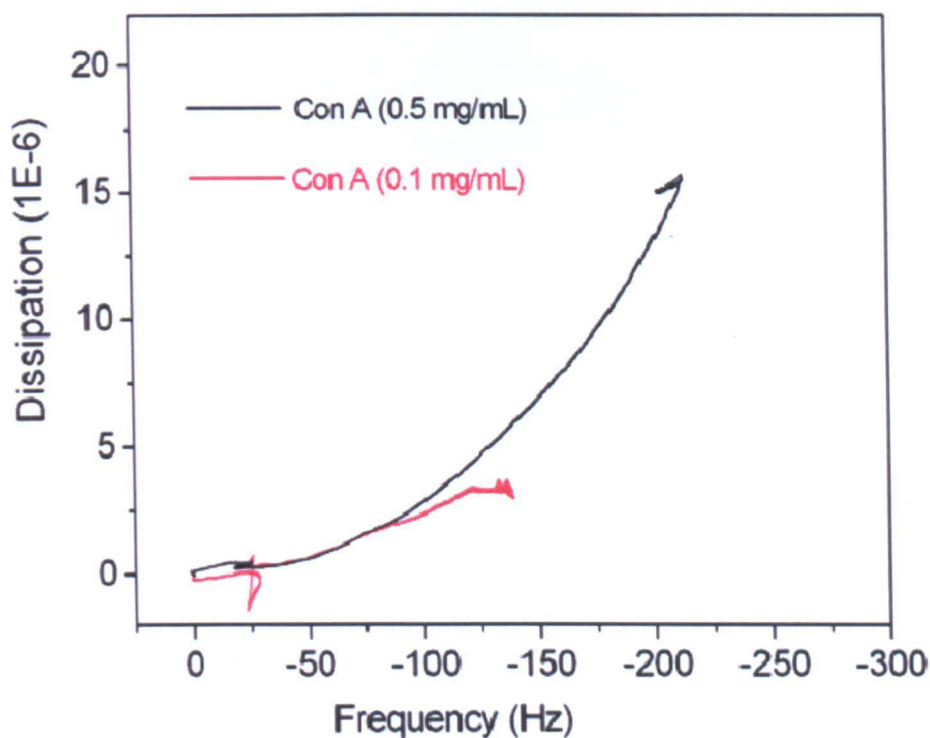


Figure 5.12 D-f plot of two layers formed by interaction between **P2** and Con A.

### 5.1.3.3 Multilayer self-assembly on Au chip surface

Lectin-glycopolymer assemblies starting with the attachment of the disulfide bonds in the polymeric backbones to quartz crystal surface provides a facile approach to multilayer bioactive films. Therefore, this method was implemented to prepare bioactive surface as shown in **Figure 5.13**.

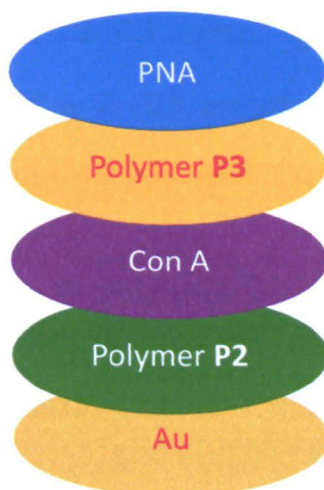


Figure 5.13 Schematic diagram of composition of the multilayer surface.

Peanut agglutinin (PNA) is a lectin isolated from peanuts as a 110 kDa tetramer composed of four identical subunits which can bind specifically to galactose.<sup>32</sup> It is a well-studied lectin which is commonly employed as a model for many investigations. Polymer **P3** was prepared by a combination of ATRP and CuAAC reactions using a mixture of mannose azide and galactose azide (mannose : galactose = 1:1), **Figure 5.14**.

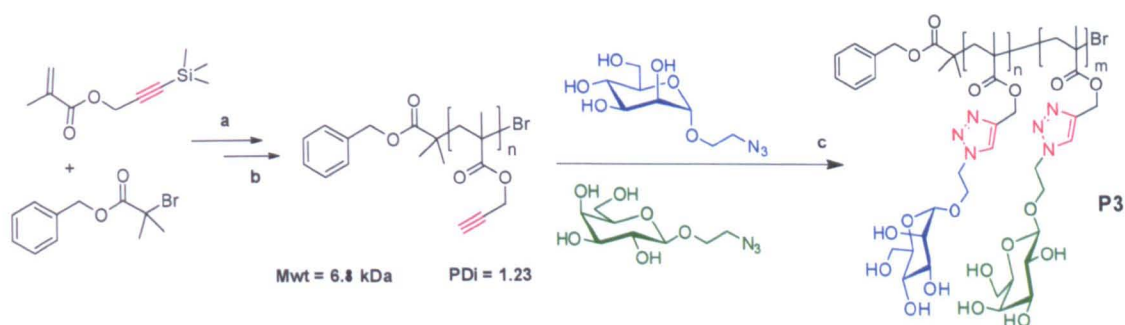


Figure 5.14 Synthesis of mannose-galactose glycopolymer **P3**: (a) *N*-(ethyl)-2-pyridylmethanimine/CuBr, toluene, 70 °C. (b) TBAF, acetic acid, THF. (c) mannose azide, galactose azide, CuBr, bipyridine, Et<sub>3</sub>N.



Disulfide mannose glycopolymer **P2** (0.5 mg/mL,  $\Delta f = -23$  Hz) was attached to the Au chip surface, followed by Con A (0.5 mg/mL,  $\Delta f = -187$  Hz) and mannose-galactose glycopolymer **P3** (0.5 mg/mL,  $\Delta f = -15$  Hz). The mannose moieties of **P3** could bind to Con A, while the galactose moieties interacted with PNA (0.5 mg/mL,  $\Delta f = -63$  Hz). Therefore, a four layer alternate assembly was achieved easily by QCM-D as shown in **Figure 5.15**.

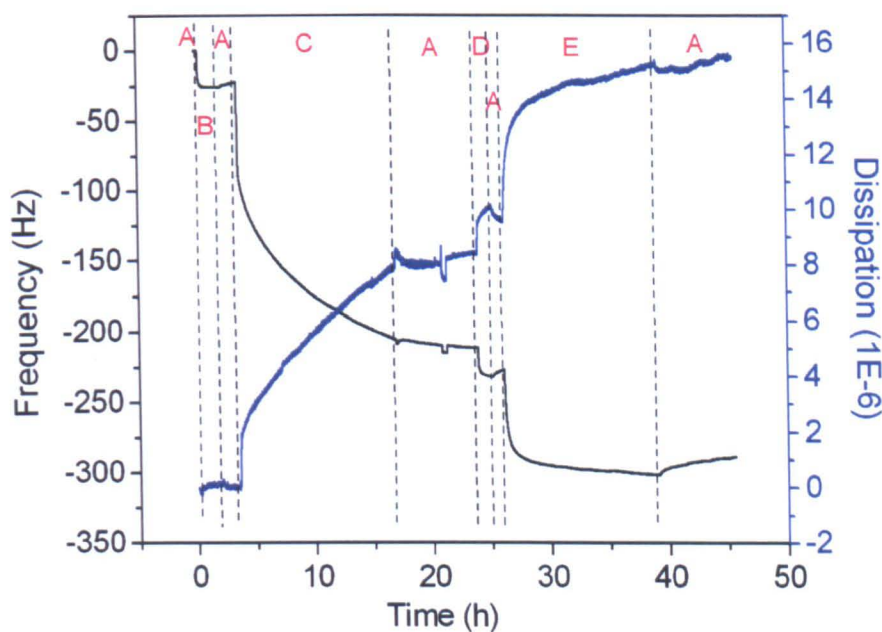


Figure 5.15 Multilayer assembly of **P2**, Con A, **P3** and PNA: (A) HBS buffer; (B) **P2** in HBS buffer (0.5 mg/mL); (C) Con A in HBS buffer (0.5 mg/mL); (D) **P3** in HBS buffer (0.5 mg/mL); (E) PNA in HBS buffer (0.5 mg/mL).

The corresponding  $D$ - $f$  plot of the multilayer assembly is shown in **Figure 5.16**. The slope of the plot for **P3** adsorption was considerably higher than that for **P2** adsorption. However, it was comparable to the slope for the lectin Con A and PNA adsorption. This indicated that the absorbed **P3** layer was much less rigid than the **P2** layer and the interactions between **P3** and Con A, PNA and **P3** were similar and no longer affected by the Au chip surface. The part of the  $D$ - $f$  plot for glycopolymer **P3**

binding was nearly linear, indicating a homo-layer was formed by glycopolymer **P3** without any conformational changes. Therefore, in some cases the binding environment should be taken into consideration when preparing platforms in order to fully investigate the lectin-carbohydrate binding kinetics.

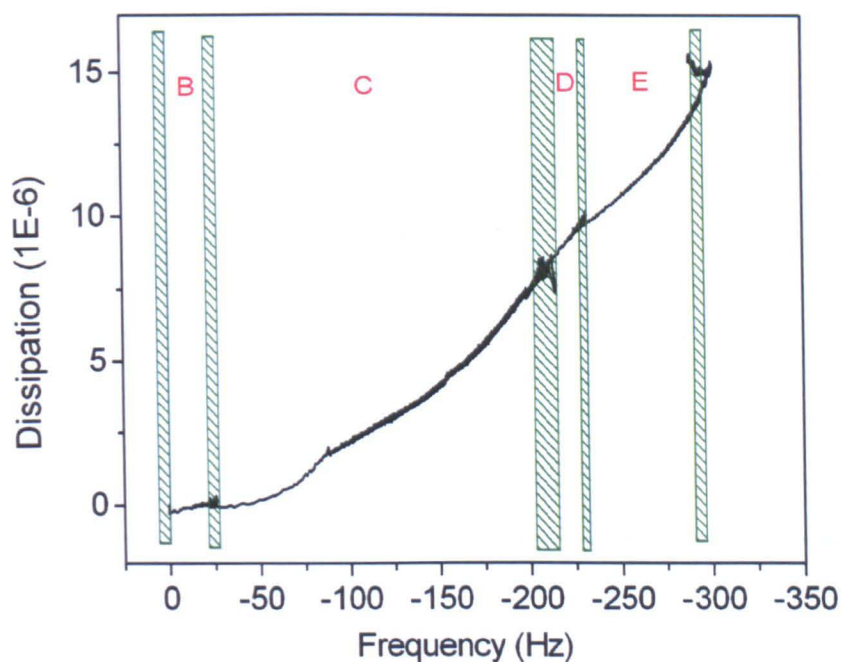


Figure 5.16 D-f plot of the multilayer films assembly.

In order to compare the efficiency and sensitivity of the LBL self-assembly between lectins and glycopolymers by different immobilisation procedures, two experiments were carried out using the same concentration (0.5 mg/mL) of lectins and glycopolymers. The comparison of the absorbed mass is given in **Table 5.1**. The mass of the rigid, uniform film on quartz crystal surface in air or vacuum can be calculated using the Sauerbrey's equation. However, modeling<sup>36</sup> of the mass is required for the viscoelastic films deposited on the Au chip surface from solution.

The mass data obtained from both Sauerbrey’s equation and Voigt modeling is shown for these two experiments.

Table 5.1 Estimated mass by two different immobilisation methods using the same concentration (T: 25 °C; pH: 7.4; flow rate: 50 µL/min; concentration: 0.5 mg/mL).

Method	Immobilisation of Con A		Immobilisation of glycopolymer P2			
	Con A	P1	P2	Con A	P3	PNA
$\Delta f$ (Hz)	37	9	23	188	13	66
$\Delta D$ (1E-6)	2.3	0.8	0.1	8.3	1.1	6.0
$\Delta m^a$ (ng/cm <sup>2</sup> )	658	163	396	3394	264	1109
$\Delta m^b$ (ng/cm <sup>2</sup> )	790	699	413	3707	319	769

(a: Sauerbrey’s Equation; b: Voigt Modeling)

It is apparent that there is a large difference between the two different methods. The binding of Con A onto the surface is much better if the gold chip surface is modified with disulfide mannose glycopolymers **P2**. The sensitivity of this method is about 5 times bigger than the method involving covalent attachment of Con A to NHS functionalised surface. Due to the larger change of energy dissipation, the layer formed by absorption of Con A is also much softer. Meanwhile, it will take less steps for the modification of quartz crystal chip using glycopolymer **P2** than using MUA, EDC and NHS. Therefore, it is more efficient to prepare the LBL self-assembled bioactive surface using carbohydrate-immobilised gold chip surface.

### 5.1.4 Conclusions

In conclusion, two different ways have been demonstrated to mimic the components on the cell surface by QCM-D to investigate the interactions between lectins and carbohydrates and also to prepare the LBL alternate self-assembled bioactive multilayer surfaces *via* the biological affinities of different lectins and their specific carbohydrates. The Au chip needs to be chemically modified by MUA, EDC and NHS in order to attach the lectin Con A to form a stable layer. If the carbohydrates are desired to be immobilised first, the disulfide glycopolymers can be used to bind directly to the Au chip surface. Along with the *in-situ*, and label free measurement of QCM-D, these two methods afford new ways to prepare the bioactive surfaces to investigate the interactions of lectins and carbohydrates and open new horizons to the controlled LBL multilayer self-assembly of lectins and synthetic glycopolymers.

## 5.2 Lectin-glycopolymer interactions monitored by QCM-D

The binding affinity of synthetic glycopolymers with lectins depends on many architectural properties such as chain length, valency and flexibility, *etc.* In this work, synthetic linear mannose glycopolymers with different chain length are compared with respect to their interactions with model lectin Con A and DC-SIGN using QCM-D measurements. Besides the binding mass obtained from frequency



change, the kinetic parameters and viscoelastic properties of the binding events can also be estimated. The synthetic glycopolymers used in this study are shown in **Figure 5.17**. Using the same monomer, TMS-protected propargyl methacrylate, glycopolymer **P4** and **P5** were prepared by CCTP and CuAAC click reactions, while **P6** and **P1** were synthesised by ATRP and CuAAC click reactions. The molecular weight and polydispersity index of these polymers were obtained from gel permeation chromatography (GPC) eluted by DMF (with 1 mg/mL LiBr) at 50°C.

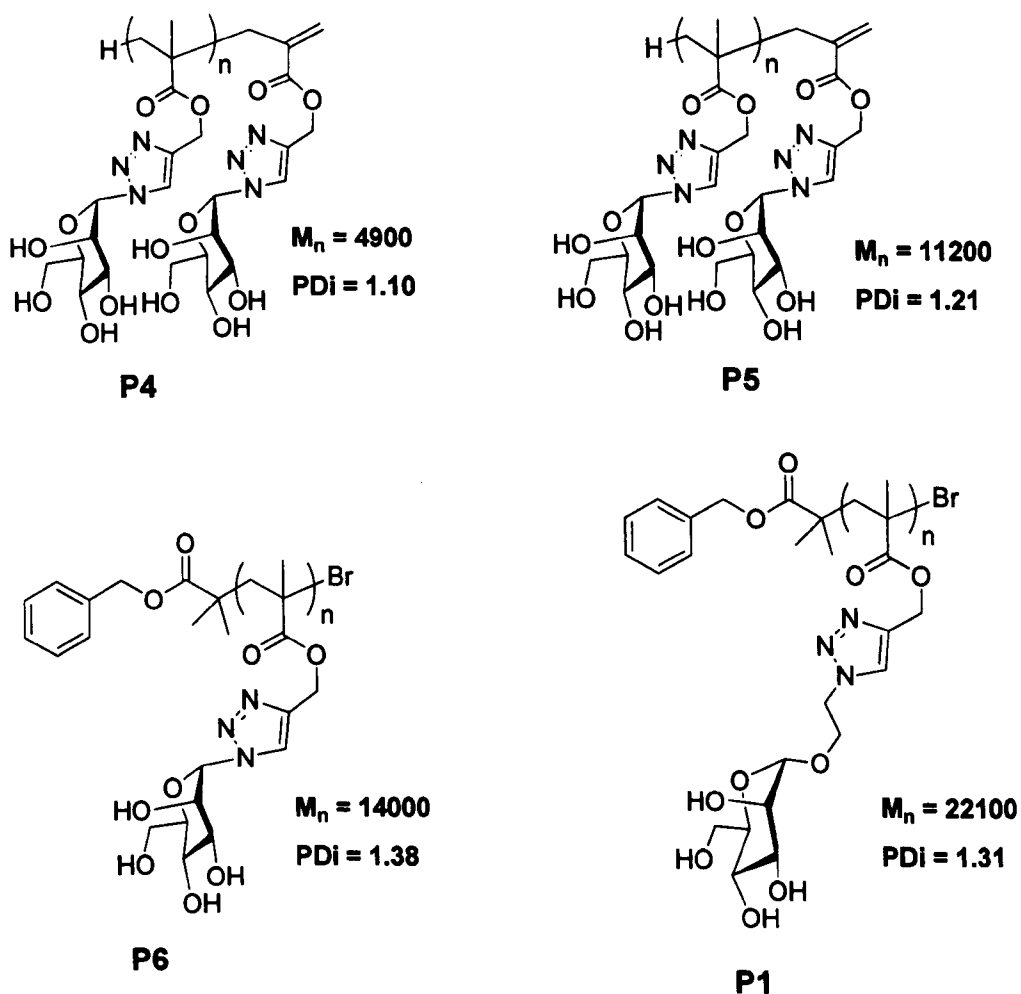


*Figure 5.17 Synthetic glycopolymers employed in QCM-D measurements.*

### 5.2.1 Interactions of Con A with glycopolymers

Con A was employed as a model lectin to interact with these four different mannose glycopolymers. The effect of chain length of glycopolymers on their binding affinities was investigated by QCM-D experiments. HBS buffer (10 mM HEPES, 150 mM NaCl, pH 7.4) containing 1 mM  $\text{Ca}^{2+}$ ,  $\text{Mg}^{2+}$  and  $\text{Mn}^{2+}$  was used to prepare the solution of the analytes. The flow rate was set to  $50 \mu\text{Lmin}^{-1}$  and the temperature was controlled at 25 °C. Before changing to a different solution of analytes, HBS buffer was always passed over the quartz crystal chip to wash until the frequency reached a new plateau for all the QCM-D experiments in this study. The gold chip surface was modified with MUA, EDC and NHS by aforementioned method. Con A was immobilised on the surface by passing Con A buffer solution (0.1 mg/mL) over the quartz crystal chip, followed by ethanolamine hydrochloride (1M, pH = 8.5) to deactivate unreacted NHS groups. The solution of glycopolymer was injected to the system to interact with the immobilised Con A layer on the gold surface. By using different concentration of the glycopolymer, kinetic parameters were calculated from these experimental results.

#### 5.2.1.1 Glycopolymer P4 binding with Con A

Concentration assays of glycopolymer **P4** were carried out keeping the concentration of Con A the same as 0.1 mg/mL. The frequency change and the corresponding concentration of the glycopolymer are shown in **Figure 5.18**. The red line is a sigmoidal fit to the experimental data points.

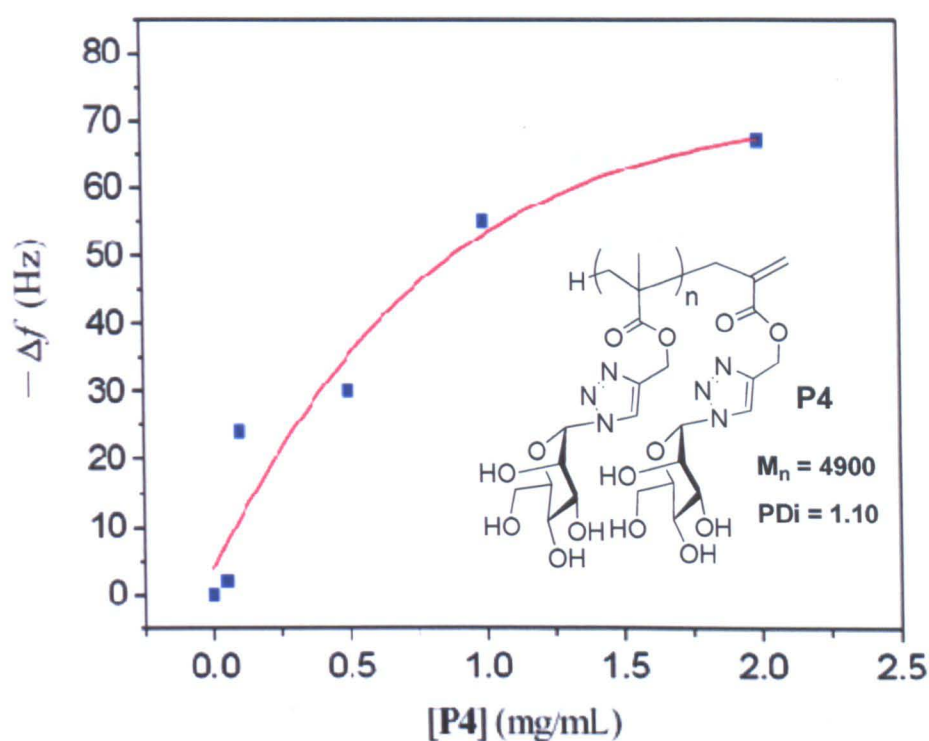


Figure 5.18 The frequency changes with different concentrations of glycopolymer **P4**.

The dependency of frequency shift on the concentration of glycopolymer **P4** follows the Langmuir-type adsorption isotherm<sup>37</sup>

$$\Delta f = \Delta f_{\max} \frac{K_a [\text{ligand}]}{1 + K_a [\text{ligand}]} \quad (1).$$

Where  $\Delta f$  is the change of frequency shift,  $\Delta f_{\max}$  is the change of frequency shift upon saturation,  $K_a$  is the association constant, and [ligand] is the concentration of a ligand solution. This equation can be rearranged as

$$\frac{1}{\Delta f} = \frac{1}{\Delta f_{\max} K_a [\text{ligand}]} + \frac{1}{\Delta f_{\max}} \quad (2).$$

The association constant can be obtained by a linear fit to the plot of  $1/\Delta f$  against  $1/[\text{ligand}]$ . Therefore, with calculation using **Equation (2)** and the experimental data in **Figure 5.18**, the association constant of the interaction between glycopolymer **P4** and Con A was estimated to be  $2.04 \times 10^4 \text{ M}^{-1}$ .

A second way for the estimation of association constant is the two-step determination of kinetic parameters, the association rate constant ( $k_1$ ) and the dissociation rate constant ( $k_{-1}$ ).<sup>38-40</sup> In the QCM-D measurement of the reversible ligand-receptor interaction with immobilised receptor on a hard surface, the change of frequency shift over the time after ejection of the ligand solution can be described by the equation

$$\Delta f = \Delta f_{\max} (1 - e^{-(1/\tau)t}) \quad (3).$$

This equation was based on the assumption that the changes of the mass on the quartz crystal surface are small enough and that the viscoelastic properties of the surface are still similar during the interaction process on the surface. The relaxation time  $\tau$  is linked with  $k_1$  and  $k_{-1}$  in the following equation

$$\tau^{-1} = k_1 [\text{ligand}] + k_{-1} \quad (4),$$

where  $\tau^{-1}$ , an inverse of the relaxation time  $\tau$ , is called as the relaxation rate constant.

In this case, two steps will be involved for the estimation of the equilibrium association constant. In the first step, the relaxation time  $\tau$  corresponding to a given

concentration of the ligand can be obtained by fitting the frequency change over time using **Equation (3)**. By applying the ligand of different concentrations to interact with the immobilised receptor, in the second step  $k_1$  and  $k_{-1}$  will be obtained from the linear fit to the plot of the relaxation rate constant  $\tau^{-1}$  against the concentration of the ligand according to **Equation (4)**.

In the interaction of glycopolymer **P4** and lectin Con A, the changes of frequency shift after ejection of glycopolymer buffer solution of different concentrations were recorded as the function of time, **Figure 5.19**. By fitting the plots with exponential decay of first order respectively, the corresponding relaxation time  $\tau$  was obtained. The slope and intercept of the plot given by **Equation (4)** were the estimation of the association rate constant ( $k_1 = 1.47 \text{ M}^{-1} \text{ s}^{-1}$ ) and the dissociation rate constant ( $k_{-1} = 4.31 \times 10^{-5} \text{ s}^{-1}$ ). Therefore, the equilibrium association constant  $K_a = k_1 / k_{-1} = 3.4 \times 10^4 \text{ M}^{-1}$ . As the results obtained from two different approaches are similar, the **Equation (2)** will be used for the estimation of association constants in the following interactions of Con A with other glycopolymers, by which the errors will be reduced because the data fitting is needed only once in this approach.

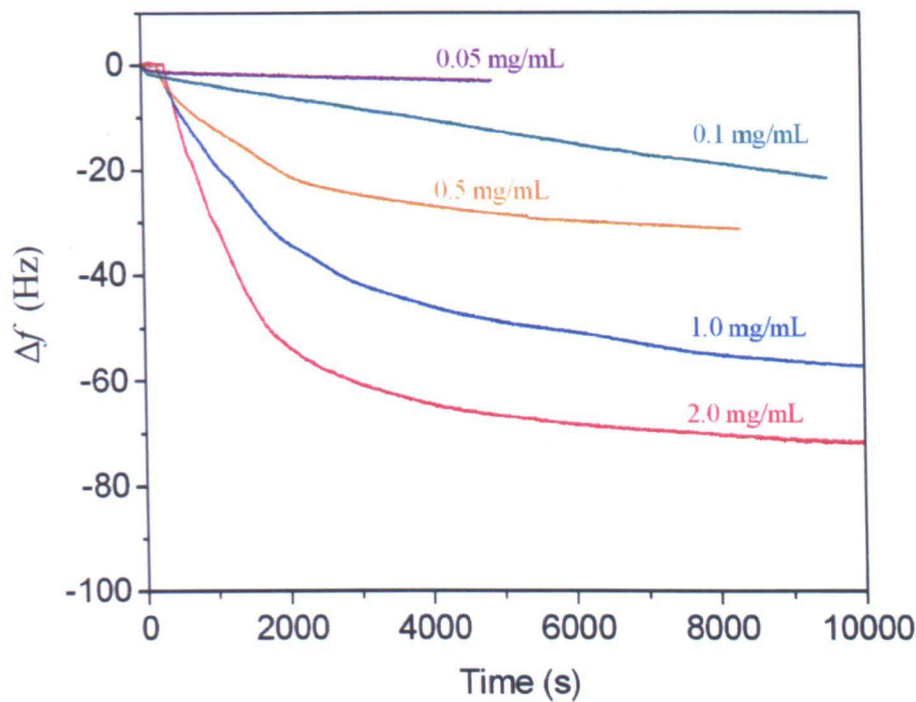


Figure 5.19 The frequency shift over time for glycopolymer **P4** of different concentrations.

With simultaneous measurements of frequency shift and energy dissipation change in QCM-D experiments, the changes of the viscoelastic properties of the materials deposited on the quartz crystal surface can be elucidated by the  $D$ - $f$  plots as shown in **Figure 5.20**. Obviously, the change of energy dissipation showed a linear dependency on the frequency shift when the concentrations of glycopolymer **P4** were low. However, the  $D$ - $f$  plots showed apparently two different periods of slope changes for high concentrations of the ligand **P4** (1 mg/mL and 2 mg/mL in this case).

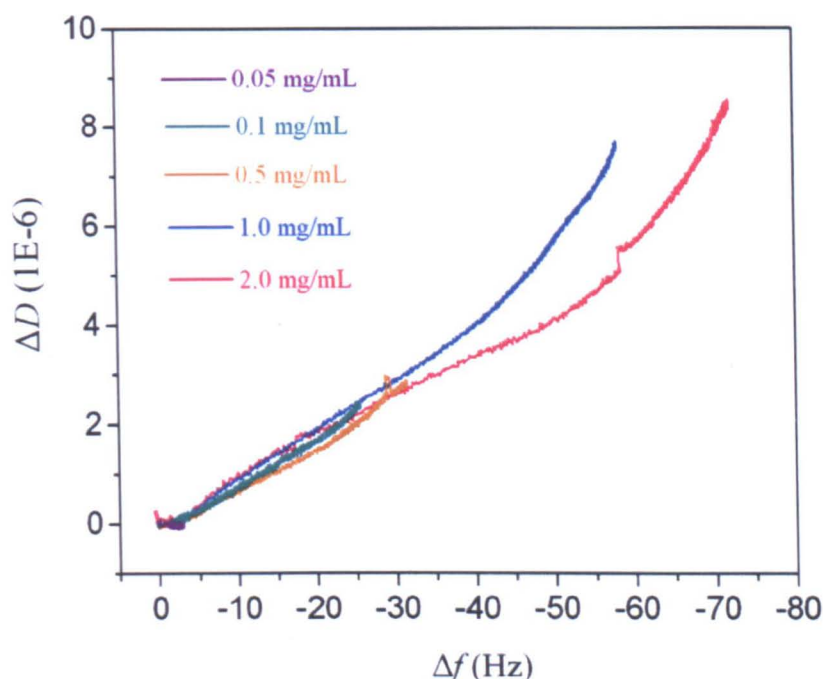


Figure 5.20 *D-f* plots of the interactions of Con A with glycopolymer **P4** of different concentration.

Initially the *D-f* plots were linear and the slopes of the plots were similar to that obtained from low ligand concentrations. In the second period this linear relationship changed as the frequency shift increased over 30 Hz and the slopes of the plots grew larger gradually. It is shown that more dissipation per added molecule during the adsorption process occurred in the second period, indicating the formation of less rigid layer over the immobilised Con A layer. The interaction process in the second period was not only kinetically controlled, but also influenced possibly by the transport limitations such as the conformational rearrangement of Con A and glycopolymer **P4**, trapped liquid in the layer or even the interfacial processes. Actually, as the two periods happened in the same interaction, the influences of the conformational rearrangement of Con A, trapped liquid and interfacial processes should be the similar for the two periods. Therefore, the slope changes of the *D-f*

plots of glycopolymer **P4** with high concentrations can be mainly due to the conformational rearrangement of the glycopolymer.

### 5.2.1.2 Glycopolymer **P5** binding with Con A

Similar to glycopolymer **P4**, glycopolymer **P5** buffer solution of different concentrations were employed to interact with Con A (0.1 mg/mL). The frequency changes with the corresponding concentration of the glycopolymer and the frequency shifts over time are shown in **Figure 5.21** and **Figure 5.22**, respectively. The red line in **Figure 5.21** is a sigmoidal fit to the experimental data points.

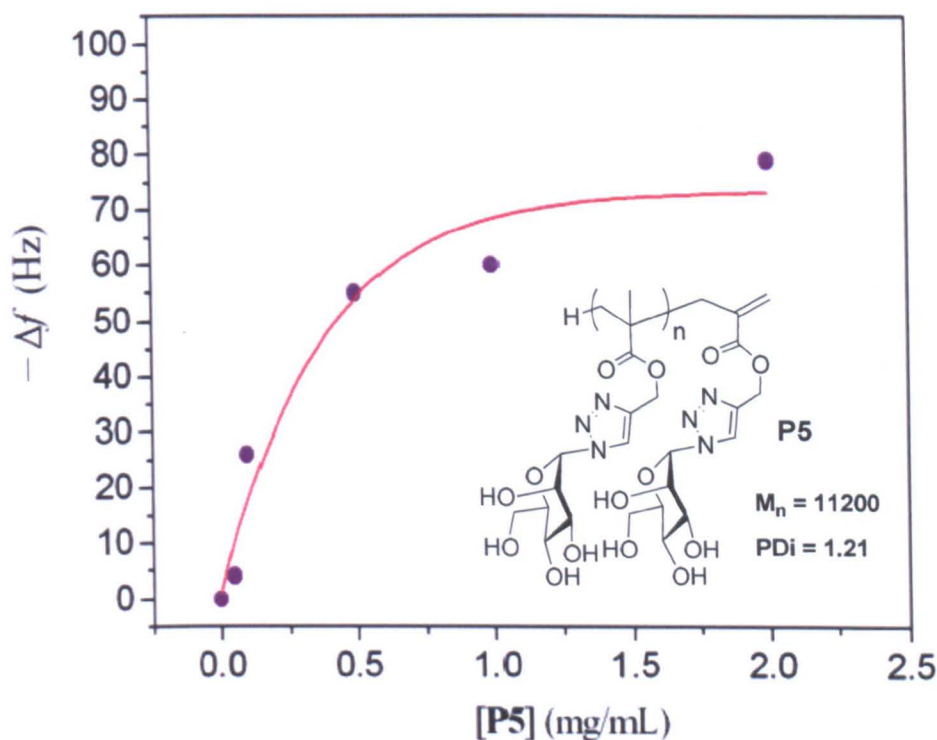


Figure 5.21 The frequency changes with different concentrations of glycopolymer **P5**.



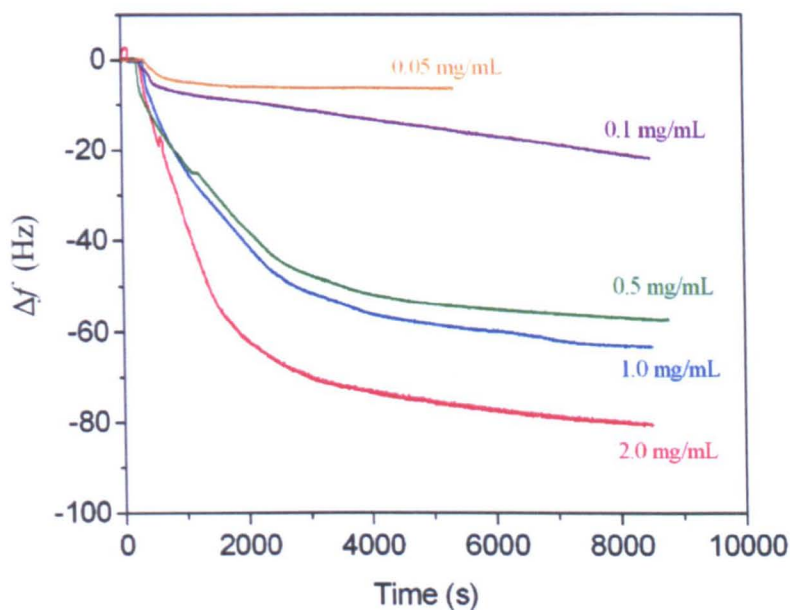


Figure 5.22 The frequency shift over time for glycopolymer **P5** of different concentrations.

The association constant of the interaction between Con A and glycopolymer **P5** were calculated according to the **Equation (2)**, which was  $K_a = 3.71 \times 10^4 \text{ M}^{-1}$ . The  $D$ - $f$  plots obtained from the QCM-D experiments are shown in **Figure 5.23**. Two different periods were also observed with respect to the slope of the plots. The conformational rearrangement of the glycopolymer **P5** became more obvious when the change of frequency was over 60 Hz.

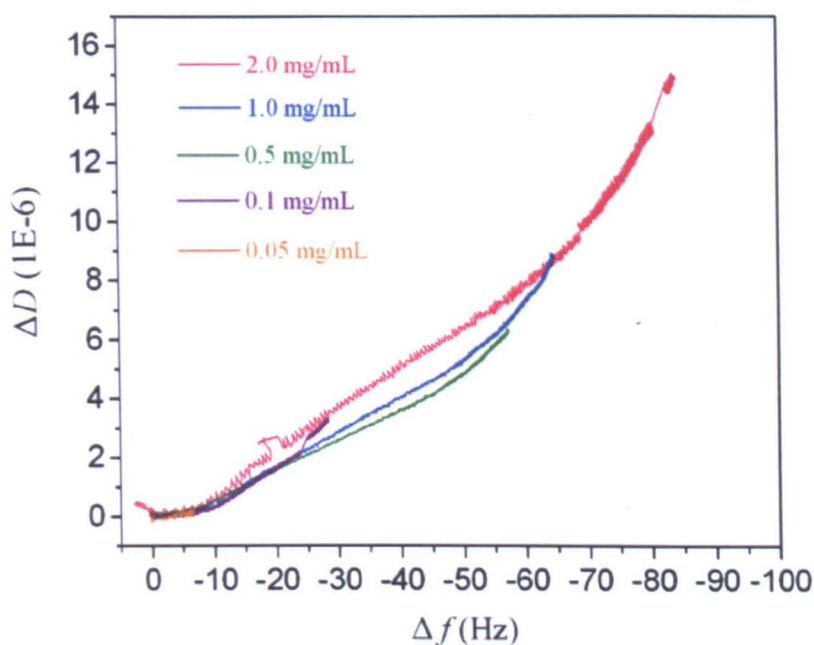


Figure 5.23 D-f plots of the interactions of Con A with glycopolymer **P5** of different concentration.

### 5.2.1.3 Glycopolymer P6 binding with Con A

According to the results from GPC, the degree of polymerisation of glycopolymer **P6** is DP = 42. Thus the chain length is longer than both glycopolymer **P4** (DP = 8) and glycopolymer **P5** (DP = 23). In the interactions of glycopolymer **P6** with Con A, the dependency of frequency changes on the concentrations of the glycopolymer are shown in **Figure 5.24** and **Figure 5.25**.

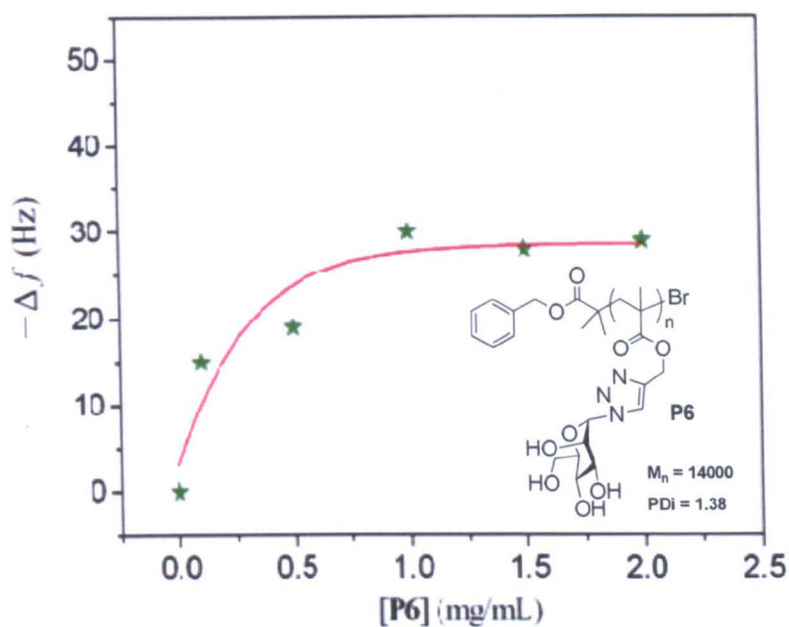


Figure 5.24 The frequency changes with different concentrations of glycopolymer **P6**.

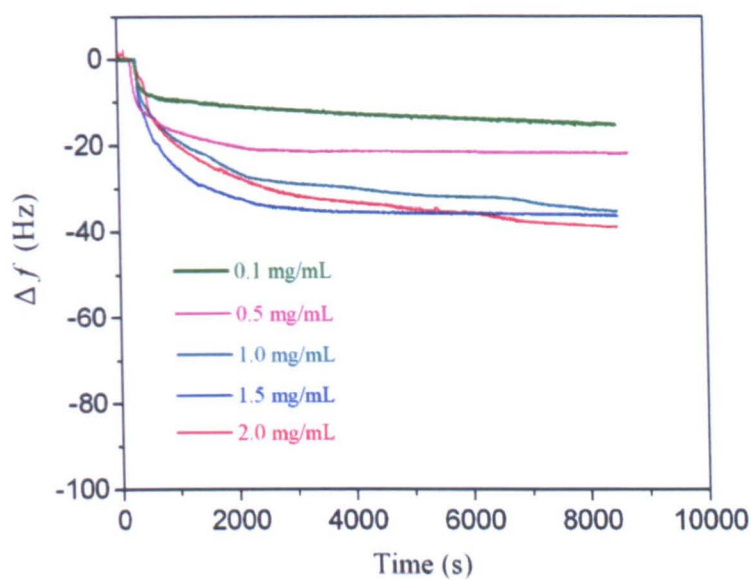


Figure 5.25 The frequency shift over time for glycopolymer **P6** of different concentrations.

The frequency shift reached a plateau (about 30 Hz) at low concentration of the glycopolymer (less than 1.0 mg/mL) and it did not change when the concentration was increased. In real time QCM-D experiments, the frequency reached the plateau very quickly for most of the measurements. The association constant of the interaction was estimated by the **Equation (2)**, which was  $K_a = 1.51 \times 10^5 \text{ M}^{-1}$ .

The  $D$ - $f$  plots are shown in **Figure 5.26**. The plots for all the concentrations from 0.1 mg/mL to 2.0 mg/mL are similar. The change of energy dissipation showed a linear relationship with the frequency shift. Due to the small changes of energy dissipation and small slopes of the plots, it can be concluded that the layer caused by adsorption of glycopolymer **P6** was relatively rigid and the influence of the transport limitations in the interaction processes was small enough to be neglected. Therefore, the viscoelastic properties of the surface did not change much during the adsorption of the glycopolymer **P6**.

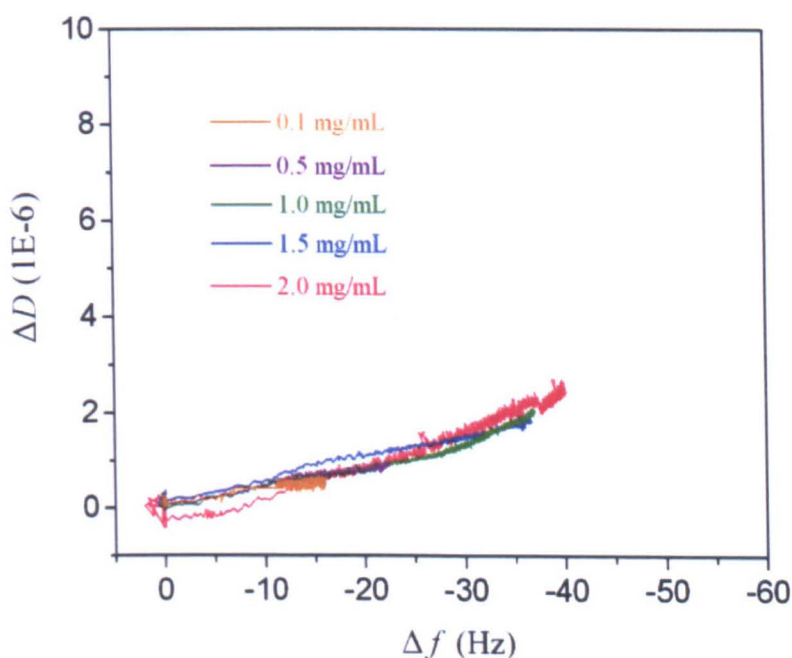


Figure 5.26  $D$ - $f$  plots of the interactions of Con A with glycopolymer **P6** of different concentration.

### 5.2.1.4 Glycopolymer **P1** binding with Con A

Glycopolymer **P1** with  $M_n = 22.1$  kDa and PDI = 1.31 was employed as a reference to interact with Con A as the chain length of this glycopolymer was the longest (DP = 58). The frequency shift over time for each concentration is shown in **Figure 5.27** and **Figure 5.28**.

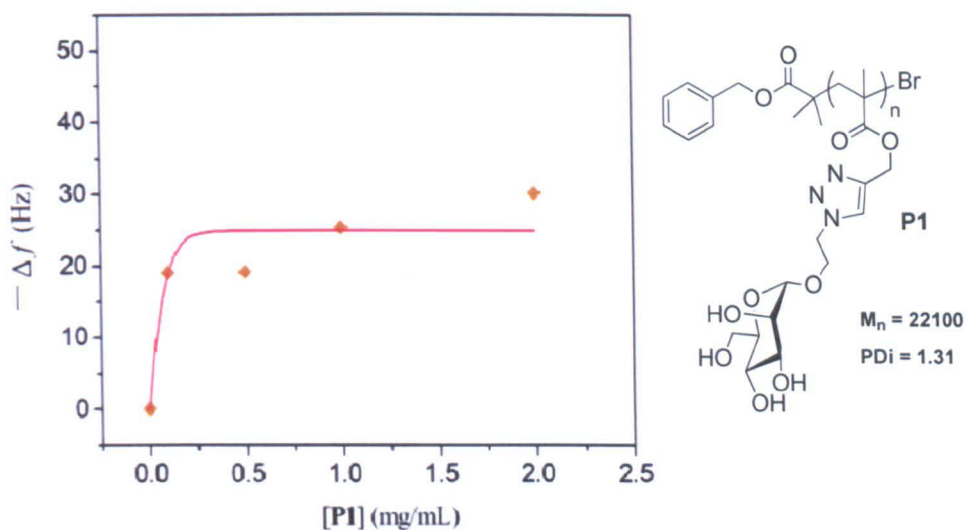


Figure 5.27 The frequency changes with different concentrations of glycopolymer **P1**.

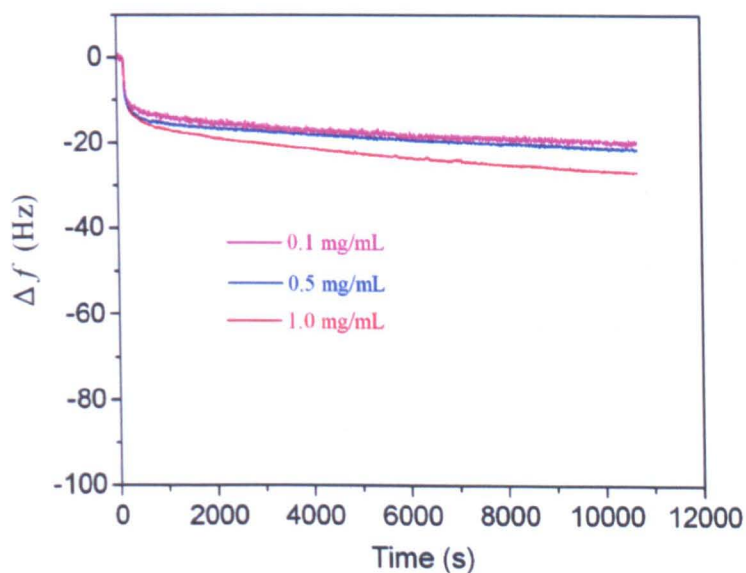


Figure 5.28 The frequency shift over time for glycopolymer **P1** of different concentrations.

The changes of frequency by adsorption of the glycopolymer **P1** were not large ( $< 30$  Hz) and the frequency also reached the plateau very quickly. The changes of energy dissipation were relatively small, as shown by the  $D$ - $f$  plots in **Figure 5.29**. Thus, glycopolymer **P1** exhibited similar properties as glycopolymer **P6** in the interactions with Con A.

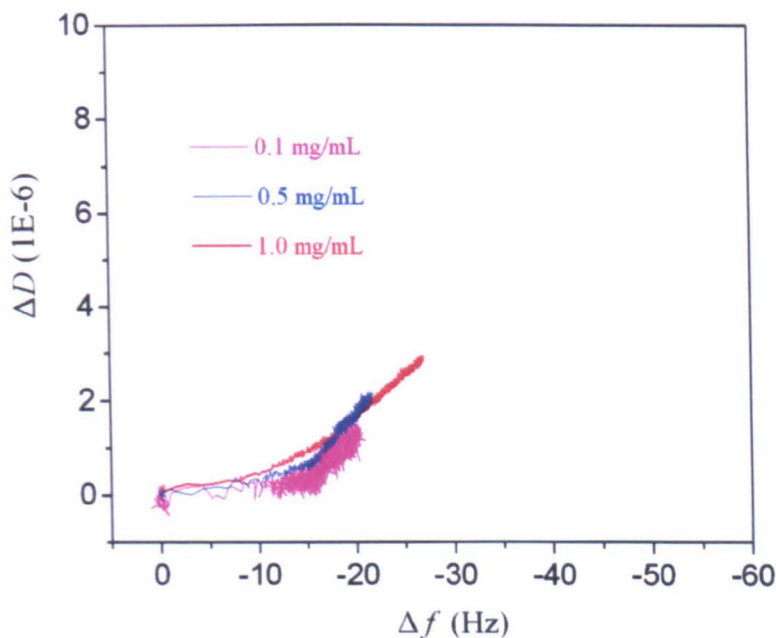


Figure 5.29  $D$ - $f$  plots of the interactions of Con A with glycopolymer **P1** of different concentrations.

#### 5.2.1.5 Comparison of all glycopolymers in the interactions with Con A

From all the results mentioned above, it seems that there are differences between the four mannose glycopolymers in their interactions with lectin Con A. However, glycopolymers **P4**, **P5** and **P6** are of most interest in the QCM-D experiments. These three glycopolymers have the same repeat unit in the polymeric backbone but are different in their chain lengths. The frequency changes for different concentrations of the three glycopolymers are shown in **Figure 5.30**.



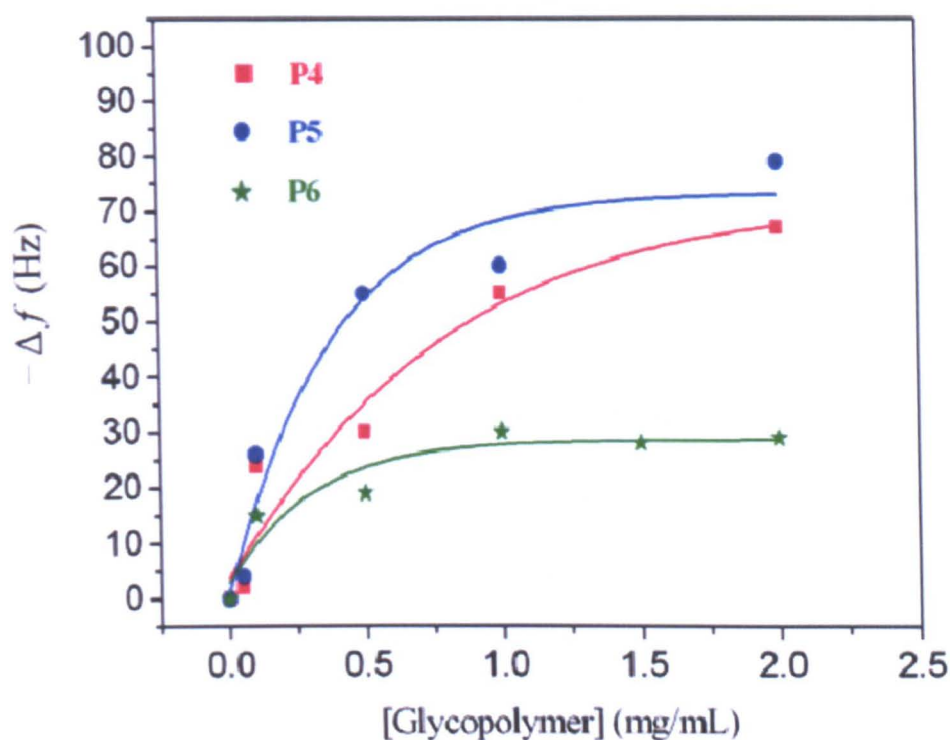


Figure 5.30 The frequency changes for different concentrations of glycopolymers.

Pendant mannose moieties are the recognition elements in these glycopolymers for them to be the ligands of Con A. From **Figure 5.30** it is clear that on the basis of mannose moieties, glycopolymer **P5** is the ligand binding most in the conjugation of Con A following an order of **P6 < P4 < P5**. In QCM-D measurements, the amounts of both glycopolymer **P4** and **P5** adsorbed onto the layer of immobilised Con A were larger than that of glycopolymer **P6**. However, on the basis of glycopolymeric chains, the association constant of glycopolymer **P6** is the biggest, **Table 5.2**. The binding affinities of the three glycopolymers to Con A are in an order of **P4 < P5 < P6**, suggesting glycopolymer **P6** is the best ligand of Con A.

Table 5.2 The association constants of different mannose glycopolymers.

Glycopolymer	P4	P5	P6
DP	8	23	42
$K_a$ (M <sup>-1</sup> )	$3.83 \times 10^4$	$5.56 \times 10^4$	$1.51 \times 10^5$

The contradictory results gave a conclusion that the binding most is not the binding best in the interactions of glycopolymers with lectin Con A. This conclusion can be further elucidated by the changes of viscoelastic properties of the quartz crystal surface during the interactions, **Figure 5.31**.

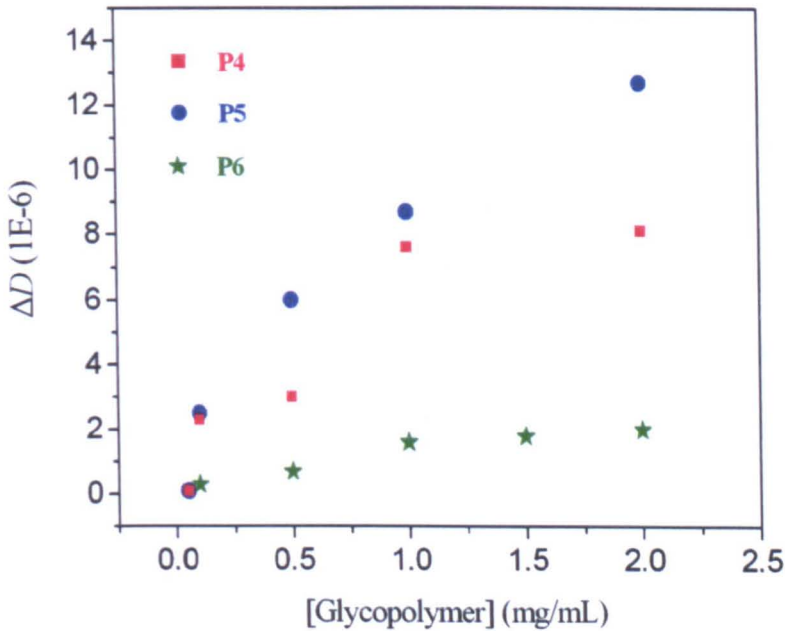
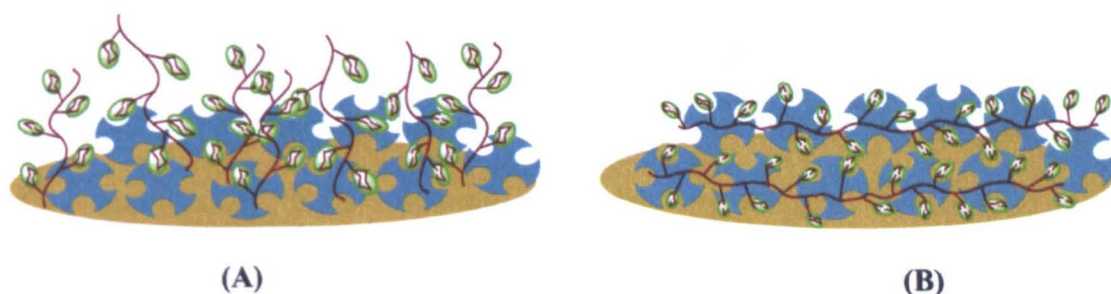


Figure 5.31 The changes of energy dissipation for different concentrations of glycopolymers.

The energy dissipation was significantly changed during the adsorption of glycopolymers **P4** and **P5**, especially when the concentration of the ligand was high.



As previously mentioned, the large changes were mostly due to the conformational rearrangement of the corresponding glycopolymers. Larger the  $\Delta D$  is, less rigid the new layer will be. The possible statuses of the glycopolymer layer are represented by schematic diagrams in **Figure 5.32**. The layer formed by glycopolymers **P4** or **P5** of high concentration was likely to be **(A)**, in which the glycopolymers with short chain lengths exist as brushes on the quartz crystal surface. In this case, more polymers were deposited on the surface but the layer was less rigid due to their weak binding with Con A. During the reversible interactions, it took more time for the glycopolymeric chains to saturate the immobilised Con A kinetically. However, the binding of glycopolymer **P6** to Con A tended to be like **(B)** as the polymer chain was longer. The conjugation of the glycopolymer with immobilised Con A led to the formation of a rigid new layer. The binding affinity enhanced by multivalency was big enough to make the conjugation process fast and the resulting lectin-glycopolymer conjugates stable on the surface. Thus the conjugated Con A tetramers became not available for further binding with other glycopolymeric chains due to the steric blockage which induced the small frequency changes in the interactions of glycopolymer **P6** with Con A. This was also confirmed by the reference binding of glycopolymer **P1** to Con A, in which both frequency shifts and changes of energy dissipation were small.



*Figure 5.32 Schematic diagrams of the glycopolymer layer on gold chip surface.*

### 5.2.2 Interactions of DC-SIGN with glycopolymers

Dendritic cell specific ICAM-3 grabbing nonintegrin (DC-SIGN) is a C-type lectin found on the surface of dendritic cells which plays a very important role in human immunity,<sup>41</sup> **Figure 5.33**. Specifically, the interactions between DC-SIGN and the HIV envelope glycoprotein gp120 regulate the adhesion and infection of the lethal opportunistic pathogen to normal host cells.<sup>42</sup> Therefore, potential new therapeutics can be based on the identification of novel ligands to inhibit the binding of DC-SIGN to gp120. As it exists as a tetramer of four identical subunits, DC-SIGN can bind to synthetic mannose/fucose-containing glycoconjugates.<sup>43-45</sup>

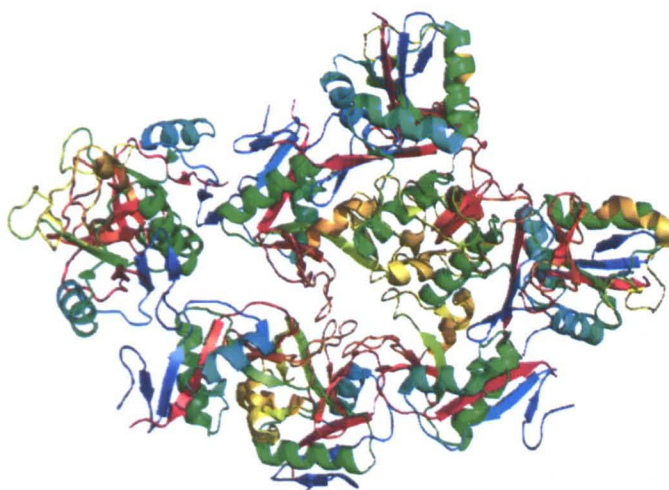


*Figure 5.33 The structure of lectin DC-SIGN from Wikipedia.*

In this work, binding properties of the well-defined mannose glycopolymer **P4**, **P5**, **P6** and **P1** to DC-SIGN were investigated by QCM-D experiments. Additionally, fucose-containing glycopolymer **P7** and **P8** were also employed for the interactions with DC-SIGN, **Figure 5.34**. Glycopolymer **P7** was synthesised by a combination of CCTP and CuAAC click reactions, while **P8** was prepared by CuAAC click chemistry following ATRP of TMS-protected propargyl methacrylate and

deprotection. Both of the glycopolymers have the same pendant recognition units ( $\beta$ -L-fucose) but different chain lengths (**P7**, DP = 23 and **P8**, DP = 58).

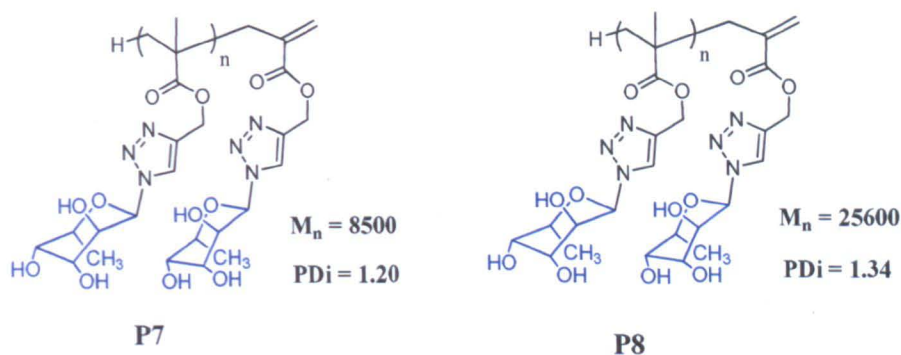


Figure 5.34 Fucose-containing glycopolymers employed in the interactions with DC-SIGN.

Using the same procedure as mentioned above, the quartz crystal chip surface was modified with 10 mM MUA, followed by 0.4 M EDC and 0.1M NHS (1:1, v/v) to activate the carboxyl groups on the gold surface. All the solid analytes were dissolved in buffer containing 25 mM HEPES, 150 mM NaCl, 5 mM  $\text{CaCl}_2$  and 0.01% Tween-20 with pH = 7.4. The buffer solution of DC-SIGN (0.1 mg/mL) was passed over the modified chip surface. The changes of frequency and energy dissipation are shown in **Figure 5.35**. Comparing with Con A solution (0.1 mg/mL), DC-SIGN exhibited much better adsorption onto the modified surface. Thus, the method used in the QCM-D experiments here is more sensitive for the investigation into the interactions of DC-SIGN with synthetic glycopolymers.



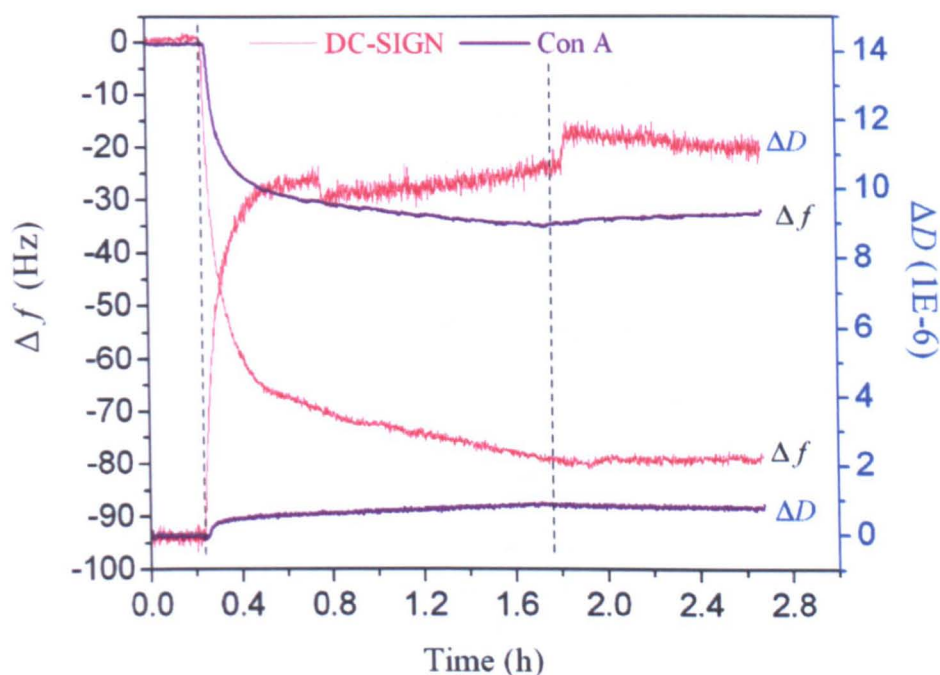


Figure 5.35 The binding of DC-SIGN to the modified gold surface comparing with Con A.

In the QCM-D measurement, the buffer solution of ethanolamine hydrochloride (1M, pH = 8.5) was also used for the deactivation of the surface after adsorption of DC-SIGN. A typical measurement is shown in **Figure 5.36**, in which a solution of glycopolymer **P4** (0.5 mg/mL) was employed to interact with DC-SIGN layer on the surface.

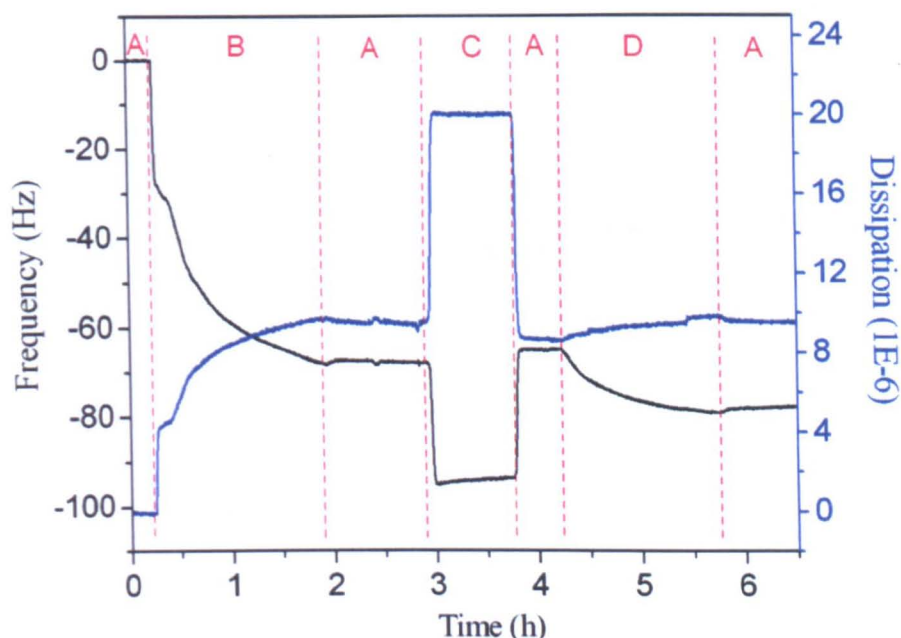


Figure 5.36 QCM-D plot of the interaction of DC-SIGN with mannose glycopolymer **P4**: (A) buffer; (B) DC-SIGN solution (0.1 mg/mL); (C) the solution of ethanolamine HCl (1M, pH 8.5); (D) the solution of glycopolymer **P4** (0.5 mg/mL).

The solution of glycopolymer **P4** was running over the lectin layer on the surface until the frequency shift reached a plateau. Unreacted polymeric molecules were washed off the quartz crystal surface by passing buffer through the system. The changes of frequency and energy dissipation were recorded for the specific concentration of the glycopolymer. After each measurement of glycopolymer solution, the lectin surface was regenerated using 10 mM glycine hydrochloride (pH 2.5), **Figure 5.37**. The solution of glycine hydrochloride was running over the surface for one hour, followed by washing with buffer. It is apparently the lectin surface was totally regenerated within the error of QCM-D measurements ( $\pm 2$  Hz).

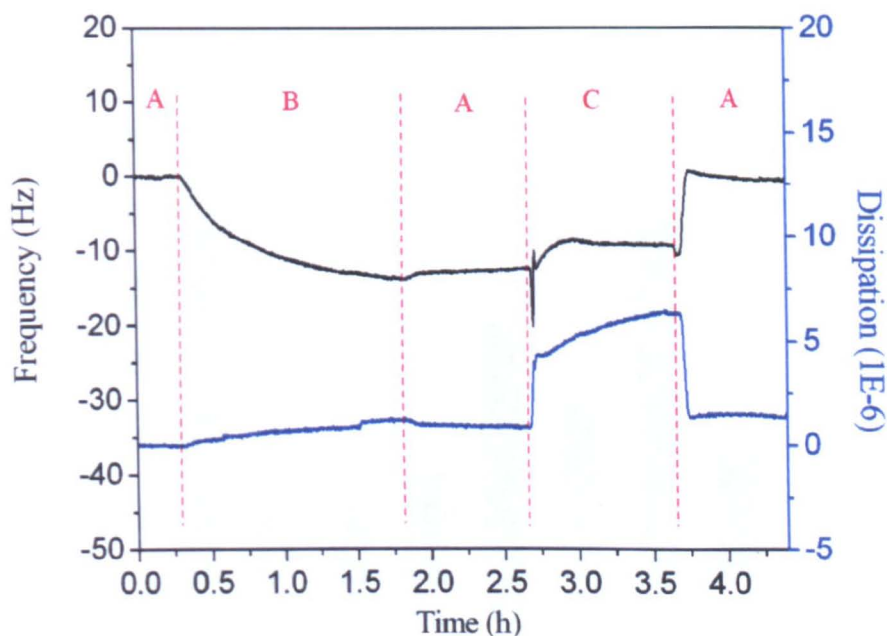


Figure 5.37 Regeneration of the lectin surface: (A) buffer; (B) glycopolymer **P4** solution (0.5 mg/mL); (C) 10 mM glycine hydrochloride, pH 2.5.

The results of QCM-D measurements for all the glycopolymers binding with lectin DC-SIGN are shown in **Figure 5.38**. The same concentration (0.5 mg/mL) was employed for all the glycopolymers in the interaction with DC-SIGN (0.1 mg/mL). Two additional experiments were carried out with glycopolymers **P4** and **P6** at the concentration of 2.0 mg/mL. Obviously it was glycopolymer **P4** that the lectin layer bound most among all the glycopolymers. The two glycopolymers **P7** and **P8** with pendant fucose moieties were more potential ligands of DC-SIGN than their mannose- containing counterparts **P5** and **P1**. In general, the changes of frequency and energy dissipation were relatively low even when the high concentration (2.0 mg/mL) was used. In a summary, the potencies of these glycopolymers as the inhibitor of DC-SIGN are limited.

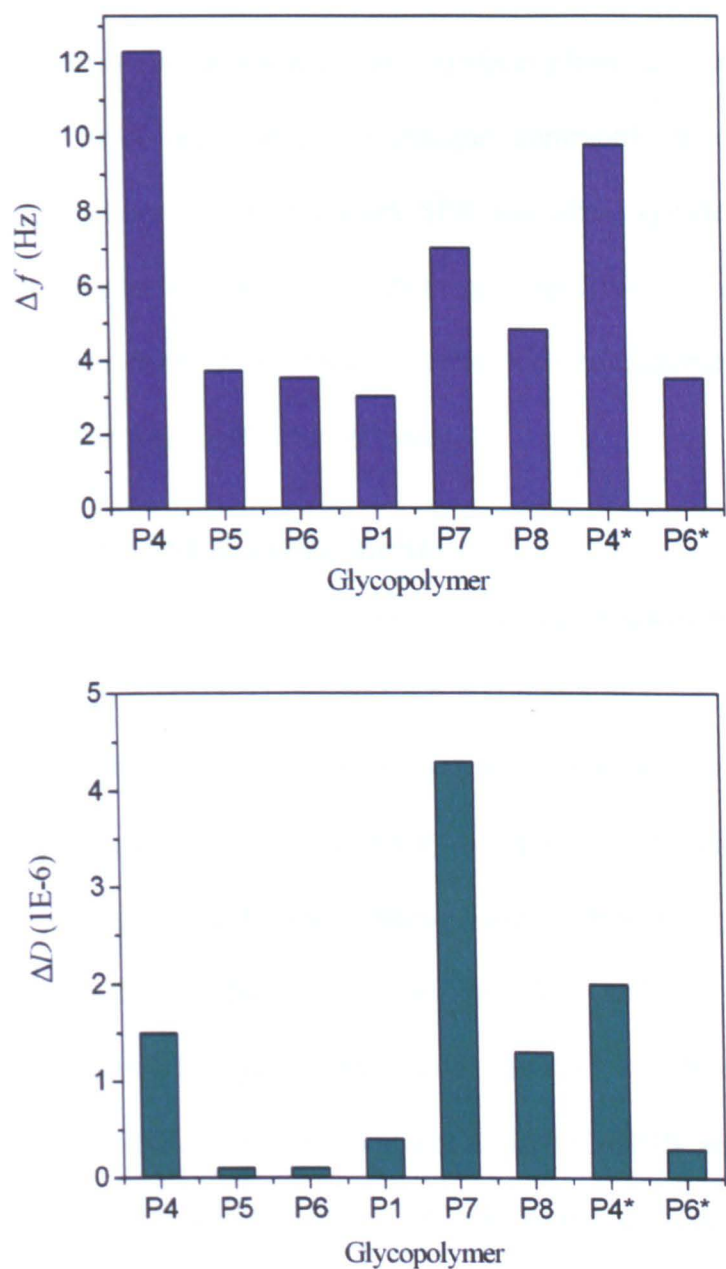


Figure 5.38 The changes of frequency and energy dissipation for all the glycopolymers (0.5 mg/mL) binding with DC-SIGN (\* The concentration was 2.0 mg/mL).

## 5.3 Investigation into the specific lectin-glycopolymer interactions by SPR

Based on the electro-optical phenomenon, surface plasmon resonance (SPR) is another powerful label-free detection technique commonly used for studies of biomolecular interactions.<sup>46-48</sup> In this work SPR was also exploited to monitor the interactions between lectins and the synthetic glycopolymers. The results will be compared with those from QCM-D experiments. The measurements of SPR were done by collaboration with Dr. C. Remzi Becer.

### 5.3.1 The routine of SPR experiments

All of the measurements were done following a similar protocol. HBS buffer (pH = 7.4) containing 25 mM HEPES, 150 mM NaCl, 5 mM CaCl<sub>2</sub> and 0.01% Tween-20 was generally used to make solutions of analytes except that the lectin DC-SIGN was dissolved in a acetate buffer (pH =5.0) for optimal immobilisation. The SPR sensor chip was bought from Biorad Company with hydrocarboxyl groups attached on the surface. The surface was then modified with a mixture of 1-[3-(dimethylamino)propyl]-3-ethyl carbodiimide (EDC) hydrochloride and *N*-hydroxysuccinimide (NHS) in order to attach lectin DC-SIGN and Con A onto the surface. Taking the interaction between DC-SIGN and glycoprotein gp120 as an example, SPR sensorgrams for a whole experimental process are shown in **Figure 5.39**. Basically, the procedure was composed of 5 different steps: (A) modification of the sensor surface by EDC and NHS; (B) immobilisation of the lectin DC-SIGN; (C) deactivation of the hydrocarboxyl groups on the surface by ethanolamine hydrochloride; (D) binding interaction of the lectin DC-SIGN with gp120 of different concentrations; (E) regeneration of the lectin surface.



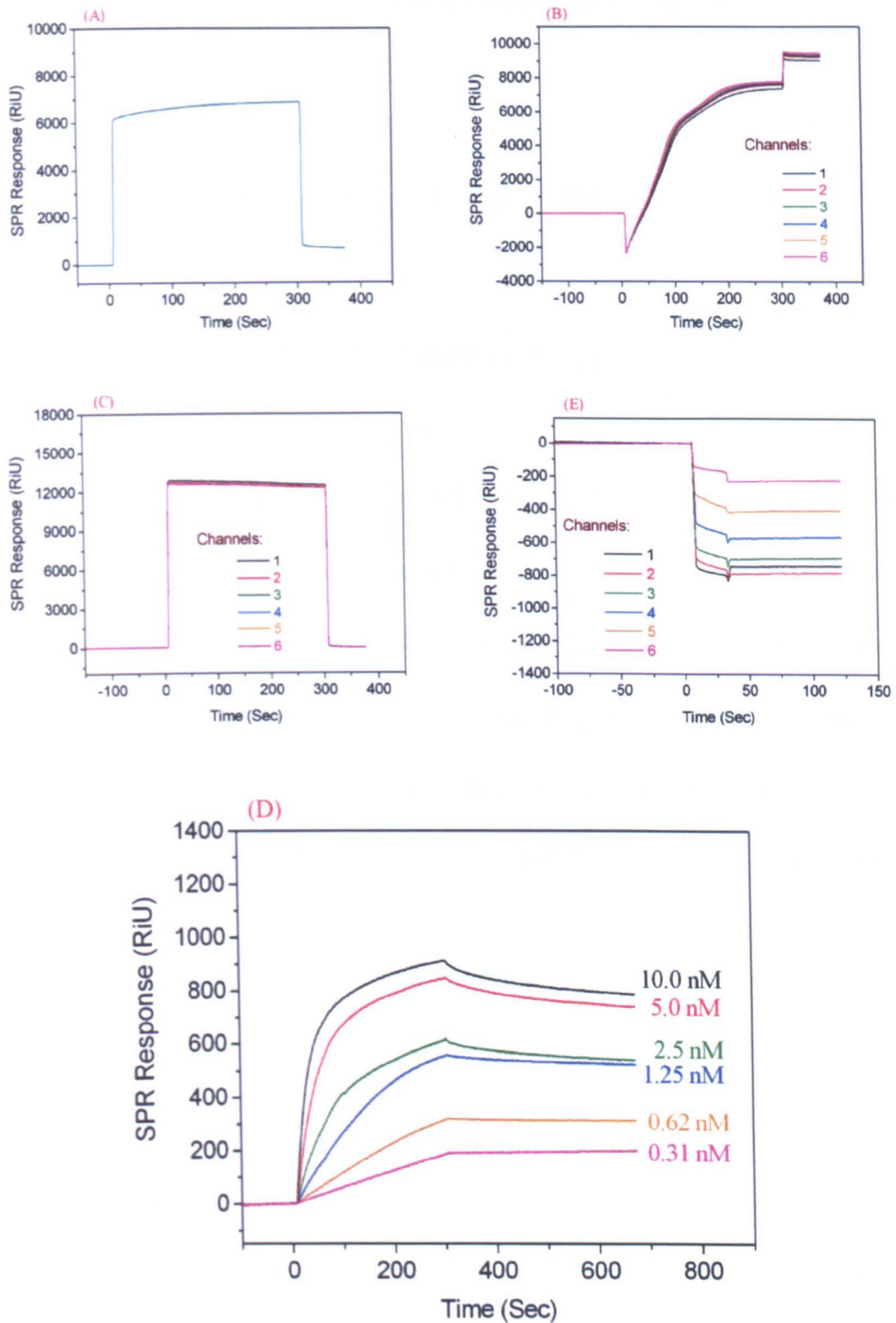


Figure 5.39 The routine for a SPR measurement of the interaction between DC-SIGN and gp120: (A) the mixture of 0.4 M EDC and 0.1M NHS (1:1, v/v); (B) the solution of DC-SIGN (50  $\mu\text{M}$ ) in acetate buffer (pH = 5.0); (C) the solution of ethanolamine HCl (1M, pH 8.5); (D) HBS buffer solutions of gp120 with different concentrations (0.31 nM ~ 10.0 nM); (E) 10 mM glycine hydrochloride, pH 2.5.

The kinetic parameters of the binding process can be determined by a combination of **Equation (5)** and **(6)**,<sup>49</sup>

$$\Delta R = \Delta R_{\max}(1 - e^{-(1/\tau)t}) \quad (5)$$

$$\tau^{-1} = k_a[\text{ligand}] + k_d \quad (6)$$

where  $\Delta R$  is the resonance response,  $\Delta R_{\max}$  is the response at steady state,  $\tau$  is the relaxation time,  $k_a$  is the association rate constant, and  $k_d$  is the dissociation rate constant. Once  $k_a$  and  $k_d$  are obtained, the apparent dissociation constant  $K_D$  will be determined by  $K_D = k_d/k_a$ . In the interaction of gp120 with DC-SIGN the kinetic constants were calculated from **Figure 5.40** by linearly fitting the data points, which are  $k_a = 1.48 \times 10^6 \text{ M}^{-1}\text{s}^{-1}$ ,  $k_d = 5.92 \times 10^{-3} \text{ s}^{-1}$ , and  $K_D = 4.0 \times 10^{-9} \text{ M}$ , respectively.

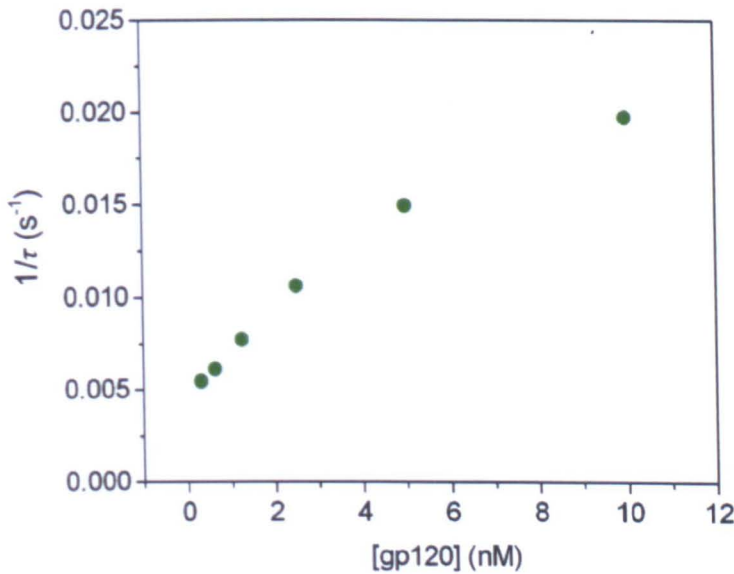


Figure 5.40 The linear dependency of the inverse of relaxation time on concentration of gp120.

### 5.3.2 Comparison of glycopolymers on the basis of sugar moieties

Glycopolymers **P5** and **P1** were employed for the measurements of their binding abilities to lectins on the basis of sugar moieties. The solution of the glycopolymer (**P5** or **P1**) with the same concentration (100  $\mu\text{g/mL}$ ) was passed over the same lectin surface (Con A or DC-SIGN) at the flow rate 25  $\mu\text{L/min}$ . After washing the surface with buffer, the changes of SPR resonance responses are shown in **Figure 5.41**.

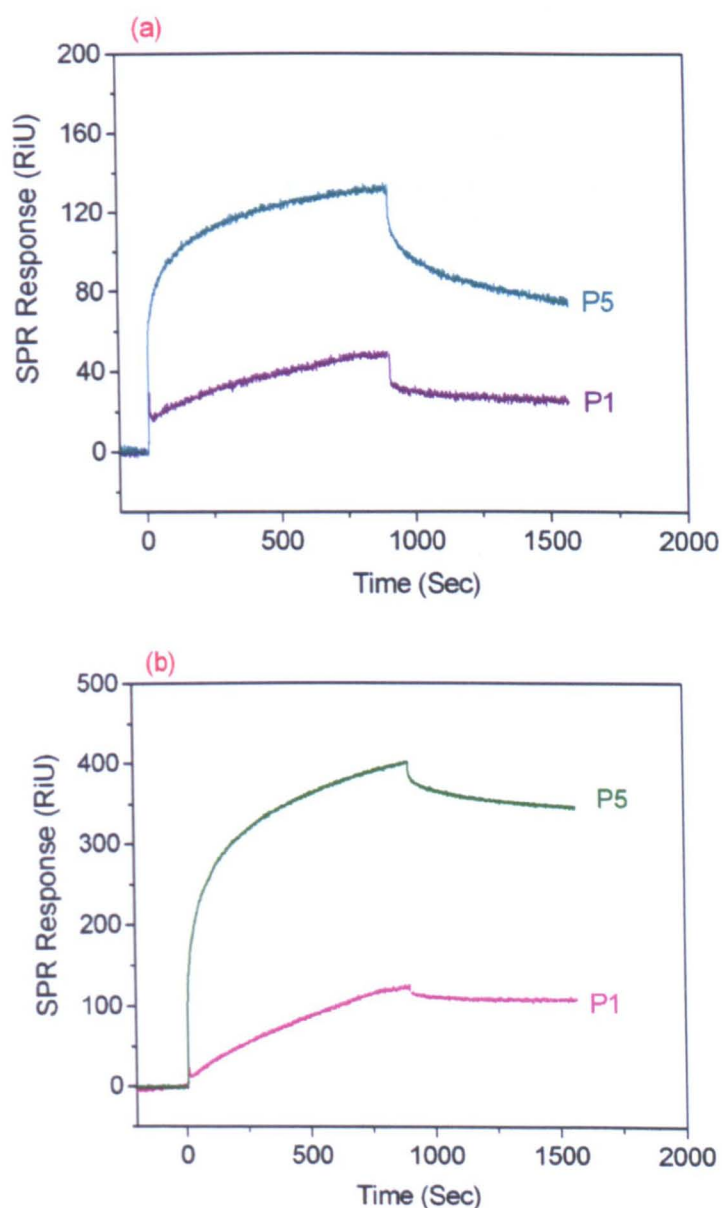


Figure 5.41 The resonance responses for the binding of glycopolymer **P5** and **P1** to the lectin (a) Con A and (b) DC-SIGN, respectively.

Similar to the results from QCM-D experiments, the amounts of the glycopolymer **P5** with short chain length ( $DP = 23$ ) attached onto the lectin surfaces were more than those of the glycopolymer **P1** ( $DP = 58$ ). In the measurements of both QCM-D and SPR, the lectins were attached covalently on the modified sensor chip surface in the same way. Therefore, the aforementioned hypothesis about the conformational status of the layer formed by binding of the glycopolymers onto the lectin layer was further supported by the results obtained from SPR experiments here.

### 5.3.3 Kinetic properties of the interaction between DC-SIGN and synthetic glycopolymers

The binding affinities of mannose glycopolymer **P5** ( $DP = 23$ ), mannose glycopolymer **P1** ( $DP = 58$ ), and fucose glycopolymer **P7** ( $DP = 23$ ) to the lectin DC-SIGN were investigated by SPR measurements, **Figure 5.42** and **Figure 5.43**. The molecular weight and polydispersity index were obtained from GPC eluted by DMF.

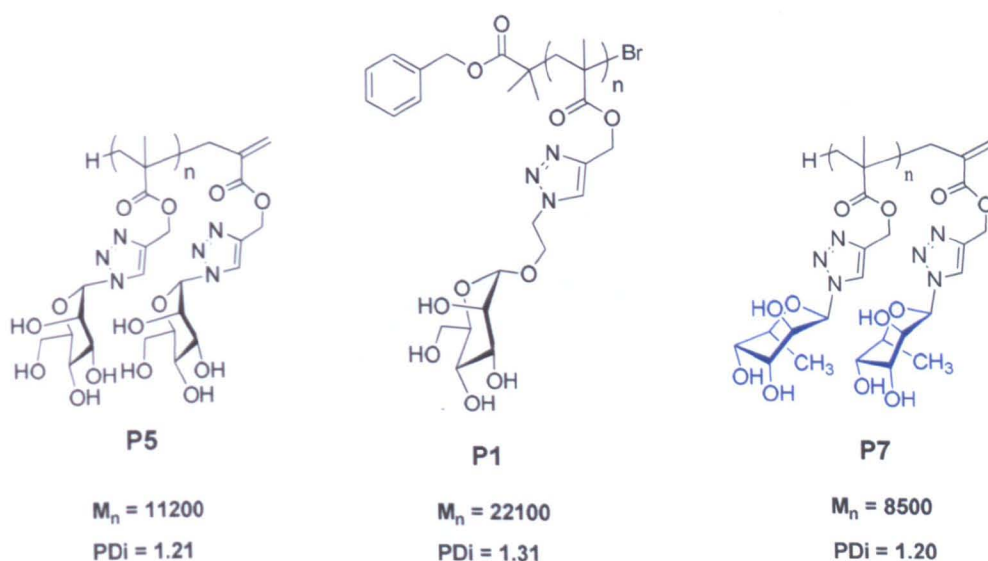


Figure 5.42 Glycopolymers used in SPR kinetic measurements.

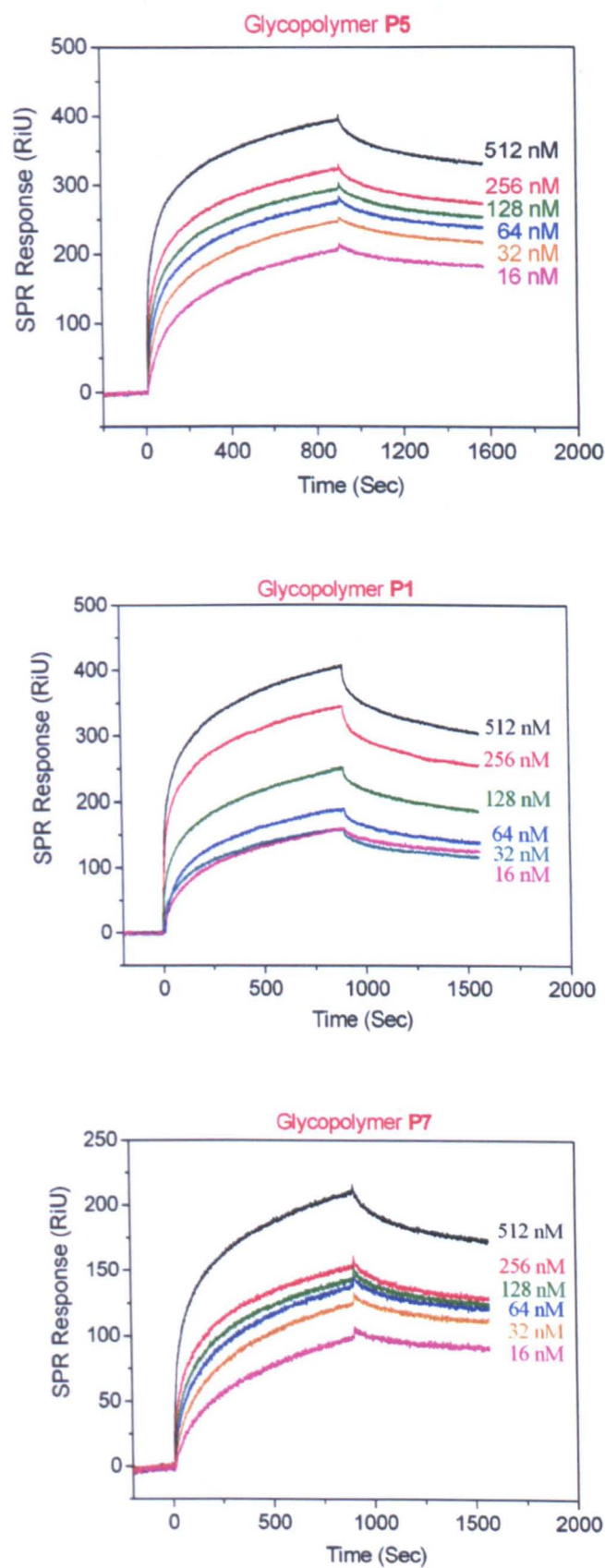


Figure 5.43 SPR sensorgrams by binding of glycopolymers to immobilised DC-SIGN with different concentrations.

Concentration assays were carried out using the same immobilised DC-SIGN surface for the interactions of different glycopolymers with a series of concentrations. All the solutions of analytes were passed over the lectin surface with the flow rate at 25  $\mu\text{L}/\text{min}$  and the contact time of 900 s. The surface was regenerated after each measurements using the solution of glycine hydrochloride with flow rate at 100  $\mu\text{L}/\text{min}$  and contact time of 27 s. The kinetic parameters were calculated by a combination of **Equation (5)** and **(6)** as shown in **Table 5.3**. The binding parameters of gp120 with DC-SIGN were used as a reference.

*Table 5.3 Kinetic parameters of the interactions between different glycopolymers and DC-SIGN.*

Ligand	Carbohydrate	$k_a (\text{M}^{-1}\text{s}^{-1})$	$k_d (\text{s}^{-1})$	$K_D (\text{M})$
<b>P5</b>	Mannose	$9.46 \times 10^3$	$4.78 \times 10^{-3}$	$5.05 \times 10^{-7}$
<b>P1</b>	Mannose	$1.61 \times 10^4$	$4.15 \times 10^{-3}$	$2.58 \times 10^{-7}$
<b>P7</b>	Fucose	$5.92 \times 10^3$	$3.72 \times 10^{-3}$	$6.28 \times 10^{-7}$
gp120	—	$1.48 \times 10^6$	$5.92 \times 10^{-3}$	$4.0 \times 10^{-9}$

It is clear that the apparent dissociation constant of glycopolymer **P1** is smaller than that of glycopolymer **P5**, which means that the binding affinity of **P1** is larger than that of **P5**. The enhancement of the binding affinity can be attributed to the "glycoside cluster effect" because of the longer chain length of glycopolymer **P1**. The binding of mannose glycopolymer **P5** to DC-SIGN is greater than fucose glycopolymer **P7** which are of the same chain length.



## 5.4 Conclusions

In summary, two powerful label-free detection techniques, QCM-D and SPR were exploited to investigate the interactions of the lectin Con A or DC-SIGN with a series of different glycopolymers.

Firstly, two different ways have been demonstrated by QCM-D experiments to prepare the LBL alternative self-assembled bioactive multilayer surfaces *via* the biological affinities of different lectins and their specific carbohydrates. Con A and PNA were used as model lectins. The Au chip surface needs to be chemically modified by MUA, EDC and NHS in order to covalently attach the lectin Con A to the surface. If the carbohydrates are desired to be immobilised first, the disulfide glycopolymers can be used to bind directly to the bare Au chip surface. Sauerbrey's equation and Voigt modeling were used to calculate the mass and thickness of the alternate self-assembly between Con A and mannose glycopolymer or the assembled multilayer by disulfide mannose glycopolymer, Con A, mannose-galactose glycopolymer and PNA. The analysis of the  $D-f$  plots of multilayer indicated the number of layers play an important role in both of the interactions happening on the quartz crystal surface and the viscoelastic properties of the resulting multilayers.

Secondly, concentration assays were carried out using QCM-D technique to analyse the effect of chain length on the binding affinities and kinetics of three mannose glycopolymers (  $DP = 8, 23, 42$  ) containing the same mannose moieties. Con A was employed as the model lectin and another mannose glycopolymer ( $DP = 58$ ) with different mannose moieties was used as a reference ligand. As the frequency shifts of the QCM-D measurements depended on the concentrations of glycopolymers

following the Langmuir-type adsorption isotherm, so the binding equilibrium association constants of the interactions were estimated. In the interactions with Con A, the amounts of glycopolymers of short chain lengths attached onto the lectin surface were more than those of longer chain lengths. However, the binding affinities of the glycopolymers of longer chain lengths were larger due to the "glycoside cluster effect". Therefore, a hypothesis was proposed about the conformational status of the layer formed by binding of the glycopolymers of different chain lengths onto the lectin layer. The interaction between DC-SIGN and the synthetic glycopolymers were also studied by QCM-D experiments. However, the changes of frequency and energy dissipation were too small to compare the influences of different chain lengths.

Finally, kinetic parameters of the interactions of DC-SIGN with glycopolymers of different chain lengths and different compositions were explored by SPR measurements. The results agreed very well with the conclusions obtained from aforementioned QCM-D experiments.

## 5.5 References

1. Decher, G., *Science* **1997**, *277*, 1232-1237.
2. Leader, H.; Popovitz-Biro, R.; Vaskevich, A.; Rubinstein, I., *Langmuir* **2011**, *27*, 1298-1307.
3. Sato, K.; Imoto, Y.; Sugama, J.; Seki, S.; Inoue, H.; Odagiri, T.; Hoshi, T.; Anzai, J.-i., *Langmuir* **2004**, *21*, 797-799.



- 
4. Sato, H.; Anzai, J.-i., *Biomacromolecules* **2006**, *7*, 2072-2076.
  5. Caruso, F.; Schuler, C., *Langmuir* **2000**, *16*, 9595-9603.
  6. Haynie, D. T.; Zhang, L.; Rudra, J. S.; Zhao, W.; Zhong, Y.; Palath, N., *Biomacromolecules* **2005**, *6*, 2895-2913.
  7. Park, M.-K.; Deng, S.; Advincula, R. C., *J. Am. Chem. Soc.* **2004**, *126*, 13723-13731.
  8. Guo, Y.; Geng, W.; Sun, J., *Langmuir* **2008**, *25*, 1004-1010.
  9. Zhang, L.; Sun, J., *Macromolecules* **2010**, *43*, 2413-2420.
  10. Clark, S. L.; Hammond, P. T., *Langmuir* **2000**, *16*, 10206-10214.
  11. Cui, X.; Pei, R.; Wang, Z.; Yang, F.; Ma, Y.; Dong, S.; Yang, X., *Biosens. Bioelectron.* **2003**, *18*, 59-67.
  12. Sato, K.; Kodama, D.; Naka, Y.; Anzai, J.-i., *Biomacromolecules* **2006**, *7*, 3302-3305.
  13. Yuan, W.; Dong, H.; Li, C. M.; Cui, X.; Yu, L.; Lu, Z.; Zhou, Q., *Langmuir* **2007**, *23*, 13046-13052.
  14. Calvo, E. J.; Danilowicz, C.; Wolosiuk, A., *J. Am. Chem. Soc.* **2002**, *124*, 2452-2453.
  15. Kang, E.-H.; Jin, P.; Yang, Y.; Sun, J.; Shen, J., *Chem. Commun.* **2006**, 4332-4334.
  16. Liu, A.; Anzai, J.-i., *Langmuir* **2003**, *19*, 4043-4046.
  17. De Cock, L. J.; De Koker, S.; De Geest, B. G.; Grooten, J.; Vervaet, C.; Remon, J. P.; Sukhorukov, G. B.; Antipina, M. N., *Angew. Chem. Int. Ed.* **2010**, *49*, 6954-6973.
  18. Lavalle, P.; Voegel, J.-C.; Vautier, D.; Senger, B.; Schaaf, P.; Ball, V., *Adv. Mater.* **2011**, *23*, 1191-1221.
-

- 
19. de Villiers, M. M.; Otto, D. P.; Strydom, S. J.; Lvov, Y. M., *Adv. Drug Delivery Rev.* **2011**, *63*, 701-715.
  20. Tang, Z.; Wang, Y.; Podsiadlo, P.; Kotov, N. A., *Adv. Mater.* **2006**, *18*, 3203-3224.
  21. Cooper, M. A.; Singleton, V. T., *J. Mol. Recognit.* **2007**, *20*, 154-184.
  22. de la Fuente, J.; Penadés, S., *Glycoconjugate J.* **2004**, *21*, 149-163.
  23. Rickert, J.; Brecht, A.; Göpel, W., *Biosens. Bioelectron.* **1997**, *12*, 567-575.
  24. Pan, N.-Y.; Shih, J.-S., *Sensor Actuat. B-Chem.* **2004**, *98*, 180-187.
  25. Okahata, Y.; Niikura, K.; Furusawa, H.; Matsuno, H., *Anal. Sci.* **2000**, *16*, 1113-1119.
  26. Marx, K. A., *Biomacromolecules* **2003**, *4*, 1099-1120.
  27. Lee, L.; Cavalieri, F.; Johnston, A. P. R.; Caruso, F., *Langmuir* **2009**, *26*, 3415-3422.
  28. Lundin, M.; Solaqa, F.; Thormann, E.; Macakova, L.; Blomberg, E., *Langmuir* **2011**, *27*, 7537-7548.
  29. Alf, M. E.; Hatton, T. A.; Gleason, K. K., *Langmuir* **2011**, *27*, 10691-10698.
  30. Martins, G. V.; Mano, J. F.; Alves, N. M., *Langmuir* **2011**, *27*, 8415-8423.
  31. Lyu, Y.-K.; Lim, K.-R.; Lee, B. Y.; Kim, K. S.; Lee, W.-Y., *Chem. Commun.* **2008**, 4771-4773.
  32. Ting, S. R. S.; Chen, G.; Stenzel, M. H., *Polym. Chem.* **2010**, *1*, 1392-1412.
  33. Ladmiral, V.; Mantovani, G.; Clarkson, G. J.; Cauet, S.; Irwin, J. L.; Haddleton, D. M., *J. Am. Chem. Soc.* **2006**, *128*, 4823-4830.
  34. Slavin, S.; Soeriyadi, A.; Voorhaar, L.; Whittaker, M. R.; Becer, C. R.; Boyer, C.; Davis, T. P.; Haddleton, D. M., *Submitted* **2011**.
-

- 
35. Höök, F.; Rodahl, M.; Brzezinski, P.; Kasemo, B., *Langmuir* **1998**, *14*, 729-734.
36. Voinova, M. V.; Jonson, M.; Kasemo, B., *Biosens. Bioelectron.* **2002**, *17*, 835-841.
37. Mahon, E.; Aastrup, T.; Barboiu, M., *Chem. Commun.* **2010**, *46*, 2441-2443.
38. Lebed, K.; Kulik, A. J.; Forr, L.; Lekka, M., *J. Colloid Interf. Sci.* **2006**, *299*, 41-48.
39. Mao, Y.; Wei, W.; He, D.; Nie, L.; Yao, S., *Anal. Biochem.* **2002**, *306*, 23-30.
40. Ebara, Y.; Okahata, Y., *J. Am. Chem. Soc.* **1994**, *116*, 11209-11212.
41. Ralph M. S., *Cell* **2000**, *100*, 491-494.
42. Geijtenbeek, T. B. H.; Kwon, D. S.; Torensma, R.; van Vliet, S. J.; van Duijnhoven, G. C. F.; Middel, J.; Cornelissen, I. L. M. H. A.; Nottet, H. S. L. M.; KewalRamani, V. N.; Littman, D. R.; Figdor, C. G.; van Kooyk, Y., *Cell* **2000**, *100*, 587-597.
43. Becer, C. R.; Gibson, M. I.; Geng, J.; Ilyas, R.; Wallis, R.; Mitchell, D. A.; Haddleton, D. M., *J. Am. Chem. Soc.* **2010**, *132*, 15130-15132.
44. Andreini, M.; Doknic, D.; Sutkeviciute, I.; Reina, J. J.; Duan, J.; Chabrol, E.; Thepaut, M.; Moroni, E.; Doro, F.; Belvisi, L.; Weiser, J.; Rojo, J.; Fieschi, F.; Bernardi, A., *Org. Biomol. Chem.* **2011**, *9*, 5778-5786.
45. van Liempt, E.; Bank, C. M. C.; Mehta, P.; Garcí'a, J. J.; Kwar, Z. S.; Geyer, R.; Alvarez, R. A.; Cummings, R. D.; Kooyk, Y. v.; van Die, I., *FEBS Lett.* **2006**, *580*, 6123-6131.
46. Papp, I.; Dervede, J.; Enders, S.; Riese, S. B.; Shiao, T. C.; Roy, R.; Haag, R., *Chembiochem.* **2011**, *12*, 1075-1083.
47. Spain, S. G.; Cameron, N. R., *Polym. Chem.* **2011**, *2*, 1552-1560.
-

48. Duverger, E.; Lamerant-Fayel, N.; Frison, N.; Monsigny, M., *Methods Mol. Biol.* **2010**, 627, 157-178.
49. Bouffartigues, E.; Leh, H.; Anger-Leroy, M.; Rimsky, S.; Buckle, M., *Nucl. Acids Res.* **2007**, 35, e39.

## **Chapter 6.**

### **Conclusions and Outlook**

## 6.1 Conclusions

The development of glycobiology can be hindered by the limited access to oligosaccharides using direct synthetic approaches. The efficient synthesis of glycomimetics offers an attractive route to solve this problem. Glycopolymers, as synthetic carbohydrate polymers, can often interact with lectins in a similar way to natural oligosaccharides in the lectin-carbohydrate interactions. In order to get a better understanding of the structure-function relationship of oligosaccharides and to mimic or even exceed the properties of natural oligosaccharides in some specific applications, much attention has been drawn to synthesis and application of glycopolymers and investigation of lectin-carbohydrate interactions in recent years.

In this work, well-defined glycopolymers were prepared by the combination of CCTP and CuAAC click reactions. Alkyne-containing polymer scaffolds were synthesised by CCTP, followed by post-modification of the *clickable* polymer scaffolds with sugar azides. By using CCTP, very small amount (*i.e.* ppm) of chain transfer agent CoBF was needed to prepare precursor polymers of low molecular weights. The double functionality of the precursor polymers enabled further modification by CuAAC, thiol-ene or thiol-yne click reactions. The one-step synthesis of sugar azide involved in this work represented a significant improvement over the traditional Koenigs–Knorr type glycosylation. The post-functionalisation strategy by CCTP and click chemistry provided a facile way to the synthesis of well-defined glycopolymers.

A library of well-defined synthetic glycopolymers featuring the same macromolecular properties (architecture, polydispersity, valency, polarity, *etc.*) with

difference only in the densities of different sugars (mannose, galactose and glucose) were employed to investigate the influence of different pendant epitopes on the interactions with a model lectin Con A. Employing four different efficient assays, quantitative precipitation, turbidimetry, inhibitory potency assay and reversal aggregation assay, we explored the behaviours of the 15 different multivalent ligands in clustering the receptor Con A. The stoichiometry of the glycopolymer-Con A conjugates, the rate of the cluster formation, the inhibitory potency of these multivalent ligands and the stability of the glycopolymer-Con A turbidity were all investigated.

Besides the traditional methods, two powerful modern detection techniques, QCM-D and SPR were also exploited to investigate the interactions of the lectin Con A, PNA, or DC-SIGN with a series of different glycopolymers. Firstly, two different ways were demonstrated by QCM-D experiments to prepare the LBL alternate self-assembled bioactive multilayer surfaces *via* the biological affinities of different lectins and their specific carbohydrates. The number of layers played an important role in both of the interactions happening on the quartz crystal chip surface and the viscoelastic properties of the resulting multilayer surface. Secondly, concentration assays were carried out to analyse the effect of chain length on the binding affinities and kinetics of three mannose glycopolymers containing the same mannose moieties. According to the amount of glycopolymers adsorbed onto the immobilised lectin surface and the estimated equilibrium association constant, a hypothesis was proposed about the conformational status of the layer formed by binding of the glycopolymers of different chain lengths onto the lectin layer. The conclusions obtained from QCM-D, SPR and the traditional methods agreed very well with each other.

The diversities of binding properties contributed by different clustering parameters can make it possible to define the structures of the multivalent ligands and densities of binding epitopes for specific functions in the lectin-carbohydrate interactions. These conclusions can be employed as the springboard to develop new glycopolymeric drugs and therapeutic agents and to assess the mechanisms by which they work.

## 6.2 Outlook

With respect to the present work, the following work can be carried out in the future:

1. Further functionalisation of the double functionality of the precursor polymers prepared by CCTP using click chemistry or preparation of copolymers using the precursor polymers as the macromonomers.
2. Synthesis of glycopolymers with different architectures such as hyperbranched or star polymers for the lectin-carbohydrate interactions investigated by traditional methods, QCM-D and SPR.
3. Preparation of thermo-, pH-sensitive glycopolymers for specific applications.
4. Preparation of micelles or nanoparticles using glycopolymers.
5. Exploration of application of glycopolymers in biological processes.



# Chapter 7.

## Experimental

## 7.1 Materials

Copper(I) bromide, tetrabutylammonium fluoride (TBAF) in THF (1.0M), acetic acid, 2,2'-bipyridyl (bipyridine), 2-chloro-1,3-dimethylimidazolinium chloride (DMC), sodium azide, L-fucose and concanavalin A (Con A) were purchased from Sigma-Aldrich. Triethylamine was purchased and used directly from Fisher Scientific. 3-(Trimethylsilyl)-2-propyn-1-ol, D-(+)-glucose, D-(+)-galactose and D-(+)-mannose were purchased from Alfa-Aesar. Copper(I) bromide was purified according to the method of Keller and Wycoff.<sup>1</sup>  $\text{CoBF}_4$ ,<sup>2,3</sup> 2-bromo-2-methylpropionic acid benzyl ester initiator<sup>4</sup> and the ligand *N*-ethyl-2-pyridylmethanimine<sup>5</sup> were prepared as described previously. All other reagents and solvents were purchased at the highest purity available from Sigma-Aldrich Chemical Company and used without further purification unless stated.

## 7.2 Characterisation

All polymerisations were carried out using standard Schlenk techniques under an inert atmosphere of oxygen-free nitrogen, unless otherwise stated.

### 7.2.1 Nuclear Magnetic Resonance

$^1\text{H}$  and  $^{13}\text{C}$  NMR spectra were obtained on a Bruker DPX-300 and Bruker DPX-400 spectrometer. All chemical shifts are reported in ppm (parts per million) relative to tetramethylsilane (TMS), referenced to the chemical shifts of deuterated solvents from Sigma-Aldrich. The following abbreviations were used to explain the multiplicities: d = doublet, m = multiplet, t = triplet. The number average molecular

weight of the polymers  $M_n$  (NMR) was calculated by comparing the integrals of the chain-end peaks and appropriate peaks related to the polymer backbone.

### 7.2.2 Gel Permeation Chromatography (GPC)

Molecular weight and the polydispersity index (PDI) of polymers were measured using gel permeation chromatography (GPC). Three systems with different eluents were used in this study depending on the solubility of the analysts. All GPC solvents and sample solutions were filtered through nylon or PVDF 0.2  $\mu\text{m}$  filters. Molecular weight and distribution data was obtained using Polymer Labs 'Cirrus' software (version 3.3).

**N, N-Dimethylformamide (DMF) GPC:** The measurements were performed on a PL 390-LC system. This system was equipped with an autosampler, two PL gel 5  $\mu\text{m}$  mixed D columns (300  $\times$  7.5 mm), one PLgel 5  $\mu\text{m}$  guard column (50  $\times$  7.5 mm), a differential refractive index (DRI) detector, a viscometer and a UV-Vis detector. The system was eluted by DMF (containing 1% LiBr) at between 0.8 ~ 1.0 mg/mL at 50°C and calibrated with PL narrow PMMA standard EasiVials (690 ~ 467,400 g/mol).

**Chloroform GPC:** The measurements were performed on a PL 390-LC system, which was equipped with an autosampler, two PL gel 5  $\mu\text{m}$  mixed D columns (300  $\times$  7.5 mm), one PL gel 5  $\mu\text{m}$  guard column (50  $\times$  7.5 mm), a DRI detector, a viscometer and a light scattering detector. The system was eluted at 1.0 mL/min by a mixture of chloroform and triethylamine (95:5, v/v) and calibrated with PL narrow PMMA standard EasiVials (690 ~ 467,400 g/mol).

**Tetrahydrofuran (THF) GPC:** The system was a PL 390-LC system equipped with an autosampler, two PL gel 5  $\mu\text{m}$  mixed D columns ( $300 \times 7.5$  mm) and one PL gel 5  $\mu\text{m}$  guard column ( $50 \times 7.5$  mm;  $200 \sim 400,000$  g/mol), a DRI detector, a dual angle light scattering detector and a photodiode array (PDA) detector. The system was eluted by THF and triethylamine (98:2, v/v) at 1.0 mL/min and calibrated by narrow molecular weight poly(methyl methacrylate) standards ( $690 \sim 467,400$  g/mol).

### ***7.2.3 Electrospray Ionization Mass Spectrometry (ESI-MS)***

The ESI-MS spectra were obtained on Bruker Esquire2000, one of the early models of Bruker's high performance trap systems. The mass range was  $50 \sim 2200$  Da with unit mass resolution and tandem mass ability. The system was coupled with an isocratic Agilent 1100 HPLC (without column) as an automatic sample delivery system.

### ***7.2.4 Matrix Assisted Laser Desorption Ionisation–Time of Flight (MALDI-TOF) Spectrometry***

MALDI-TOF analysis was performed with a Bruker Ultraflex TOF and analysed using FlexAnalysis software. The system was kept inside a vacuum at  $5 \times 10^{-6}$  Torr to avoid contamination of the sample reading and equipped with a neodymium-doped yttrium aluminium garnet laser (Nd:YAG) at 337 nm with positive ion TOF detection performed using an accelerating voltage of 25 kV. The matrix was prepared by dissolving 2, 4-dihydroxybenzoic acid (DHB) (10 mg/mL) and sodium iodide (NaI) (1 mg/mL) in THF. The calibration standard PMMA (5 mg/mL) and the

sample (5 mg/mL) were dissolved in THF separately (for glycopolymers as the sample, they were dissolved in water.). The matrix solution (1  $\mu$ L) was applied to the stainless steel plate. After the solvent was evaporated, the same volume of sample solution was applied on top of the dried matrix. By drying the overall mixture on the plate, the sample was irradiated with 200 pulsed laser shots at no greater than 30% laser power. Calibration was performed with various linear PMMA standards.

### ***7.2.5 Fourier Transform Infra Red (FTIR) Spectroscopy***

The system was a Bruker Vector-22 FTIR spectrometer with a Golden Gate diamond attenuated total reflection (ATR) cell.

### ***7.2.6 Ultraviolet (UV) Spectroscopy***

The UV-Vis data was obtained on a Jasco V-660 UV-Vis spectrometer, using 1 mL volume polycarbonate cuvettes (1 cm path length).

### ***7.2.7 Quartz Crystal Microbalance with Dissipation Monitoring (QCM-D)***

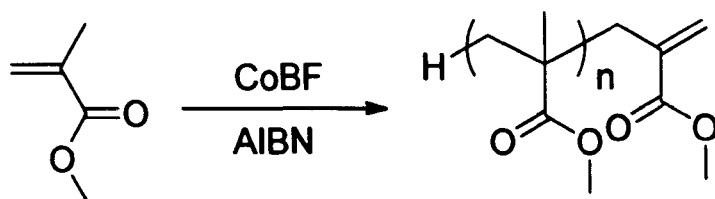
All the QCM-D experiments were performed using the Q-Sense E4 System with four sensor chambers for four parallel measurements at 25 °C. The system was equipped with QE 401 Electronics Unit, QCP 401 Chamber Platform, QFM 401 Flow Module with Ismatec IPCN Pump. The quartz crystal chip was optically polished Au coated quartz sensor (AT-cut; Diameter: 14 mm; Thickness: 0.3 mm; Surface roughness of electrode < 3 nm; Electrode layer: 10–300 nm) with fundamental resonant frequency 5 MHz.

### 7.2.8 Surface Plasmon Resonance (SPR)

All the SPR Sensorgrams were carried out in a Biorad ProteOn XPR36 SPR biosensor (Biorad, Hercules CA) using Biorad GMC sensor chips.

## 7.3 Chapter 3 Experimental

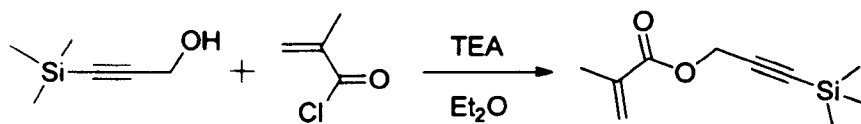
### 7.3.1 CCTP of Methyl Methacrylate (MMA)



CoBF (10 mg) was dissolved in MMA (25 mL) which was previously freeze-pump-thawed 3 times. Azobisisobutyronitrile (AIBN) (9.2 mg) was added to a Schlenk tube containing a magnetic stirrer, followed by addition of methyl methacrylate (2 mL). The solution was freeze-pump-thawed 4 times and then filled with nitrogen. The CoBF solution (810  $\mu$ L) was added into the Schlenk tube and the mixture was stirred at 60  $^{\circ}$ C under nitrogen overnight. At the end of the reaction, the mixture was cooled to ambient temperature and bubbled with air for 2 hours. The volatiles were removed by distillation under reduced pressure and the crude product was purified by precipitation in petroleum ether (Conversion = 17.3%,  $M_n$  = 1100 Da, PDi = 2.44)

### 7.3.2 Synthesis of TMS-Protected Propargyl Methacrylate

TMS-protected propargyl methacrylate was synthesised as previously described using **3-(trimethylsilyl)-2-propyn-1-ol** and methacryloyl chloride.<sup>6</sup>



A solution of trimethylsilyl propyn-1-ol (40.0 g, 312 mmol) and triethylamine (TEA) (56.6 mL, 406 mmol) in diethyl ether (250 mL) was cooled to 0 °C. A solution of methacryloyl chloride (45 mL, 406 mmol) in diethyl ether (150 mL) was added dropwise into the mixture using a dropping funnel. The mixture was stirred at this temperature for 1 h and at ambient temperature overnight under nitrogen. The solution was passed through a basic alumina column and washed with diethyl ether. After removal of the volatiles under reduced pressure, the crude product was purified by kugelrohr distillation. 47.4 g colourless oil was obtained as the product (yield = 77.4 %).

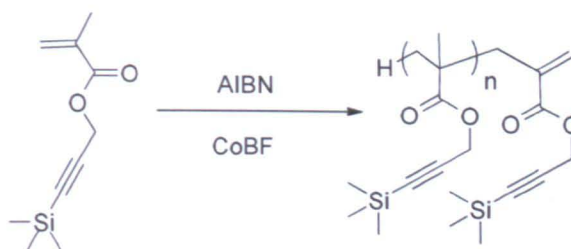
<sup>1</sup>H NMR (400.03 MHz, CDCl<sub>3</sub>, 298 K) δ (ppm) = 0.20 (s, 9H, Si(CH<sub>3</sub>)<sub>3</sub>), 1.94 (s, 3H, CH<sub>3</sub>C=CH<sub>2</sub>), 4.80 (s, 2H, OCH<sub>2</sub>), 5.58 (s, 1H, C=CH<sub>H</sub>), 6.07 (s, 1H, C=CH<sub>H</sub>).

<sup>13</sup>C NMR (100.59 MHz, CDCl<sub>3</sub>, 298 K) δ (ppm) = 0 (3C, Si(CH<sub>3</sub>)<sub>3</sub>), 17.9 (1C, CH<sub>3</sub>C=CH<sub>2</sub>), 52.7 (1C, OCH<sub>2</sub>), 91.1 (1C, C≡CSi(CH<sub>3</sub>)<sub>3</sub>), 100.3 (1C, C≡CSi(CH<sub>3</sub>)<sub>3</sub>), 126.7 (1C, CH<sub>3</sub>C=CH<sub>2</sub>), 135.3 (1C, CH<sub>3</sub>C=CH<sub>2</sub>), 166.6 (1C, C=O).

FTIR (neat):  $\tilde{\nu}$  (cm<sup>-1</sup>) = 2961, 2186, 1722, 1638, 1452, 1367, 1314, 1292, 1250, 1145, 1051, 970, 942, 839, 813, 759, 700, 644.

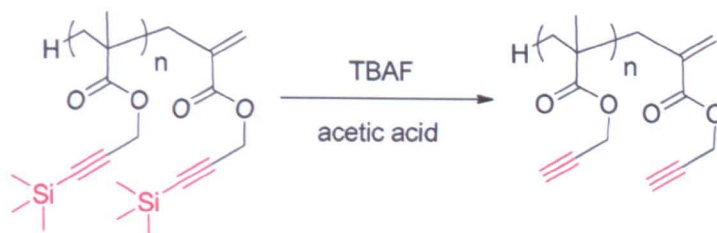
Mass Spectrometry (ESI-MS):  $m/z$  = 219.0 [M+Na]<sup>+</sup>.

### 7.3.3 CCTP of TMS-Protected Propargyl Methacrylate (General Procedure)



CoBF (5.0 mg) was dissolved in MEK (10.0 mL) which was previously freeze-pump-thawed 3 times. AIBN (50 mg) was added to a Schlenk tube containing a magnetic stirrer, followed by addition of TMS-protected propargyl methacrylate (10 mL). The solution was freeze-pump-thawed for 3 times and then filled with nitrogen. The CoBF solution (500  $\mu$ L) was added into the Schlenk tube and the mixture was stirred at 60  $^{\circ}$ C under nitrogen overnight. At the end of the reaction, the mixture was diluted with 20 mL MEK and bubbled with air for 2 hours. The volatiles were removed by distillation under reduced pressure and the polymer was used for deprotection (Conversion = 88%;  $M_n$  = 3100 Da, PDi = 1.74).

### 7.3.4 Deprotection of TMS-Protected Polymers (General Procedure)



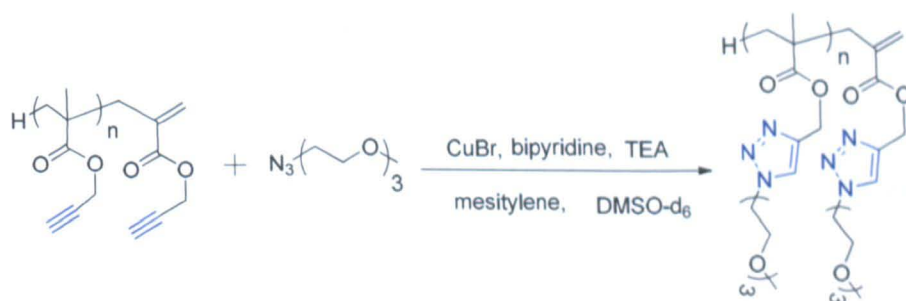
The TMS-protected polymers (2 g, 10.2 mmol TMS groups) and acetic acid (3 g, 51 mmol) were dissolved in THF (100 mL). Nitrogen was bubbled for ten minutes and the solution was cooled to -20  $^{\circ}$ C. A 0.20 M solution of TBAF (15.3 mmol) in THF was added dropwise into the mixture. The resulting solution was stirred at this



temperature for 1 hour and then warmed to ambient temperature. After stirring overnight Amberlite IR-120 ion-exchange resin was added and stirred with the reaction mixture for 2 hours. The resin was removed by filtration and the resulting solution was concentrated under reduced pressure. The polymer was purified by precipitation in petroleum ether (0.6 g, yield = 47.6%;  $M_n = 2900$ ,  $PDi = 1.53$ ).

### 7.3.5 CuAAC of Clickable Polymers and Poly(ethylene glycol) (PEG)

#### Azide



A solution of PEG azide (41.8 mg, 0.288 mmol), clickable polymer (30 mg, 0.24 mmol alkyne groups), bipyridine (7.5 mg, 48  $\mu$ mol), triethylamine (4.86 mg, 48  $\mu$ mol), mesitylene (4 mg, internal NMR standard) in  $DMSO-d_6$  (1.0 mL) was put into an NMR tube and the resulting solution was analysed by  $^1H$  NMR. This solution was then transferred into a small vial and degassed for 20 minutes under nitrogen. The solution was then cannulated into to a Youngs-tap NMR tube, which was previously evacuated and filled with nitrogen, containing  $CuBr$  (3.44 mg, 24  $\mu$ mol). The Youngs-tap NMR tube was immediately placed into an NMR spectrometer set at 60  $^{\circ}C$ . The reaction was analysed by  $^1H$  NMR at regular intervals of time (5 minutes). At the end of the reaction, the brown reaction solution was passed through a short neutral alumina column and subsequently washed with DMSO. The solution

was dialysed against water for 2 days followed by freeze-drying to give the product (Conversion = 100%).

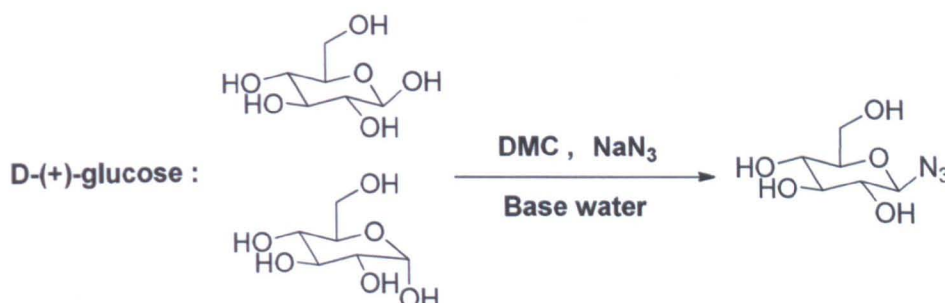
### 7.3.6 Thiol-ene reaction of Clickable Polymers with Benzyl Mercaptan



Dimethylphenylphosphine (DMPP) stock solution (1 mg/mL) was made by dissolving DMPP (2.1  $\mu\text{L}$ , 0.0148 mmol) in acetone- $\text{d}_6$  (2 mL). The clickable polymers (50 mg, 16.7  $\mu\text{mol}$  alkyne groups), benzyl mercaptan (4  $\mu\text{L}$ , 33.33  $\mu\text{L}$ ), DMPP stock solution (230  $\mu\text{L}$ ), and deuterated acetone were transferred into a Youngs-tap NMR tube. The tube was immediately placed into an NMR spectrometer. The reaction was analysed by  $^1\text{H}$  NMR at regular intervals of time (5 minutes) overnight at ambient temperature (Conversion = 85%).

### 7.3.7 One-Step Synthesis of Sugar Azides

The synthesis was performed in large scale following a modified procedure.<sup>7</sup>



**Synthesis of  $\beta$ -D-glucopyranosyl azide:** 2-Chloro-1, 3-dimethylimidazolium chloride (DMC) (2.82 g, 16.7 mmol), D-(+)-glucose (1.00 g, 5.6 mmol), triethylamine (7.7 mL, 55 mmol) and sodium azide (3.61 g, 55.5 mmol) were

dissolved in H<sub>2</sub>O (20 mL). After stirring for 1 h at 0 °C, the reaction mixture was concentrated under reduced pressure and ethanol (40 mL) was added. The resulting white solid was removed by filtration and the volatiles were removed under reduced pressure. The yellowish crude product was dissolved in H<sub>2</sub>O (10 mL) again and washed with dichloromethane (3 × 15 mL), before being passed through a short column of prewashed Amberlite IR-120. The resulting aqueous solution was freeze-dried for two days to give β-D-glucose azide (1.0 g, 5.3 mmol) as an off-white solid. <sup>1</sup>H NMR (400.03 MHz, D<sub>2</sub>O, 298 K) δ (ppm) = 3.25 (t, J = 8.95 Hz, 1H, CH), 3.41 (t, J = 9.50 Hz, 1H, CH), 3.51 (t, J = 9.00 Hz, 1H, CH), 3.54 (m, 1H, CH), 3.74 (m, 1H, CHH), 3.92 (m, 1H, CHH), 4.74 (d, J = 8.78 Hz, 1H, CH). <sup>13</sup>C NMR (100.59 MHz, D<sub>2</sub>O, 298 K) δ (ppm) = 60.5 (1C, CH<sub>2</sub>), 69.1 (1C, CH), 72.8 (1C, CHCH<sub>2</sub>), 75.7 (1C, CH), 77.9 (1C, CH), 90.1 (1C, CHN<sub>3</sub>).

FTIR (neat):  $\tilde{\nu}$  (cm<sup>-1</sup>) = 2116 (-N<sub>3</sub>)

Mass Spectrometry (ESI-MS):  $m/z$  = 228.1 [M+Na]<sup>+</sup>.

**Synthesis of α-D-mannopyranosyl azide:** D-(+)-Mannose (10 g, 55.5 mmol), DMC (28.2 g, 0.167 mol), diisopropylethylamine (DIPEA) (96.7 mL, 0.55 mol) and sodium azide (36.1 g, 0.55 mol) were dissolved in H<sub>2</sub>O (200 mL). After stirring for 5h at 0 °C, the reaction mixture was concentrated under reduced pressure and ethanol (200 mL) was added. The resulting white solid was removed by filtration and the volatiles were removed under reduced pressure. The yellowish crude product was dissolved in H<sub>2</sub>O (80 mL) again and washed with dichloromethane (3 × 100 mL), before being passed through a short column of prewashed Amberlite IR-120. The resulting aqueous solution was freeze-dried for two days to give α-D-mannopyranosyl azide as an off-white solid.

$^1\text{H}$  NMR (400.03 MHz,  $\text{D}_2\text{O}$ , 298 K)  $\delta$  (ppm) = 3.65 (m, 1H,  $\text{CHCH}_2$ ), 3.74 (m, 1H, CH), 3.77 (m, 2H,  $\text{CH}_2$ ), 3.89 (m, 1H, CH), 3.94 (m, 1H, CH), 5.48 (d,  $J = 1.7$  Hz, 1H, CH).  $^{13}\text{C}$  NMR (100.59 MHz,  $\text{D}_2\text{O}$ , 298 K)  $\delta$  (ppm) = 60.82 (1C,  $\text{CH}_2$ ); 66.40 (1C, CH); 69.77 (1C, CH); 69.84 (1C, CH); 74.65 (1C,  $\text{CHCH}_2$ ); 89.74 (1C,  $\text{CHN}_3$ ). FTIR (neat):  $\tilde{\nu}$  ( $\text{cm}^{-1}$ ) = 3318, 2932, 2116, 1652, 1410, 1237, 1091, 1059, 934, 881, 803, 668.

Mass Spectrometry (ESI-MS):  $m/z = 228.1$  [  $\text{M}+\text{Na}$  ] $^+$ .

**Synthesis of  $\beta$ -D-galactopyranosyl azide:** D-(+)-Galactose (10 g, 55.5 mmol), DMC (28.2 g, 0.167 mol), diisopropylethylamine (DIPEA) (96.7 mL, 0.55 mol) and sodium azide (36.1 g, 0.55 mol) were dissolved in  $\text{H}_2\text{O}$  (200 mL). After stirring for 5 h at 0  $^\circ\text{C}$ , the reaction mixture was concentrated under reduced pressure and ethanol (200 mL) was added. The resulting white solid was removed by filtration and the volatiles were removed under reduced pressure. The yellowish crude product was dissolved in  $\text{H}_2\text{O}$  (80 mL) again and washed with dichloromethane ( $3 \times 100$  mL), before being passed through a short column of prewashed Amberlite IR-120. The resulting aqueous solution was freeze-dried for two days to give an off-white solid. Both  $\beta$ -D-galactopyranosyl azide and  $\alpha$ -D-galactopyranosyl azide were obtained (82:18).

$^1\text{H}$  NMR (400.03 MHz,  $\text{D}_2\text{O}$ , 298 K)  $\delta$  (ppm) = 3.51 (m, 1H, CH), 3.66 (m, 1H, CH), 3.75 (m, 2H,  $\text{CH}_2$ ), 3.78 (m, 1H, CH), 3.95 (d,  $J = 3.2$  Hz, 1H, CH), 4.65 (d,  $J = 8.5$  Hz, 1H,  $\text{CHN}_3$ ).  $^{13}\text{C}$  NMR (100.59 MHz,  $\text{D}_2\text{O}$ , 298 K)  $\delta$  (ppm) = 60.95 (1C,  $\text{CH}_2$ ), 68.52 (1C, CH), 70.32 (1C, CH), 72.65 (1C, CH), 77.21 (1C,  $\text{CHCH}_2$ ), 90.55 (1C,  $\text{CHN}_3$ ).

FTIR (neat):  $\tilde{\nu}$  ( $\text{cm}^{-1}$ ) = 3320, 2909, 2365, 2119, 1683, 1399, 1245, 1040, 781.

---

Mass Spectrometry (ESI-MS):  $m/z = 228.1$  [M+Na]<sup>+</sup>.

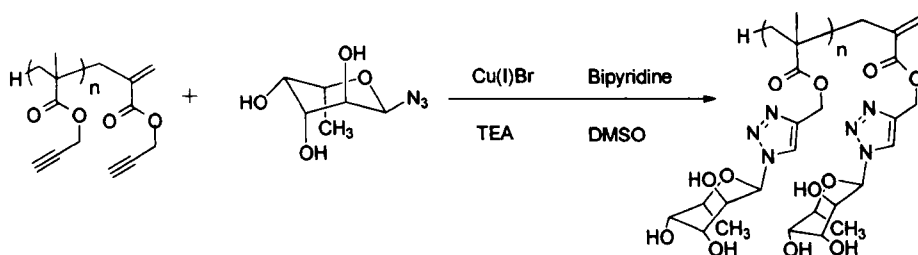
**Synthesis of  $\beta$ -L-fucopyranosyl azide:** L-(+)-Fucose (5.00 g, 30.5 mmol), DMC (15.5 g, 91.4 mmol), DIPEA (53.1 mL, 0.31 mol) and sodium azide (19.8 g, 0.31 mol) were dissolved in H<sub>2</sub>O (100 mL). After stirring for 1 h at 0 °C, the reaction mixture was concentrated under reduced pressure and ethanol (100 mL) was added. The resulting white solid was removed by filtration and the volatiles were removed under reduced pressure. The yellowish crude product was dissolved in H<sub>2</sub>O (50 mL) again and washed with dichloromethane (3  $\times$  100 mL), before being passed through a short column of prewashed Amberlite IR-120. The resulting aqueous solution was freeze-dried for two days. <sup>1</sup>H and <sup>13</sup>C NMR showed that the product was a mixture of the two anomeric epimers ( $\alpha/\beta = 16:84$ ).

<sup>1</sup>H NMR (400.03 MHz, D<sub>2</sub>O, 298 K)  $\delta$  (ppm) = 1.24 (d, J = 6.50 Hz, 3H, CH<sub>3</sub>); 3.55 (m, 1H, CH); 3.79 (m, 2H, CH); 3.88, 4.20 (m, 1H, CH); 4.75 (d, J = 8.65 Hz, 1H, CHN<sub>3</sub>). <sup>13</sup>C NMR (100.39 MHz, D<sub>2</sub>O, 298 K)  $\delta$  (ppm) = 15.50 (1C, CH<sub>3</sub>); 68.08 (1C, CH); 70.86 (1C, CH); 71.66 (1C, CH); 72.92 (1C, CH); 92.20 (CHN<sub>3</sub>).

FTIR (neat):  $\tilde{\nu}$  (cm<sup>-1</sup>) = 3275, 2894, 2115, 1644, 1375, 1249, 1165, 1031, 996, 899, 752, 664.

Mass Spectrometry (ESI-MS):  $m/z = 212.2$  [M+Na]<sup>+</sup>.

### 7.3.8 CuAAC of Clickable Polymers with Sugar Azides (General Procedure)

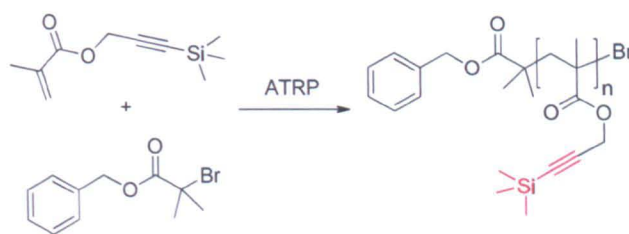


The clickable polymer (0.1 g, 0.81 mmol alkyne groups),  $\beta$ -L-fucopyranosyl azide (0.305 g, 1.61 mmol), 2, 2'-bipyridine (25.2 mg, 0.16 mmol) and TEA (23  $\mu$ L, 0.165 mmol) were dissolved in DMSO (3 mL). The solution was freeze-pump-thawed for 3 times before being cannulated over to another Schlenk tube which was previously evacuated and filled with nitrogen, containing Cu(I)Br (12 mg, 0.084 mmol). The resulting brown solution was stirred at ambient temperature for 3 days. At the end of the reaction, the solution was passed through a short neutral alumina column and washed with DMSO. The mixture was transferred to a dialysis tube and dialyzed against water for 3 days, followed by freeze-drying to give the glycopolymer as a white solid (0.21 g, yield = 79%; Conversion = 100%;  $M_n$  = 8500 Da, PDI = 1.26).

## 7.4 Chapter 4 Experimental

The library of glycopolymers used in this chapter was made by former PhD student in the group, Jin Geng, using the combination of ATRP and CuAAC. The procedures are as following:

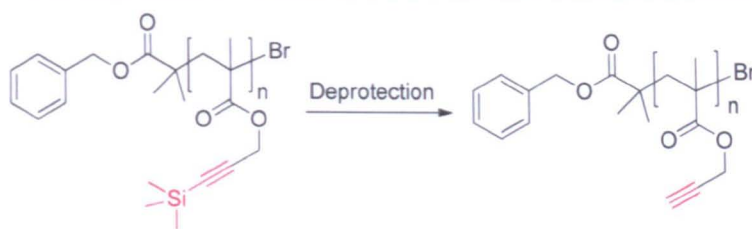
### 7.4.1 Synthesis of TMS-Protected Polymers by ATRP (General Procedure)



TMS-protected propargyl methacrylate (2.00 g, 10.2 mmol), *N*-(ethyl)-2-pyridylmethanimine ligand (0.078 mL, 0.51 mmol), initiator (0.094 g, 0.26 mmol) and mesitylene (0.5 mL) were dissolved in toluene (8.0 mL) in a Schlenk tube. After five freeze-pump-thaw cycles, the solution was then transferred under nitrogen into a second Schlenk tube, which was previously evacuated and filled with nitrogen containing Cu(I)Br (0.036 g, 0.25 mmol). The solution was stirred at 70 °C and samples were taken out periodically using a degassed syringe. At the end of the reaction the mixture was diluted with 20 mL of toluene and then bubbled through with air for 4 h. The solution was passed through a short neutral alumina column and sequentially washed with toluene. The volatiles were removed under reduced pressure and the residues were dissolved in THF (10 mL) prior to precipitation into 200 mL solution of methanol/water (10:2, v/v). The product was isolated as white solid by filtration.

### 7.4.2 Deprotection of the TMS-Protected Polymers (General Procedure)

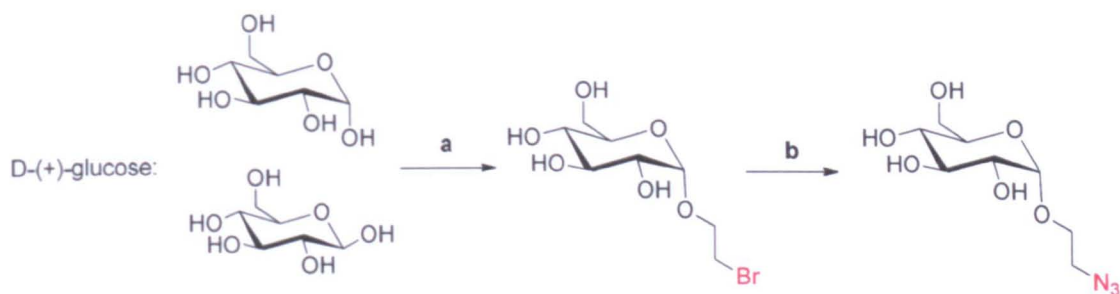




The TMS-protected polymer (1.5 g, 7.653 mmol TMS-alkyne groups) and acetic acid (2.19 mL, 0.0382 mol) were dissolved in THF (100 mL). Nitrogen was bubbled for ten minutes and the solution was cooled to  $-20\text{ }^{\circ}\text{C}$ . A 0.20 M THF solution of TBAF $\cdot$ 3H $_2$ O (0.0114 mol) was added dropwise into the reaction mixture. The resulting solution was stirred at this temperature for 30 minutes and then at ambient temperature overnight. Amberlite IR-120 ion-exchange resin was added and stirred with the solution for 30 min. The resin was removed by filtration and the filtrate was concentrated under reduced pressure. The clickable polymer was purified by precipitation in petroleum ether as white powder (0.46 g, yield = 48 %).

### 7.4.3 Synthesis of Sugar Azides

The experiments followed a procedure as previously described.<sup>6, 8-9</sup>



**a):** A suspension of 2-bromoethanol (78.5 mL, 1.20 mol) and prewashed Amberlite IR-120 (40.0 g) was heated and refluxed at  $90\text{ }^{\circ}\text{C}$  for 30 minutes. D-(+)-glucose



(20.1 g, 0.11 mol) was added into the mixture and the resulting solution was stirred at this temperature for 2.5 h. The solution was filtered, followed by addition of 100 mL deionised water. The excess of 2-bromoethanol was removed by extraction of the mixture using dichloromethane (4×100 mL). The aqueous part was concentrated under reduced pressure to a volume 30 mL and used for next step without further purification.

**b):** Sodium azide (9.2 g, 0.23 mol), deionised water (20 mL) and acetone (250 mL) were added to the previously obtained 2'-bromoethyl- $\alpha$ -D-glucopyranoside aqueous solution. The mixture was heated to reflux for 20 h. Acetone was removed under reduced pressure and the aqueous solution was freeze-dried to give an oily residue. The residue was dissolved in methanol, followed by addition of 100 g silica. The mixture was stirred for 1 h and the silica was removed by filtration. After removal of methanol under reduced pressure, the product was purified by a silica column with a mixture of dichloromethane and methanol (5:1, v/v) as the eluent. The solvent was removed to give 2'-azidoethyl-O- $\alpha$ -D-glucopyranoside (20.1 g, 0.0807 mol, 73 %) as a white solid.  $^1\text{H}$  and  $^{13}\text{C}$  NMR showed that the product was a mixture of the two anomeric epimers ( $\alpha$  and  $\beta$ ).

#### **Azidoethyl -O- $\alpha$ -D-glucopyranoside**

$^1\text{H}$  NMR (400.03 MHz,  $\text{D}_2\text{O}$ , 298 K)  $\delta$  (ppm) = 3.32, 3.52 (m, 2H,  $\text{CH}_2\text{N}_3$ ); 3.57-3.61 (m, 2H,  $\text{CH}_2\text{CH}_2\text{N}_3$ ); 3.61-3.69 (m, 2H,  $\text{CH}_2\text{OH}$ ); 3.71-3.97, 3.97-4.14 (m, 4H, 4×CH); 4.57 (d,  $J$  = 7.92 Hz, 1H,  $\text{C}_{\text{anomeric}}\text{H}$ ), 5.03 (d,  $J$  = 3.65 Hz, 1H,  $\text{C}_{\text{anomeric}}\text{H}$ ).

$^{13}\text{C}$  NMR (100.39 MHz,  $\text{D}_2\text{O}$ , 298 K)  $\delta$  (ppm) = 50.45, 50.62 (1C,  $\text{CH}_2\text{N}_3$ ); 60.59, 60.78 (1C,  $\text{CH}_2\text{OH}$ ); 66.30, 68.57 (1C,  $\text{CH}_2\text{CH}_2\text{O}$ ); 69.56, 69.65 (1C, CH); 71.24, 72.01 (1C, CH); 72.95, 73.13 (1C, CH); 75.72, 75.97 (1C, CH); 98.29 ( $\text{C}_{\text{anomeric}}$ ), 102.33 ( $\text{C}_{\text{anomeric}}$ ).

FTIR (neat):  $\tilde{\nu}$  (cm<sup>-1</sup>) = 3358, 2927, 2097, 1644, 1301, 1262, 1132, 1056, 976, 913, 881, 812.

Mass Spectrometry (ESI-MS):  $m/z$  = 272 [M+Na]<sup>+</sup>.

### 2'-Azidoethyl -O- $\alpha$ -D-mannopyranoside

<sup>1</sup>H NMR (400.03 MHz, D<sub>2</sub>O, 298 K)  $\delta$  (ppm) = 3.45 (m, 2H, CH<sub>2</sub>N<sub>3</sub>), 3.55-3.60 (m, 2H, CH<sub>2</sub>CH<sub>2</sub>N<sub>3</sub>), 3.61-3.67 (m, 2H, CH<sub>2</sub>OH), 3.67-3.91 (m, 4H, 4 $\times$ CH), 4.92 (d,  $J$  = 1.5 Hz, 1H, CH). <sup>13</sup>C NMR (100.59 MHz, D<sub>2</sub>O, 298 K)  $\delta$  (ppm) = 50.20 (1C, CH<sub>2</sub>N<sub>3</sub>), 60.91 (1C, CH<sub>2</sub>OH), 66.30 (1C, CH<sub>2</sub>CH<sub>2</sub>O), 66.68 (1C, CH), 69.97 (1C, CH), 70.39 (1C, CH), 72.89 (1C, CH), 99.81 (C<sub>anomeric</sub>).

IR (neat):  $\tilde{\nu}$  (cm<sup>-1</sup>) = 3358, 2927, 2097, 1644, 1301, 1262, 1132, 1056, 976, 913, 881, 812.

Mass Spectrometry (ESI-MS):  $m/z$  = 272 [M+Na]<sup>+</sup>.

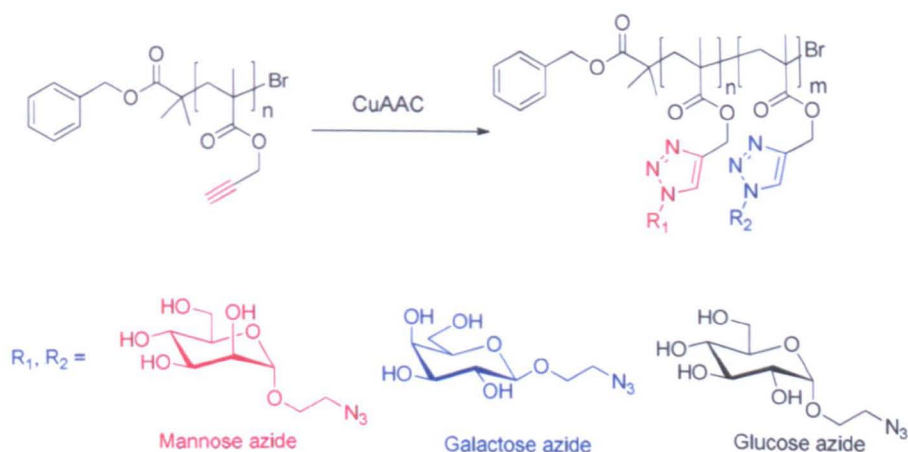
### 2'-Azidoethyl -O- $\beta$ -D-galactopyranoside

<sup>1</sup>H NMR (400.03 MHz, D<sub>2</sub>O, 298 K)  $\delta$  (ppm) = 3.57 (m, 2H, CH<sub>2</sub>N<sub>3</sub>), 3.60 (m, 1H, CH), 3.64-3.72 (m, 2H, CH<sub>2</sub>CH<sub>2</sub>N<sub>3</sub>), 3.76-3.80 (m, 2H, CH<sub>2</sub>OH), 3.83 (m, 1H, CH), 3.93 (m, 1H, CH), 4.05 (m, 1H, CH), 4.46 (d,  $J$  = 7.78 Hz, 1H, CH). <sup>13</sup>C NMR (100.59 MHz, D<sub>2</sub>O, 298 K)  $\delta$  (ppm) = 50.55 (1C, CH<sub>2</sub>N<sub>3</sub>), 60.95 (1C, CH<sub>2</sub>OH), 68.38 (1C, CH<sub>2</sub>CH<sub>2</sub>O), 68.63 (1C, CH), 70.69 (1C, CH), 72.71 (1C, CH), 75.18 (1C, CH), 102.89 (C<sub>anomeric</sub>).

IR (neat):  $\tilde{\nu}$  (cm<sup>-1</sup>) = 3322, 2953, 2098, 1644, 1303, 1265, 1121, 1061, 998, 910.

Mass Spectrometry (ESI-MS):  $m/z$  = 272 [M+Na]<sup>+</sup>.

### 7.4.4 Synthesis of Glycopolymers by CuAAC (General Procedure)



The clickable polymer (0.012 g, 0.092 mmol alkyne groups), 2'-azidoethyl-O- $\alpha$ -D-mannopyranoside (0.026 g, 0.097 mmol), 2'-azidoethyl-O- $\beta$ -D-galactopyranoside (0.009g, 0.032 mmol) and 2,2'-bipyridine (0.014 g, 0.091 mmol) were dissolved in DMSO (10 mL). The solution was degassed by bubbling nitrogen for 20 minutes. Cu(I)Br (0.006 g, 0.04 mmol) was added into the mixture under nitrogen. The resulting solution was stirred at ambient temperature for 3 days, followed by addition of 50 mL of deionised water. The solution was bubbled with air for 6 hours before transferred into a dialysis tube. The solution was dialyzed against water for 2 days, followed by freeze-drying to give the glycopolymers as a white solid.

### 7.4.5 Quantitative Precipitation

The assay was followed a modified procedure.<sup>6, 10</sup> Con A was dissolved in the HBS buffer (0.10 M HEPES, 0.9 M NaCl, 1 mM MgCl<sub>2</sub>, 1 mM CaCl<sub>2</sub> and 1 mM MnCl<sub>2</sub>, pH 7.4) to make fresh stock solution and the concentration was 60  $\mu$ M (assuming Con A tetramers with a molecular weight of 106 kDa). Glycopolymers solutions in

HBS buffer were also prepared with a series of different concentration. Then Con A solution and the glycopolymer solution were mixed (1:1, v/v) energetically and incubated for 5 hours at 22 °C. So the final concentration of Con A was 30  $\mu$ M. White precipitates were separated from solution by centrifugation at  $5000 \times g$  for 2 minutes, followed by removal of the supernatants very carefully using pipette. Then the pellets were resuspended in cold buffer again. These washing steps were repeated twice. After removal of the supernatants, the precipitates were dissolved in a HBS buffer solution of methyl- $\alpha$ -D-mannopyranoside (1 mL, 1 M). With complete dissolution, the Con A content was determined by measuring the absorbance at 280 nm.

#### 7.4.6 Turbidimetry

It was carried out *via* a previously described procedure by Kiessling, *et al.*<sup>10</sup> Con A was fully dissolved in HBS buffer (approximately 1 mg/mL). The exact concentration of Con A was determined by measuring the absorbance at 280 nm ( $A_{280} = 1.37 \times [\text{mg/mL Con A}]$ ). The solution was then diluted to 1  $\mu$ M. After addition of 0.50 mL glycopolymer (50  $\mu$ M) into a dry polycarbonate cuvette (1 mL, 1 cm pathlength), the cuvette was placed in the UV spectrometer. By adding 0.50 mL of the diluted Con A solution into the cuvette *via* a pipette, the absorbance of the mixture was quickly recorded at 420 nm for 10 min every 0.12 s. The relative rate of interaction was determined by a linear fit of the steepest portion of the initial aggregation. Each experiment was repeated 3 times.

### 7.4.7 Reversal Aggregation Assay

As previously described,<sup>6</sup> following the turbidity measurement, the absorbance  $A_{420}$  of the solution after 2 hours at room temperature was recorded as  $A_{420}(t=0)$ . Then 0.1 mL methyl- $\alpha$ -D-mannopyranoside (54 mM) in HBS buffer solution was added to the cuvette. The mixed solution was quickly placed in the spectrometer and the absorbance at 420 nm was recorded for 10 minutes.  $A_{420}(t=10)$  was calculated as an average of the last 10 seconds of each experiment. The percent change in absorbance was determined as  $(A_{420}(t=0) - A_{420}(t=10)) / A_{420}(t=0)$ .

### 7.4.8 Inhibitory Potency Assay

Con A was dissolved in HBS buffer to make fresh stock solution and the concentration was 5  $\mu$ M (assuming Con A tetramers with a molecular weight of 106 kDa). The stock solution of Glycopolymer in HBS buffer was also prepared (5  $\mu$ M). The glycopolymer solution (0.25 mL) and methyl- $\alpha$ -D-mannopyranoside (0.05 mL) of different concentration were mixed together, followed by addition of Con A solution (0.25 mL). The solution was mixed energetically and incubated for 5 hours at 22 °C and then the absorbance of the solution at 420 nm was measured.

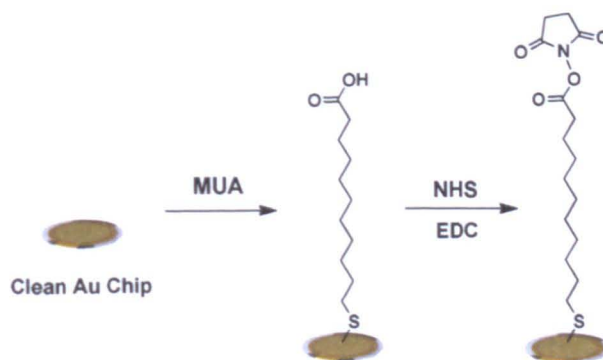
## 7.5 Chapter 5 Experimental

### 7.5.1 Typical Conditions for QCM-D Experiment



HBS buffer (10 mM HEPES, 0.15 M NaCl, pH 7.4) containing 1 mM metal ions ( $\text{Ca}^{2+}$ ,  $\text{Mg}^{2+}$  and  $\text{Mn}^{2+}$ ) was pumped through the QCM-D system at a flow rate 50  $\mu\text{L}/\text{min}$  to get stable flat baselines of frequency and energy dissipation at 25 °C. Then a solution of disulfide mannose glycopolymer (0.5 mg/mL) in HBS buffer was passed over the QCM-D gold chips in the flow-through module to ensure maximum surface coverage of the glycopolymer. There was a decrease of the frequency and an increase of the dissipation. After a plateau is reached for both  $f$  and  $D$ , HBS buffer was passed over the chip to remove any unbounded glycopolymers. The frequency increased suggesting removal of non-adsorbed mass but the dissipation decreased indicating the formation of a more rigid film, during the rinsing process before the flat baselines were achieved again. After which Con A (0.5 mg/mL) was injected, followed by the HBS buffer rinse. The changes in frequency and dissipation which were caused by glycopolymers and lectin were monitored simultaneously by the QCM-D system and modelled afterwards using QTools software.

### 7.5.2 Modification of Au Chip with MUA, EDC and NHS



Au chips were cleaned in a mixture of 35 % of  $\text{NH}_3$ , 33 % of  $\text{H}_2\text{O}_2$  and Milli-Q water (1:1:5, v/v) for 10 min and then rinsed with Milli-Q water and dried by a stream of nitrogen. Then the chips were immediately immersed into the solution of

10 mM 11-mercaptoundecanoic acid (MUA) in ethanol and kept overnight at ambient temperature to obtain the thiol self-assembled monolayer (SAM) on the gold surfaces. The gold chips were washed with ethanol and Milli-Q water sequentially and then immersed into a freshly prepared water solution of 0.4 M 1-[3-(dimethylamino)propyl]-3-ethyl carbodiimide (EDC) hydrochloride and 0.1M *N*-hydroxysuccinimide (NHS) (1:1, v/v) to activate the carboxyl groups on the Au surface. After washed with Milli-Q water and dried with a stream of nitrogen, the gold chips were mounted in the QCM-D cell. HBS buffer was run through the system until flat baselines of frequency and dissipation were achieved.

### ***7.5.3 Typical Conditions for SPR Experiment***

HBS buffer (pH = 7.4) containing 25 mM HEPES, 150 mM NaCl, 5 mM CaCl<sub>2</sub> and 0.01% Tween-20 was generally used to make solutions of analytes except that the lectin DC-SIGN was dissolved in a acetate buffer (pH = 5.0) for optimal immobilization. The following solutions were passed through the system sequentially: (A) the mixture of 0.4 M EDC and 0.1M NHS (1:1, v/v) at 30  $\mu$ L/min with contact time at 300 s and volume at 150  $\mu$ L, followed by buffer; (B) the solution of DC-SIGN (50  $\mu$ M) in acetate buffer (pH = 5.0) at 25  $\mu$ L/min with contact time at 900 s and volume at 375  $\mu$ L, followed by buffer; (C) the solution of ethanolamine HCl (1M, pH 8.5) at 25  $\mu$ L/min with contact time at 900 s and volume at 375  $\mu$ L, followed by buffer; (D) HBS buffer solutions of gp120 with different concentrations (0.31 nM ~ 10.0 nM) at 25  $\mu$ L/min with contact time at 900 s and volume at 375  $\mu$ L, followed by buffer; (E) 10 mM glycine hydrochloride, pH 2.5 at 100  $\mu$ L/min with contact time at 27 s and volume at 45  $\mu$ L, followed by buffer.



---

## 7.6 References

1. Keller, R. N.; Wyckoff, H. D., *Inorg. Synth.* **1946**, 2, 1-4.
2. Bakak, A.; Espenson, J. H., *J. Am. Chem. Soc.* **1984**, 106, 5197-5202.
3. Suddaby, K. G.; Haddleton, D. M.; Hastings, J. J.; Richards, S. N.; O'Donnell, J. P., *Macromolecules* **1996**, 29, 8083-8091.
4. Hovestad, N. J.; van Koten, G.; Bon, S. A. F.; Haddleton, D. M., *Macromolecules* **2000**, 33, 4048-4052.
5. Haddleton, D. M.; Crossman, M. C.; Dana, B. H.; Duncalf, D. J.; Heming, A. M.; Kukulj, D.; Shooter, A. J., *Macromolecules* **1999**, 32, 2110-2119.
6. Ladmiral, V.; Mantovani, G.; Clarkson, G. J.; Cauet, S.; Irwin, J. L.; Haddleton, D. M., *J. Am. Chem. Soc.* **2006**, 128, 4823-4830.
7. Vinson, N.; Gou, Y.; Becer, C. R.; Haddleton, D. M.; Gibson, M. I., *Polym. Chem.* **2011**, 2, 107-113.
8. Geng, J.; Mantovani, G.; Tao, L.; Nicolas, J.; Chen, G.; Wallis, R.; Mitchell, D. A.; Johnson, B. R. G.; Evans, S. D.; Haddleton, D. M., *J. Am. Chem. Soc.* **2007**, 129, 15156-15163.
9. Geng, J.; Lindqvist, J.; Mantovani, G.; Chen, G.; Sayers, C. T.; Clarkson, G. J.; Haddleton, D. M., *QSAR. Comb. Sci.* **2007**, 26, 1220-1228.
10. Cairo, C. W.; Gestwicki, J. E.; Kanai, M.; Kiessling, L. L., *J. Am. Chem. Soc.* **2002**, 124, 1615-1619.